

**Genetic and Functional Characterisation
of the *LIMD1* Promoter and Gene
Product: From Lung Cancer to the
Hypoxic Response**

Daniel E. Foxler, BSc (Hons)

**Thesis submitted to the University of Nottingham for the
degree of Doctor of Philosophy.**

July 2012

Abstract

LIM domain containing protein 1 (LIMD1) is a tumour suppressor located at 3p21.3, a region that harbours multiple tumour suppressor genes and is commonly subject to homozygous deletions and loss of heterozygosity in many cancers. The mechanism of LIMD1 tumour suppressive activities are not fully elucidated, however to date it has been shown to bind to the retinoblastoma protein (pRb) and repress E2F driven transcription as well as being a critical component of miRNA mediated gene silencing. Recent work has also identified LIMD1 as a possible negative regulator of hypoxia inducible factor α (HIF1 α) and the hypoxic response. In lung cancer, LIMD1 protein expression is down regulated in up to 79% of tumours when compared to normal tissue with gene deletion and loss of heterozygosity accounting for 32 and 12% respectively, leaving 30% of tumours with unexplained mechanism of LIMD1 protein loss.

In an aim to identify other possible mechanisms of LIMD1 loss, scrutinisation of the *LIMD1* promoter identified a CpG Island in the 5' promoter region, within which a small region was found to be critical for transcriptional activation. This region was methylated in the non-LIMD1 expressing MDA-MB435 cell line, but became hypomethylated and *LIMD1* expressed following treatment with the DNA methylation inhibitor 5-Aza-2'-deoxycytidine. In primary lung tumours, analysis of genomic DNA also identified increased methylation of this region as well as a reduction in *LIMD1* mRNA levels when compared to matched normal lung tissue. Furthermore, *in silico* analysis identified a conserved binding motif for the Ets transcription factor PU.1. Experimentally PU.1 was verified as binding to the *LIMD1* promoter with siRNA mediated depletion of PU.1 significantly reducing endogenous LIMD1 protein levels, thus identifying two possible novel mechanisms of *LIMD1* silencing. Transcription of *LIMD1*, like that of other HIF1 α regulatory proteins, was enhanced when cells were exposed to hypoxia (1% O₂), facilitated by HIF1 α binding a hypoxic responsive element (HRE) within the promoter. At the molecular level, *in vivo* LIMD1 forms an endogenous complex with proline hydroxylase 2 (PHD2) and the von Hippel-Lindau (VHL) protein, with LIMD1 loss decreasing the efficiency of HIF1 α degradation and impeding the resultant cellular adaptation to chronic hypoxia.

In summary these studies identified epigenetic silencing of *LIMD1* as a possible explanation for LIMD1 protein loss in transformed cells. Furthermore, *LIMD1* transcription was identified as being activated by PU.1 and enhanced by HIF1 α , and a revised, LIMD1 integrated, model of HIF1 α regulation is proposed.

Publications

- 1 **The LIMD1 protein bridges an association between the Prolyl Hydroxylases and VHL to repress HIF1 activity.**
Daniel E. Foxler, Katherine S. Bridge, Victoria James, Thomas M. Webb, Maureen Mee1 , Sybil C. K. Wong, Yunfeng Feng, Constantin-Teodosiu D, Thorgunnur Eyfjord Petursdottir, Johannes Bjornsson, Sigurdur Ingvarsson, Peter J. Ratcliffe, Gregory D. Longmore and Tyson V. Sharp
Nature Cell Biology In press 2012.

- 2 **Human feeder cell line for derivation and culture of hESc/hiPSc.**
McKay TR, Camarasa MV, Iskender B, Ye J, Bates N, Miller D, Fitzsimmons JC, Foxler D, Mee M, Sharp TV, Aplin J, Brison DR, Kimber SJ.
Stem Cell Res. 2011 Sep;7(2):154-62. Epub 2011 May 16

- 3 **PU.1 is a major transcriptional activator of the tumour suppressor gene LIMD1.**
Foxler DE, James V, Shelton SJ, Vallim TQ, Shaw PE, Sharp TV.
FEBS Lett. 2011 Apr 6;585(7):1089-96. Epub 2011 Mar 12.

- 4 **LIM-domain proteins, LIMD1, Ajuba, and WTIP are required for microRNA-mediated gene silencing.**
James V, Zhang Y, Foxler DE, de Moor CH, Kong YW, Webb TM, Self TJ, Feng Y, Lagos D, Chu CY, Rana TM, Morley SJ, Longmore GD, Bushell M, Sharp TV.
Proc Natl Acad Sci U S A. 2010 Jul 13;107(28):12499-504. Epub 2010 Jun 28.

- 5 **The chromosome 3p21.3-encoded gene, LIMD1, is a critical tumor suppressor involved in human lung cancer development.**
Sharp TV, Al-Attar A, Foxler DE, Ding L, de A Vallim TQ, Zhang Y, Nijmeh HS, Webb TM, Nicholson AG, Zhang Q, Kraja A, Spendlove I, Osborne J, Mardis E, Longmore GD.
Proc Natl Acad Sci U S A. 2008 Dec 16;105(50):19932-7. Epub 2008 Dec 5.

Acknowledgements

I would like to first thank Tyson for letting me work in his lab, and all the advice, support, and help he has given me since I started. His open door and enthusiasm with my project has certainly paid off. I also have pay tribute to the regular 'I've had a thought' and 'what's going on' that he's given me since I started. It's certainly made it a more enjoyable experience.

I would also like to thank Rob Layfield for all his help and advice, and I just hope I managed to entertain you on all those days you told your lab not to bother coming in?

There are then all of the lab members (or I maybe feel like I should call them friends after so long) that I need to mention. Starting (in chronological order) with the Sharpies first; Pierre, you were the first one to introduce me to the concept of LIMD1, lab work, and eating/drinking/sleeping at your desk. But also thank you for all the help and advice you gave me as an undergraduate. Then there is Tom, have our girlfriends learnt to wash up yet I wonder? I still get mocked for how much we would complain about that. We had some good banter in the lab, and also got some good science done too before you deserted me for a different world (that sounds like you've died...I should say to work for GSK). Vicky, thank you for all the help and advice in the lab, the qRT-PCR and being the only person I could feel safe around knowing that they wouldn't steal The Sun at morning coffee. Then came Katherine, who I admire (even though she's turned to the dark side with her phone) for laughing at my same old jokes every day of the week (except for the days you go off to Tesco late at night to buy The Sun) and Mo, who can always be found in tissue culture, thanks for all the ordering and help around the lab. I still don't know what you mean when you said Katherine was becoming more like me? Also thank you to the past members Nisha, Nektaria and Tom.

Moving on to the Layfield lot... Jo, you've been here with me since the start, thank you for all the entertainment provided by your stories, and all the mutual work and social advice we exchange. And if you want to reply to this please write it on one of your many lists. Then there's Alice 'tea?' Goode, my caffeine intake has rocketed since you've started, and I still don't forgive you anytime you (or Mr Atkins come to think of it) get to the paper before I do. But I still enjoy the tea breaks, chats and moans all the same! Also thank you to Barry and James.

I would then like to thank my family for their love and attempting/pretending/trying to understand science. Mum, those days I worked late and don't get chance to phone you, no my finger's weren't broken I was working hard. Dad, yes you'll understand this page, but after this you probably won't understand it regardless of what you think. Becky, explain to mum and dad what those comments mean, and don't do a PhD unless you want to do your version of the next 200 pages. And finally Gemma, because nobody tells you anything at home, I've submitted my thesis...

I also want to thank all of my other family and friends for their help and support both in and out of the lab, as well as Laura for her patience, love and support I've needed whilst writing this novel.

Finally I would like to thank the British Lung Foundation, the BBSRC and the School of Biomedical Sciences (University of Nottingham) for funding my research.

Abbreviations

A	Adenine
ALDOC	aldolase C, fructose-bisphosphate
AP-1	activator protein 1
aPKC	atypical protein kinase C
bHLH	basic helix loop helix
BNIP3	BCL2/adenovirus E1B 19kDa interacting protein 3
bp	base pairs
BRE	TFIIB recognition element
BSA	bovine serum albumin
C	Cytosine
C3CER1	chromosome 3 commonly eliminated region 1
CAGE	CAP analysis of gene expression
cfu	colony forming unit
ChIP	chromatin immunoprecipitation
CSC	cancer stem cell
Cul2	cullin 2
Deep-seq	Deep Sequencing
DMOG	Dimethylxallylglycine
DNA	deoxyribonucleic acid
Dnmt	DNA methyl transferase
DPE	downstream promoter element
EC	embryonal carcinoma
ECM	extra-cellular matrix
Elo B	elongin B
EMSA	electrophoretic mobility shift assay
Epo	Erythropoietin
ERO1L	endoplasmic reticulum oxidoreductin-1-like
ES	embryonic stem-cell
EST	expressed sequence tag
FIH	factor inhibiting HIF1 α
G	Guanine
GST	glutathione-s-transferase
GTF	general transcription factor
HAT	histone acetyltransferases
HDAC	histone deacetylase
HIF	hypoxia inducible factor
HKMT	histone lysine methyltransferases
HNSCC	head and neck squamous cell carcinoma
HRE	hypoxic responsive element
HRE	hypoxia response element
HSC	hematopoietic stem cell
HTF	HpaII tiny fragment
ICR	imprinting control regions
IKK	I κ B kinase
Inr	initiator element

IVTT	in vitro transcription and translation
JMJD1A	jumonji domain containing 1A
kbp	kilobase pairs
kDa	kilo Daltons
LIMD1	Lim domain containing protein 1
LOH	loss of heterozygosity
LPP	lipoma preferred partner
MAPK	mitogen activated protein kinase
MBD	methyl CpG binding domain
miRNA	micro-ribonucleic acid
M-MuLV	Moloney murine leukemia virus
mRNA	messenger RNA
MSP	methylation specific PCR
MTase	methyltransferase
mtDNA	mitochondrial DNA
MXI1	MAX interacting protein 1
NuRD	nucleosome remodelling and deacetylase
ODD(D)	oxygen dependent degradation (domain)
PBS	phosphate buffered saline
PCR	polymerase chain reaction
PHD	proline hydroxylase
PIC	pre-initiation complex
Pol II	RNA polymerase II
pRB	Retinoblastoma protein
Pu	purine
Py	pyrimidine
qRT-PCR	quantitative real time PCR
RANK	Receptor activator of NFκB
RANK-L	Receptor activator of NFκB ligand
RISC	RNA induced silencing complex
RLC	RISC loading complex
RM	restriction modification
RMCE	recombinase mediated cassette exchange
RNA	ribonucleic acid
SCID	severely combined immunodeficient
SFFV	spleen focus forming virus
Spi-1	SFFV proviral integration protein
SV40	Simian virus 40
T	thymine
TAE	Tris-acetate-EDTA
TBP	TATA binding protein
TMA	tissue microarray
TRAF	TNF receptor associated factor
TRBP	TAR RNA binding protein
TSG	tumour suppressor gene
TSS	transcription start site
VEGF	vascular endothelial growth factor A

VHL	von Hippel-Lindau protein
VO	vector only
WSB1	WD repeat and SOCS containing 1

Table of Contents

Abstract	i
Publications	ii
Acknowledgements	iii
Abbreviations	v
Chapter 1 Introduction	1
1.1 Thesis Overview	2
1.2 Genetic and Epigenetic Alterations are the Underlying Cause of Cancer	3
1.3 Chromosome 3 Deletions in Cancer	4
1.4 LIM Domain Containing Proteins	7
1.5 The Zyxin Family of LIM Domain Containing Proteins	8
1.6 LIMD1	10
1.6.1 Identification of LIMD1	10
1.6.2 LIMD1 in Lung Cancer	10
1.6.3 LIMD1 in Breast Cancer	11
1.6.4 LIMD1 in Head and Neck Squamous Cell Carcinomas	12
1.6.5 LIMD1 is involved in multiple Intracellular Signalling Pathways	14
1.6.6 LIMD1 interacts with pRb and is a Repressor of E2F Driven Transcription	14
1.6.7 LIMD1 is a Critical Component of miRNA Silencing	15
1.6.8 LIMD1 is a Regulator of Osteoblast and Osteoclast Function	18
1.7 The Ajuba/Zyxin Family of Proteins	23
1.7.1 Zyxin	23
1.7.2 LPP	23
1.7.3 TRIP6	23
1.7.4 Migfilin	24
1.7.5 Ajuba	25
1.7.6 WTIP	25
1.8 Control of Gene Transcription	26
1.8.1 Features of RNA Polymerase II Promoters	27
1.8.2 Active Transcription requires an Open Euchromatin Structure	30
1.9 DNA Methylation and Epigenetic Silencing	32
1.9.1 5-Methyl Cytosine	32
1.9.2 CpG Islands	33
1.9.3 CpG Islands are Aberrantly Hypermethylated in Multiple Cancers	35
1.9.4 DNA Methylation is Epigenetic	38
1.9.5 DNA Methylation is Carried out by DNA Methyltransferases (Dnmts)	38
1.9.6 CpG Methylation is Critical for Normal Cell Physiology	42
1.9.7 Promoter Methylation as a Cause of Transcriptional Silencing	45
1.9.8 Methyl CpG Binding Domain Proteins	47
1.10 Preliminary Data	49
1.10.1 The LIMD1 Promoter contains a Putative CpG Island	49
1.11 Ets Family of Transcription Factors	51
1.11.1 The Ets Domain	51
1.11.2 PU.1 (Spi1)	53
1.12 Hypoxia	58
1.12.1 Identification of the HIF1 Transcription Factor	58
1.12.2 HIF1 Allows for Cellular Adaptation to Low Oxygen Tensions	60

1.12.3	Regulation of HIF1 α Protein Degradation	62
1.12.4	The von Hippel-Lindau (VHL) Protein	63
1.12.5	Proline Hydroxylase (PHD) Proteins	64
1.12.6	Regulation of HIF1 α Transcriptional Activation	65
1.12.7	Phosphorylation of HIF1 α	67
1.12.8	Summary of HIF1 α Regulation	68
1.12.9	Regulation of HIF1 α in Hypoxia	70
1.13	Preliminary Data	73
1.13.1	The Role of LIMD1 in Regulation of Hypoxia	73
1.13.2	LIMD1 binds to the Proline Hydroxylases and VHL	73
1.13.3	LIMD1 Bridges the Association between PHD2 and VHL	75
1.13.4	Loss of LIMD1 Inhibits HIF1 α Degradation	76
1.14	Thesis Aims and Objectives	77
Chapter 2 Materials and Methods		78
2.1	Materials	79
2.1.1	Media and Selection Drugs	79
2.1.2	Antibiotics and Selection Drugs	80
2.1.3	Buffers and Solutions	80
2.1.4	Bacteriological Buffers and Solutions	80
2.1.5	DNA Buffers	80
2.1.6	Cell Lysis/Wash Buffers	81
2.1.7	Solutions for Sodium Dodecyl Sulphate-Polyacrylamide Gel Electrophoresis (SDS-PAGE) and Immunoblotting	82
2.1.8	Dual-Luciferase Reporter Assay Solutions	83
2.1.9	Human Tumour Samples	83
2.1.10	Antibodies	84
2.2	Methods	85
2.2.1	Bacterial Culture methods	85
2.2.2	Preparation of Chemically-Competent Cells	85
2.2.3	Transformation and Propagation of Chemically Competent <i>DH5α</i> Bacteria	85
2.2.4	Nucleic Acid Techniques	86
2.2.5	Plasmid DNA Extraction	86
2.2.6	Genomic DNA Extraction	87
2.2.7	RNA Extraction and cDNA Synthesis	87
2.2.8	Quantification of DNA/RNA Concentration	88
2.2.9	DNA Sequencing	88
2.2.10	Bisulphite Treatment of Genomic DNA	88
2.2.11	Site-directed Mutagenesis	88
2.2.12	Polymerase Chain Reaction (PCR)	90
2.2.13	TA Cloning of PCR Products	91
2.2.14	Cell Culture Techniques	91
2.2.15	Cell Maintenance and Passaging of Adherent Cells	91
2.2.16	Cell Maintenance and Passaging of Suspension Cells	91
2.2.17	Cell Freezing	92
2.2.18	Cell Counting	92
2.2.19	Cell Seeding	92
2.2.20	Hypoxic Treatment of Cells	92
2.2.21	Transfection of DNA into Monolayer Adherent Cells	92
2.2.22	Transfection of siRNA into Monolayer Adherent Cells	93
2.2.23	Transfection of siRNA into Suspension Cells	93
2.2.24	DNA/RNA Analysis Techniques	94
2.2.25	Bioinformatic Analysis	94
2.2.26	CpG Island and Transcription Factor Binding Motif Analysis	94

2.2.27	Methylation Specific PCR	94
2.2.28	Bisulphite Sequencing	95
2.2.29	qRT-PCR Analysis	95
2.2.30	5-Aza-2'-Deoxycytidine Treatment	96
2.2.31	Protein-DNA Interaction Techniques	96
2.2.32	Mapping and hypoxic responsiveness of the <i>LIMD1</i> Promoter	96
2.2.33	Chromatin Immunoprecipitation	96
2.2.34	Electrophoretic Mobility Shift Assay (EMSA)	97
2.2.35	Protein-Protein Interaction Analysis Techniques	98
2.2.36	Recombinant protein purification	98
2.2.37	Direct Binding Assay	100
2.2.38	Dephosphorylation Assay	100
2.2.39	Immunoprecipitation (IP)	101
2.2.40	Western Blot Analysis	101
Chapter 3 <i>LIMD1</i> transcription and promoter methylation in lung cancer		103
3.1	Introduction	104
3.2	The <i>LIMD1</i> Promoter contains a Single CpG Island	104
3.2.1	The CpG Island within the <i>LIMD1</i> Promoter Contains Both Negative and Positive Regulatory Regions	106
3.3	Analysis of <i>LIMD1</i> Promoter Methylation	108
3.3.1	Identification of the Methylation Status of the <i>LIMD1</i> promoter in <i>LIMD1</i> expressing and non-expressing cell lines.	108
3.3.2	Methylation within IR5 of the <i>LIMD1</i> promoter increases in primary lung tumours compared to normal control tissue.	110
3.3.3	Optimisation of methylation specific PCR (MSP)	111
3.3.4	MSP of Primary Lung Tissue and Matched Lung Tumours	113
3.3.5	Optimisation of Bisulphite Sequencing the <i>LIMD1</i> Promoter	117
3.3.6	Bisulphite Sequencing of the IR5 Region within the <i>LIMD1</i> Promoter identified Aberrant Methylation in Primary Lung Tumours	119
3.4	<i>LIMD1</i> and <i>Rassf1a</i> mRNA Expression is Reduced in the Majority of Primary Lung Tumours Examined	122
3.5	Epigenetic Silencing of <i>LIMD1</i>	125
3.5.1	Optimisation of 5-azacytidine Treatment	125
3.5.2	<i>LIMD1</i> is Epigenetically Silenced in the non- <i>LIMD1</i> Expressing MB435 Cell Line	126
3.6	Summary	127
Chapter 4 Identification of <i>PU.1</i> as a Major Transcriptional Activator of <i>LIMD1</i>		128
4.1	Introduction	129
4.1.1	IR5 within the <i>LIMD1</i> Promoter is Perfectly Conserved Between Different Mammalian Species	129
4.2	<i>In Silico</i> Analysis of the <i>LIMD1</i> Promoter identified a Binding Motif for an Ets Transcription Factor	130
4.2.1	Mutation of the DNA Consensus for Ets Factor Binding within IR5 Reduces <i>LIMD1</i> Promoter Driven Transcription	132
4.3	Identification of <i>PU.1</i> Binding to <i>LIMD1</i> Promoter and Activating Transcription	135
4.3.1	Sub-cloning of <i>PU.1</i> into pcDNA4 His/Max TOPO and pCMV-HA Vectors	135
4.3.2	<i>PU.1</i> binds the IR5 region of the <i>LIMD1</i> Promoter <i>in vitro</i> as demonstrated by Electrophoretic Mobility Shift Assay	141
4.3.3	The Ets-domain alone of <i>PU.1</i> binds to the <i>LIMD1</i> Promoter	143
4.3.4	siRNA Mediated Depletion of <i>PU.1</i> reduces <i>LIMD1</i> Protein Levels	144

4.4	Summary	148
Chapter 5 <i>LIMD1</i> as a Regulator of the Hypoxic Response		149
5.1	Introduction	150
5.2	The <i>LIMD1</i> Promoter is Responsive to Hypoxia	150
5.2.1	<i>LIMD1</i> Promoter Driven Transcription Increases Following Hypoxic Exposure	150
5.2.2	<i>LIMD1</i> Protein Levels Increase Following Prolonged Hypoxic Exposure	153
5.3	Characterisation of the Hypoxic Responsive Element in the <i>LIMD1</i> Promoter	154
5.3.1	The IR3 Region of the <i>LIMD1</i> Promoter is required for Hypoxic Responsiveness.	154
5.3.2	Mutagenesis of the HRE or HIF1 α Depletion Abolishes the Hypoxic Response of the <i>LIMD1</i> Promoter	156
5.3.3	Depletion of Endogenous HIF1 α Significantly Reduces Endogenous <i>LIMD1</i> Protein.	158
5.4	The role of <i>LIMD1</i> in Regulation of the Hypoxic Response	159
5.4.1	<i>LIMD1</i> Binds Directly to PHD2 <i>in vitro</i>	160
5.4.2	<i>LIMD1</i> interacts Endogenously with PHD2, VHL and VCB Complex Proteins	162
5.4.3	Optimisation of Endogenous Co-immunoprecipitations Methods	162
5.4.4	Endogenous VHL, <i>LIMD1</i> and PHD2 Co-Immunoprecipitate <i>In Vivo</i> .	166
5.4.5	<i>LIMD1</i> Protein Loss Inhibits Adaptation to Chronic Hypoxia	172
5.5	HIF1 α is Post Translationally Modified by Phosphorylation	176
5.5.1	Phosphorylation of HIF1 α Affects Transcription of HRE Containing Genes	179
5.6	Summary	181
Chapter 6 Discussion		182
6.1	<i>LIMD1</i> Gene Transcription and Promoter Methylation	183
6.1.1	The <i>LIMD1</i> Promoter is Methylated in the Non- <i>LIMD1</i> expressing MDA-MB435 Cell Line	183
6.1.2	The <i>LIMD1</i> Promoter is Methylated in Primary Lung Tumours	184
6.1.3	<i>LIMD1</i> mRNA Expression is Down-Regulated in Lung Tumours	186
6.1.4	<i>LIMD1</i> is Epigenetically Silenced in MDA-MB435 Cells	187
6.2	Identification of PU.1 as a Major Transcriptional Activator of <i>LIMD1</i>	189
6.2.1	IR5 is Perfectly Conserved between <i>LIMD1</i> Expressing Species and Harbours an Ets Family Member/PU.1 Binding Motif	189
6.2.2	The <i>LIMD1</i> Promoter Contains a putative Second PU.1 Binding Site	192
6.3	Additional (Unconfirmed) Features of the <i>LIMD1</i> Promoter	194
6.4	<i>LIMD1</i> is a Regulator of the Hypoxic Response	195
6.4.1	<i>LIMD1</i> driven Transcription and Protein Levels are increased in Hypoxia	195
6.4.2	HIF1 α Modulates <i>LIMD1</i> Transcription but is not a Major Transcriptional Activator	196
6.4.3	Promoter Methylation may Prevent Transcription Factor Binding to the <i>LIMD1</i> Promoter	197
6.4.4	<i>LIMD1</i> Forms an Endogenous Complex with PHD2 and VHL/VCB Complex Proteins	197
6.4.5	<i>LIMD1</i> Loss Reduces the Efficiency of HIF1 α Degradation and Inhibits Adaptation to Chronic Hypoxia	198
6.4.6	<i>LIMD1</i> Expression does not Effect HIF1 α Phosphorylation	199
6.4.7	Loss of <i>LIMD1</i> Expression Affects HIF-1 Driven Gene Expression	200
6.4.8	<i>LIMD1</i> forms a Negative Regulatory Pathway of HIF1 α Degradation	201
Chapter 7 Future Work		204
7.1	Future Work	205
7.1.1	Methylation Analysis of the Full <i>LIMD1</i> Promoter and Gene	205

7.1.2	The Identification of PU.1 as an Activator of <i>LIMD1</i> Transcription May Imply a Hematopoietic Lineage Related Function of LIMD1	206
7.1.3	PU.1 and LIMD1 are Both Critical Regulators of Osteoclast Differentiation	209
7.1.4	Loss of LIMD1 Expression May Initiate Cell Transformation and Growth through Pathways Involving PU.1 or HIF1 α	212
7.2	Final Conclusions	213
Chapter 8 Appendix		214
8.1.1	Nucleic Acid Sequence of the <i>LIMD1</i> Promoter	215
8.1.2	The LIMD1 Promoter Showing the Relative Positions of the confirmed PU.1 and HIF1 α Binding Sites	216
8.1.3	Sequencing Chromatograms of Primary Lung Tumours that Exhibited a Change in Methylation of IR5 Compared to Matched Normal Lung Tissue	217
8.1.4	Sequencing Chromatograms of Point Mutations Created Within and Downstream of the PU.1 Binding Motif	218
8.1.5	Sequencing chromatogram of PU.1 cDNA Sub-cloned into pcDNA4 His/Max TOPO Vector	220
8.1.6	Sequencing Chromatograms of Point Mutations Created Within the putative Hypoxic Response Elements within the <i>LIMD1</i> Promoter	221
Chapter 9 References		223

Chapter 1 Introduction

1.1 Thesis Overview

This thesis focuses on advancing our knowledge and understanding of the physiological control and intracellular role of the tumour suppressor protein LIM domain containing 1 (LIMD1). *In vivo*, loss of LIMD1 protein expression has been demonstrated in a variety of cancers; however, the reasons for this loss could not be fully explained by genetic alterations. Furthermore, the precise mechanism of control of *LIMD1* expression at a transcriptional level was unknown, and whether disruption of this regulation could contribute to loss of protein expression. Also, mechanistically, little is known about how LIMD1 exerts its tumour suppressive effects.

To address these questions, each results chapter presents experimental findings that address three areas of distinct LIMD1 biology; epigenetic silencing of *LIMD1*, transcriptional control of *LIMD1* and the role of LIMD1 in regulating the hypoxic response.

The first two results chapters focus upon transcriptional regulation of LIMD1 and correlate these findings with loss of LIMD1 protein expression in cancer. In the first results chapter, investigations centre on the *LIMD1* promoter, where LIMD1 expressing and non-expressing cell lines along with a cohort of human lung tumour and matched normal tissue are used to investigate epigenetic silencing of LIMD1. Following identification of a region critical for transcription within the *LIMD1* promoter, the second results chapter focuses upon this region and identifies the transcription factor PU.1 as a major transcriptional activator of *LIMD1* gene transcription. In the final results chapter, following analysis of transcription factor binding motifs, a functional hypoxic response element within the *LIMD1* promoter is identified and validated. This is then integrated with investigations into the molecular role that LIMD1 has in regulation of the hypoxic response post transcriptionally, and the possible discovery of a negative regulatory feedback loop for hypoxic regulation is presented.

Therefore the background to these distinct, yet often overlapping areas of biochemistry will be introduced.

1.2 Genetic and Epigenetic Alterations are the Underlying Cause of Cancer

All multicellular organisms are somatically mosaic, which is defined as 'multiple populations of cells with distinct genotypic expression in one individual, whose developmental lineages trace back to a single fertilised egg.' (De, 2011). The differences in genotypic expression within the same individual are due to a combination of factors, including erroneous DNA replication or repair mechanisms, transposable elements, translocations, recombinations, chromosomal loss or gains, epigenetic alterations, carcinogens, UV light and nicotine (De, 2011).

When a mutation is introduced into genomic DNA, there can be different consequences depending upon the genetic location. Mutations that do not affect the expression or product of either a protein coding or non-protein coding (e.g. microRNAs, non-coding RNAs) gene, or is part of the true 'junk' DNA (i.e. is not associated with either a coding or non-coding gene or type of RNA) will not exert any detrimental effects on the cell and go unperturbed. However, a mutation that does affect gene expression or the protein/RNA product could have damaging consequences, and the larger the mutation (e.g. chromosomal translocations, amplifications, deletions or loss of heterozygosity) the greater the chance of one or more genes being affected.

Proto-oncogenes are genes that stimulate proliferation, and include both protein coding genes and non translated RNAs. A mutation within one allele of a proto-oncogene, which results in a positive activating phenotype, can cause it to become oncogenic and contribute to cellular transformation. Therefore these mutations tend to be dominant. Conversely, mutations within tumour suppressor genes that have a negative effect on their expression or activity are recessive as long as there is still one functional allele (Wijnhoven et al., 2001), a hypothesis originally put forward by Knudson (Knudson, Jr., 1971) It is therefore mutations of this class within (proto) oncogenes and tumour suppressors that can lead to de-regulated cellular proliferation and ultimately cancerous transformation.

Chromosomal deletions have been described as a common occurrence in a variety of tumours since the early 20th century, with all 23 chromosomes exhibiting chromosomal abnormalities in solid tumours/neoplasms and haematological malignancies (Mitelman et al., 1997). One of the most common universal chromosomal alterations in human solid tumours occurs on the short arm of chromosome 3; within 3p, homozygous deletions and loss of

heterozygosity are characterised early events in lung, breast, head and neck, gastrointestinal, cervical and kidney cancers (Zabarovsky et al., 2002; Hesson et al., 2007), with losses occurring in up to 100% of small cell lung cancers (SCLC) (Angeloni, 2007).

1.3 Chromosome 3 Deletions in Cancer

Loss of heterozygosity and cytogenetic analysis has shown the chromosomal region of 3p21-22 to be the most frequently deleted in all lung tumours (Kok et al., 1994; Murata et al., 1994; Zabarovsky et al., 2002). This was identified through the use of elimination assays. Human chromosome 3- A9 mouse fibrosarcoma microcell hybrids were inoculated into severely combined immunodeficient (SCID) mice and any resultant tumours which grew in the SCID mice were examined for chromosome 3 deletions, which would implicate the presence of tumour suppressive genes. These investigations identified regions of 3p (but not 3q) that were frequently eliminated in the resultant tumours, most specifically 3p21.3-p22 (Kholodnyuk et al., 2002; Imreh et al., 1997). This frequently deleted region was named the chromosome 3 commonly eliminated region (C3CER1; also sometimes referred to as CER). A transcriptional map compiled by Kiss *et al* following elimination tests and PAC sequencing characterised C3CER1 as spanning ~1.4Mb and containing 19 genes and 3 pseudogenes (Kiss et al., 2002) (Figure 1.1). Kost-Alimova *et al* more recently updated the transcriptional map of C3CER1 to span ~2.4Mb (from Mb 43.32-45.74) and contain 32 genes (Kost-Alimova and Imreh, 2007).

Loss of heterozygosity analysis of C3CER1 in 576 tumours revealed deletions in 70-94% of nine tumour types investigated (breast, gastric, colorectal, lung, endometrial, ovarian, testicular, renal and thyroid) with soft tissue sarcomas exhibiting lower deletions of 40%. These C3CER1 deletions were greater than that of other commonly eliminated regions of chromosome 3 (3p14.2 and 3p25.3) (Petursdottir et al., 2004).

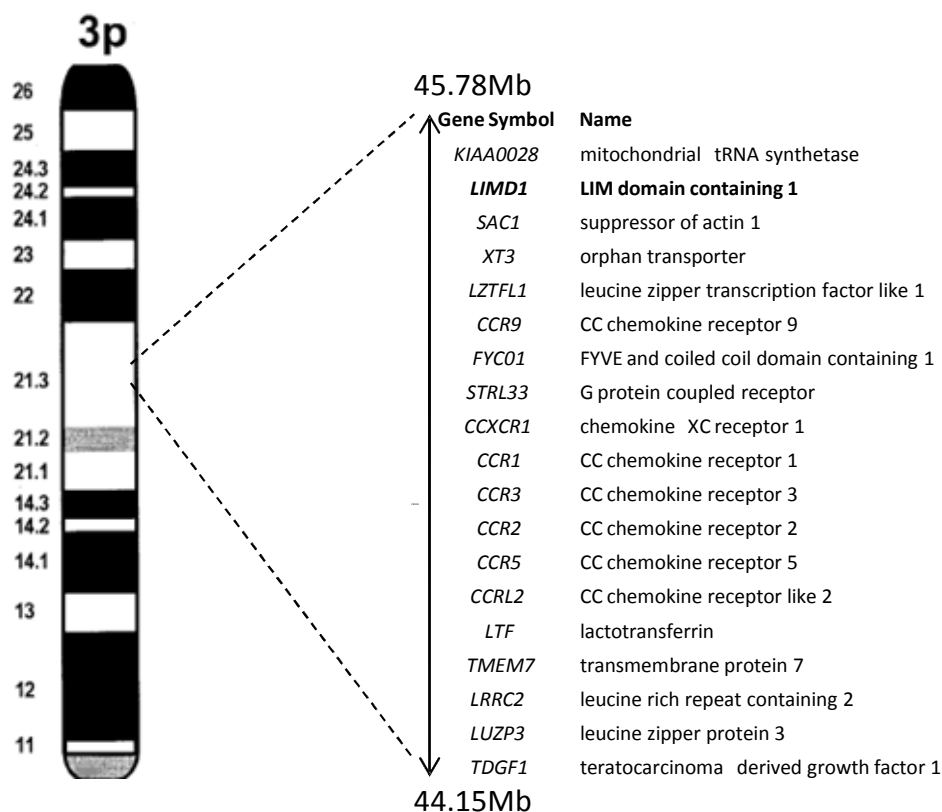


Figure 1.1: Gene map of the chromosome 3 commonly eliminated region 1 (C3CER1). C3CER1 spans 1.4Mb within 3p21.3 and contains a total of 19 genes, including 7 chemokine receptors. Chromosomal deletions and LOH of this region have been reported in up to 94% of solid tumours (Kost-Alimova and Imreh, 2007).

As C3CER1 deletions are frequently found in cancers, this is highly indicative that these genes may possess tumour suppressive functions, as their loss is found within with a transformed/tumour cell. The genes that are in close proximity to *LIMD1* within 3p21.3 have been shown to possess one or more tumour suppressive functions. *LTF* has been reported to be down-regulated in nasopharyngeal (NP) carcinomas, and when re-expressed causes a blockage of cell cycle progression and resultant cell growth inhibition (Zhang et al., 2011a). Furthermore, *LTF* expression blocks infection of the carcinogenic Epstein-Barr virus in primary B lymphocytes and NP epithelial cells, thus demonstrating another tumour suppressive action (Zheng et al., 2012). *LZTFL1* has little published function; however it has been demonstrated to be down-regulated in gastric cancers, with over-expression inhibiting anchorage independent growth and tumour cell survival, possibly through promoting the stabilisation of E-cadherin mediated cell junctions and regulation of ciliary trafficking of signalling proteins (Wei et al., 2010; Seo et al., 2011). *TMEM7* is down-regulated in

hepatocellular carcinomas, and like with the other C3CER1 genes described, ectopic expression reduced tumour cell growth and reduced tumour formation in nude mice (Zhou et al., 2007).

As will be further described later for the published expression profiles and molecular functions of LIMD1, there is clear molecular evidence that it also is a tumour suppressor protein. For instance, LIMD1 inhibits transcription of E2F responsive genes, both dependently and independently of the well characterised pRb tumour suppressor protein (Sharp et al., 2004). This subsequently results in inhibition of cell cycle progression, a classical feature of a tumour suppressor. Furthermore, as LIMD1 is able to do this independently of pRb, this alone attributes it to being a tumour suppressor protein. The tumour suppressive functions of LIMD1 are further demonstrated through *Limd1* gene knockout mice, which exhibit increased size and numbers of lung tumours, as well as decreased survival rates compared to control *Limd1* expressing mice (Sharp et al., 2008). Furthermore, as a critical component of miRNA mediated gene silencing (James et al., 2010), a process which is well characterised as being de-regulated in cancer and disease (Naoghare et al., 2011), it could be postulated that LIMD1 loss, like that of other miRNA pathway proteins such as AGO2 and Dicer, would contribute to the transforming properties of de-regulated miRNA silencing.

1.4 LIM Domain Containing Proteins

The protein LIM domain was initially identified within the MEC-3 protein from *C. elegans* as a protein that contained a characterised DNA binding homeodomain along with a novel cys-his domain (Way and Chalfie, 1988). The first homology of this domain was identified following identification and cloning of the rat gene *Isl1* (Karlsson et al., 1990) and the *C. elegans* gene *lin-11* (Freyd et al., 1990). As such the domain was named a LIM domain after these three proteins (*lin-11*, *Isl1* and *MEC3*). The LIM domain within *lin-11* was initially reported as being a metallodomain being able to bind both iron and zinc (Li et al., 1991), however this was superseded by Michelsen *et al* who confirmed LIM domains are double zinc fingers, tetrahedrally binding two zinc ions (Michelsen et al., 1993). The first solution structure of a LIM domain within the protein CRP1 was published in 1994 (Perez-Alvarado et al., 1994).

A LIM domain has the broad consensus sequence $C(X)_2C(X)_{16-23}H/C(X)_{2/4}C/H/E(X)_2C(X)_2C(X)_{14-21}C/H(X)_{2/1/3}(C/H/D)X$, with 8 conserved cysteine and histidine residues co-ordinating 2 zinc ions (Figure 1.2) (Kadmas and Beckerle, 2004). Initially it was presumed that LIM domains would solely participate in DNA binding; the first identified LIM domain containing protein MEC-3 contained a homeodomain, which participates in DNA binding and other characterised transcription factors interact with DNA through zinc finger motifs, for example the GATA family of transcription factors. However, this has since been superseded by the identification of non DNA binding LIM proteins (Scott et al., 1989; Kadmas and Beckerle, 2004).

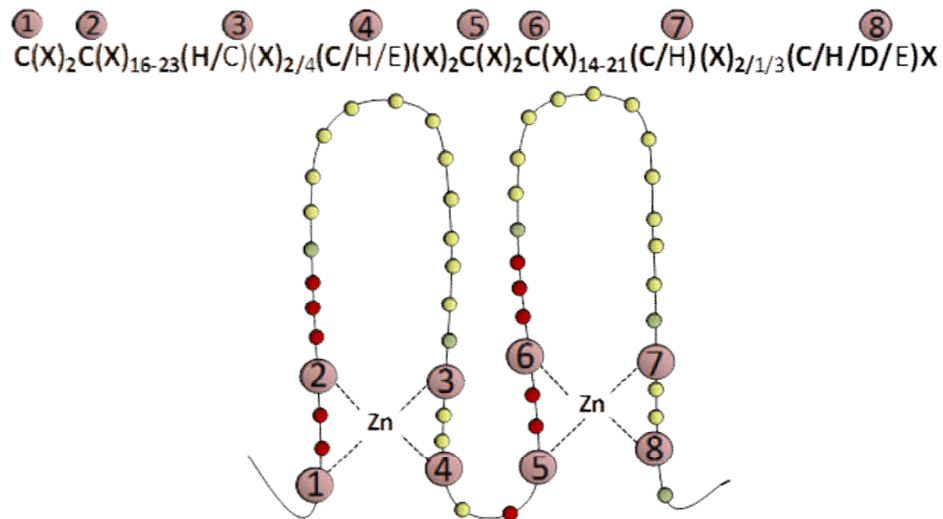


Figure 1.2: Schematic representation of a protein LIM domain. A protein LIM domain has the consensus $C(X)_2C(X)_{16-23}H/C(X)_{2/4}C/H/E(X)_2C(X)_2C(X)_{14-21}C/H(X)_{2/1/3}(C/H/D)X$. 8 conserved cysteine and histidine residues co-ordinate 2 zinc ions to form a double zinc finger that is subsequently able to facilitate protein-protein interactions.

LIM domain containing proteins can be characterised into 4 groups (Kadmas and Beckerle, 2004; Dawid et al., 1998). Group 1 contains LIM homeodomain and nuclear LIM-domain only proteins, group 2 contains proteins that are almost solely comprised of LIM domains and can shuttle between the cytoplasm and nucleus, group 3 contains proteins with C-terminal LIM domains and other protein-protein binding domains, and group 4 which contain LIM domains along with a catalytic kinase or mono-oxygenase domain. LIMD1 belongs to the Zyxin family of LIM domain containing proteins, which belongs to Group 3.

1.5 The Zyxin Family of LIM Domain Containing Proteins

The zyxin family of LIM domain containing proteins is comprised of Zyxin, Trip6, LPP, LIMD1, Ajuba, WTIP and migfilin (Figure 1.3A). Phylogenetically, the family can be sub-divided into the Ajuba sub-family (LIMD1, Ajuba and WTIP) and the Zyxin sub-family (Zyxin, Trip6, LPP and migfilin) (Figure 1.3B), and this correlates with their differing functional roles; the Zyxin family are primarily located at sites of cell adhesion and participate in cytoskeletal arrangements, whereas the Ajuba family are identified as being located more in cytoplasmic vesicles and more recently to participate in microRNA (miRNA) mediated gene silencing (James et al., 2010) and negative regulation of the hypoxic response (Foxler et al 2012, Nature Cell Biology, in press 2012).

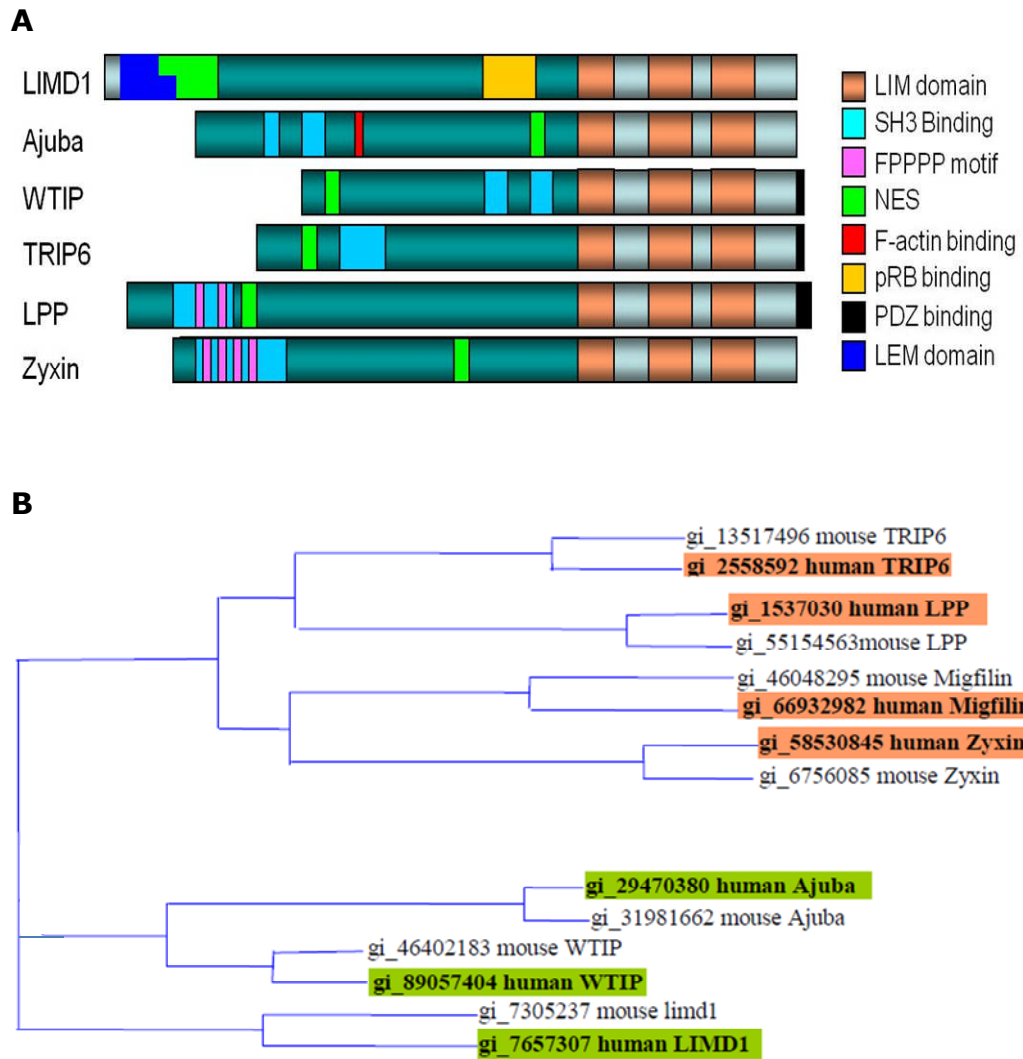


Figure 1.3: The Zyxin family of LIM proteins. (A) Schematic diagram of the Zyxin family of proteins, composed of LIMD1, Ajuba, WTIP, LPP, Trip6, Zyxin and Migfillin, all of which commonly share three tandem C-terminal LIM domains. (B) The Zyxin family can then be phylogenetically sub-divided into the Zyxin (orange) and Ajuba (green) subfamilies, which are shown along with their mouse homologues and gi (GenBank) identification numbers that link to the proteins amino acid and nucleotide sequence.

1.6 LIMD1

1.6.1 Identification of LIMD1

Using an elimination test assay in severe combined immunodeficiency (SCID) mice, the human chromosomal 3p21.3 region was identified as being frequently deleted during malignant growth and as such was named the chromosome 3 commonly eliminated region 1 (C3CER1) (Kholodnyuk et al., 1997). Utilising a one megabase PAC contig that covered C3CER1 (Yang et al., 1999), LIMD1 was first characterised (along with its mouse homologue) in 1999 (Kiss et al., 1999) and was named LIMD1 following a BLAST search which revealed high homology with other LIM containing proteins (LIM Domain containing 1).

Since the identification of LIMD1 in 1999, which occurred prior to completion of sequencing of the human genome, changes in expression in lung, breast and head and neck carcinomas have been identified. However, relatively little is known about the mechanism of action and function of LIMD1 within the cell, and how loss of LIMD1 may promote cellular transformation.

1.6.2 LIMD1 in Lung Cancer

In normal lung tissue LIMD1 is expressed in bronchiolar epithelia, distal alveolar epithelia, alveolar endothelia, inflammatory and stromal cells (Sharp et al., 2008). Tissue microarray data from 185 human lung tumours identified 80% of tumours to have reduced LIMD1 expression compared to a normal control, which supported a previous smaller study where 83% of human lung cancer cell lines had reduced LIMD1 expression (Sharp et al., 2004; Sharp et al., 2008).

The tumour suppressive properties of LIMD1 expression in lung tumours have been validated *in vivo*. *Limd1*^{-/-} mice develop both a higher number of lung tumours, and greater volume tumours when exposed to the chemical lung carcinogen urethane when compared to wild type mice (Sharp et al., 2008). K-Ras is a proto-oncogene that is activated and mutated (to become oncogenic) in up to 25% of all human cancers, the effect of which is increased downstream cell signalling, proliferation and cancerous transformation (Monticone et al., 2008; Tuveson et al., 2004). When *LIMD1*^{-/-} mice were bred with oncogenic *K-Ras*^{G12D} expressing mice, *Limd1* null mice developed more and larger volume of tumours when compared to wild type controls. After 12 months *K-Ras*^{G12D}/*Limd1*^{-/-} mice exhibited a 90% mortality rate, *K-Ras*^{G12D}/*Limd1*^{+/+} mice only showed a 30% mortality rate further indicating *Limd1* as a critical tumour suppressor, with loss contributing to lung cancer development in mice (Sharp et al., 2008).

There is no evidence that *LIMD1* undergoes any base pair mutations in lung cancers. The *LIMD1* gene contains 8 exons, and sequencing of these along with the intron-exon boundaries in 188 adenocarcinomas did not identify any genetic alterations. However, analysis of 357 matched normal and tumour adenocarcinomas identified 32% of tumours had *LIMD1* gene deletion, which is comparable to other genes in the C3CER1 cluster. The percentage deletion is greater than that for other TSGs implicated in lung cancer including *p53* (22%), *RB1* (8%) and *RASSF1A* (21%) (Sharp et al., 2008) (Figure 1.4). A further 12% of tumours analysed exhibited loss of heterozygosity (LOH) at the *LIMD1* gene locus (Sharp et al., 2008).

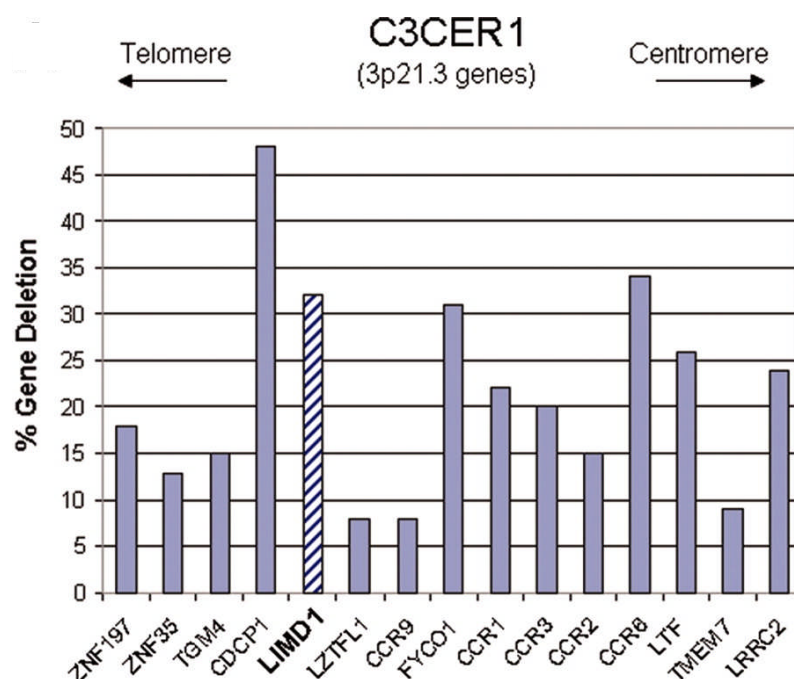


Figure 1.4: Gene deletion of *LIMD1* and surrounding 3p21.3 genes in human lung cancer. Sequencing data from the NHGRI tumour sequencing project lung adenocarcinoma data set of cancer and matched normal tissue was scrutinised and the percentage gene deletion for the indicated C3CER1 genes is displayed in the above histogram. *LIMD1* gene deletion (32%) is comparable to that of the other C3CER1 genes. Taken from (Sharp et al., 2008).

1.6.3 *LIMD1* in Breast Cancer

In normal breast tissue *LIMD1* is highly expressed in the epithelia of terminal duct lobular units but not in surrounding breast stroma or foam cells. Using a Tissue Microarray (TMA), corresponding to 495 different cases of primary invasive breast carcinomas, 98.8% of tumourous cores tested had *LIMD1* expression. However clinicopathological data correlated decreased patient

prognosis/survival with decreased LIMD1 staining; absent or weak staining had a mortality rate of 15.7%, this decreased to 5.3% with strong staining (Spendlove et al., 2008).

There is an indication that LIMD1 mRNA levels are altered in breast tumours; *LIMD1* mRNA has been shown to be both decreased by up to 66% and increased by up to 260% in sporadic breast tumours when compared to a pool of cell line RNA (Huggins and Andrulis, 2008). However, as the control standard was a pool of cell line RNA from a range of tissue types, no definitive conclusions can be drawn about the *LIMD1* mRNA levels in breast cancer as for this tumour samples need to be compared to matched normal breast tissue from the same patient.

E-cadherin is a transmembrane protein that forms homodimers with E-cadherin proteins on adjacent cells to form cell-cell contacts. Loss of E-cadherin expression facilitates the progression from adenoma to invasive carcinoma, and is associated with malignant epithelial metastases (Batlle et al., 2000; Wijnhoven et al., 2000). E-cadherin binds to β -catenin intracellularly, and is thought to sequester it from binding to T-cell factor (TCF) and forming an active transcription factor complex to transduce Wnt signalling pathways; loss of E-cadherin leads to an increase in β -catenin/TCF signalling and increased metastatic potential, whereas over-expression of E-cadherin leads to cell growth arrest (Gottardi et al., 2001). LIMD1 and co-family member Ajuba repress E-cadherin transcription through association with the Slug/Snail transcriptional repressor complex, and as such loss of LIMD1 in breast cancer could contribute to increased invasiveness (Ayyanathan et al., 2007).

1.6.4 LIMD1 in Head and Neck Squamous Cell Carcinomas

Head and neck squamous cell carcinoma is the collective term for cancers of the upper aerodigestive tract, including nasal, oral, pharynx and larynx cancers. These cancers account for up to 40% of all malignancies in the Indian subcontinent and 5% in the Western countries. The stark difference in incidence can be explained in part due to the environmental risk factors of tobacco, betel quid, alcohol and the human papillomavirus, which are more prevalent in the Indian subcontinent (Hogg et al., 2002; Ghosh et al., 2008). Genetic deletions of 9p (70-80% of HNSCC cases), 3p (60-70%), 17p (50-70%), 11q (30%) and 13q (30%) are well characterised events in HNSCC (Perez-Ordenez et al., 2006). Within 3p, a number of smaller regions of common loss including 3p14, 21, 22, 24 and 26 have been identified as early events present in dysplastic lesions (Masayeva et al., 2004; Garnis et al., 2003; Perez-Ordenez et al., 2006).

Ghosh *et al* identified 3 regions of 3p21.3 as having high incidences of gene deletions, which they referred to as D1, D2 and D3 (Figure 1.5). These regions showed deletions of 33-43%, 44-49% and 26-38% respectively (Ghosh *et al.*, 2008), with the *LIMD1* locus found within D1 (Figure 1.5). Microsatellite-based deletion mapping unveiled that in mild dysplastic lesions, D1 and D3 were highly deleted and the percentage deletion remained relatively unchanged during tumour progression, whereas deletion of D2 increased, implicating loss of genes in D1 and D3 contribute to dysplastic lesion development, whereas those in D2 to carcinoma development.

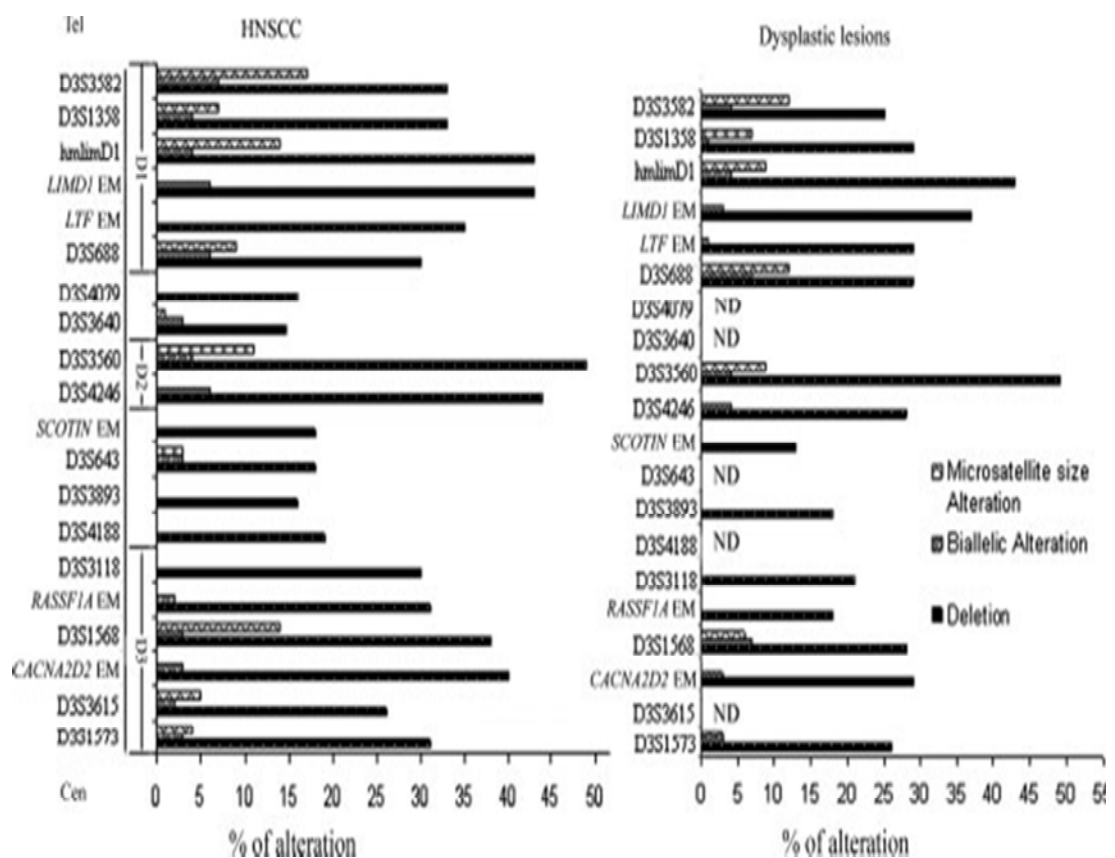


Figure 1.5: Occurrence of 3p21.3 genetic alterations in head and neck squamous cell carcinomas and early dysplastic lesions. The indicated regions D1, D2 and D3 are chromosomal areas identified as areas of high genetic deletions (loss of heterozygosity and homozygous gene deletions). *LIMD1* resides within D1. Adapted from (Ghosh *et al.*, 2008).

The *LIMD1* promoter was highly methylated in both mild dysplastic and HNSCC cases (59-69%), with other genes at the same locus, *LTF*, *CACNA2D2* and *RASSF1A*, exhibiting lower levels of methylation of 49-52%, 42-44% and 17-21% respectively. However in corresponding normal tissue, there was also

promoter methylation of *LIMD1*, *LTF* and *CACNA2D2* showing an incidence of 10%, 5% and 6% respectively. This could be an indication that epigenetic silencing through promoter methylation (discussed later) could be an initial or early event in carcinogenesis. Deletion and methylation of *LIMD1* (50%) did not significantly change through progression from mild dysplasia to carcinoma, contrary to *LTF*, *CDC25A* and *CACNA2D2*, which all significantly increased. This again implied *LIMD1* is involved with initiation of transformation, rather than tumour progression in HNSCC.

LIMD1 mRNA is reduced in HNSCC by a mean of 53.2% in tumour compared to matched normal tissue; for reference in the same study the highest reduction was seen with *LTF* (67.6%), and the lowest of only 0.58% for *SCOTIN* and these can be significantly correlated to the presence of any genetic alterations of either the gene or promoter (Ghosh et al., 2008).

A screen of exons 1 and 5 of *LIMD1* in 83 primary head and neck lesions revealed 40% contained at least one of six novel mutations within exon 1 (two of which caused amino acid substitutions, two which didn't and a further two caused a frame shift mutation due to a single base deletion) or at the intron 4-exon 5 splice junction (Ghosh et al., 2010). Mutation of *LIMD1* however was less frequent in dysplastic lesions than in Stage I and II or III and IV tumours, further indicating methylation and genetic deletions are early events in tumorigenesis. Furthermore, *LIMD1* mRNA expression was decreased more significantly than *pRB* mRNA expression in tumour samples when normalised to their matched normal tissue (Ghosh et al., 2010).

1.6.5 LIMD1 is involved in multiple Intracellular Signalling Pathways

1.6.6 LIMD1 interacts with pRb and is a Repressor of E2F Driven Transcription

In 1971 Alfred Knudson first hypothesised that retinoblastomas in children were caused by two mutational events, one that was either inherited or sporadic, followed by an additional sporadic event (Knudson, Jr., 1971). The esterase D enzyme had previously been mapped to the chromosomal region 13q14, and a reduction in enzyme activity of about half was observed in some patients who had suffered from a retinoblastoma, and this reduction in activity correlated with loss of one allele due to chromosomal deletions (Sparkes and Sparkes, 1983). A proportion of retinoblastoma sufferers were found to have chromosomal

deletions at the same broad genetic locus 13q14, which implicated this region as containing a gene or genes responsible for retinoblastoma growth (Sparkes et al., 1983). Identification of a patient who had 50% esterase D activity, no chromosomal deletion at the broad 13q14 region but still suffered from a retinoblastoma (Benedict et al., 1983) along with further finer chromosomal mapping, identification of reduced mRNA and chromosomal alterations in retinoblastomas identified a retinoblastoma susceptibility (RB) gene at 13q14.2 (Lee et al., 1987).

pRB binds to the E2F family of transcription factors, which regulate the transcription of multiple genes needed for progression through the G1 and S phase of the cell cycle and for DNA metabolism. Upon binding, pRB turns E2F from a positive regulator of transcription to a negative regulator, thus acting as a negative regulator of cell cycle progression (Grana et al., 1998; Harrington et al., 1998).

LIMD1 binds to pRB (Sharp et al., 2004), identified initially through a yeast two-hybrid screen and confirmed by *in vivo* co-immunoprecipitation of endogenous LIMD1 with exogenous pRB. pRB's role in repressing E2F driven transcription is well characterised, and LIMD1 was found to augment the same in a concentration dependent manner. LIMD1 also repressed E2F driven transcription in the absence of Rb, and introduction of LIMD1 into the non-LIMD1 expressing MDA-MB435 cell line caused the reduced expression of 85% of E2F responsive genes, implicating a likely role of LIMD1 as a general tumour suppressor. Introduction of LIMD1 into MDA-MB435 cells inhibited proliferation, and ectopic expression in transformed A549 and HEK293 cell lines decreased colony formation by 80%. Injection of A549 cells transduced with lentiviral-HA-LIMD1 into tail veins of nude mice gave a significant reduction in lung metastases incidence compared to lentiviral-HA-vector only (Sharp et al., 2004). This was the first published study to identify a possible tumour suppressive function of LIMD1.

1.6.7 LIMD1 is a Critical Component of miRNA Silencing

MicroRNAs (miRNA) are short ~22nt non coding RNA molecules that are responsible for the post-transcriptional silencing of many genes involved in normal cellular differentiation, development and proliferation, with miRNA expression frequently deregulated in a variety of cancers, briefly reviewed in (Deng et al., 2008). The first miRNA to be discovered was in *C. elegans* in 1993,

a short *lin-4* transcript that did not code for a protein but was complementary to a sequence in the 3' untranslated region (UTR) of *lin-4* mRNA (Lee et al., 1993). miRNA silencing is a major form of post-transcriptional gene silencing.

Most miRNA genes are transcribed by RNA polymerase II and like most mRNAs contain a 5' 7-methyl guanylate cap and a 3' poly(A) tail (Lee et al., 2004). This primary transcript is known as a pri-miRNA and may be several kb in length and contain one or more stem loop structures (Figure 1.6A). miRNA transcripts can also originate from the introns of mRNAs following splicing, with as many as 40% of miRNAs originating this way (Davis and Hata, 2010) (Figure 1.6C). The nuclear protein DGCR8 then recognises the region between the single stranded RNA loop and double stranded RNA stem and guides the RNase III enzyme Drosha to cleave the RNA approximately 11 base pairs from the single strand-double strand RNA junction (Denli et al., 2004; Han et al., 2004) to create a 60-70 nucleotide hair pin RNA with a 3' 2 nucleotide overhang, known as a precursor miRNA (pre-miRNA) (Lee et al., 2003)(Figure 1.6B). The pre-miRNA is then exported out of the nucleus into the cytoplasm by Exportin 5 and the cofactor Ran-GTP (Yi et al., 2003) (Figure 1.6D). In the cytoplasm, the RNase III enzyme Dicer, along with TAR RNA binding protein (TRBP) and protein kinase R activating protein (PACT) bind to the pre-miRNA in a RNA induced silencing complex (RISC) loading complex (RLC) and cleaves it into a mature double strand miRNA, again with a 3' two nucleotide overhang (Zhang et al., 2004a) (Figure 1.6E). The RLC is then loaded into RISC, with TRBP and the mature miRNA binding to AGO2 (Chendrimada et al., 2005) (Figure 1.6F). The less thermodynamically stable strand of the double strand RNA, the guide strand, is unwound and presented for mRNA target recognition by one of a family of Argonaute proteins, and the more stable strand, the passenger strand, is degraded (Figure 1.6G). Binding of the miRNA to its target mRNA (usually in the 3' UTR) then results in translational repression and/or degradation of the mRNA (Filipowicz et al., 2008).

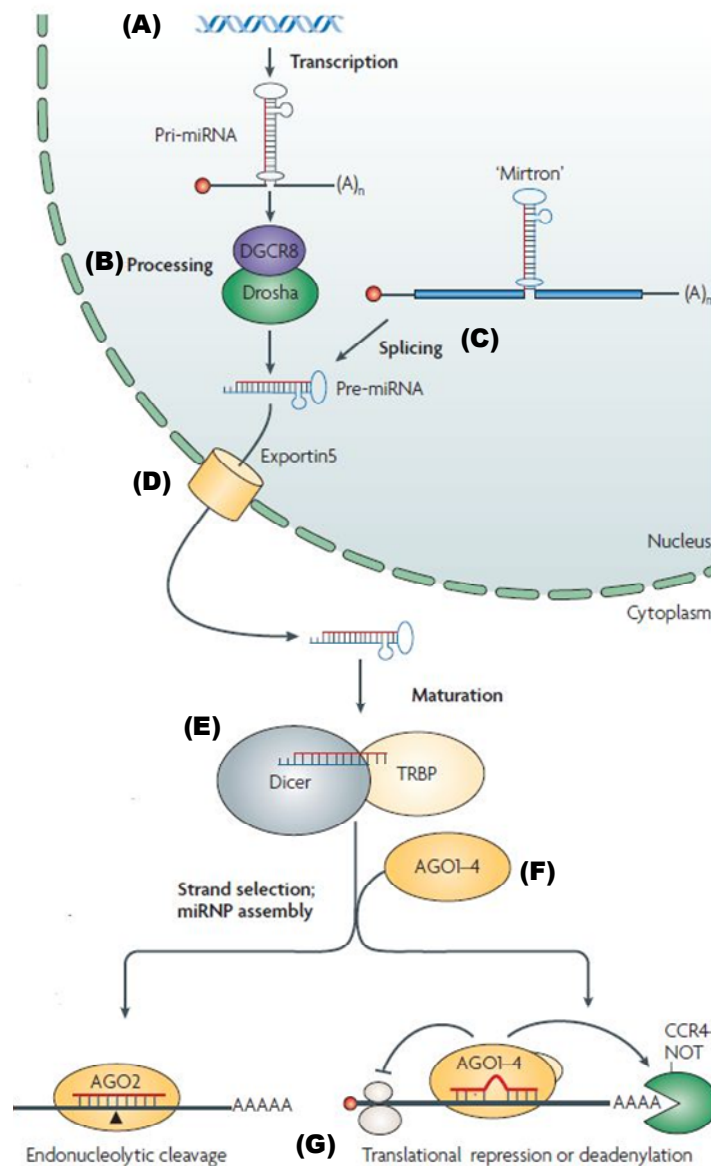


Figure 1.6: The miRNA biogenesis pathway. (A) miRNA genes are transcribed from miRNA coding genes within the genomic DNA by RNA polymerase II to produce pri-miRNA transcripts containing one or more stem-loop structures. (B) The stem-loops are recognised and cleaved by a Drosha-DGCR8 complex to form a pre-miRNA. (C) Splicing of introns from mRNA can also produce pre-miRNA transcripts. (D) The pre-miRNA is shuttled out of the nucleus by Exportin5/Ran-GTP into the cytoplasm where (E) it is further cleaved by Dicer in the RNA induced silencing (RISC) loading complex (RLC) to form a mature double stranded miRNA. (F) This is then loaded into an argonaute protein in the RISC, where it is unwound by an argonaute protein to yield a single stranded miRNA that is (G) capable of binding a target mRNA causing translational repression and or cleavage. Adapted from (Filipowicz et al., 2008).

When a target mRNA is recognised and bound into the RISC complex, it is translationally repressed either through being degraded or stored in GW182/P-bodies. P-bodies were first characterised as being cytoplasmic foci containing the mRNA decapping enzyme DCP2 and the 5'-3' endonuclease XRN1 as well as other 5'-3' mRNA decay associated proteins including LSM and RCK, and more recently also GW182 (Cougot et al., 2004; Eystathioy et al., 2002). P-bodies are sites of mRNA storage and or degradation, however they are a consequence of RNA induced silencing rather than being a requirement for this pathway; depletion of the RNA silencing machinery, including AGO2, Dicer, Drosha and GW182 or inhibition of early steps of degradation like deadenylation causes a decrease in number of P-bodies, whereas inhibition of XRN1 progression along mRNAs causes an increase in size and number of P-bodies. Furthermore miRNA mediated silencing also occurs in the absence of microscopically visible P-bodies (Eulalio et al., 2007; Eulalio et al., 2008).

LIMD1 colocalizes with and co-immunoprecipitates the P-body and RNAi associated proteins RCK, DCP2 and AGO2. Endogenous depletion of LIMD1 by siRNA causes a decrease in miRNA, but not siRNA, mediated silencing, with over-expression increasing silencing potency. This has been demonstrated using both a luciferase reporter with a synthetic *let-7a* miRNA site in its 3' UTR, and a luciferase fused to the full length endogenous 3' UTR of the HMGA2 (high mobility group AT hook 2) gene (James et al., 2010). With respect to HMGA2 repression, inhibition of *let-7* in a LIMD1 depleted background did not give any further increases in HMGA2 protein expression, demonstrating that LIMD1 activity was probably not independent from the *let-7* pathway. Furthermore LIMD1 depletion did not affect *HMGA2* mRNA levels demonstrating the increase in HMGA2 protein following LIMD1 loss was due to release of the mRNA from translational repression.

1.6.8 LIMD1 is a Regulator of Osteoblast and Osteoclast Function

Bone remodelling is part of normal bone homeostasis with bone formation and bone resorption in equilibrium. These two processes are carried out by osteoblast and osteoclast cells respectively, with any disturbances or deregulation leading to diseases such as osteoporosis and Paget disease of the bone (Cundy and Bolland, 2008; Raisz, 2005).

Osteoclasts are generated from bone marrow derived macrophages (BMDM) (Figure 1.7). Following stimulation by macrophage colony stimulating factor (M-

CSF), preosteoclasts are formed, which further divide and then fuse following stimulation by receptor activator of NF- κ B ligand (RANK-L) to form a fused polykaryon. Further RANK-L stimulation then results in a mature activated multinucleated osteoclast (Boyle et al., 2003; Eriksen, 2010). Osteoclast differentiation is negatively regulated by the RANK antagonist OPG, which competes for binding to RANK-L, thus inhibiting it from binding to RANK and promoting osteoclast development (Boyle et al., 2003; Raisz, 2005; Eriksen, 2010).

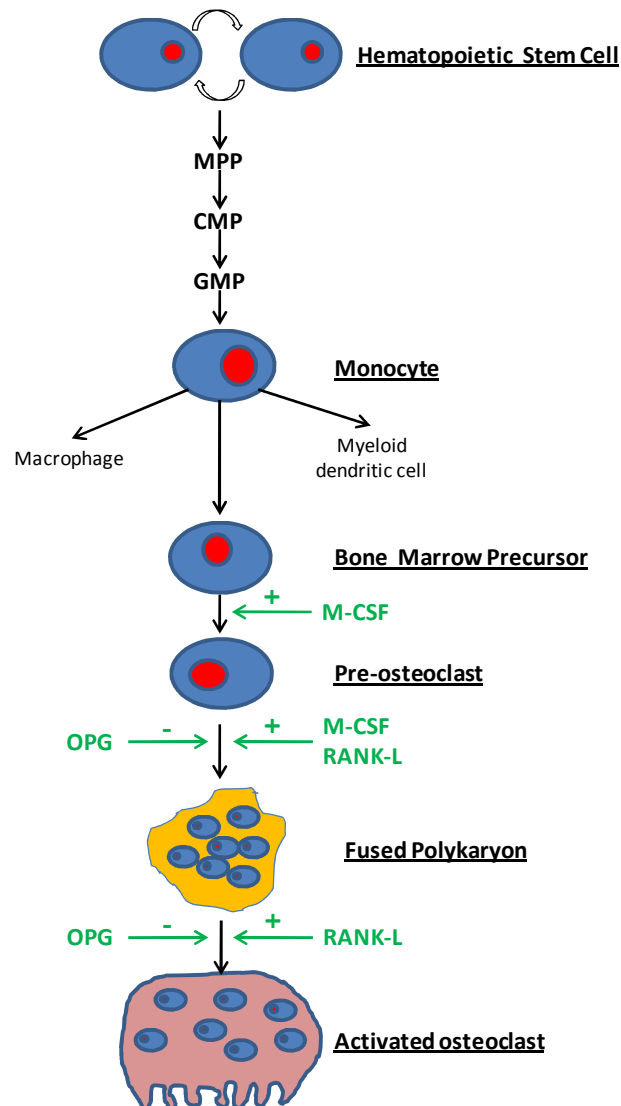


Figure 1.7: Schematic diagram of osteoclast differentiation from hematopoietic stem cells. Osteoclasts are originally derived from hematopoietic stem cells. Monocytes differentiate into bone marrow precursor cells, which upon stimulation by M-CSF further differentiate into pre-osteoclasts. Further stimulation by M-CSF and RANK-L facilitates formation of multi-nucleated fused polykaryons, which ultimately form activated osteoclasts following RANK-L stimulation. OPG is a RANK antagonist and competes for binding with RANK-L, meaning it is a negative regulator/inhibitor of osteoclast development. MPP, multipotent progenitor cell; CMP, common myeloid progenitor cell; GMP, granulocyte-macrophage progenitor; M-CSF, macrophage-colony stimulating factor; RANK-L, receptor activator of NF- κ B ligand; OPG, osteoprotegerin.

When RANK-L binds to RANK, the receptor trimerizes, which facilitates association with TNF receptor associated factors (TRAFs), in particular TRAF6. TRAF6 then binds as part of a complex to atypical protein kinase C and p62 in a multiprotein complex referred to as the sequestosome and this is the start of a signalling cascade which ultimately leads to the activation of the transcription factors Activator Protein 1 (AP-1) and NF- κ B, which activate genes critical for osteoclast development as well as the I κ B kinases (IKKs) and mitogen activated protein kinases (MAPKs) (Boyle et al., 2003; Feng et al., 2007).

LIMD1 binds to both p62 and Traf6 (Feng and Longmore, 2005; Feng et al., 2007). During RANK-L osteoclast differentiation, and concurrent with Traf6 levels, Limd1 levels are significantly induced and positively regulate the activation of AP-1 through TRAF6 (Figure 1.8). *Limd1*^{-/-} mice show normal bone density and osteoclast numbers when compared to wild type mice, however the null mice showed a significantly reduced response to stimulation with RANK-L, but this effect was rescued with reintroduction of Limd1.

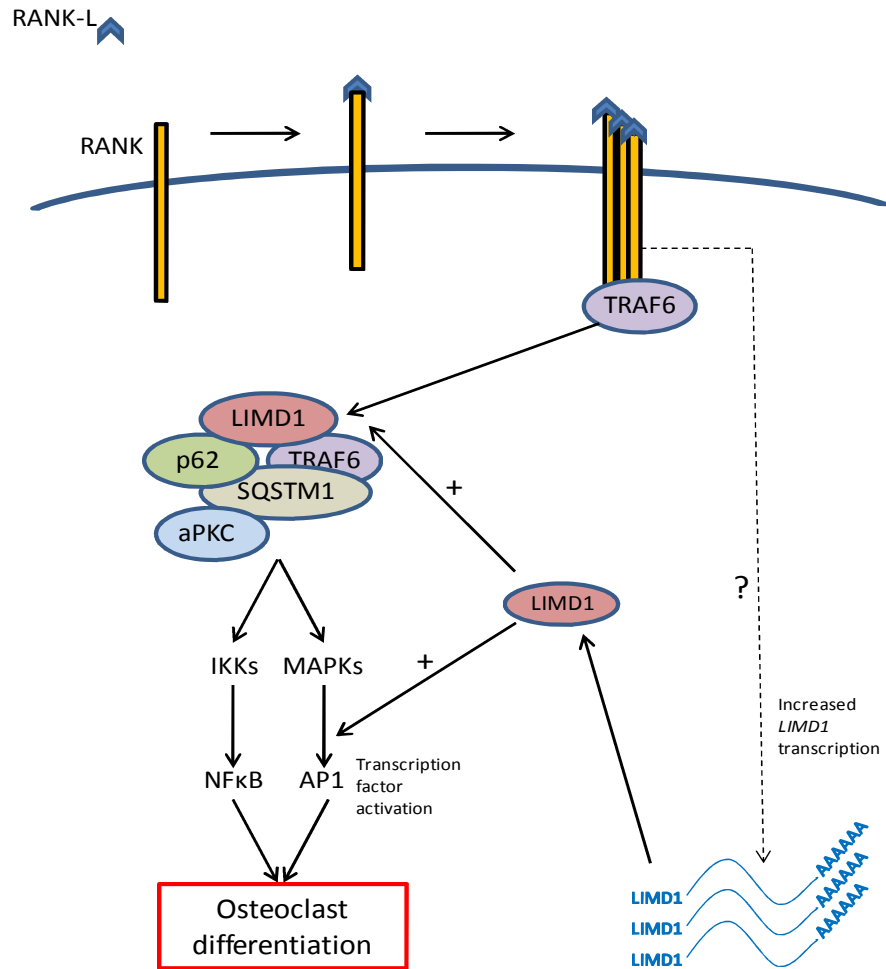


Figure 1.8: RANK-L mediated osteoclast differentiation. RANK-L binding to its receptor, RANK, causes trimerisation of the receptor. This facilitates association with TRAF proteins, especially TRAF6. TRAF6 then facilitates the formation of the sequestosome, a multiprotein complex including p62 and atypical protein kinase C (aPKC). The sequestosome, through a signalling cascade, causes the activation of the transcription factors NFκB and AP1, which are critical for osteoclast differentiation. Trimerisation of RANK also correlates with an increase in LIMD1 mRNA and protein levels. LIMD1 has been shown to bind TRAF6 and p62, and positively regulate AP1 activation.

In summary, LIMD1 expression is down regulated in significant proportions of lung, breast and head and neck squamous cell carcinomas. In lung cancer, down-regulation has been attributed to both homozygous and heterozygous chromosomal gene deletions, with epigenetic silencing also evident in breast and HNSCC (Sharp et al., 2004; Sharp et al., 2008; Spendlove et al., 2008; Huggins and Andrulis, 2008; Ghosh et al., 2008).

Mechanistically, loss of LIMD1 protein expression has not been directly correlated with tumour suppressive activities. LIMD1 interacts with pRb and co-represses E2F driven transcription, which may enhance the function of pRb, and in doing so act as a tumour suppressor in this specific pathway (Sharp et al., 2004). Similarly, LIMD1 is required for microRNA mediated gene silencing, and ablation of expression would deregulate this pathway, a phenomena that is already a well characterised event in cancer development (Karube et al., 2005; Sharp et al., 2008; Melo et al., 2009; Melo et al., 2009; Wu et al., 2010). LIMD1 is also a regulator of osteoclast differentiation and function, and as such LIMD1 loss could contribute to diseases of the bone, including osteoporosis and osteopetrosis (Feng et al., 2007).

1.7 The Ajuba/Zyxin Family of Proteins

The other members of the Ajuba/Zyxin family of LIM domain containing proteins share both similar and discrete functions to LIMD1, but as they are not the focus of this thesis will only be briefly described.

1.7.1 Zyxin

To date zyxin is the most well characterised member of the family originating from its identification as a novel protein at sites of cell-substrate adhesion and cell-cell contacts (Beckerle, 1986; Crawford and Beckerle, 1991). Zyxin has been shown to be important in actin polymerisation (Fradelizi et al., 2001) and assembly of complexes required for cell motility (Drees et al., 1999; Hoffman et al., 2006). In a recent study of cells in a 3D matrix, where focal adhesions are greatly reduced when compared to 2D culture, depletion of zyxin resulted in increased cell motility (Fraley et al., 2010). Zyxin shuttles between the cytoplasm and nucleus and as such may transduce signals from the cell periphery to the nucleus influencing cell dynamics (Nix et al., 2001). In Ewing tumours which have a highly disrupted actin cytoskeleton, zyxin is expressed at very low levels and diffusely through the cytoplasm, but ectopic introduction of zyxin results in organisation of the actin skeleton, coupled with reduced anchorage independent growth and reduced tumour formation when introduced into mice (Amsellem et al., 2005).

1.7.2 LPP

Lipoma preferred partner (LPP) was initially identified as a gene at 3q27-28 that commonly translocated with the HMGIC gene at 12q15 in a major subset of lipomas (Petit et al., 1996). LPP shares 41% homology with zyxin, and like its family member is located at focal adhesions, can shuttle to and from the nucleus (Petit et al., 2000) where it is a co-activator of the ETS transcription factors PEA3 and ER81 (Guo et al., 2006). LPP also binds the actin polymerisation associated proteins VASP and α -actinin (Petit et al., 2000) and is localized to focal adhesions through interaction with the tumour suppressor protein Scrib (Petit et al., 2005).

1.7.3 TRIP6

Thyroid hormone interacting protein 6 (TRIP6) was identified as a binding partner for the thyroid hormone receptor following a yeast 2 hybrid screen (Yi

and Beckerle, 1998). TRIP6 is located on chromosome 7q22, a chromosomal region that is commonly deleted in uterine leiomyomas (benign smooth muscle neoplasms) and malignant myeloid diseases (Yi and Beckerle, 1998). TRIP6 is able to shuttle between focal adhesions and the nucleus, where it is able to transactivate transcription, but is not able to directly bind to DNA (Wang and Gilmore, 2001). Similar to LPP, TRIP6 also binds to Scrib, but this interaction is not what localises TRIP6 to focal adhesions or sites of cell-cell contact (Petit et al., 2005). Petit *et al* briefly discussed unpublished preliminary evidence that LPP could homodimerize as well as heterodimerise with TRIP6 (Petit et al., 2005). TRIP6 interacts with RIP2 following stimulation by IL-1 or TNF, and facilitates NF- κ B activation (Li et al., 2005). More recently, TRIP6 was identified as being able to bind to the scaffold protein MAGI-1b, which in turn recruits the tumour suppressor PTEN to sites of cell-cell contacts where it binds to and stabilises E-cadherin dependent cell contact complexes (Chastre et al., 2009). TRIP6 is over expressed in colon cancers, which could be the reason for their invasiveness as ectopic expression of TRIP6 in epithelial MDCK cells also increased their invasiveness in collagen gel invasiveness assays (Chastre et al., 2009).

1.7.4 Migfilin

Migfilin was the most recently identified member of the Zyxin family. It was identified through a yeast 2 hybrid assay looking at binding partners of the cell-extra cellular matrix adhesion site complex protein Mig 2 (Tu et al., 2003). Mig-2 localises migfilin to these adhesion sites, where it binds to the actin binding protein filamin and influences cell spreading, shape modulation and actin assembly (Tu et al., 2003). Like other Zyxin family members, migfilin binds to VASP and shuttles between the cytosol and nucleus (Akazawa et al., 2004; Wu, 2005). Migfilin is only expressed at very low levels in normal smooth muscle cells. However in leiomyosarcomas (malignant neoplasms composed of cells that exhibit distinct smooth muscle differentiation) migfilin is found to be expressed at much higher levels within the cytoplasm, putatively suggesting a role in it aiding progression of invasiveness within these malignancies (Papachristou et al., 2007). In mice migfilin does not appear to be necessary for development or tissue homeostasis as migfilin null mice developed normally and show no phenotypic differences (Moik et al., 2011). Migfilin also interacts with the cardiac homeobox transcription factor CSX/NKX2-5, where following stimulation by Ca^{2+} migfilin translocates into the nucleus and activates CSX/NKX2-5 target gene transcription and promotes myocardial cell differentiation (Akazawa et al., 2004).

1.7.5 Ajuba

Ajuba was identified in 1999 as a binding partner of the erythropoietin receptor (EPO-R) in a yeast 2 hybrid screen (Goyal et al., 1999). Following serum stimulation ajuba binds the adapter protein Grb2, which transduces signals from membrane receptors to Ras and downstream MAP kinase (Goyal et al., 1999). Furthermore in *Xenopus* oocytes ajuba promotes maturation in a Grb2/MAP kinase dependent manner (Goyal et al., 1999). There is contradictory evidence to the cellular localisation of ajuba; it has been reported to be both absent (Goyal et al., 1999) and present (Kanungo et al., 2000; Marie et al., 2003) from focal adhesions. It contains a nuclear export and localisation signal and as such shuttles between the cytosol and nucleus (Goyal et al., 1999; Kanungo et al., 2000). Ajuba binds to F-actin and α -catenin which localises it to cadherin dependent cell junctions (Marie et al., 2003). Over expression of full length ajuba (or just the pre-LIM region) enhanced proliferation of P19 embryonal cells, whilst LIM domains alone had the converse effect and induced endodermal differentiation in a JNK MAP kinase dependent manner (Kanungo et al., 2000). Ajuba binds the SNAG transcriptional repressor domain within the SNAIL protein, and co-represses transcription by forming a repressional complex within the nucleus. Specifically ajuba contributes to epithelial-mesenchymal transitions (EMT), through co-repressing SNAIL activity which reduces E-cadherin expression, a glycoprotein involved in cell-cell contacts and loss of which is intimately involved in invasiveness of breast cancers (Langer et al., 2008; Ayyanathan et al., 2007). Ajuba is a negative regulator of the Hippo pathway that regulates cancer development and tissue size; ajuba null *Drosophila* tissues have increased apoptosis and reduced proliferation leading to smaller cell/tissue size (Das et al., 2010). More recently ajuba has been shown to be a critical component of microRNA mediated gene silencing, a process involved in cell cycle regulation, homeostasis, disease and cancer progression (James et al., 2010).

1.7.6 WTIP

Wilm's tumour interacting protein (WTIP) was again initially identified in a yeast 2 hybrid screen that was looking for binding partners of the Wilm's tumour protein (WT1), a transcription factor essential for normal nephrogenesis that is mutated in a high proportion of Wilm's tumours (Srichai et al., 2004). WTIP contains a nuclear export signal and is able to shuttle between the cytoplasm and nucleus where it represses WT1 activated transcription (Srichai et al., 2004). WTIP is localised both at cytoplasmic spots (Srichai et al., 2004) and at the cell membrane where it interacts with Ror2, a receptor tyrosine kinase, and represses Wnt induced β -catenin signalling (van Wijk et al., 2009). WTIP is

located at cell adheren junctions in podocytes, however it translocates to the nucleus, via the actin motor protein dyein, following injury and altering actin dynamics and subsequent podocyte shape (effacement) (Rico et al., 2005; van Wijk et al., 2009; Kim et al., 2010a). shRNA mediated silencing of WTIP in podocytes resulted in altered actin dynamics and cell morphology (Kim et al., 2010a). WTIP is also able to homodimerise via it's LIM domains (van Wijk et al., 2009) and like ajuba, is also a critical regulator of microRNA mediated silencing (James et al., 2010).

The Ajuba/Zyxin family therefore have important physiological and tumour suppressive roles. However, the focus of this thesis is the encoded 3p21.3 LIMD1 tumour suppressor gene.

Chromosomal deletions or loss of heterozygosity of a region of genomic DNA that encodes a tumour suppressor gene will cause a complete loss or reduction in expression respectively, and this has been demonstrated with loss of LIMD1 expression in adenocarcinomas (Sharp et al., 2008). However, reduced expression of TSGs cannot always solely be accounted for by chromosomal alterations; where protein loss is observed independent of chromosomal deletions it is indicative that loss of expression could be due to deregulation of gene transcription. This may indeed be the case with LIMD1 as 79% of lung tumours show LIMD1 protein loss, but only 44% show genetic deletions (Sharp et al., 2008).

Therefore to investigate if LIMD1 expression is down-regulated at a transcriptional level, and before describing my investigations into the transcriptional control of *LIMD1* gene expression, it is necessary to describe the basis of regulation of general gene transcription.

1.8 Control of Gene Transcription

In eukaryotes there are 3 different RNA polymerases that transcribe different classes of genes. RNA polymerase I transcribes 18S and 28S RNA (Grummt,

2003); RNA polymerase II transcribes mRNA (Smale and Kadonaga, 2003); and RNA polymerase III transcribes 5S ribosomal RNA, tRNA and other small catalytic RNAs (Schramm and Hernandez, 2002). As RNA polymerase II is the polymerase that transcribes protein coding RNA transcripts, only this polymerase will be focused on.

Transcription of a specific gene requires RNA pol II to bind to genomic DNA 5' to the ATG translation initiation codon, at a region known as the core promoter. A core promoter is defined as 'the minimal stretch of contiguous DNA sequence that is sufficient to direct accurate initiation of transcription by the RNA polII machinery' (Butler and Kadonaga, 2002). Essentially, a core promoter is the minimal consensus that through interactions with transcription factors is able to facilitate transcription. Binding of RNA polII to the core promoter is facilitated by trans-acting general transcription factors (GTFs) that together make up the pre-initiation complex (PIC), and is the culmination of associations between cis-acting transcription factors that bind to proximal promoters, silencers, enhancers or insulators, and chromatin remodelling factors (Baumann et al., 2010).

1.8.1 Features of RNA Polymerase II Promoters

There are 2 types of RNA pol II promoters, ones that contain a TATA box and ones that do not (TATA-less). A TATA box (or Goldberg-Hogness box after its discoverers) is a core sequence of TATAAA that was initially identified as being present 25-30 bp upstream of the transcription start site in almost all RNA pol II transcribed genes examined from mammalian, viral and *Drosophila* protein coding genes (Smale and Kadonaga, 2003; Baumann et al., 2010). However, more recent analysis of 1031 genes by cap analysis of gene expression (CAGE) showed only approximately 32% of genes contained a TATA box within their promoters (Suzuki et al., 2001), with this figure decreasing to as low as 10% in a separate bioinformatic analysis study (Zhu et al., 2008). Further CAGE sequencing methods have revealed over 70% of TATA boxes are located between -33 and -28 from the actual transcriptional start site (TSS), with the majority at positions -31 or -30 (Carninci et al., 2006). The TATA binding protein (TBP) was initially identified as being part of a subunit of the general transcription factor TFIID, and it is this subunit that binds the TATA box, and ultimately recruits RNA pol II (Nakajima et al., 1988; Smale and Kadonaga, 2003; Burley and Roeder, 1996; Greenblatt, 1991).

Another common feature of RNA pol II associated promoters is an initiator element (Inr) that encompasses the actual transcription start site, and is present in up to 85% of promoters (Suzuki et al., 2001). It has the general consensus sequence $Py_2-A-N-A/T-Py_2$, (Py=pyrimidine, N=any base) with transcription commonly initiating from the 'A' (Smale and Kadonaga, 2003; Baumann et al., 2010). Inrs are found in both TATA and TATA-less promoters. When the Inr is located ~30bp from the TATA box, the two elements act synergistically to enhance transcription, however, both can also act independently to initiate transcription with TATA being predominant over Inr (O'Shea-Greenfield and Smale, 1992). When independent of each other TATA initiates transcription ~25bp downstream and Inr initiates at its specific nucleotide within its consensus sequence (Smale and Kadonaga, 2003). The Inr is recognised by a complex of TAF1 and 2, which are part of the complex that includes TBP that form the general transcription factor TFIID (Chalkley and Verrijzer, 1999). *In vitro*, RNA pol II is able to weakly bind to the Inr; the interaction and transcription enhanced through the addition of TFIID, and TFIID is required even in promoters that lack a TATA consensus (Carcamo et al., 1989; Carcamo et al., 1991).

Downstream promoter elements (DPE) are also found in up to 85% of gene promoters. The DPE is found at exactly +28 to +32 relative to the initiating A within the Inr, has the general consensus $A/G_{(+28)}-G-A/T-C/T-G/A/C_{(+32)}$ and is often only found in TATA-less promoters (Kadonaga, 2002; Butler and Kadonaga, 2002). In *Drosophila*, the DPE is roughly found at the same frequency as TATA boxes, however in humans there is no correlation between the presence of a TATA sequence and a DPE (Kutach and Kadonaga, 2000; Gershenson and Ioshikhes, 2005). TFIID, through its TAF6 and 9 subunits, binds the DPE (Burke and Kadonaga, 1997).

The TFIIB recognition element (BRE) is the only other characterised core promoter motif that is bound by a general transcription factor other than TFIID. The BRE consensus sequence is $G/C-G/C-G/A-C-G-C-C$ and is immediately upstream of the TATA (Lagrange et al., 1998). Contradictory observations have been published regarding the function of the BRE. Lagrange et al identified TFIIB binding to the BRE enhanced formation of the transcription initiation complex (Lagrange et al., 1998). However, Evans *et al* observed an inhibitory effect on basal transcription which was reversed by addition of a transcriptional activator, and this observation corroborated with previous studies that identified mutations of the (then uncharacterised) BRE sequence directly upstream of the TATA box

that increased levels of transcription (Evans et al., 2001). It was more recently discovered that there are BREs downstream of the TATA box, with the consensus G/A-T-T/G/A-T/G-G/T-T/G-T/G (Deng and Roberts, 2005). As such the original upstream BRE is referred to as BRE^U and the more recent downstream one as BRE^D. The effect of BRE^D is promoter dependent; it has a positive increase on transcription in promoters that lack a BRE^U but a negative effect on transcription in promoters that also contain a BRE^U (Deng and Roberts, 2006). The two different BREs are bound by different binding domains within TFIIB (Deng and Roberts, 2005).

GC boxes are present in almost all gene promoters (Suzuki et al., 2001). Studies on the DNA tumour Simian virus 40 (SV40) to identify sequences essential for its transcriptional activation identified three 21bp repeats, within which were 6 repeated GC rich repeats of GGGCGG. This gave rise to the GC box general consensus sequence of 5'-G/T-G/A-GGCG-G/T-G/A-G/A-C/T-3', which when present were found to be critical for transcriptional activation (Dynam et al., 1985; Gidoni et al., 1985; Imataka et al., 1992). Further studies revealed that the transcription factor Sp1 binds to these GC boxes and activates transcription (Briggs et al., 1986; Dynam and Tjian, 1983).

The final feature of gene promoters to be described is CpG Islands, which will subsequently be shown to be a critical feature of the *LIMD1* promoter and thus gene expression. These are short DNA sequences approximately 1kb in length that contain a high frequency of 5'-CG-3' dinucleotides, further referred to as CpG, and are associated with up to 100% of all housekeeping genes and approximately 70% of genes in total (Saxonov et al., 2006; Illingworth and Bird, 2009). Promoters of genes that contain one or more CpG Islands often do not contain TATA boxes or DPEs, however they are usually rich in GC boxes (both in 5' and 3' CpG Islands) that harbour multiple Sp1 binding sites (Gardiner-Garden and Frommer, 1987). CpG Islands will be discussed in more detail later on.

The different promoter elements are represented schematically in Figure 1.9.

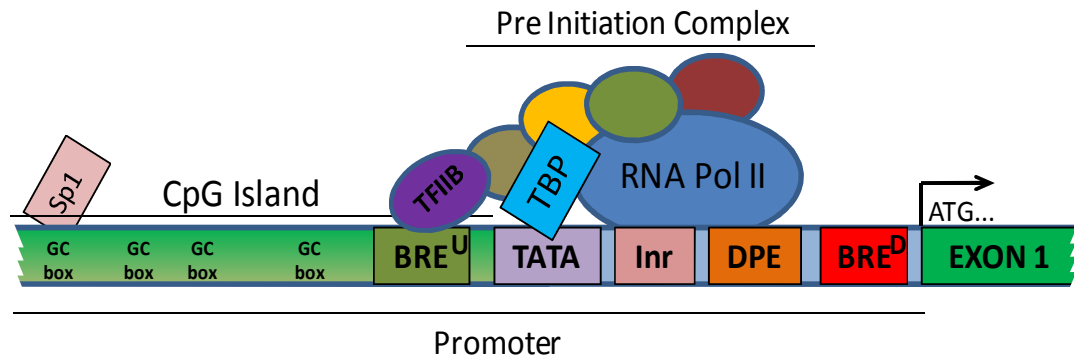


Figure 1.9: Schematic diagram of a RNA Pol II promoter. A typical transcribed gene contains a 5' promoter region that contains elements to facilitate transcription through the binding of transcriptional activators. Up to 70% of all genes contain a CpG Island within their promoter that may harbour multiple GC boxes for Sp1 binding. Some promoters may also contain a TATA box, where the TATA binding protein (TBP) binds or an upstream or downstream TFIIB recognition element (BRE^{U/D}) for binding of TFIIB. Both TBP and TFIIB recruit other general transcription factors and RNA Pol II to form the pre-initiation complex and initiate transcription from within the initiator element (Inr). Often in TATA-less promoters, the presence of a downstream promoter element (DPE) facilitates the recruitment of TFIID and the PIC.

Assembly of the general transcription factors and RNA pol II into a pre-initiation complex onto the DNA is the preceding step to transcription. The presence of TATA boxes and other promoter elements helps guide the transcriptional machinery to the promoter. However, in order for the Pol II basal machinery to bind to the promoter, the DNA needs to be in an accessible open or active conformation.

1.8.2 Active Transcription requires an Open Euchromatin Structure

In its native state DNA is tightly packaged around nucleosomes, which are octomers of histone proteins that has ~146bp of DNA wrapped around. The N terminal tails of Histone2B and H3 protrude through the grooves of the DNA where lysines and argenines interact with the phosphate groups of the DNA to facilitate the packaging (Ruthenburg et al., 2007; Schnitzler, 2008). Post translational modifications to the histone tails alters the affinity of the histones for the DNA, and allows for the DNA to alter between a tightly packaged, transcription factor inaccessible heterochromatin structure, and a more open and accessible euchromatin conformation. When referring to histone modifications a standardised nomenclature is used. The first part of a reference is the histone (e.g. H3), the next letter is the amino acid being modified, and the final number is the residue of the amino acid; e.g. H3K9 refers to a modification of lysine 9 of histone H3.

One of the major histone modifications associated with active promoters is acetylation. Histones are reversibly acetylated on lysines within their N-terminal tails by histone acetyltransferases (HATs). Acetylated histones are associated with euchromatin, facilitating interactions of transcription factors with the DNA. Experimentally, permanently acetylated histones are unable to adapt a heterochromatic conformation (Shogren-Knaak et al., 2006; Garcia-Ramirez et al., 1995). Many transcriptional co activator proteins contain histone acetylase activities, for example p300/CBP that is able to link activators including c-Jun, Elk-1, AF-2, HIF-1 and CREB to the basal Pol II apparatus to increase transcription (Iyer et al., 2004). Conversely, deacetylation by histone deacetylases (HDACs) is associated with inhibition of transcriptional activator association and thus gene silencing, with some transcriptional repressors including Sin3 and NCoR/SMRT associated with HDACs (Pazin and Kadonaga, 1997). As well as acetylation, histones are also methylated on specific residues by histone lysine methyltransferases (HKMTs). Methylation of H3K9, 27 and H4K20 are associated with gene repression, whilst of H3K4, 36 and 79 with activation; in X chromosome inactivation, the silenced X chromosome has a significant enrichment H3K9 methylation and reduced H3K4 methylation (Boggs et al., 2002). Methylation of H4K20 by PR-Set7 has been shown to induce silencing through preventing acetylation of H4K16 by the transcriptional co-activator p300 (Nishioka et al., 2002).

Many factors contribute to the formation of either a euchromatin or heterochromatin structure. One of the major factors that promote a closed DNA structure is DNA methylation. Methylation facilitates the binding of transcriptional repressor proteins to the DNA, causing an inactive DNA conformation, which results in gene silencing. This process often occurs aberrantly in cancers, and will now be fully introduced.

1.9 DNA Methylation and Epigenetic Silencing

Epigenetic silencing refers to the heritable change (silencing) of gene expression that cannot be accounted for by a change in the DNA sequence (Bird, 2007). In mammals, epigenetic silencing is due to both pre-programmed and aberrant DNA methylation of cytosine bases, and this will now be introduced.

1.9.1 5-Methyl Cytosine

In higher eukaryotic organisms from plants to humans, the only base that is observed to be naturally modified by methylation is cytosine, and this normally occurs on the 5' position of the cytosine pyrimidine ring in the context of a CpG dinucleotide (Ehrlich and Wang, 1981; Suzuki and Bird, 2008). m^5C accounts for approximately 1% of bases in human somatic cells (Ehrlich et al., 1982), however the occurrence of CpG dinucleotides in many animals is much less than would be statistically expected. The total C and G content of human genomic DNA is ~40% and so as such the probability of a CpG dinucleotides occurring statistically would be $0.2 \times 0.2 = 0.04$. However the observed frequency of CpG is 0.008, significantly lower than expected (Bird, 1980; Simmen, 2008).

The amount of CpG methylation varies between different species, initially identified with restriction endonuclease isochizomers that discriminate against methylation. The restriction endonuclease HpaII will cleave the sequence CCGG, however not C^m CGG, whereas MspI will cleave both sequences indiscriminately. Therefore a sequence of DNA that is cleaved equally by HpaII and MspI must be unmethylated, whereas a sequence that is only cleaved by MspI but not HpaII must be methylated. It was this methodology that revealed the genomic DNA in *Drosophila melanogaster* and other insects is largely unmethylated, whereas vertebrate genomes are heavily methylated, with other species e.g. *Echinus esculentus* (sea urchin) are inbetween these extremes and considered to be partially methylated (Bird and Taggart, 1980).

There is a correlation between the amount of cytosine methylation and CpG frequency within genomes. Bird *et al* noted that insects, which have poorly methylated genomes, are not deficient in CpG dinucleotides, however vertebrates, which have highly methylated genomes, are deficient in CpG dinucleotides, and organisms with intermediate amounts of methylation have CpG content between the two extremes (Bird, 1980). This can be explained as methylated cytosines (within CpG dinucleotides) are prone to spontaneous deamination into thymine, thus resulting in TpG rather than CpG. This theory is also supported by the observation that genomes which have a deficiency in CpG

have a correlated increase in TpG and CpA dinucleotide frequency (Bird, 1980). Therefore, organisms with high ^mCpG content exhibit a slow decay to give rise to a significantly increased TpG content.

1.9.2 CpG Islands

CpG Islands were originally identified as being small regions of DNA that were CpG rich, and unmethylated. Digestion of vertebrate genomic DNA with the restriction nuclease MspI that cuts both CCGG and C^mCGG sequences, resulted in extensive cleavage of DNA. However, digestion with the methylation resistant nuclease HpaII that only recognises the sequence CCGG but not C^mCGG gave mainly larger fragments of undigested methylated genomic DNA, along with some smaller digested fragments, representing areas of genomic DNA that were unmethylated (Cooper et al., 1983).

Further investigations using hybridisation, methylation specific restriction digests and sequencing revealed that the small HpaII digested regions of DNA (also called HTFs; HpaII tiny fragments) were mostly unmethylated. Contrary to previous observations of significantly low CpG frequency compared to the overall GC content (Cooper et al., 1983), these undigested regions were found to be both GC rich and not deficient in CpG dinucleotides (which were found at a similar frequency to GpC dinucleotides) (Bird et al., 1985). Furthermore the occurrence of these unmethylated HTF 'Islands' were clustered in ~1kb regions of the genome and contained HpaII sites at 10 times the frequency found in genomic DNA as a whole (Bird et al., 1985).

Analysis of the hamster adenine phosphoribosyl transferase (*aprt*) and dihydrofolate reductase (*dhfr*) genes revealed that both genes were highly methylated intragenically, except for the 5' flanking region that was both unmethylated and contained a high CpG content (Stein et al., 1983). The *aprt* gene had previously been shown to be transcriptionally inactive following *in vitro* methylation prior to transfection into *aprt*⁻ mouse cells (Stein et al., 1982). This therefore led to one of the earliest evidence based predictions that methylation of a normally unmethylated 5' CpG rich region of a gene could cause it to be silenced (Stein et al., 1983).

The murine α 2 collagen gene was discovered to be unmethylated in the region surrounding the transcriptional start site, but methylated within and at the 3' end of the gene itself, and within the tissues examined the methylation remained constant regardless of expression of the gene (McKeon et al., 1982). Comparably, the albumin gene was also found to be consistently unmethylated

at the 5' end, with varying degrees of methylation within the rest of the gene, and in hepatoma cells hypomethylation of the 5' region was necessary for expression. The methylation status of the gene could not be directly correlated with expression, however the 5' proximal gene regions were consistently found to be unmethylated (Ott et al., 1982).

These identified 5' regions of genes that were CpG rich but unmethylated were termed CpG Islands. An initial definition of a CpG Island was put forward by Gardiner-Garden and Frommer of 'a region of at least 200bp with a GC percentage that is greater than 50% and with an observed/expected CpG ratio that is greater than 60%' (Gardiner-Garden and Frommer, 1987). Alu repeats are small interspersed DNA repeats that are ~280bp in length, that were originally introduced by integration of a retrotransposon, and there are approximately 1×10^6 Alu repeats in the human genome, accounting for ~10% of the total genome (Mighell et al., 1997). Alu repeats are GC rich, and as such the Gardiner-Garden and Frommer CpG Island definition could not always discriminate between these and actual CpG Islands. Following analysis of chromosomes 21 and 22 with a range of algorithms in order to avoid detecting Alu repeats, the more recent and widely accepted definition of a CpG Island was put forward by Takai and Jones of 'a region of DNA greater than 500bp with a GC content of at least 55% and an observed/expected CpG ratio of at least 0.65' (Takai and Jones, 2002).

There are 20-30,000 protein coding genes within the human genome (Lander et al., 2001; Venter et al., 2001) and CpG Islands are present in the promoters of up to 70% of all genes in total, with 100% of constitutively expressed housekeeping genes having one or more promoter CpG Islands (Kundu and Rao, 1999; Illingworth and Bird, 2009). The majority of CpG Islands do not contain TATA boxes or DPEs (Butler and Kadonaga, 2002). Promoters with TATA boxes and other core promoter elements tend to have either a single focused transcription start site, or a few closely clustered start sites within ~40bp. However, CpG Islands are promoters that give rise to multiple transcription start sites from within a larger range of ~100bp (Juven-Gershon et al., 2008).

CpG Islands contain multiple binding sites for the transcription factor Sp1 (Butler and Kadonaga, 2002). Sp1 is a ubiquitously expressed, multi faceted transcription factor that has been shown to be critical in maintaining the hypomethylated state of CpG Island promoters; the human and mouse *aprt* gene contains a 5' CpG Island with multiple Sp1 sites. The CpG Island is

unmethylated, but mutation of the Sp1 sites in ES cells resulted in promoter methylation (Brandeis et al., 1994). Sp1 also binds to the chromatin remodelling factors SNI/SWF and the p300/CBP co-activator complex, as well as recruiting TBP to TATA-less promoters in order to activate transcription (Butler and Kadonaga, 2002; Esteve et al., 2007). In HepG2 and 3B cells, Sp1 was shown to be critical for a euchromatic structure and transcriptional activation of the *CD151* gene, a gene that in liver cancer is a positive effector of metastasis and high expression correlates with poor prognosis (Wang et al., 2010).

However, Sp1 also binds to the HDAC 1/2 and Sin3A transcriptional repressor complex to repress transcription (Li and Davie, 2010). Furthermore, it binds to the *survivin* gene promoter and recruits transcriptional co-repressors including the methyltransferase Dnmt1 and HDAC1 that leads to methylation of H3K9 on the promoter, and represses transcription (Esteve et al., 2007). Therefore, the presence of the Sp1 binding motifs within CpG Islands appears to both repress and activate transcription in a gene dependent manner.

As well as containing multiple Sp1 sites, CpG Island promoters have a high incidence of other transcription factor binding motifs, including E2F, Nrf-1 and ETS family transcription factors (Landolin et al., 2010). Furthermore, in mouse studies, the presence of these motifs within CpG Islands was indicative of a constitutively expressed housekeeping gene (Rozenberg et al., 2008).

1.9.3 CpG Islands are Aberrantly Hypermethylated in Multiple Cancers

Initially cancer cells were identified as having a global reduction in m⁵C content (Gama-Sosa et al., 1983) and this has since been characterised as being a global phenomenon in cancers. Early analysis using methylation sensitive restriction digests of genomic DNA from a cohort of 23 human normal, neoplastic or polyp colonic cancers showed specific hypomethylation in a selection of genes in the polyps or neoplasms when compared to normal tissue, including γ -crystallin, growth hormone, α -chorionic gonadotropin and γ -globin, which are genes that are hypermethylated and not expressed in normal colonic epithelium (Goelz et al., 1985). However, converse to global hypomethylation that had to date been identified in cancers, Baylin *et al* then identified the calcitonin gene as having an increase in methylation in small cell lung cancer and lymphoma cell lines and in tumour samples from patients with Non-Hodgkins T and B cell lymphoid neoplasms and acute non-lymphocytic lymphomas when compared to non-neoplastic cells (Baylin et al., 1987). Since then, CpG Islands within the 5' proximal promoter regions of many genes have been identified as becoming

hypermethylated in cancers, including BRCA1, p14^{ARF}, p16^{Ink4A} and Rassf1a (Esteller, 2007).

Observations obtained using restriction landmark genomic scanning (RLGS) analysis of 1184 CpG Islands in 98 tumour samples revealed stark differences in aberrant methylation between different tumour types. For example breast, head and neck and testicular cancers showed low (or no) aberrant methylation, whereas childhood acute myeloid leukaemias and neuroectodermal tumours, colon and gliomas showed a significantly higher frequency of methylation (Costello et al., 2000). Furthermore some CpG Islands were commonly methylated between different tumour types, whereas others were specific for one type of cancer (Costello et al., 2000).

Different genes all appear to succumb to different extents of methylation, and this also varies between different cancer types. Esteller *et al* produced a 'CpG Island hypermethylation profile of human cancer,' illustrating the frequency of which 20 commonly hypermethylated gene promoters are methylated in 18 different primary cancers (Esteller, 2007) (Figure 1.10). This identified that different cancers show different extents of CpG gene promoter methylation; ovarian, skin cancers and sarcomas have relatively little hypermethylation in general compared to colonic, breast, HNSCC, lung and haematological malignancies. Furthermore, the same genes between different cancers show the varied levels of hypermethylation. For example the p16^{INK4A} tumour suppressor gene is reported to be hypermethylated in up to 50% of colon, lung cancer and lymphomas, whereas has no reports of hypermethylation in ovarian, pancreatic or stomach cancers (Esteller, 2007).

More recently with the development of high throughput, genome wide sequencing technologies, deep sequencing (Deep-seq) has been used to quantify CpG Island methylation in a range of cancers, with simultaneous identification of methylation within thousands of CpG Islands within the same genome. This allows for a global comparison of methylation between normal cells and cancer cells, facilitating the identification of potential tumour suppressor genes. In a cohort of prostate cancer samples, Deep-seq of methylated CpG enriched genomic DNA identified 2,481 cancer specific promoter hypermethylation occurrences, including almost all of 56 previously reported pancreatic cancer hypermethylated genes (Kim et al., 2011). In a cohort of breast cancer cell lines, deep-seq analysis identified differential methylation within the promoters of 162 genes that were differentially expressed between estrogen receptor expressing

and non-expressing cells, which has implications for the understanding and development of clinical therapeutics (Sun et al., 2011). The large increase in data obtainable from deep-seq methodology therefore further corroborates promoter hypermethylation as a characteristic and possible transformation initiating event in cancer.

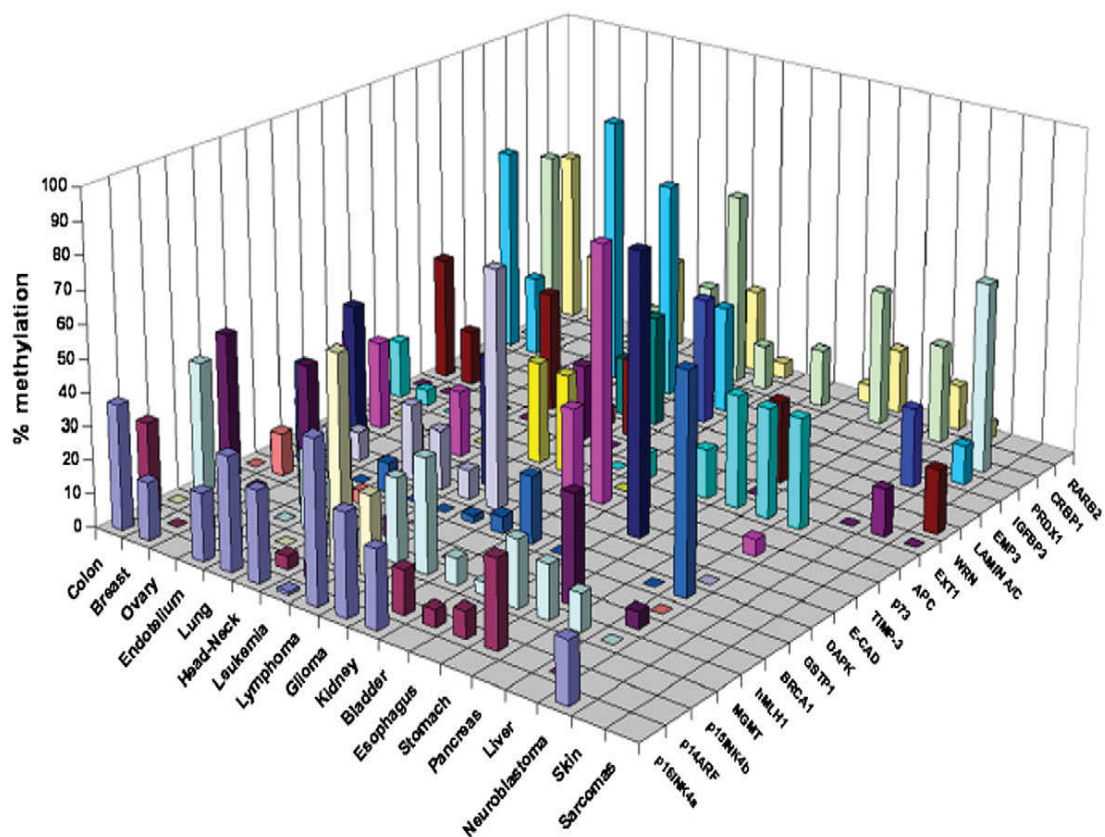


Figure 1.10: A CpG Island Hypermethylation Profile of human cancer. An illustrated histogram of 20 commonly hypermethylated genes in 18 different primary malignancies (Esteller, 2007).

1.9.4 DNA Methylation is Epigenetic

Both normal cell and aberrant tumour cell DNA methylation patterns are inherited following mitosis, and as such methylation is known as an epigenetic DNA modification. Epigenetics is defined as 'the study of mitotically and/or meiotically heritable changes in gene function that cannot be explained by changes in DNA sequence' (Bird, 2007). The first evidence to show the heritable trait of methylation patterns was when *in vitro* methylated plasmid DNA was transfected into cells, and following multiple rounds of host cell replication the methylation status of the original plasmid was maintained. Furthermore, as the methylation pattern was maintained this also indicated the presence of a 'maintenance' methyltransferase (Wigler, 1981; Wigler et al., 1981). Two DNA methyltransferases of molecular weights 150 and 175kDa were then purified from murine erythroleukaemia cells and shown to have the highest activity towards hemi-methylated DNA (Bestor and Ingram, 1983). The identified DNA methyltransferases (MTase) was subsequently cloned in 1988 (Bestor et al., 1988).

During gametogenesis, fertilisation and placental implantation, the methylation pattern of the DNA goes through both transiently dynamic and permanent changes. Methylation specific restriction analysis initially identified that methylation decreases post fertilization and then increases again after implantation (Monk et al., 1987). Pre-implantation embryos are observed to become globally hypomethylated compared to the fertilising oocyte and sperm (which themselves are hypomethylated when compared to somatic cells), and then the level of methylation is increased following implantation (Kafri et al., 1992; Kafri et al., 1993; Lei et al., 1996). Observations with an anti-5-methylcytosine antibody that showed the amount of methylation from single cell embryo to blastocyst decreased (Rougier et al., 1998). Furthermore, it has been proven that the paternally derived DNA is actively demethylated (as it occurs prior to DNA replication) whereas the maternal DNA is passively demethylated following replication due to the absence of a maintenance MTase (Mayer et al., 2000).

1.9.5 DNA Methylation is Carried out by DNA Methyltransferases (Dnmts)

From the initial cloning of MTase (Bestor et al., 1988), the existence of additional methyl transferases came following experimentation using murine embryonic cells.

Infection of the Moloney murine leukemia virus (M-MuLV) into murine embryonal carcinoma (EC) cells (stem cells of teratocarcinomas that are developmentally totipotent) produced genomes that contained integrated viral DNA. However, no significant expression of viral specific RNA was detected. Infection into differentiated EC cells however, resulted in both genomic integration and successful virus production. DNA analysis revealed that in the EC cells the viral DNA had become methylated, whereas in the differentiated cells it was unmethylated. Treatment with the DNA methylation inhibitor 5-azacytidine demethylated the viral DNA in the undifferentiated EC cells and induced viral expression (Figure 1.11). These observations indicated that the dynamics of methylation change following differentiation. Furthermore, and contrary to previous findings of a preference of the DNA methylase for methylating hemi-methylated DNA (Bestor and Ingram, 1983), these results indicated the presence of *de novo* DNA methylation in undifferentiated/pluripotent cells (Stewart et al., 1982).

Further evidence to support the existence of a *de novo* methyltransferase came following the production of ES cells with mutations in the MTase gene that rendered a non-functional protein. Infection of M-MuLV into wild type ES cells rendered identical results to those observed by Stewart *et al*; the viral DNA became integrated and then methylated (Figure 1.11). Following viral integration into ES cells with the non functional MTase the levels of *de novo* methylation were again identical to those seen in the wild type ES cells, indicating the presence of another methyltransferase that exhibited *de novo* methylation capabilities. After 8 days, when the levels of methylation peaked in both cell types, the amount of methylation decreased in the MTase mutant cells, which was attributed to the lack of a functional 'maintenance' methyltransferase (MTase) to preserve the methylation status. These observations therefore indicated other DNA methyltransferases enzymes existed (Stewart et al., 1982; Lei et al., 1996).

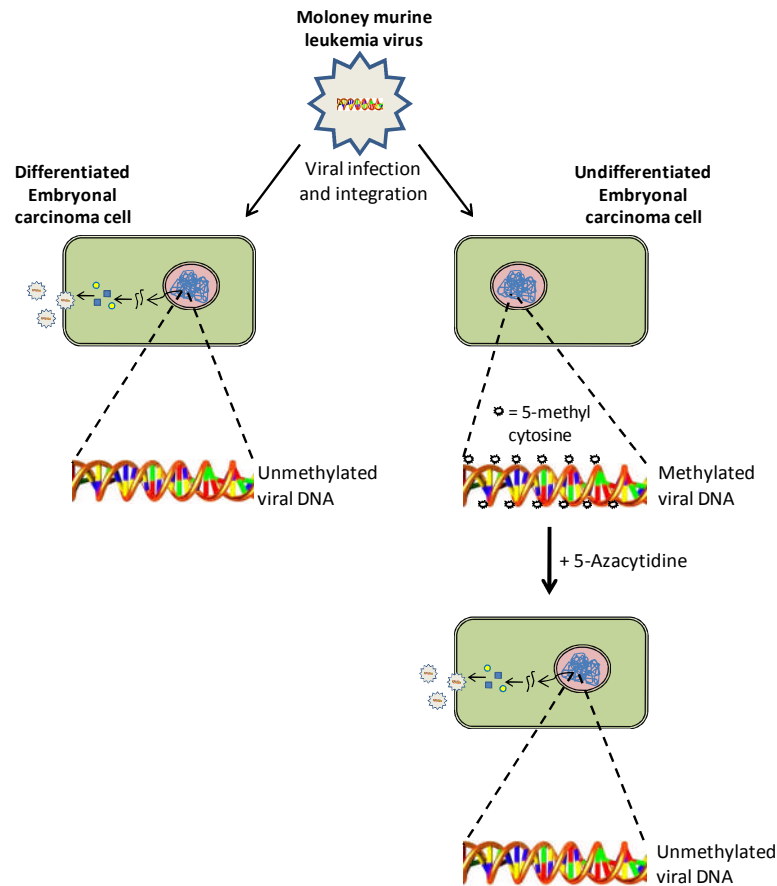


Figure 1.11 Undifferentiated embryonic cells contain an active *de novo* methyltransferase, whereas differentiated cells lose the ability of *de novo* methylation. Undifferentiated or differentiated embryonic cells were infected with the Moloney murine leukaemia virus, and viral DNA was integrated into the host genome. The differentiated cells produced viral encoded RNA and virus, however the undifferentiated cells did not; this difference was due to the integrated DNA becoming methylated in the latter cell type. Treatment with the DNA methylation inhibitor 5-azacytidine prevented methylation of the integrated DNA, and resulted in viral expression, proving the existence of an active *de novo* methyltransferase in undifferentiated cells (Stewart et al., 1982).

Sequence comparisons of 13 prokaryotic cytosine methyltransferases revealed 5 highly conserved domains (Posfai et al., 1989). Using this as a query sequence, 4 human EST clones were identified (Okano et al., 1998a). These were named DNA methyltransferase (Dnmt) 2, Dnmt3a and Dnmt3b (along with the already identified Dnmt1/MTase). Human Dnmt3a and b exhibit 98 and 94% homology respectively with their mouse homologues, whereas only 60% homology is seen between murine and human Dnmt1 (Okano et al., 1998a; Xie et al., 1999). Unlike Dnmt1 which shows a preferential activity towards hemi-methylated DNA (Bestor and Ingram, 1983), Dnmt3a and b were equally active towards both hemi and un-methylated DNA (Xie et al., 1999). Gene knockout of Dnmt3a and/or Dnmt3b revealed that homozygous mutant ES cell lines failed to

differentiate, $Dnmt3a^{-/-}$ mice developed to term but died after ~ 1 month and $Dnmt3b^{-/-}$ mice had multiple development and growth defects and no viable mice survived to birth (Okano et al., 1999). Double $Dnmt3a$ and b null ES cell lines were unable to methylate integrated M-MuLV DNA (Okano et al., 1999), demonstrating that both $Dnmt3a$ and b are required for *de novo* methylation, whereas $Dnmt1$ is required to maintain methylation states.

$Dnmt2$, the other identified mammalian DNA methyltransferase (Yoder and Bestor, 1998) is not required for either *de novo* or maintenance methylation (Okano et al., 1998b) and is localised to both the cytosol and the nucleus in contrary to the nuclear localisation of $Dnmt1$ and 3 (Schaefer and Lyko, 2010). Mice, that harboured inactivating mutations in $Dnmt2$ were viable, fertile and had almost identical phenotypes and genotypes to wild-type controls (Goll et al., 2006). $Dnmt2$ specifically methylates cytosine 38 in aspartic acid, glycine and valine transfer RNA (tRNA) both *in vivo* and *in vitro* (Goll et al., 2006; Schaefer and Lyko, 2010; Schaefer et al., 2010). Under oxidative or heat induced stress $Dnmt2$ localises to stress granules and RNA processing bodies, and that the methylation of the tRNAs protects them against stress induced angiogenin cleavage (Schaefer et al., 2010).

1.9.6 CpG Methylation is Critical for Normal Cell Physiology

Even though aberrant CpG methylation is observed in cancer cells, it is also a normal physiological event that is critical for normal differentiation and development of cells. This is specifically exemplified by X chromosome inactivation and genetic imprinting.

In somatic cells, diploid organisms contain two copies (alleles) of each gene, one maternal and one paternal. The only exception to this is the sex chromosome, where a female inherits two copies of the X chromosome, and a male only one. In order that the expression of X linked genes is equal between the different sexes, one X chromosome in human females is silenced, a phenomenon known as X-chromosome inactivation and is an example of dosage compensation.

The processes involved in X chromosome inactivation are not fully elucidated or understood. However, briefly, inactivation is dependent on an X-inactivation centre (Xic) locus that (through undiscovered mechanisms) is responsible for X chromosome counting to ensure all but one X chromosome is inactivated. Xic contains a gene called X-inactive specific transcript (Xist) which is transcribed as a 17kb untranslated RNA, which physically binds and coats the X chromosome to be inactivated in cis. The active X chromosome produces an anti-sense transcript Tsix, which represses Xist expression through altering Xist chromatin during transcription of Tsix. This prevents the active X chromosome from being coated with Xist. Xist then recruits the chromatin remodelling Polycomb repressor complex. This ultimately results in modified histone proteins and gene promoter methylation. The inactive X chromosome exhibits high levels of CpG promoter methylation in comparison to the active chromosome, and the few genes in the inactive chromosome that escape inactivation are unmethylated in both copies of the X chromosome, indicating the critical role of CpG methylation in silencing of genes in the inactive chromosome (Figure 1.12). (Heard, 2004; Kalantry, 2011; Kim et al., 2009; Leeb et al., 2009).

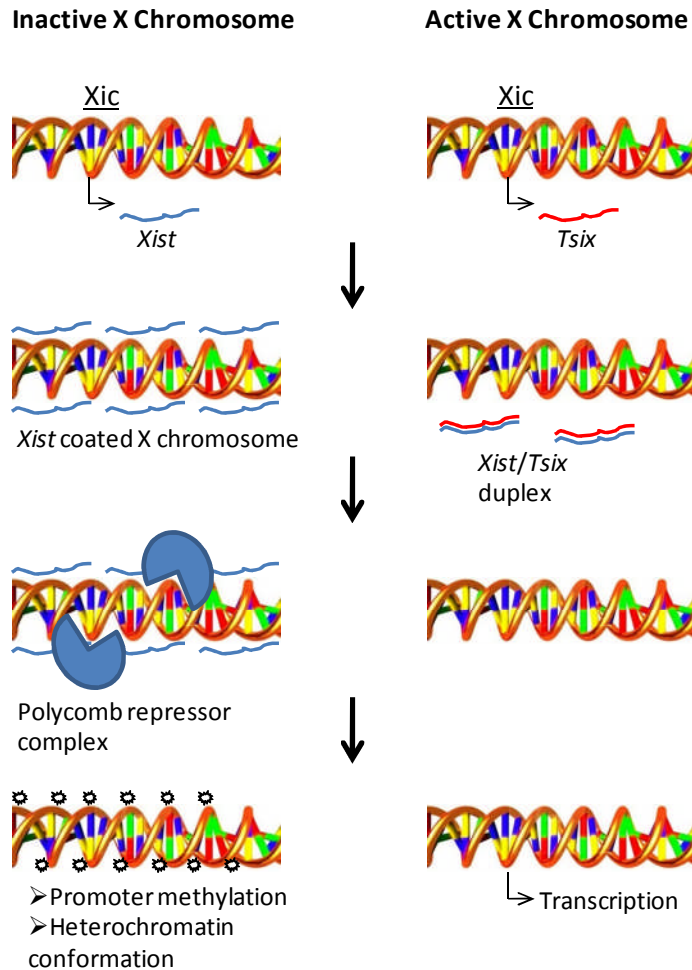


Figure 1.12 Schematic diagram of X chromosome inactivation. To maintain equal expression of X linked genes in males and females, one X female X chromosome is inactivated following fertilisation. The mechanism of this is not fully elucidated however, an X chromosome inactivation locus (Xic) is responsible for counting the X chromosomes to ensure all but one is inactivated. Xic encompasses the X-inactive specific transcript gene which is transcribed as a 17kb untranslated RNA that physically coats the X chromosome that is to be inactivated. At the same time the active chromosome transcribes the complementary transcript *Tsix*, which forms a duplex with *Xist*, preventing it from coating the chromosome. *Xist* on the coated chromosome then recruits the Polycomb repressor complex, resulting in chromatin remodelling and hypermethylation of the contained genes, rendering the chromosome inactive (Kalantry, 2011).

Similar to X chromosome inactivation is genetic imprinting, which is the expression of certain genes in a parent specific manner; i.e. one allele of a gene is inactivated so that expression of a gene is solely from either the maternally or paternally inherited chromosome. In humans and mice there are 53 and 96 (37 common) functionally characterised imprinted genes respectively (Morison et al., 2005). During gametogenesis, the methylation status of the maternal/paternal imprinted gene is erased and then re-imprinted; this is so that the gametes contain methylation information that is specific to parent it was inherited from,

rather than from the gene itself. The precise methylation is controlled by cis-acting imprinting control regions (ICRs), which are CpG rich sequences. Following fertilisation, the methylation status of the ICR is maintained (even though there is global hypomethylation), and the genes associated with the ICR if appropriate are *de novo* methylated by Dnmt3. The gene methylation is then preserved through differentiation and proliferation by Dnmt1, resulting in maternal or paternal specific expression of a gene (Kim et al., 2009; Wood and Oakey, 2006).

Regulated promoter methylation in normal cells has also been shown to regulate tissue specific silencing of genes. Methylation analysis from normal peripheral blood leukocytes identified 258 genes that had CpG islands within their promoters that were methylated, which corresponded to 4% of all gene promoters assayed (Shen et al., 2007). The identified methylated genes could broadly be characterised as being involved in intracellular membrane bound organelle function, metal ion binding and signalosome function and were shown to be hypomethylated in multiple cancer cell lines. Furthermore, expression of the genes in the cell lines correlated with hypomethylation of the promoter (either by 5-aza deoxycytidine treatment or Dnmt1 and 3b knockout) (Shen et al., 2007). The promoter of the breast cancer tumour suppressor gene *serpin* is unmethylated and expressed in normal epithelia, however is methylated and not expressed in normal hematopoietic, liver, kidney and heart cells (Futscher et al., 2002). *MAGE1*, a gene only expressed in testis and some melanomas, as well as other multiple testis specific genes, are methylated in normal somatic cells, meaning they are not expressed, but unmethylated specifically in the testis/spermatozoa where they are expressed (Zendman et al., 2003; Strathdee et al., 2004). The *HOXA5* gene product is involved in differentiation of both haematopoietic and epithelial cells, and is also a candidate tumour suppressor in breast cancer. The *HOXA5* promoter was methylated in mesenchymal cells, had ~50% methylation in haematopoietic cells and unmethylated in epithelial cells, and this correlated with mRNA expression (Strathdee et al., 2007).

Methylation is therefore important for maintaining normal silencing of certain genes. As previously described, aberrant methylation of gene promoters is also a well characterised event in multiple cancers. It is therefore important to understand how methylation of a gene or its promoter results in transcriptional silencing of the gene.

1.9.7 Promoter Methylation as a Cause of Transcriptional Silencing

The biochemical link between promoter methylation and transcriptional silencing was first presented over 20 years ago. de Bustros *et al* confirmed the earlier findings by Baylin *et al* of methylation of the 5' region of the calcitonin gene in lung cancer, gastrointestinal tumour and teratocarcinoma cell lines (Baylin *et al.*, 1987; de *et al.*, 1988). They used restriction enzymes to target recognition sites within the 5' gene region and compared the restriction digests from cells that were methylated to those that were unmethylated. They discovered that in unmethylated cells, all restriction sites were accessible and so cleaved by the enzymes, whereas in the methylated cells not all sites were accessible as demonstrated by reduced DNA cleavage (Figure 1.13). This led to the conclusion that methylation could be linked to a closed chromatin structure, and furthermore, could prevent transcription from this site (de *et al.*, 1988). More recently, methylated DNA has been shown using FRET to induce a more compact and rigid nucleosome structure when compared to unmethylated DNA (Choy *et al.*, 2010).

Cytosine methylation can directly inhibit binding of transcription factors to their consensus motifs. AP-2 is inhibited from binding within the human proenkephalin gene promoter (Comb and Goodman, 1990) and E2F from binding to the enhancer of the adenoviral *E1A* gene (Kovesdi *et al.*, 1987), thus directly inhibiting transcriptional activation. However some transcription factors are unaffected by methylation, for example Sp1 (Harrington *et al.*, 1988), and as such, direct inhibition of transcription factor binding is unlikely to be the major reason for transcriptional silencing.

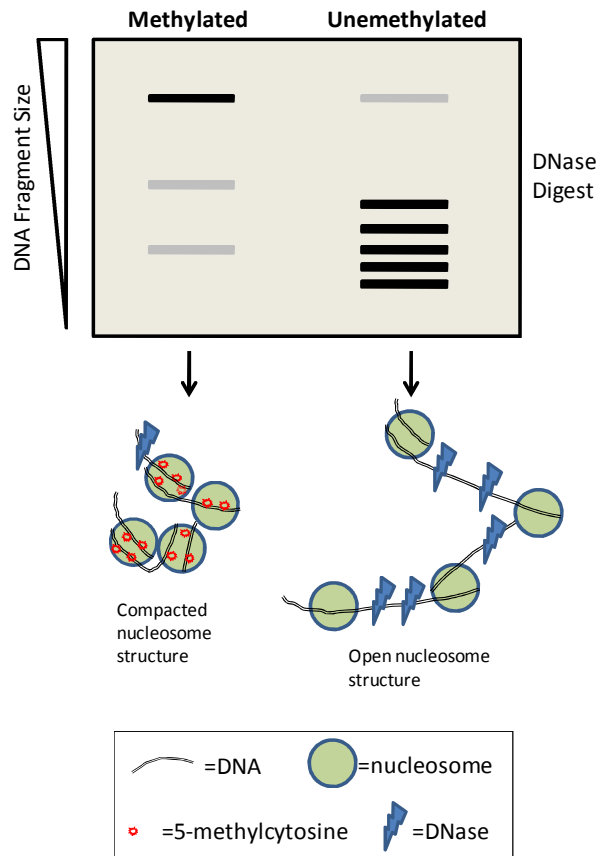


Figure 1.13: DNase activity is inhibited by methylation. The calcitonin gene promoter was observed to become hypomethylated in a subset of lung carcinomas (de et al., 1988). Restriction digest of this region in cells with an unmethylated promoter resulted in extensive digestion of the DNA. However, in cells where the promoter was methylated, the amount of digestion was significantly reduced, which was hypothesised to be due to a closed chromatin structure inhibiting DNA accessibility.

Other mechanisms of silencing were uncovered by the use of *in vitro* methylated DNA. An *in vitro* methylated Herpes simplex virus-thymidine kinase transfected into cells was expressed at the same rate as the unmethylated control DNA 48 hours post transfection. Levels of transcription did not decrease in the *in vitro* methylated cells until after 100 hours (Buschhausen et al., 1985), suggesting that whilst some transcription factors may be inhibited from binding by methylation, it is more likely methylation causes an indirect mechanism of silencing.

In 1989, a specific methyl CpG binding protein (MBD) was identified as a 120kDa protein that bound to a synthetic cluster of methylated CpGs (Meehan et al., 1989) and named MeCP2, giving the first indication that recruitment of proteins specifically to methylated DNA could cause indirect alterations to silence transcription (Wakefield et al., 1999). Further studies that identified MeCP2 could

recruit the transcriptional repressor Sin3A and histone deacetylases to methylated DNA, implicated a mechanistic connection between DNA methylation and chromatin remodelling/gene silencing (Jones et al., 1998).

1.9.8 Methyl CpG Binding Domain Proteins

To date, there are 5 characterised mammalian methyl CpG binding domain proteins; MeCP2, MBD1, MBD2, MBD3 and MBD4.

MeCP2 contains a MBD that interacts with symmetrically methylated CpGs in the major groove of DNA (Wakefield et al., 1999) and forms a complex with the histone deacetylases HDAC1 and 2 containing transcriptional repressor complex mSin3A, (Nan et al., 1998; Jones et al., 1998). It also forms a complex with the transcriptional co-repressors c-Ski and NCoR (Kokura et al., 2001) and has more recently also been shown to cause methylation of H3K9 (Fuks et al., 2003).

MBD1, and its 5 isoforms, are able to repress transcription from both methylated and unmethylated promoters through recruitment of the H3K9 methylases Suv39h1 and SETDB1 as well as HDAC1 and 2, facilitating the formation of heterochromatin (Fujita et al., 2003; Fujita et al., 2000). siRNA mediated depletion of MBD1 causes a loss of H3K9 methylation and expression of the normally silenced p53BP2 gene in HeLa cells (Sarraf and Stancheva, 2004).

MBD2 is part of the MeCP1 transcriptional repressor complex, associating with HDAC1 and 2 (Ng et al., 1999), and is able to anchor the Mi2/NuRD (Nucleosome Remodelling and Deacetylase) complex to methylated DNA (Zhang et al., 1999). MBD2 knockdown in cancer cell lines reduces their ability for anchorage independent growth, the ability to implant *in vivo* in nude mice and knockdown of MBD2 within already implanted A549 HCT116 tumours reduced their *in vivo* growth and tumorigenicity. On the converse MBD2 protein had no effect on the growth of anchorage dependent normal or tumour cells (Campbell et al., 2004).

MBD3 does not bind to methylated CpGs *in vivo*, however it is a component of the NuRD complex, where it binds directly to HDAC1 and MTA2 to facilitate formation of heterochromatin (Saito and Ishikawa, 2002).

MBD4 possesses a different function from the other MBD proteins; it binds to ^mCpG:TpG mismatches and excises the mis-matched thymine (or uracil) and initiates DNA repair through interaction with the mismatch repair protein MLH1

(Hendrich et al., 1999). *Mbd4*^{-/-} mice show a significant increase in C to T mutations and a three-fold increase in CG to TA transitions (Millar et al., 2002). MBD4 has also been shown to form a complex with mSin3A and HDAC1 and repress reporter driven transcription *in vivo* and to associate with the *p16INK4a* and *hMLH1* gene promoters in a methylation specific manner (Kondo et al., 2005).

The importance of gene structure and epigenetic modifications has been shown to be critical for accessibility of RNA polymerase to gene promoter elements. For example in cancers, when aberrant epigenetic modifications such as CpG Island hypermethylation occurs, this promotes the association of MBD proteins and chromatin remodelling factors that cause a heterochromatic structure and inhibit transcription, ultimately causing silencing of the gene. It is this specific aspect of gene expression that will first be addressed regarding LIMD1 biology.

1.10 Preliminary Data

1.10.1 The *LIMD1* Promoter contains a Putative CpG Island

The *LIMD1* promoter region encompassing 2039bp relative to the *LIMD1* ATG translation initiation codon had previously been cloned into a pGL4.10 vector (WT-P). This allowed for activity of the *LIMD1* promoter to be assayed indirectly through transcription and translation of a downstream luciferase gene (Sharp et al., 2008). Furthermore, a putative CpG Island had been identified, and 3 large deletion mutants created; Δ 1-P which removed 500bp from the 5' end of the promoter, Δ 2-P which removed an extra 240bp, leaving no promoter sequence 5' to the CpG Island, and Δ 3-P which removed all of the predicted CpG Island. Initial experiments in the A549, MB435 and U2OS cell lines revealed that the putative CpG Island was necessary for transcriptional activation from the promoter (Figure 1.14). The methylation status of the CpG Island in normal or cancer cells could therefore be a mechanism to control *LIMD1* gene expression.

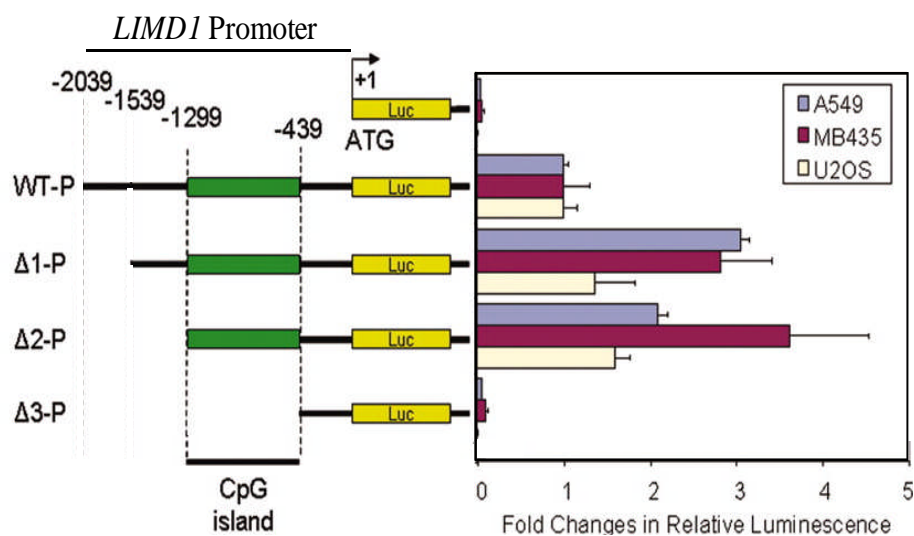


Figure 1.14: The *LIMD1* Promoter contains a putative CpG Island that is critical for *LIMD1* promoter driven transcription. The *LIMD1* promoter encompassing ~2kb 5' proximal to the ATG initiation codon was cloned into a pGL4.10 vector (WT-P), along with 3 large promoter truncation deletions (Δ 1-P, Δ 2-P and Δ 3-P). The promoter plasmids were co-transfected with a pGL3 renilla plasmid for normalisation into the indicated cell lines and resultant luciferase activity assayed. The putative CpG Island is critical for transcription as deletion of it (Δ 3-P) ablated transcriptional activity (Sharp et al., 2008).

To promote transcription from genes, i.e. enhance RNA polymerase binding, the association of transcription factors to a gene promoter can facilitate the binding of the general transcription factor machinery/RNA pol II. Some transcription factors also contain histone acetyl transferase activity to acetylate histone tails and promote a euchromatin structure. Therefore, loss or deregulation of a transcription factor can affect the basal expression of genes under its control, which if a tumour suppressor, can have detrimental consequences for the cell.

The second results chapter discusses how the Ets family of transcription factors may control *LIMD1* expression and thus biology. Therefore this family of proteins will next be discussed.

1.11 Ets Family of Transcription Factors

The Ets family of proteins is one of the largest families of transcription factors characterised to date. The first member of the Ets family of transcription factors, v-ets, was identified in 1983 in the E26 avian transforming retrovirus, a retrovirus that causes avian leukaemias (Leprince et al., 1983). This gave rise to the name Ets; the E26 transformation specific family and to date 28 human Ets family members have been identified (Hsu et al., 2004) (Figure 1.15).

1.11.1 The Ets Domain

The common feature of the family is the Ets domain, which is an evolutionary conserved sequence of 80-85 amino acids forming a DNA binding domain that binds the core consensus sequence GGAA. Initially identified as a winged helix-turn-helix, structural studies on Ets-1, PU.1, GABPa, SAP-1 and Elk-1 revealed the domain is more specifically comprised of 3 α -helices and 4 β -sheet strands. DNA binding specificity is controlled by the third α -helix, the wing between β -strands 3 and 4, and the loop between α -helices 2 and 3 (Sharrocks, 2001). The flanking Ets domain amino acids and the flanking DNA base pairs around the core consensus confer specificity and affinity of binding for a particular family member, with as little as one amino acid conferring specificity of one Ets protein over another (Verger and Duterque-Coquillaud, 2002).

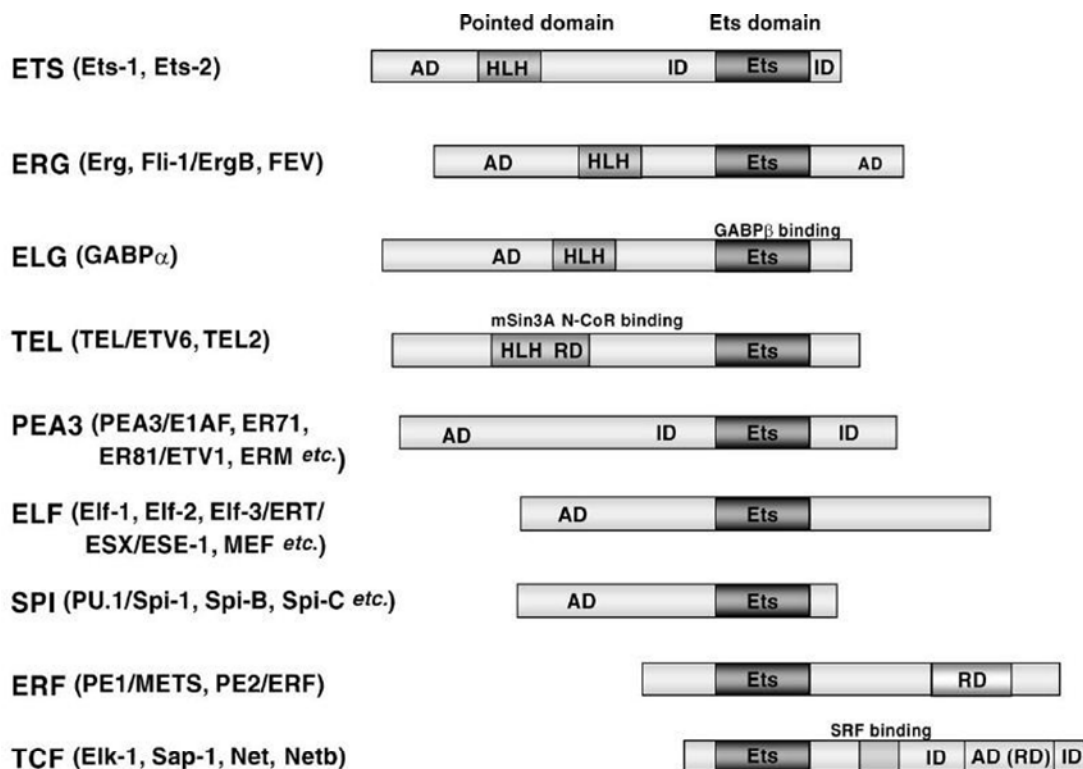


Figure 1.15: Schematic diagram of the general structures of the Ets transcription factor subfamilies. As well as harbouring an Ets domain the Ets family can be subdivided into smaller groups based on their structures. AD activation domain; HLH helix loop helix; ID auto-inhibitory domain; RD repression domain. Adapted from (Oikawa and Yamada, 2003).

The Ets family targets over two hundred genes including those involved in apoptosis, differentiation, development, angiogenesis and transformation; examples include p53 (Ets 1 and 2), NF- κ B1 (Ets 1), cyclin D1 (Ets 2), Rb (GABP), IL 1-5 (Ets 1 and 2, PU.1) and TNF α (Elk-1) (Sementchenko and Watson, 2000). Whereas some family members are ubiquitously expressed (e.g. Ets-2, GABP α , TEL and TCF subfamily) others have tissue specific distribution; Ets-1 in the brain, lymphoids, and vascular endothelial cells, PEA3/E1AF in epidermis and mammary glands, Elf-1 in liver, kidney and intestines, Elf-5 in lung epithelia, Elf-1 in hematopoietic cells, ESE-1 in epithelial cells and PU.1 in macrophages, neutrophils and B cells (Oikawa and Yamada, 2003).

The majority of Ets proteins are associated with transcriptional activation, however a few including YAN, ERF, NET, PU.1 and TEL have been shown to exhibit negative effects upon gene transcription (Mavrothalassitis and Ghysdael, 2000). One mechanism of transcriptional repression is the recruitment of HDACs. Activation of ERK MAP kinase causes an association of Elk-1 with the mSin3A-HDAC1 co-repressor complex, resulting in histone deacetylation and gene

silencing (Yang et al., 2001). TEL also recruits the mSin3A complex, as well as harbouring gene repressor properties independent of characterised co-repressors (Chakrabarti and Nucifora, 1999).

1.11.2 PU.1 (Spi1)

Spi-1 (SFFV proviral integration protein) was initially identified in 1988 as a putative oncogene in murine erythroleukemias that were induced by the retroviral spleen focus forming virus (SFFV), with its' mRNA found in 95% of the examined erythroid tumours (Moreau-Gachelin et al., 1988). Spi-1 was cloned in 1990, and renamed PU.1, so called due to its binding to a purine rich sequence, 5'-GAGGAA-3' that was present in the promoter of the MHC class II gene following screening with a cDNA library (Klemsz et al., 1990). PU.1 exhibits high homology with other Ets family members and is most closely related overall to Spi-B and Spi-C (Kastner and Chan, 2008).

PU.1 contains four distinct protein domains; an acidic domain, a Gln rich domain, a PEST (proline, glutamic acid, serine and threonine rich) domain and an Ets domain (Nishiyama et al., 2004; Lloberas et al., 1999) (Figure 1.16). The acidic and Gln regions are required for transactivation of genes, through mediation with PU.1 interacting proteins including the general transcription factors TFIID/TBP and the transcriptional co-activators p300/CBP (Klemsz and Maki, 1996). The PEST domain interacts with interferon regulatory proteins, including PU.1 interacting partner (PIP), to mediate transcription of interferons in order to activate the immune defence (Tenen, 2003).

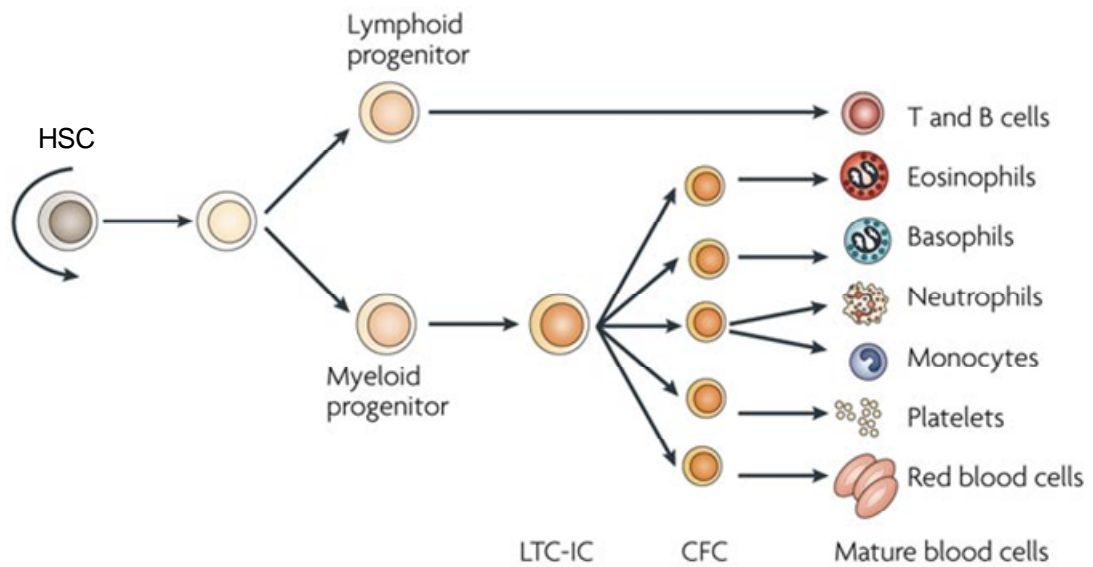


Figure 1.17: Schematic overview of haematopoiesis. Pluripotent haematopoietic stem cells (HSC) give rise to lymphoid and myeloid progenitors. Lymphoid progenitors subsequently give rise to T and B cells. Myeloid progenitors differentiate into colony forming cells, which in turn produce mature eosinophils, basophils, neutrophils, monocytes, platelets and red blood cells. LTC-IC, long term culture initiating cells; CFC, colony forming cell. Adapted from (Corey et al., 2007).

Phosphorylation of PU.1 modulates its protein and DNA binding activity. Haematopoietic progenitor cells contain levels of PU.1 that are both hypo and hyper phosphorylated, and the equilibrium of phosphorylation changes following external stimulation (Gross et al., 2006). For example, activation of Protein Kinase C delta (PKC δ) causes phosphorylation of the transactivation domain of PU.1 to promote its transcriptional activation capacity, but does not affect its DNA binding ability, facilitating the differentiation of HSCs into dendritic cells (Hamdorf et al., 2011). There is also evidence showing phosphorylation of PU.1 by PKC δ can stimulate DNA binding and is correlated with inhibition of leukemic cell growth (Carey et al., 1996). Furthermore, phosphorylation of ser148 within PU.1 is required for binding to the nuclear factor NF-EM5 and transcriptional activation of the immunoglobulin K 3' enhancer (Pongubala et al., 1993) as well as interaction with PU.1 interaction partner (PIP) (Eisenbeis et al., 1995). Phosphorylation of ser41 by AKT kinase affects PU.1 transcriptional activity and B cell proliferation (Gross et al., 2006).

1.11.2.1 Pathogenic Role of PU.1

PU.1 deregulation is associated with 2 major hematopoietic associated diseases; Friend's erythroleukaemia and acute myeloid leukaemia.

(i) Friend's Erythroleukaemia

PU.1 was initially identified as the over expressed oncogene that was targeted by the SFFV in murine Friend's erythroleukaemias (Moreau-Gachelin et al., 1988). Transgenic mice that over-expressed PU.1 developed normally, with no mortality observed until 6 weeks after birth, where 50% of mice developed multi-step erythroleukaemia, facilitated by an increase in pro-erythroblasts that were unable to differentiate (Moreau-Gachelin et al., 1996). It has since been shown that PU.1 expression blocks erythroblasts from differentiating (Dahl and Simon, 2003). PU.1 activation is required for growth of erythroleukaemic cells (Hegde et al., 2009), and siRNA mediated depletion of PU.1 in erythroleukaemias abrogates the PU.1 mediated block of differentiation and allows for terminal growth arrest (Papetti and Skoultchi, 2007). As such PU.1 exhibits oncogenic properties in erythroleukaemias.

(ii) Acute Myeloid Leukaemia

Conditional deletion of *PU.1* in adult mice causes fatal myeloid leukaemia (Metcalf et al., 2006). Acute myeloid leukaemia is the most common leukaemia in adults and is characterised by increased levels of undifferentiated granulocyte and monocytes precursors in the blood and bone marrow. PU.1 acts as a tumour suppressor in myeloid cells, which is opposite to its oncogenic properties in erythroleukaemias, with multiple studies identifying reduced PU.1 levels associated with leukemogenesis (Mueller et al., 2002; Cook et al., 2004). As little as a 20% reduction in PU.1 expression results in an increase in pre-leukemic haematopoietic cell number (Stirewalt, 2004).

In mice, deletion of an upstream regulatory element in the *PU.1* promoter reduces PU.1 protein expression by 80%; up to 2 months in age these mice were the same size and had the same behaviour as the control mice, but by 8 months of age 98% of mice had died from a disease akin to human myeloid leukaemia, all exhibiting enlarged spleens and livers (Rosenbauer et al., 2004). Using Cre-recombinase, deletion of the PU.1 Ets domain again resulted in mice with enlarged spleens and high populations of undifferentiated granulocytes that died of myeloid leukaemia, demonstrating the DNA binding ability of PU.1 is critical for its function (Metcalf et al., 2006).

PU.1 is essential for myeloid differentiation; when PU.1 mediated differentiation/maturation of myeloid precursors is inhibited or blocked this gives rise to development of leukaemia (Dahl and Simon, 2003). Unsurprisingly, mutations that effected PU.1 DNA binding, transactivation or protein-protein binding have been identified in patients suffering from AML (Mueller et al., 2002).

In the final chapter of results, focus switches from silencing and major transcriptional activation of LIMD1 to its enhanced expression and concurrent role in hypoxia. Therefore the identification and concepts of the cellular response to hypoxia will now be introduced.

1.12 Hypoxia

1.12.1 Identification of the HIF1 Transcription Factor

Using squamous lung carcinomas as an initial study, Thomlinson and Gray identified that tumours contained a core of necrotic cells surrounded by viable tumour cells. Furthermore, the necrotic core appeared to correlate with the distance oxygen was able to diffuse through a solid tumour and distance it was from the oxygen containing stroma (Thomlinson and Gray, 1955). This suggested that the necrotic core was the result of anoxia (no oxygen). Otto Warburg then observed that cancer cells, irrespective of oxygen availability, had a high rate of anaerobic glycolysis and lactic acid fermentation rather than aerobic respiration (mitochondrial pyruvate oxidation), and postulated this aberrant change in metabolism to be an underlying cause of cancer- the Warburg effect (Warburg, 1956).

From these initial observations of tumours exhibiting areas of hypoxia (low oxygen tensions/concentrations) and respiring anaerobically, further investigations identified a global decrease in protein synthesis under conditions of hypoxia, except for a few proteins whose intensity on a stained SDS-PAGE gel increased following hypoxic/anoxic exposure. Two of these uncharacterised proteins were positively identified with molecular weights of 76 and 97kDa (Sciandra et al., 1984). Levels of specific mRNAs including erythropoietin and glycolysis related enzymes were also observed to be increased following hypoxic conditions (Webster, 1987; Schuster et al., 1989).

Further investigations on the Epo gene using Dnase foot printing, reporter and EMSA analysis revealed there was a 50bp hypoxic responsive enhancer 3' to the poly-adenylation signal, and this bound to both constitutively expressed proteins as well as a protein that only bound following hypoxic exposure (1% O₂) (Semenza et al., 1991; Semenza and Wang, 1992). This protein was given the name hypoxia inducible factor 1, HIF-1 (Semenza and Wang, 1992) and was subsequently found to be active in a variety of cells (Wang and Semenza, 1993c; Wang and Semenza, 1993b). HIF-1 levels were shown to peak at 4 hours following hypoxic exposure and remain stable until after 16 hours; however 5 minutes in 20% oxygen following 4 hours hypoxia reduced HIF-1 levels by 66% (Wang and Semenza, 1993a). HIF-1 was able to be induced through either cobalt ions or the iron chelator desferrioxamine (Wang and Semenza, 1993b). In this same study HIF-1 DNA binding activity and induction of Epo RNA was

ablated by either treatment with the protein kinase inhibitor 2-aminopurine or calf intestinal alkaline phosphatase (Wang and Semenza, 1993a).

Using DEAE ion exchange and DNA affinity chromatography, HIF1 was purified and identified as being composed of 2 subunits; a 120kDa HIF1 α and a 94kDa HIF1 β (also referred to as ARNT) subunit (Wang and Semenza, 1995). Scrutinisation of available sequenced genomes revealed both HIF1 α and HIF1 β contained regions homologous to those found in the *Drosophila* proteins Per and Sim, as well as the mammalian aryl hydrocarbon receptor, AHR. This domain as such was called a PAS domain; Per, AHR and Sim (Wang et al., 1995a). They were also found to contain a basic helix loop helix (bHLH) domain and so as such are referred to as bHLH-PAS proteins (Wang et al., 1995a). HIF1 α and β heterodimerise both *in vivo* and *in vitro* in both in the presence or absence of DNA (Jiang et al., 1996).

Depletion of HIF1 α in embryonic stem cells resulted in the reduced expression of many glycolytic pathway enzymes in hypoxia, and furthermore HIF1 α ^{-/-} ES cells proliferate much slower in hypoxia than HIF1 α ^{+/+} ES cells but have no difference in normoxia (20% O₂/atmospheric O₂ tension) (Iyer et al., 1998). HIF1 α ^{-/-} mice are also not viable, and even though non-hypoxic ES cells have constitutively high levels of HIF1 α , depletion of HIF1 α does not affect pre-implantation development (Iyer et al., 1998).

Two other proteins homologous to HIF1 α were also identified. HIF2 α (also called endothelial PAS protein 1, EPAS1; HIF1 α -like factor, HLF; HIF-related factor, HRF) is 48% homologous to HIF1 α and also dimerises with HIF1 β where it activates transcription from hypoxic response elements (HREs) within gene promoters (O'Rourke et al., 1999; Tian et al., 1997). HIF3 α (also called inhibitory PAS domain protein, IPAS), unlike HIF1 and 2 α , impairs induction of hypoxic inducible genes (acting in a dominant negative fashion when co-expressed with HIF1 α). It binds HIF1 α reducing its DNA/HRE binding ability (Makino et al., 2001). HIF3 α (and its splice variants) doesn't contain a C terminal activation domain and as such is unable to function as an effective transcriptional activator (Figure 1.18). Furthermore, HIF3 α contains a HRE within its promoter that causes an increase in mRNA and protein levels in hypoxia in a HIF1 α dependent manner, implicating it as a negative regulator of hypoxia (Makino et al., 2007; Pasanen et al., 2010).

HIF1 α and HIF1 β mRNA are constitutively expressed in a wide variety of human tissues, with transcription of both remaining constant regardless of oxygen

tension (Huang et al., 1996; Gradin et al., 1996). However, in hypoxia, the levels of HIF1 α protein significantly increase, whilst the level of HIF1 β does not change and this will be further elaborated upon in Section 1.12.3.

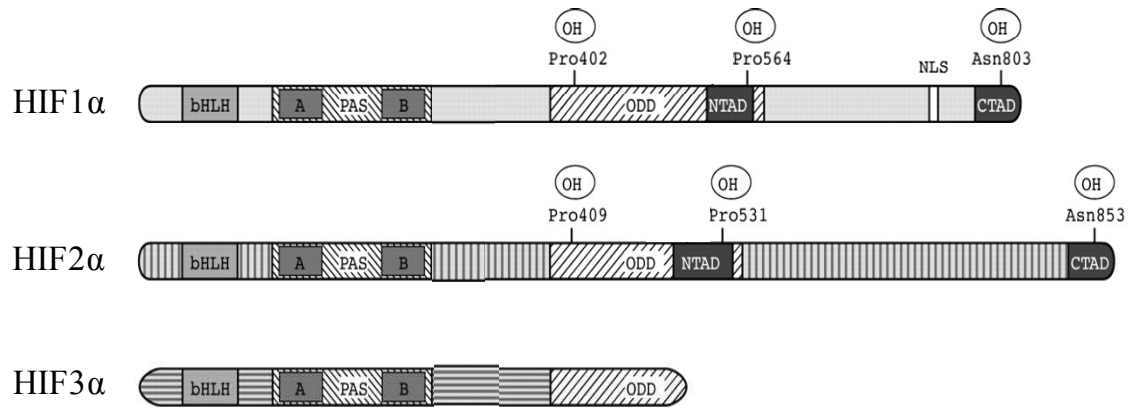


Figure 1.18: Schematic diagram of the homologous HIF1, 2 and 3 α proteins. The HIF α proteins all share high homology, with conserved functional domains illustrated. Oxygen dependent hydroxylation sites on HIF1 and 2 α are also illustrated. The functional domains include a basic helix-loop-helix (bHLH) that mediate DNA binding; two Per/Ahr-ARNT/Sim (PAS) domains to mediate interaction with HIF1 β ; one oxygen dependent degradation (ODD) domain that encompasses residues required for oxygen dependent hydroxylation and degradation; N-terminal and C-terminal transactivation domains (NTAD/CTAD) that facilitate interaction with the p300/CBP transcriptional co-activator and a nuclear localisation signal (NLS). Hydroxylation of the ODD localised prolines is facilitated by proline hydroxylase proteins (PHDs), whereas asparagine hydroxylation is facilitated by factor inhibiting HIF (FIH). Adapted from (Gaber et al., 2005).

1.12.2 HIF1 Allows for Cellular Adaptation to Low Oxygen Tensions

HIF1 allows for cellular survival under low oxygen tensions, through the transcription of multiple genes that stimulate the activation of different pathways. With low oxygen tensions, aerobic respiration is unable to effectively proceed and a switch to glycolysis is observed; this was initially observed by Warburg (Warburg, 1956). Therefore enzymes involved in the anaerobic glycolytic pathway are increased, for example glyceraldehyde-3-phosphate dehydrogenase (GAPDH) (Graven et al., 1999). In association with glycolytic enzymes, enzymes that increase the availability of glucose for respiration are also upregulated, this includes for example the glucose transporters 1 and 3 (Iyer et al., 1998; Semenza, 1999; Zagorska and Dulak, 2004) (Figure 1.19). In order to try and re-establish the oxygen supply, proteins involved in angiogenesis and red blood cell production/maturation are also increased; this includes the growth factor VEGF, which stimulates vasculogenesis and angiogenesis (Forsythe et al., 1996) and the hormone erythropoietin (EPO) that

stimulates maturation of erythrocyte precursors into mature red blood cells (Semenza and Wang, 1992).

Most of the genes up-regulated by HIF1 appear to be adaptive in nature, however HIF1 α can also induce apoptosis. In hypoxia, the lack of oxygen, inhibits the electron transport chain, causing a decrease in mitochondrial membrane potential, hyperpermeability of the inner mitochondrial membrane and cytochrome C release, which initiates the cascade leading to apoptosis (Greijer and van der Wall, 2004). In addition, hypoxia causes a HIF1 α dependent up-regulation in the expression of some pro-apoptotic tumour suppressors, including WT1 and BNIP3 (Wagner et al., 2003; Guo et al., 2001).

In what seems a counter-intuitive manner, hypoxia also induces expression of inhibitor of apoptosis protein 2 (IAP-2), which inhibits apoptosis (Dong et al., 2001). Furthermore, in the human tongue squamous cell carcinoma cell lines SCC-4 and 9, depletion of HIF1 α resulted in inhibition of cell proliferation and induction of apoptosis (Zhang et al., 2004b). HIF-1 therefore appears to exert both pro- and anti- apoptotic functions. The equilibrium that exists between hypoxia induced pro-apoptotic and adaptive responses is not fully understood; for example many cancer cells that express high levels of HIF1 α have been found to be resistant to hypoxia induced apoptosis, and so further investigations are therefore required to elucidate and distinguish HIF1 pro- and anti-apoptotic functions (Greijer and van der Wall, 2004).

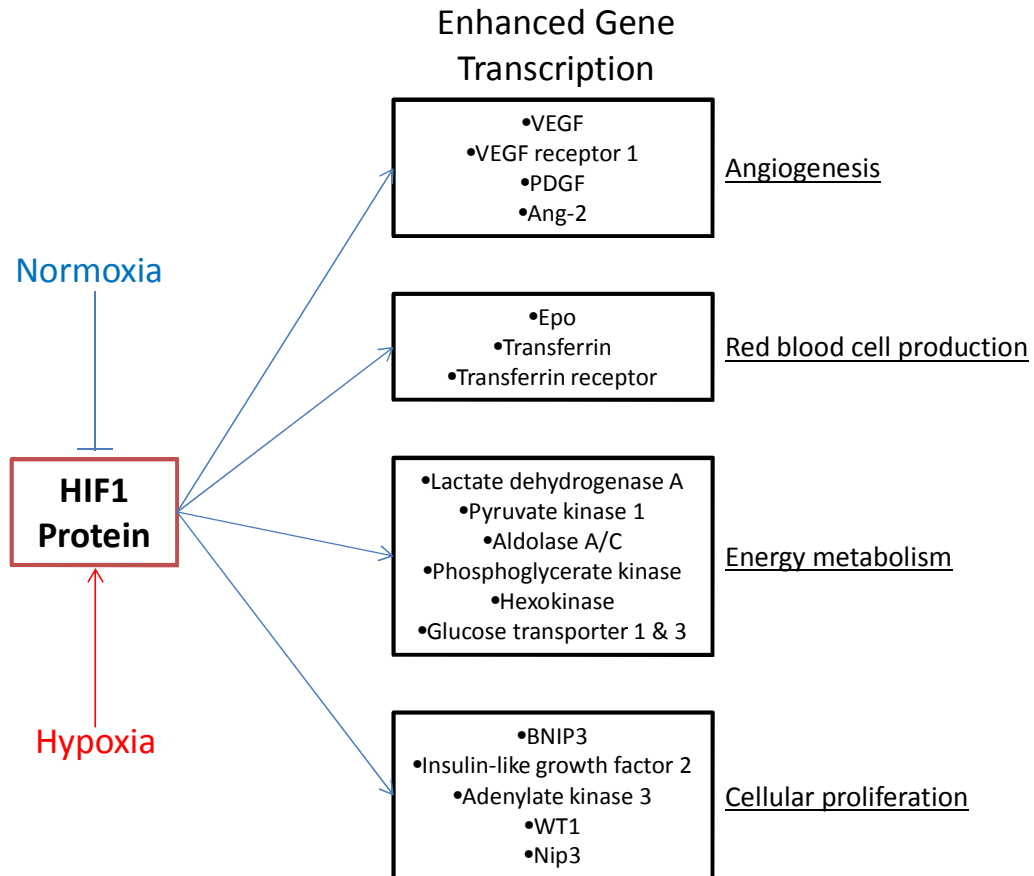


Figure 1.19: Transcriptional targets of HIF1. Multiple genes belonging to many different pathways are upregulated by HIF1 in order to allow for adaptation to low oxygen tensions. Unsurprisingly a lot of these genes are found upregulated in solid malignancies. These genes involved include VEGF and PDGF which are involved in angiogenesis; Epo and transferrin which are crucial for red blood cell production/maturation; lactate dehydrogenase and glucose transporters 1 and 3 that increase the uptake of glucose and anaerobic respiration (glycolysis); insulin-like growth factor and WT1 that are involved in cell proliferation and apoptosis respectively. Adapted from (Zagorska and Dulak, 2004).

1.12.3 Regulation of HIF1 α Protein Degradation

The HIF1 transcription factor is only active under hypoxic conditions; deregulated activation under normoxic conditions could lead to inappropriate proliferation of cells coupled with expression of genes that would promote anaerobic glycolytic respiration rather than the more efficient aerobic respiration. The discovery of regulation of HIF1 α protein was accomplished through observations of changes in HIF1 α protein levels following treatment with inhibitors of translation or redox reagents. Inhibition of translation by cyclohexamide following 2 hours hypoxic incubation did not cause a change in levels of HIF1 α , demonstrating that the hypoxic increase in HIF1 α was not due to an increase in translation rates (Huang et al., 1996). However, incubation of cells with the redox reagent H₂O₂ prevented HIF1 α protein accumulation and

DNA binding without effecting HIF1 α mRNA levels or translation (or HIF1 β protein or mRNA), suggesting that regulation of HIF1 α was due to a redox reaction targeted against the protein itself (Huang et al., 1996). Similar observations were also detected with the redox reagents N-ethylmaleimide, diamide and DTT (Huang et al., 1996; Wang et al., 1995b).

Specific inhibition of the ubiquitin 26S proteasome with lactocystin or MG132, but not of other cellular proteases prevented degradation of HIF1 α in normoxia following hypoxic exposure (Salceda and Caro, 1997). This gave the first indication that HIF1 α was regulated by ubiquitination and 26S proteasomal degradation. Comparison of the human HIF1-3 α , mouse HIF1 α and highly homologous *Drosophila* Sim protein revealed a highly conserved 15 amino acid sequence (corresponding to amino acids 557-571 of human HIF1 α). When this sequence alone was expressed in cells, it exhibited the same normoxic/hypoxic regulation as the full length protein and as such was named the oxygen dependent degradation (ODD) domain (Huang et al., 1998; Srinivas et al., 1999).

1.12.4 The von Hippel-Lindau (VHL) Protein

von Hippel-Lindau (VHL) disease is a hereditary human cancer syndrome that predisposes sufferers to highly angiogenic tumours, particularly of the kidney or blood vessels (haemangioblastomas). In these cancers, or in VHL deficient renal cell carcinoma cell lines (RCC4 and 786-0 cells), constitutive high expression of genes that contain HRE elements including VEGF and GLUT1 is observed, and this expression was down-regulated following re-expression of functional VHL (Maxwell et al., 1999). These findings indicated a possible role that VHL may have in regulation of HIF1 α . VHL was subsequently found to bind to HIF1 α and its expression to decrease HIF1 α protein levels without affecting its mRNA expression. Furthermore, in VHL negative cell lines (that have constitutively high HIF1 α protein levels) normoxic HIF1 α regulation was restored following functional VHL expression (Maxwell et al., 1999).

VHL is composed of an α and β domain; the α domain is able to bind cullin 2, elonginB/C and Rbx, This complex of proteins is collectively known as the VBC complex, which is a functional E3 ligase. The β domain is responsible for binding to the ODD domain of HIF1 α and specifically causes its ubiquitination leading to subsequent 26S proteasomal degradation (Stebbins et al., 1999; Ohh et al., 2000). However, the VBC complex was unable to ubiquitylate recombinant HIF1 α

that was produced in *E. Coli* unless it was pre-incubated with mammalian cell extracts, indicating VHL recognised a modified HIF1 α (Ivan et al., 2001).

1.12.5 Proline Hydroxylase (PHD) Proteins

MALDI-TOF and substitution analysis of amino acids within the ODD domain of HIF1 α showed that VHL only recognised HIF1 α when Prolines 402 and 564 were hydroxylated, however the identity of the endogenous hydroxylase was unknown (Ivan et al., 2001; Jaakkola et al., 2001; Yu et al., 2001; Masson et al., 2001). Multiple groups commonly identified HIF1 α ubiquitylation/degradation as being inhibited by 2-oxoglutarate analogues, iron chelators and hypoxia (Wang and Semenza, 1993a; Goldberg et al., 1988; Wang and Semenza, 1993b; Epstein et al., 2001). This implicated that proline hydroxylation could be facilitated by a member of the 2-oxoglutarate-dependent-oxygenases, as this family is dependent upon oxygen, iron and 2-oxoglutarate as cofactors.

Subsequent identification and cloning of *C. elegans* HIF-1 revealed it exhibited the same regulatory properties as the human homologue. It was rapidly degraded under normoxic conditions and stabilised in hypoxia with no change in mRNA levels. Furthermore VHL^{-/-} *C.elegans* had high HIF-1 levels in normoxia, and *in vitro* transcribed and translated (IVTT) VHL and HIF-1 only interacted following pre-incubation of HIF-1 with *C.elegans* lysate. This was found to be the result of hydroxylation of Proline 621 within HIF-1 (Epstein et al., 2001). Bioinformatic analysis of the *C. elegans* genome revealed a potential hydroxylase, *egl-9*, that when depleted in mutant *C. elegans* resulted in a significant increase in HIF-1 levels in normoxia.

Subsequent bioinformatic scrutinisation of the human genome identified 3 prolyl hydroxylase domain (PHD) containing proteins 1, 2 and 3 that were homologous to *egl-9*. These 3 proteins were able to hydroxylate HIF1 α and is the critical first step required in order for VHL recognition. Furthermore, in agreement with earlier studies, the PHD proteins were inhibited by cobalt ions, iron chelators and 2-oxoglutarate analogues (Epstein et al., 2001; Bruick and McKnight, 2001). Further mutational mapping identified the proline residues 402 and 564 within HIF1 α as the targets for PHD hydroxylation (Figure 1.18), with mutation of either causing a stabilisation of HIF1 α protein levels (Masson et al., 2001).

The PHD proteins are therefore the major oxygen sensors within the cell. When oxygen is abundant (20% O₂, normoxia), the PHD proteins are active and

hydroxylate HIF1 α , leading to recognition by VHL and subsequent ubiquitylation and degradation. However, under low oxygen concentrations (hypoxia) the activity of the PHDs is significantly reduced, allowing HIF1 α to escape hydroxylation and VHL recognition, thus causing an increase in HIF1 α protein levels. This is the central dogma of the regulation of HIF1 α and the subsequent intracellular response to low oxygen tensions (Figure 1.20).

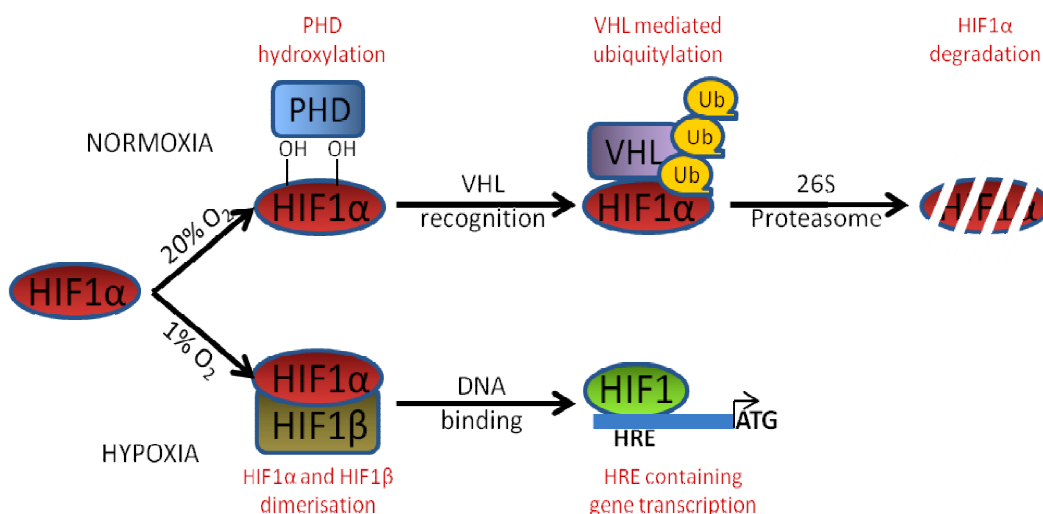


Figure 1.20: Overview of oxygen dependent regulation of HIF1 α . In high O₂ tensions (20%, normoxia), HIF1 α becomes hydroxylated at Pro402 and 564 by PHD2, allowing for recognition by the VHL component of the VBC E3 ubiquitin ligase, ubiquitination and degradation by the 26S proteasome. In hypoxia, HIF1 α dimerises with HIF1 β to form the active HIF1 transcription factor, which can bind to HREs within selected gene promoters and enhance their transcription in hypoxia.

1.12.6 Regulation of HIF1 α Transcriptional Activation

HIF1 and 2 α have 2 activation domains that were mapped using deletion analysis of a HIF1 α cDNA containing reporter plasmid; a centrally located N-terminal transactivation domain (NAD) (residues 531-575 of HIF1 α) and a C-terminal transactivation domain (CAD) (residues 786-826 of HIF1 α) (Pugh et al., 1997). The two transactivation domains contain less than 20% similarity, and appear to regulate different sets of hypoxic genes, however to date it is still not clear how or why this is the case (Dayan et al., 2006). Furthermore, as the NAD overlaps with the ODD domain of HIF1 α , experimentally it has been difficult to isolate its function.

Under hypoxic conditions, HIF-1 activates transcription by directly binding to the p300/CBP transcriptional activator proteins (Arany et al., 1996; Ebert and Bunn, 1998). p300/CBP is able to induce transcriptional activation through both the NAD and CAD. HIF-1 also binds in a hypoxia dependent manner to the transcriptional activators SRC-1 and TIF-2 (Carrero et al., 2000). However, to date this interaction has not been proven to be direct, and as such the p300/CBP interaction has been the most studied. p300/CBP acts as a co-activator, simultaneously binding HIF-1 and recruiting the general transcription factors to enhance PIC formation on the promoter, ultimately enhancing the rate of transcription. (Arany et al., 1996; Ebert and Bunn, 1998; Kallio et al., 1998).

In addition to the identification of the PHD proteins that hydroxylate HIF1 α , in 2001 through a yeast 2 hybrid screen another protein, factor inhibiting HIF-1 (FIH) was identified as binding to the CAD within HIF1 α (Mahon et al., 2001). Depletion of FIH induces HIF1 α responsive gene expression (Stolze et al., 2004) and through further studies, differential functions of the NAD and CAD have been observed, as FIH depletion only effects transcriptional activation of the CAD (Dayan et al., 2006).

FIH, like the PHDs is an oxygen and Fe²⁺ dependent hydroxylase (Lando et al., 2002a). FIH hydroxylates asparagine 803 (which lies within the CAD) under normoxic conditions and prevents HIF's association with the transcriptional co-activators p300/CBP, meaning HIF is only transcriptionally active in hypoxia (Hewitson et al., 2002; Lando et al., 2002b). The interaction between FIH and HIF1 α is largely abrogated in hypoxia, and in normoxia the interaction is mediated by VHL (Li et al., 2011). It has been shown that VHL and FIH can bind to histone deacetylases 1-3 (HDAC1-3) and this could possibly be a further mechanism of transcriptional inactivation (Mahon et al., 2001).

PHD2 and FIH have different K_m values with respect to oxygen, with the latter still active at lower oxygen tensions than PHD2. It has therefore been proposed that this could reflect differing degrees of HIF1 α mediated gene transcription depending on the distance from the blood vessel. Cells that are in close physical proximity to the blood supply will have inactive HIF1 α , due to high oxygen tensions allowing for PHD2 and FIH to be active. As the distance from the blood supply increases and oxygen tension decreases, PHD2 becomes inactivated, leading to an increase in HIF1 α protein levels, however as FIH is still active, only the NAD is transcriptionally active. As the distance increases even further,

approaching anoxic conditions, FIH is then inactivated, resulting in an active NAD and CAD to fully adapt to the hypoxic environment (Dayan et al., 2006).

Oxygen dependent degradation of HIF1 α is required to avoid normoxic activated HIF-1 gene transcription. Inhibition of HIF1 α degradation in normoxia by saturating the HIF1 α -degradation pathway through ectopic over-expression of a region of HIF1 α encompassing the ODD domain or treatment of cells with the PHD inhibitor DMOG or the 26S proteasome inhibitor MG132 all increased endogenous normoxic HIF1 α protein levels, nuclear accumulation and HIF-1 driven transcription (Hagg and Wennstrom, 2005). Therefore, even in normoxia, un-degraded HIF1 α is active and capable of initiating a hypoxic response.

1.12.7 Phosphorylation of HIF1 α

Before the cloning or regulatory pathways of HIF1 α had been identified, it was observed that HIF-1 DNA binding activity and induction of Epo RNA was ablated by either treatment with the protein kinase inhibitor 2-aminopurine or calf intestinal alkaline phosphatase (Wang and Semenza, 1993a). This evidence indicated that HIF-1 was positively regulated by phosphorylation.

SDS-PAGE analysis of *in vitro* transcribed and translated (IVTT) HIF1 α and lysates from different cultured cells identified differences in HIF1 α motilities; the IVTT HIF1 α was one discrete band, whereas the hypoxic extracts ran as a diffuse pattern, with a molecular weight of up to 12kDa more (Richard et al., 1999). Treatment of the hypoxic extracts with the general protein phosphatase lambda phosphatase abrogated the diffuse pattern observed. Treatment of cells with serine/threonine phosphatase inhibitor okadaic acid caused an increase in molecular weight of HIF1 α .

Observations of hypoxic phosphorylation of Elk-1 by mitogen activated protein kinases (MAPKs) lead to the identification of the p42 and p44 MAPKs as phosphorylating HIF1 α , but not HIF1 β , *in vitro* and *in vivo*. Furthermore, p42/44 MAPK activation enhanced HIF-1 transcriptional activity (Richard et al., 1999; Berra et al., 2000). It has also been postulated that other kinases are crucial for HIF1 α activity. Inhibition of the MEK1/ERK pathway did not affect HIF1 α stabilisation, but was crucial for HIF-1 transcriptional activities (Michiels et al., 2001). The PI-3K/Akt pathway when inhibited also caused an inhibition of hypoxic VEGF transcription (Minet et al., 2001). On a side note Akt is negatively regulated by PTEN; glioblastoma cell lines that lack functional PTEN, or

mutations within the catalytic domain of PTEN, all exhibit increased Akt activity, and more relevant increased VEGF transcription even in normoxia (Minet et al., 2001).

This evidence therefore shows phosphorylation of HIF1 α is critical for its DNA binding activity. The exact mechanisms and contributing factors are still unclear with regards to HIF1 α phosphorylation. The requirement of phosphorylation for HIF1 α transcriptional activity is evident, but further studies are required to determine the responsible kinases and if the kinases are universal or cell type specific.

1.12.8 Summary of HIF1 α Regulation

In 20% oxygen (normoxia), O₂ dependent hydroxylation of two conserved proline residues (402 and 564) by PHDs1-3 within the ODD domain of HIF1 α allows for recognition by the VHL containing E3 ubiquitin ligase VBC complex, subsequently causing HIF1 α ubiquitination and degradation by the 26S proteasome. Furthermore, the oxygen dependent asparagine hydroxylase, FIH, hydroxylates Asn803 within HIF1 α , preventing association with p300/CBP and inhibiting the ability of HIF1 to activate transcription. Combined, these two hydroxylase driven pathways prevent HIF1 α activity in normoxic conditions. In hypoxia the very low rate limiting oxygen tension prevents PHD hydroxylation and therefore a stabilisation of HIF1 α protein. This allows for HIF1 α phosphorylation, translocation to the nucleus and dimerisation with HIF1 β , to form HIF1. HIF1 then binds to hypoxic responsive elements (HRE) within the promoters of genes, and due to inactive FIH, associates with the transcriptional co-activator p300/CBP to enhance their transcription (Figure 1.21).

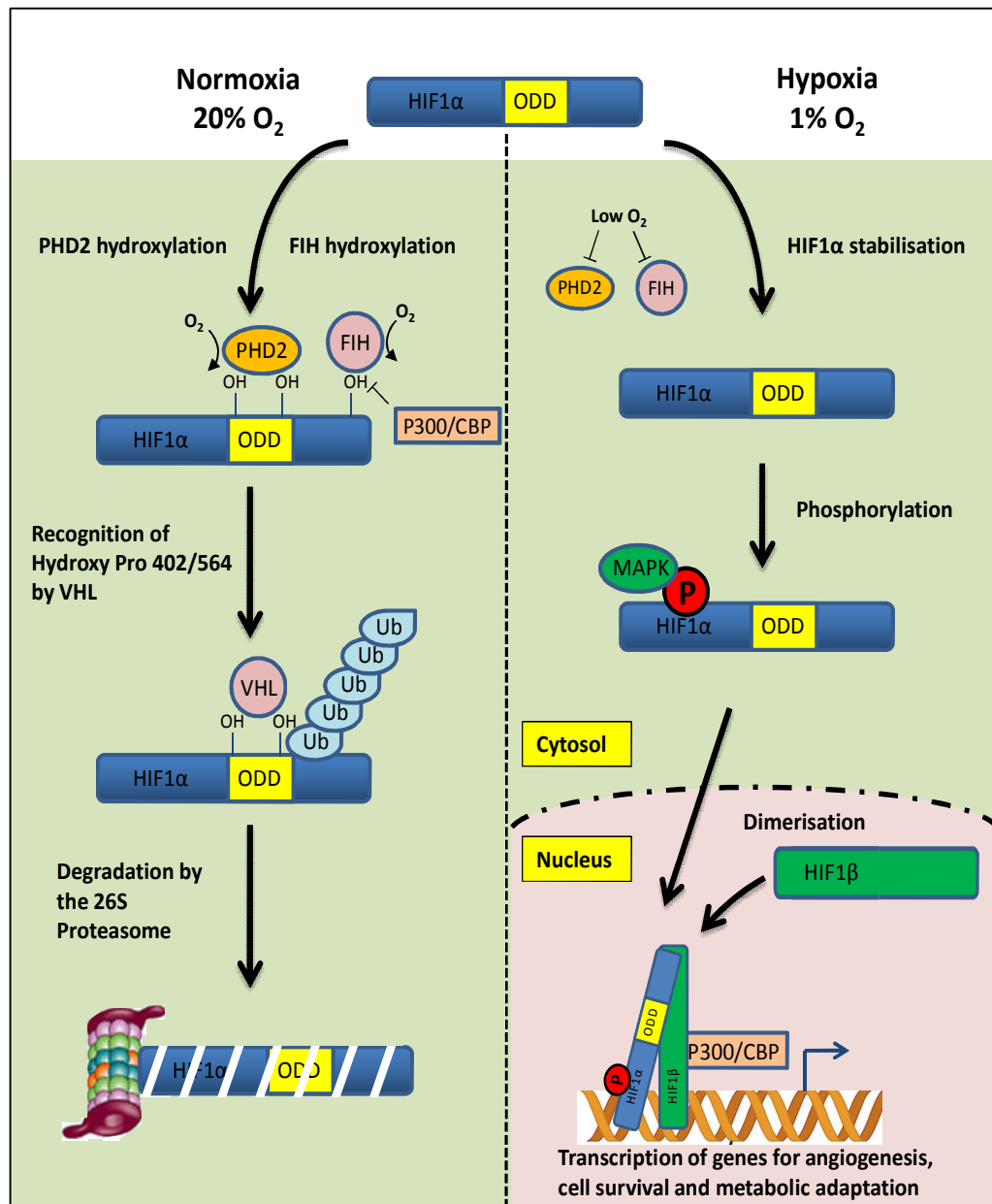


Figure 1.21: HIF1 α is rapidly degraded under high oxygen tensions. Under high oxygen tensions (20% O₂), Pro 402 and 564 within the ODD domain of HIF1 α are hydroxylated by PHD2. PHD2 uses oxygen as a cofactor, and is the rate limiting variable for PHD2 activity. Hydroxylation of HIF1 α allows for recognition by VHL, which is a component of the VBC E3 ubiquitin ligase complex. This leads to ubiquitination and subsequent 26S mediated degradation of HIF1 α . Furthermore under high oxygen tensions, HIF1 α is also hydroxylated by FIH on Asn 803. This hydroxylation prevents association with the transcriptional co-activator p300/CBP complex, meaning any undegraded HIF1 α in normoxia remains inactive. Under low oxygen tensions (hypoxia), PHD2 and FIH are inactive, and so HIF1 α protein is stabilised. This allows for subsequent phosphorylation, translocation into the nucleus and dimerisation with HIF1 β to form the active transcription factor HIF1. HIF1 then binds to hypoxic responsive elements (HREs) within selected genes that allow for adaptation to low oxygen conditions, recruits p300/CBP, causing transcriptional activation of the HRE containing genes.

1.12.9 Regulation of HIF1 α in Hypoxia

In hypoxia, stabilised HIF1 α protein allows for formation of the HIF1 transcription factor and subsequent enhanced transcription of HRE containing genes. However, if levels of HIF1 α protein continued to increase in hypoxia, this would lead to an exponential increase in expression of genes that allow for adaptation and cellular growth in low oxygen conditions, ultimately resulting in uncontrolled cellular proliferation. Therefore, following an initial stabilisation of HIF1 α it is critical that expression levels become attenuated.

Following an initial increase in HIF1 α protein within 4 hours of hypoxia, HIF1 α protein levels decrease following chronic hypoxic exposure (over 24 hours), whilst, in a seemingly counter-intuitive manner, levels of PHD2 increase (Ginouves et al., 2008). However, from recent studies it is now clear that in both acute and chronically hypoxic cells there is PHD2 activity still present, acting to degrade HIF1 α (Chan et al., 2005; Stiehl et al., 2006; Ginouves et al., 2008). Indeed the study by Stiehl *et al* demonstrated that siRNA targeted depletion of PHD2 in hypoxia resulted in a significant increase of HIF1 protein levels, showing PHD2 to be active in these conditions. This was a surprising observation given that low oxygen tension was thought to render PHD2 inactive, as molecular oxygen is the rate limiting K_m for PHD2 activity (Stolze et al., 2004).

In vitro assays with recombinant PHD2 revealed that under hypoxic conditions, significant PHD2 mediated hydroxylation of HIF1 α was still observed. Furthermore, increasing the amount of PHD2 protein under hypoxic conditions compensated for the lower enzymatic activity (due to very low levels of O₂ as a co-factor) and could restore the amount of HIF1 α hydroxylation in hypoxia to levels observed in normoxia (Stiehl et al., 2006). This suggested that the *in vivo* increase in PHD2 protein observed in hypoxia is a compensatory mechanism to allow for hypoxic hydroxylation and subsequent degradation of HIF1 α .

PHD1, 2 and 3 mRNA are all up-regulated in both primary and cultured cell lines (Marxsen et al., 2004; Aprelikova et al., 2004), observed after as little as 60 minutes hypoxic exposure, and remaining elevated even after 7 days hypoxia (Stiehl et al., 2006; Ginouves et al., 2008). The up-regulation was dependent upon HIF1 α , as either siRNA mediated depletion of HIF1 α or *HIF1 α* gene knockout in MEF cells ablated the hypoxic upregulation of the PHDs (Stiehl et al., 2006; Marxsen et al., 2004).

SAG (sensitive to apoptosis gene) belongs to the same family as Rbx1, a component of the VHL containing VBC ubiquitin ligase complex. Under hypoxia,

SAG mRNA and protein are up-regulated, again in a HIF1 α dependent manner. Under hypoxic conditions SAG forms a complex with VHL and facilitates hypoxic HIF1 α ubiquitination and degradation. In a similar effect to that observed with PHD2 depletion, siRNA mediated depletion of SAG resulted in a stabilisation of HIF1 α protein levels in both normoxia and hypoxia (Tan et al., 2008).

FIH protein levels are unaffected by either hypoxia or hypoxia mimics (e.g. DMOG) (Stolze et al., 2004). Again, unexpectedly, FIH was observed to be active and repress HIF1 α mediated gene expression in oxygen tensions as low as 0.2%. Furthermore, at this lower oxygen tension, in a concurrent experiment, PHD2 was totally inactive (Stolze et al., 2004). siRNA mediated depletion of FIH resulted in an up-regulation of PHD2 and 3, presumably through relief of Asn 802 hydroxylation (Stolze et al., 2004). These proteins are upregulated in hypoxia in a HIF1 α dependent manner (Stiehl et al., 2006), and as such FIH could be viewed as a further hypoxic regulator of both PHDs and HIF1 α .

Therefore, a hypoxic negative feedback loop appears to exist to regulate the expression of HIF1 α and explain the observed decrease in HIF1 α protein levels following prolonged (chronic) hypoxia (Figure 1.22). A decrease in rate limiting oxygen tension reduces the activity of PHD2, which reduces hydroxylation and VHL mediated ubiquitination of HIF1 α . This causes an increase in levels of HIF1 α protein which leads to increased levels of active HIF-1. Furthermore, FIH also becomes inactive, increasing association with p300/CBP and HIF1 α driven gene transcription. As the time in hypoxia increases, the increased transcriptionally active HIF1 α causes an increase in PHD2 mRNA and protein, which facilitates increased hydroxylation of HIF1 α . Furthermore, levels of SAG protein also increases, facilitating VHL mediated ubiquitination and degradation of hydroxylated HIF1 α . Concurrently however, FIH still exerts inhibitory effects on HIF1 α driven transcription as it is still active at oxygen tensions lower than that required for PHD2 activity. This causes a slight repression of PHD2 transcription, contributing to the time lag prior for maximal HIF1 α degradation as well as inhibiting other HRE driven gene transcription.

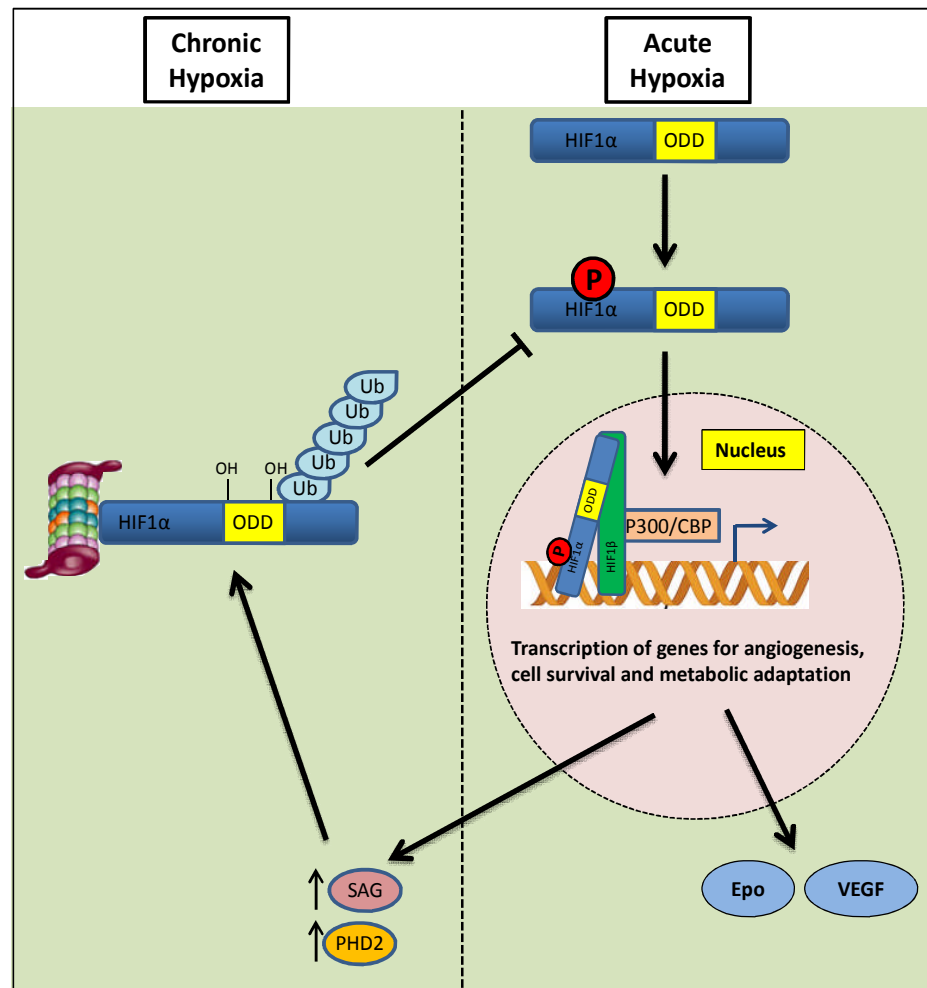


Figure 1.22: Levels of HIF1 α protein are regulated by negative feedback loops in hypoxia. Under low oxygen tensions, PHD2 has significantly reduced activity due to low levels of its rate limiting cofactor O₂. This results in no hydroxylation of HIF1 α , leading to stabilised protein levels. HIF1 α is then phosphorylated and translocates into the nucleus, where it dimerises with HIF1 β to form a HIF1 dimer. HIF1 binds to hypoxic responsive elements (HREs) that are contained in the promoters of many genes that allow the cell to adapt to low oxygen tensions. PHD2 and SAG both contain functional HREs and are upregulated in hypoxia. The upregulation of PHD2 compensates for its reduced activity, restoring hydroxylation of HIF1 α and its subsequent degradation. This results in decreased HIF1 formation and a decrease in associated transcription. Furthermore, FIH is active even under conditions that approach anoxia, and acts as a further negative regulator of transcription by hydroxylating Asn803 on HIF1 α and preventing association with p300/CBP.

In summary, cells are able to adapt and survive in low oxygen tensions by up regulating expression of proteins and enzymes involved in glycolysis, glucose uptake, angiogenesis, vascularisation and red blood cell production and maturation through the transcription factor HIF1. Following prolonged exposure to hypoxia, up-regulation of PHD and SAG proteins facilitate the hypoxic degradation of HIF1 α (as in normoxia), providing a negative regulatory feedback loop and preventing an exponential increase in HIF1 α protein and subsequent HRE containing genes.

1.13 Preliminary Data

1.13.1 The Role of LIMD1 in Regulation of Hypoxia

In a yeast-2-hybrid screen to identify LIMD1 interacting partners, LIMD1 amino acids 1-363 (denoted $\Delta 364-676$) fused to a GAL4 DNA binding domain was screened against a HeLa cell cDNA library. This obtained a cDNA encoding one of the HIF1 α prolyl hydroxylases, PHD1, as being a potential binding partner (Figure 1.23).

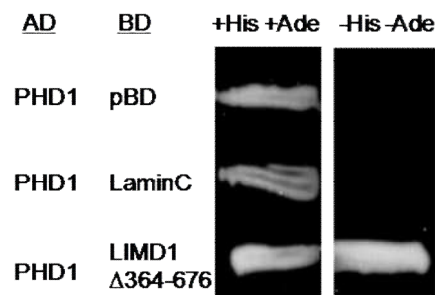


Figure 1.23: LIMD1 interacts with prolyl hydroxylase 1 in a yeast 2 hybrid screen. A Y2H screen with LIMD1 amino acids 1-363 (denoted $\Delta 364-676$) fused to a GAL4 DNA binding domain identified PHD1 (fused to a GAL4 activation domain) as a binding partner from a HeLa cDNA library. Binding domain vector only or laminC were used as negative controls (Dr T. Sharp, unpublished data).

1.13.2 LIMD1 binds to the Proline Hydroxylases and VHL

The interaction with PHD1 was then confirmed through co-immunoprecipitation studies using ectopically over-expressed PHD1, 2 and 3 with LIMD1 and the other Zyxin family members. This confirmed that LIMD1 bound PHD1, and also was the only Zyxin family member to bind to PHD2 and 3 (Figure 1.24). As PHD2 is the main proline hydroxylase involved in HIF1 α hydroxylation, and uniquely bound to LIMD1 (but not the other Zyxin family members), this was the main focus of subsequent studies.

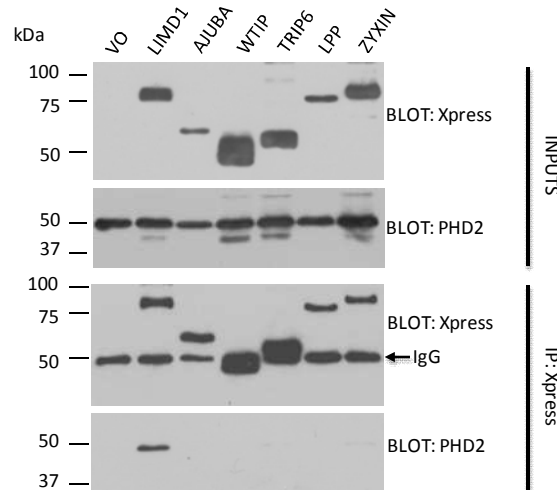


Figure 1.24: LIMD1 binds to PHD2 in vivo. Xpress tagged Zyxin family members were co-transfected with un-tagged PHD2 into U2OS cells, and immunoprecipitated with an anti-Xpress antibody. Following immunoprecipitation of the family members, PHD2 only co-immunoprecipitated with LIMD1 (Dr T. Webb, unpublished data).

Under normoxic conditions HIF1 α is initially hydroxylated by PHD2 and then recognised by VHL, leading to its ubiquitination and subsequent proteasomal degradation. As LIMD1 bound to PHD2, further investigations were performed to examine if VHL also bound to LIMD1, which was indeed found to be the case (Figure 1.25).

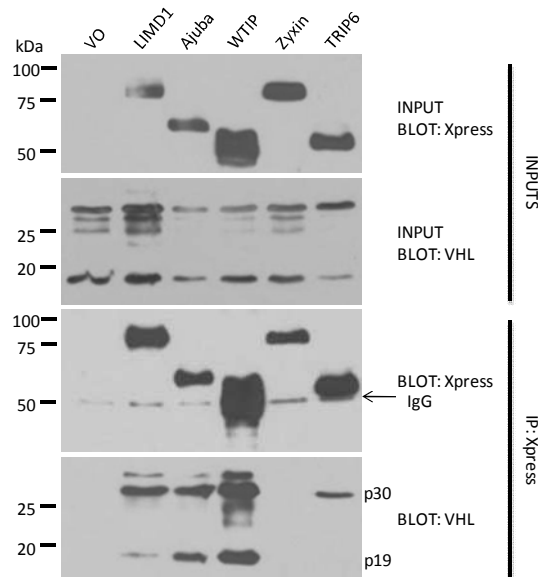


Figure 1.25: LIMD1 binds to VHL in vivo. Xpress tagged Zyxin family members were co-transfected with V5 tagged VHL into U2OS cells and the family members immunoprecipitated with anti-Xpress antibody. VHL expresses as both p19 and p30 isoforms due to an internal initiation codon, and both isoforms specifically co-immunoprecipitated with LIMD1, Ajuba and WTIP (Dr T. Webb, unpublished data).

1.13.3 LIMD1 Bridges the Association between PHD2 and VHL

LIMD1 was found to bind both PHD2 and VHL, however, as PHD2 and VHL do not directly interact, it was reasoned that LIMD1 could either exist in the same complex as, or form a scaffold between, these two proteins. In ectopic expression studies, immunoprecipitation of VHL in the absence of transfected LIMD1 resulted in only very low levels of associated PHD2, however, when LIMD1 was co-transfected this resulted in significantly increased co-immunoprecipitation of PHD2 with VHL (Figure 1.26). From these observations the hypothesis was suggested that LIMD1 was acting as a scaffold to bridge the association between VHL and PHD2 into a single complex, thus creating an 'enzymatic niche' to enhance the efficiency of HIF1 α degradation.

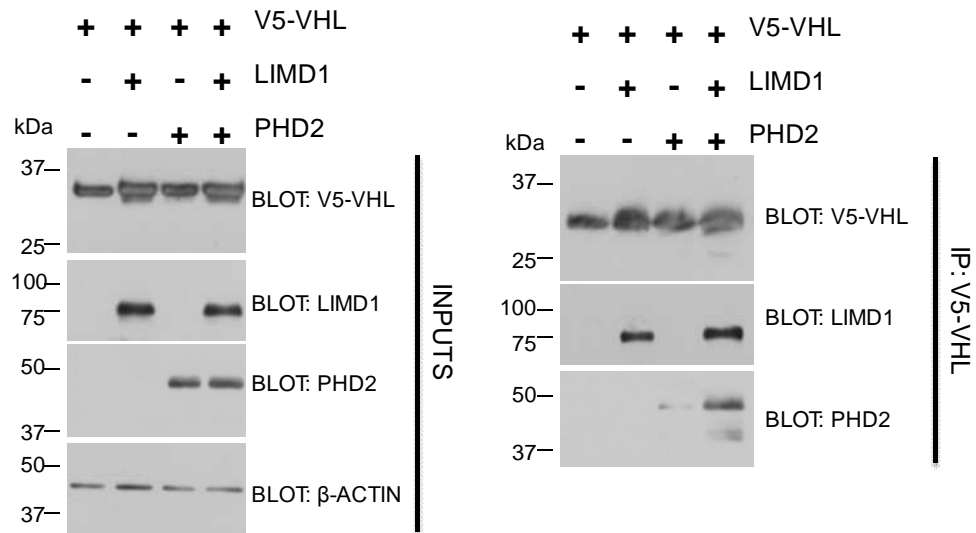


Figure 1.26: LIMD1 acts as a scaffold protein to simultaneously bind VHL and PHD2. VHL was co-transfected with LIMD1 and PHD2 either individually or in combination into U2OS cells and VHL immunoprecipitated. (A) 2% input blots indicate protein expression prior to immunoprecipitation. (B) LIMD1 co-immunoprecipitated both in the presence and absence of PHD2. However, co-immunoprecipitation of PHD2 was significantly enhanced upon expression of LIMD1 (Dr T. Webb, unpublished data).

1.13.4 Loss of LIMD1 Inhibits HIF1 α Degradation

It was next reasoned that if LIMD1 was indeed forming an enzymatic complex with PHD2 and VHL, it was reasoned that upon LIMD1 loss/depletion, the HIF1 α degradation pathway would be inhibited and result in an increase in HIF1 α protein levels. siRNA mediated depletion of LIMD1 resulted in an increase in HIF1 α protein levels, akin to that seen following depletion of PHD2 (Figure 1.27).

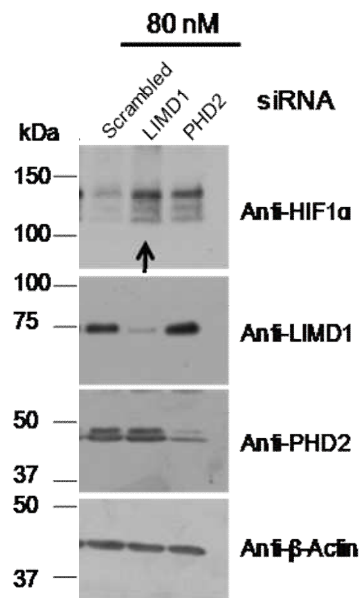


Figure 1.27: siRNA mediated depletion of LIMD1 causes an increase in HIF1 α protein levels. HEK293 cells were transfected with 20 or 80nM siRNA targeting LIMD1, PHD2 or a scrambled control. 48 hours post-transfection cells were lysed and lysates assayed by Western blot. Depletion of LIMD1 or PHD2 caused a significant increase in levels of HIF1 α protein (Dr T. Webb, unpublished data).

Collectively, these observations suggest that LIMD1 acts as a scaffold to bridge the association between VHL and PHD2, concentrating their respective activities into an enzymatic niche. Furthermore, loss of LIMD1 disrupts this complex formation, inhibiting HIF1 α degradation and resulting in an increase in HIF1 α protein levels in normoxia.

1.14 Thesis Aims and Objectives

There are three distinct areas of LIMD1 biology that form the aims and objectives of this thesis.

1. LIMD1 protein expression is down regulated in up to 80% of lung cancers, as well as in breast cancer and chromosomal alterations identified in HNSCC and childhood acute lymphoblastic leukaemias (Sharp et al., 2004; Sharp et al., 2008; Spendlove et al., 2008; Ghosh et al., 2008). Specifically in lung adenocarcinomas, LIMD1 protein loss could be attributed to gene deletion (32%) and loss of heterozygosity (12%). However, these 44% of genetic alterations was significantly lower than the observed 79% of lung cancers exhibiting protein loss. It was therefore hypothesised that this 35% shortfall could be explained by *LIMD1* promoter methylation within the putative CpG Island (Figure 1.14), causing epigenetic silencing of the gene. Therefore the first aim was to investigate if the *LIMD1* promoter is methylated in transformed cells, and if so does it correlate with silencing of the *LIMD1* gene.
2. From the preliminary data, the putative CpG Island appeared to be critical for transcription. The second aim was to identify why the CpG Island was so important for transcription, and to identify possible transcription factors that may bind to the promoter to activate *LIMD1* gene expression. Identification of the transcription factor(s) that activates *LIMD1* transcription could provide another explanation for LIMD1 protein loss in transformed cells.
3. Preliminary studies had identified LIMD1 as a negative regulator of HIF1 α (Figure 1.27). The working hypothesis was through formation of a complex with the oxygen dependent proline hydroxylase PHD2 and the VHL containing E3 ubiquitin ligase VBC complex, LIMD1 facilitated HIF1 α degradation, identifying a novel tumour suppressive function of LIMD1. Therefore, the final distinct objective within this thesis was to investigate if LIMD1 expression changes in hypoxia, and to obtain endogenous data to further the understanding and evidence that LIMD1 may form a complex with PHD2/VHL to regulate the intracellular hypoxic response.

Chapter 2 Materials and Methods

2.1 Materials

2.1.1 Media and Selection Drugs

2.1.1.1 Bacterial Media

LB Broth (LB) (L3522-1KG, Sigma-Aldrich, Saint Louis, USA). LB was dissolved in distilled water (2.5% w/v) and autoclaved at 121°C for 20 minutes. Stored at room temperature with required antibiotics added immediately prior to use.

LB-Agar (L2897-1KG, Sigma-Aldrich, Saint Louis, USA). LB-agar was dissolved in distilled water (3.5%w/v) and autoclaved at 121°C for 20 minutes. The agar was allowed to cool to ~50°C and the required antibiotic was added, mixed well and poured into sterile petri dishes (25ml/plate). Plates were allowed to set at room temperature and stored for up to 4 weeks at 4°C.

2.1.1.2 Cell Culture Media

Dulbecco's Modified Eagle's Medium (DMEM) (D6429, Sigma-Aldrich, Saint Louis, USA). DMEM contained 4500mg/L glucose, 2mM L-glutamine and 100mg/L sodium pyruvate and was supplemented with 10% (v/v) Foetal calf serum (FCS) and 1% (v/v) penicillin/streptomycin and stored at 4°C. Selection drugs were added immediately prior to use.

RPMI-1640 Medium: (R8758, -Aldrich, Saint Louis, USA). RPMI contained 2000mg/L glucose and was supplemented with 10% (v/v) Foetal calf serum (FCS) and 1% (v/v) penicillin/streptomycin and stored at 4°C.

Fetal Bovine Serum (FBS): (F9665, Sigma-Aldrich, Saint Louis, USA). FBS was aliquoted into 50ml aliquots and stored at -20°C. FBS was added to cell medium within a cell culture fume hood.

1x Trypsin/EDTA Solution: (T3924, Sigma-Aldrich, Saint Louis, USA). The solution contained 0.5g/100ml porcine trypsin, 0.2g/100ml EDTA per litre of Hanks' Balanced Salt Solution (HBSS) and phenol red. Working aliquots were stored at 4°C and pre-warmed to 37°C in a water bath prior to use.

Opti-MEM®: (31985, GIBCO, N.Y. USA). Opti-MEM® serum free media was aliquoted and stored at 4°C.

2.1.2 Antibiotics and Selection Drugs

5-Aza-2'-deoxycytidine: (A3656, Sigma-Aldrich, Saint Louis, USA). A stock solution was prepared at a concentration of 100mM in DMSO and stored at -80°C.

Ampicillin: (A2804-50MG, Sigma-Aldrich, Saint Louis, USA). A stock solution of ampicillin was prepared at a concentration of 100mg/ml in distilled water, filter sterilised through a 0.2µm filter and stored at -20°C. The standard working concentration was 100µg/ml.

Chloramphenicol: (C0378, Sigma-Aldrich, Saint Louis, USA). A stock solution of chloramphenicol was prepared at a concentration of 50mg/ml in 100% ethanol and stored at -20°C. The standard working concentration was 50µg/ml.

Kanamycin: (420311, Merck Chemicals, Germany). A stock solution of kanamycin was prepared at a concentration of 50mg/ml in distilled water, filter sterilised through a 0.2µm filter and stored at -20°C. The standard working concentration was 50µg/ml.

Penicillin/Streptomycin: (P0781, Sigma-Aldrich, Saint Louis, USA). Penicillin/Streptomycin solution contained 10,000 units of Penicillin and 10mg/ml Streptomycin in 0.9% NaCl. Working aliquots were stored at 4°C.

2.1.3 Buffers and Solutions

2.1.4 Bacteriological Buffers and Solutions

Transformation Buffer (TB): 15mM CaCl₂, 250mM KCl and 10mM PIPES were dissolved in distilled water and the pH adjusted to 6.7 with 1M KOH. 55mM MnCl₂ was then dissolved after the pH was adjusted (otherwise it would fall out of solution) and was filter sterilised through a 0.2µm filter.

PreScission Protease Buffer: 50mM Tris-HCl pH7.0, 150mM NaCl, 1mM EDTA, 1mM DTT were dissolved in water and stored at 4°C.

2.1.5 DNA Buffers

Tris-Acetate-EDTA (TAE) (50X): 2M Tris base, 250mM Sodium Acetate, 50mM EDTA were dissolved in distilled water and the pH adjusted to 8.0 with HCl. The 50X stock solution was stored at room temperature and diluted to a 1X working solution with distilled water.

DNA Agarose Gel Loading Buffer (10x): 50% (v/v) glycerol and 0.25% (w/v) Bromophenol Blue were dissolved in 1X TAE and stored at room temperature. When added to a DNA sample the final concentration was 1X.

Oligo Annealing Buffer (1X): 10mM Tris-HCl pH 7.5, 50mM NaCl, 1mM EDTA were dissolved in distilled water and stored at room temperature.

2.1.6 Cell Lysis/Wash Buffers

Phosphate Buffer Saline (PBS) (10 X): (11666789001, Roche Diagnostics GmbH, Mannheim, Germany). Premixed 10x PBS contained 2.5mM KH_2PO_4 , 25mM Na_2HPO_4 , 0.34 M NaCl, 6.75mM KCl, pH 7.4 was diluted to 1 X with distilled water and stored at room temperature.

RIPA: 150 mM NaCl, 1% (v/v) IGEPAL-630, 0.5% (w/v) sodium deoxycholate, 0.1% (w/v) SDS and 50mM Tris were dissolved in distilled water, the pH adjusted to 8 and stored at 4°C.

Passive Lysis Buffer (PLB) (5 X): (E1941, Promega, Madison, USA). 5 x PLB, was stored at -30°C and diluted to 1 X with distilled water immediately before use, with subsequent lysates stable for 6 hours at room temperature.

Chromatin Immunoprecipitation Lysis Buffer: 50mM Tris-HCl pH8.0, 1% SDS, 10mM EDTA. Stored at room temperature.

Hypotonic Lysis Buffer: 20mM HEPES, pH 7.9, 50mM NaCl, 1mM EDTA, 1mM EGTA, 20mM NaF, 1mM Na_3VO_4 , 1mM $\text{Na}_4\text{P}_2\text{O}_7$, 2mM benzamide, 1mM dithiothreitol were dissolved in distilled water and stored at 4°C.

Hypertonic Lysis Buffer: 20mM HEPES, pH 7.9, 420mM NaCl, 1mM EDTA, 1mM EGTA, 20mM NaF, 1mM Na_3VO_4 , 1mM $\text{Na}_4\text{P}_2\text{O}_7$, 2mM benzamide, 1mM dithiothreitol, 20% glycerol were dissolved in distilled water and stored at 4°C.

Protease and Phosphatase Inhibitors: (Roche, Mannheim, Germany). One Complete™ EDTA free Protease Inhibitor Cocktail tablet and two PhosSTOP™ Phosphatase Inhibitor Cocktail tablets were dissolved in 20ml of lysis buffer and either stored at 4°C <1 week or at -20°C for <1 month.

MG-132 Proteasome Inhibitor: (PI102-0005, Biomol International, Enzo Life Sciences Ltd, UK). A 10mM MG-132 stock solution was prepared by dissolving

MG-132 powder in sterile DMSO (Dimethyl Sulfoxide, D2438, Sigma-Aldrich) and stored at -80°C for <2 months. Standard working concentration was 10µM.

2.1.7 Solutions for Sodium Dodecyl Sulphate-Polyacrylamide Gel Electrophoresis (SDS-PAGE) and Immunoblotting

5 x SDS-PAGE Sample buffer: 50% (v/v) Glycerol, 250mM Tris-HCl pH 6.8, 5% (w/v) SDS, 5% (v/v) β-Mercaptoethanol and 0.05% (w/v) Bromophenol Blue were dissolved in distilled water and the buffer aliquoted and stored at -20°C.

PBS-Tween: 0.05% (v/v) Tween[®]20 (P2287-500ml, Sigma-Aldrich, Saint Louis, USA) was added to 1 x PBS and stored at room temperature.

SDS-PAGE Running Buffer (10 X): 0.25M Tris, 1.92M Glycine and 1% (w/v) SDS were dissolved in distilled water and stored at room temperature. A 1 x solution was prepared by diluting the 10 x stock in distilled water.

Transfer Buffer: Tris-Glycine transfer buffer solution (10 X) (250mM Tris-HCl pH 7.5, 2M glycine, [93015, Fluka, Sigma-Aldrich, UK]) was diluted to 1X in distilled water containing 10% (v/v) methanol and stored at 4°C.

Blocking Solution: Marvel dried skimmed milk powder (5% w/v) was dissolved in 1 x PBS-Tween and stored <1 day at 4°C.

Coomassie Blue Protein Stain: 0.12% (w/v) Coomassie Brilliant Blue R, 50% (v/v) Methanol and 20% (v/v) Glacial Acetic Acid solution were dissolved in distilled water, filtered through 3MM filter paper and stored at room temperature.

Coomassie Blue De-staining solution: 10% (v/v) Methanol and 10% (v/v) Glacial Acetic Acid were dissolved in distilled water and stored at room temperature.

Ponceau S Protein Stain: 0.1% [w/v] Ponceau S and 10% (v/v) Glacial Acetic Acid solution were dissolved in distilled water and stored at room temperature.

Resolving Gel Buffer: ddH₂O and bis-acrylamide (30% stock solution) were supplemented with 0.375M Tris pH8.8 and 0.1% SDS. The amount of bis-acrylamide was altered to achieve the desired percentage gel depending upon

the size of protein to be resolved. Generally, 15% bis-acrylamide gels were used to resolve proteins below 37kDa, and 8% gels used to resolve proteins between 25 and 150kDa. 0.1% ammonium persulphate was added (to cross-link the acrylamide), and this was catalysed by addition of 0.01% N,N,N',N'-tetramethylethylenediamine (TEMED) immediately before pouring. A straight horizontal gel was achieved by overlaying with 100% EtOH whilst polymerising.

Stacking Gel Buffer: 5% bis-acrylamide was supplemented with 0.125M Tris pH6.8, 0.1% SDS and 0.1% ammonium persulphate. 0.01% TEMED was added to catalyse polymerisation of the gel. Gel combs were inserted straight after pouring the stacking gel to create wells in the gel to load sample.

2.1.8 Dual-Luciferase Reporter Assay Solutions

Dual-Luciferase Reporter Assay System: (E1960, Promega, Madison,USA). The kit comprised of 5x Passive Lysis Buffer (see above), a Luciferase Assay Buffer and Stop & Glo[®] Reagent for the measurement of firefly and renilla luciferase respectively. Components were stored at -20°C and once reconstituted at -20°C for <1 month or -80°C for <6 months.

2.1.9 Human Tumour Samples

One sample each of fresh tumour tissue and normal lung parenchyma distant from tumour were collected from patients undergoing operative resection of lung cancer at the Royal Brompton Hospital. Samples were snap-frozen in isopentane and stored at -80°C. Specific consent for usage of tissue for non-diagnostic use was obtained from patients. Ethical approval for the study was obtained from the Brompton, Harefield and NHLI Research Ethics Committee, U.K by Dr Andrew Nicholson (Ref 03-112).

2.1.10 Antibodies

Antigen	Dilution for Western Blot	Host Species	Molecular Weight (kDa)	Company	Catalogue Number
Primary Antibodies					
LIMD1	1:500	Mouse	72	(Sharp <i>et al</i> 2004)	N/A
Xpress	1:5000	Mouse	N/A	Invitrogen	46-0528
HA	1:1000	Rabbit	N/A	Sigma-Aldrich	H6908
GFP	1:1000	Mouse	27	Roche	11814460001
β -Actin	1:50000	Mouse	42	Sigma-Aldrich	A1978
PU.1	1:1000	Rabbit	32-42	Cell Signalling	#2266
Ets-1	1:1000	Mouse	50	BD Transduction Laboratories™	E34620
Elk-1	1:1000	Rabbit	45	Santa Cruz	SC22804
HIF1 α	1:500	Mouse	120	BD Transduction Laboratories™	610959
PHD2	1:1500	Rabbit	46	Abcam	AB4561
PHD2	1:1500	Mouse	46	Millipore	05-1327
VHL	1:400	Mouse	19-30	BD Transduction Laboratories™	536347
Elongin B	1:750	Rabbit	18	Santa Cruz	SC11447
Cullin 2	1:750	Rabbit	87	Abcam	AB1870
Secondary Antibodies					
Mouse	1:2500-5000	Goat	-	DAKO	P0447
Rabbit	1:5000	Goat	-	DAKO	P0448

Table 1: Table of primary and secondary antibodies used for immunoblotting with the working dilutions, host species, predicted molecular weight, manufacturing company and catalogue number indicated.

2.2 Methods

2.2.1 Bacterial Culture methods

2.2.2 Preparation of Chemically-Competent Cells

2ml of a starter culture of DH5 α *E.coli* was used to inoculate 200ml of sterile LB. The bacteria were grown at 22°C overnight with vigorous shaking (220rpm) until they reached an OD₆₀₀ of ~0.5. The culture was then chilled on ice for 15 minutes, divided into 4 and pelleted by centrifugation. The bacterial pellets were each resuspended in 20ml of filter sterilised ice cold transformation buffer (TB) and the 4 suspensions combined into 2. Cells were then chilled on ice for 10 minutes and then re-centrifuged (15 minutes, 4000g, 4°C). The pellets were again resuspended in 20ml of ice cold TB and centrifuged as before. The resulting pellets were then each resuspended in 5ml of ice cold TB, recombined into one tube and DMSO added (10% v/v). The bacteria were then incubated on ice for 10 minutes and aliquoted into sterile 1.5ml eppendorf tubes (200 μ l/tube), flash frozen in liquid nitrogen and stored at -80°C.

2.2.3 Transformation and Propagation of Chemically Competent DH5 α Bacteria

200 μ l aliquots of chemically competent DH5 α bacteria were gently thawed on ice and gently tapped to ensure complete resuspension of the cells. 5 μ l of ligated DNA or 10ng of plasmid DNA were added to the bacteria and incubated on ice for 30 minutes. The bacteria were heat shocked in a still water bath (42°C, 45 seconds) and then returned to ice to recover for 2 minutes. 500 μ l of Luria Broth (LB) was added to the bacteria before being incubated at 37°C with vigorous shaking (220 rpm) for 60 minutes. 10-200 μ l of the bacteria were spread onto LB-agar plates containing the appropriate antibiotic and incubated overnight at 37°C.

Plates were removed from the incubator the next morning and stored at 4°C. Late afternoon individual colonies were picked with a sterile 10 μ l pipette tip and inoculated in 5ml of LB containing the same appropriate antibiotic. Inoculated cultures were then incubated overnight (37°C, 220rpm) for a maximum of 16hours and the bacteria harvested through centrifugation (6,000g, 15 minutes).

2.2.4 Nucleic Acid Techniques

2.2.5 Plasmid DNA Extraction

Plasmid DNA was extracted from small scale cultures of transformed bacteria (<10ml) using the QIAprep Spin Miniprep Kit (27106, QIAGEN, Maryland, USA). Briefly, harvested bacteria were resuspended in 250µl of RNase A containing buffer P1 and transferred into sterile 1.5ml microcentrifuge tubes. Bacteria were lysed by addition and gentle mixing of 250µl alkaline lysis buffer P2 and incubated at room temperature for 5 minutes. Alkaline lysis was neutralised and cell debris, lipids, chromosomal DNA and SDS precipitated by addition of 350µl neutralisation buffer N3 followed by centrifugation at 13,000g for 10 minutes. Plasmid DNA was then bound to the silica membrane within the QIAprep spin column by passing the cleared supernatant through and centrifugation for 1 minute at 13,000g. Residual salt and other bacterial contaminants were removed by washing the column with 750µl of wash Buffer PE, followed by centrifugation for 2 minutes into a clean microcentrifuge tube to remove residual ethanol from the wash buffer that could interfere with downstream processes. Plasmid DNA was then eluted into a clean microcentrifuge tube by addition of 75µl HPLC H₂O and centrifugation for 1 minute at 13,000g.

For large cultures (50ml), plasmid DNA was extracted using the Qiagen Plasmid Midi Kit (12143, QIAGEN, Maryland, USA). Briefly, bacteria were harvested and resuspended in 4ml of Buffer P1, lysed through the addition of 4ml Buffer P2 for 5 minutes and neutralised with 4ml Buffer P3. After 15 minute incubation on ice to aid precipitation of SDS, chromosomal DNA, lipids and cell debris the lysate was cleared by centrifugation at 20,000g for 30 minutes at 4°C. The cleared lysate was decanted into a clean centrifuge tube and further cleared by centrifugation for another 15 minutes. The plasmid DNA was then bound to a QIAGEN-100 tip (equilibrated with 4ml Buffer QBT) by passing the supernatant through under gravity flow. The tip was washed by passing 2X 10ml of Buffer QC through under gravity before elution into a clean centrifuge tube by addition of 5ml Buffer QF. Eluted plasmid DNA was precipitated with 3.5ml isopropanol and centrifuged at 15,000g for 30 minutes at 4°C. The resultant DNA pellet was washed and resuspended in 3ml 70% (v/v) ethanol and centrifuged at 15,000g for 15 minutes at 4°C. The DNA pellet was then air-dried for 15 minutes and resuspended in 400µl HPLC H₂O.

2.2.6 Genomic DNA Extraction

Genomic DNA from cultured cells and lung tissue samples was extracted using the QIAamp DNA Mini Kit (51306, QIAGEN, Maryland, USA). Briefly, 5×10^6 adherent monolayer cells were washed twice in ice cold PBS and then scraped and resuspended in 1ml of ice cold PBS. Cells were centrifuged 3,500g for 5 minutes at 4°C and the resultant cell pellet resuspended in 200µl ice cold PBS. 20µl of proteinase K and 4µg RNase A was then added. 200µl of lysis Buffer AL was added and pulse-vortexed for 15seconds prior to incubation at 56°C for 10minutes. 200µl of 100% ethanol was then added, pulse-vortexed for 15seconds, the liquid transferred to a QIAamp Mini spin column and centrifuged at 8,000g for one minute to bind the DNA to the column. The column was then sequentially washed and centrifuged (13,000g, one minute) with 500µl each of wash buffer AW1 and AW2. The column was then centrifuged for an additional minute to remove any residual wash buffer and the DNA eluted in 2x 200µl of HPLC H₂O.

For lung tissue samples, 50µl of PBS was added to 20mg of tissue in a 1.5ml microcentrifuge tube and the tissue homogenised until no solid tissue was visible. 100µl of lysis Buffer ATL and 20µl of proteinase K were added and incubated at 56°C for 10minutes. 4µg of RNase A was then added and incubated at room temperature for 2 minutes. 200µl of Buffer AL were then added, pulse-vortexed for 15seconds and incubated at 70°C for 10minutes. 200µl of 100% ethanol was then added and the remaining steps carried out identically to the method for monolayer cells above.

2.2.7 RNA Extraction and cDNA Synthesis

RNA was extracted from lung tissue using TriPure Isolation Reagent (11667157001 Roche Applied Science, Germany). 50mg of flash frozen lung tissue was homogenised in 1ml of TriPure and incubated at room temperature for 5 minutes to allow for complete lysis. Homogenates were then clarified of insoluble polysaccharides, lipids and membranes by centrifugation at 13,000g for 10 minutes at 4°C. 0.2ml of chloroform was added and the homogenates vortexed vigorously for 15 seconds prior to phase separation by centrifugation at 13,000g for 15 minutes. After centrifugation there was 3 phases; an upper aqueous phase containing RNA and a middle and lower phase containing DNA and protein. The upper aqueous phase was transferred to a sterile RNA free microcentrifuge tube containing 0.5ml isopropanol and incubated at room temperature for 10 minutes to allow precipitation of RNA, which was then pelleted by centrifugation at 13,000g for 10 minutes at 4°C. The pellet was then

washed in 1ml of 75% ethanol, re-centrifuged as before and after allowing the pellet to air dry for 10 minutes, resuspended in 50µl DEPC treated H₂O and stored at -80°C.

2.2.8 Quantification of DNA/RNA Concentration

DNA and RNA concentrations were quantified using a NanoDrop® ND-1000 spectrophotometer (NanoDrop Technologies Inc., Wilmington, USA). Pre and post use the pedestals were wiped clean with 100% ethanol and DEPC treated water. The instrument was blanked with 1µl of the same buffer that the DNA/RNA was dissolved in. 1µl of the RNA/DNA sample was used per quantification with both a 260nm and 280nm light absorbance values measured. Readings were measured in duplicate and an average value taken.

2.2.9 DNA Sequencing

DNA sequencing was performed by Source BioScience UK Limited (previously Geneservice, Nottingham) on an Applied Biosystems 3730 DNA Analyzer.

2.2.10 Bisulphite Treatment of Genomic DNA

Genomic DNA was bisulphite treated using the EZ DNA Methylation-Gold Kit (D5006, Zymo Research, Orange, CA, USA). 500ng of genomic DNA was diluted to a final volume of 20µl using ddH₂O. To this 130µl of CT Conversion Reagent was added and mixed to form a homogeneous solution. The DNA was then denatured by heating to 98°C for 10 minutes, followed by bisulphite conversion of unmethylated cytosines into uracil by incubation at 65°C for 2.5 hours. The bisulphite DNA was then added to 600µl of M Binding Buffer preloaded into a Zymo-Spin™ IC Column and centrifuged (13,000g, 1 minute). 100µl of M-Wash Buffer was added to the column to wash the bound DNA and centrifuged (13,000g, 1minute). 200µl of M-Desulphonation Buffer was then added to the column and incubated for 20minutes at room temperature to desulphonate the DNA, followed by centrifugation as before. DNA was then washed with 2 x 200µl M-Wash Buffer and eluted in 10µl ddH₂O. Eluted DNA was stored at -20°C prior to PCR analysis.

2.2.11 Site-directed Mutagenesis

Site directed mutagenesis reactions were performed using QuikChange XL Site-Directed Mutagenesis Kit (Stratagene #200517). This allows for mutation (addition, deletion or substitution) of DNA base pairs within a super-coiled plasmid. Primers were designed that incorporated the mutation flanked by 15-25bp of complimentary base pairs either side. The primers anneal to the denatured plasmid, and are extended around the plasmid with *PfuUltra* DNA

polymerase, resulting in a parent strand-mutated strand plasmid duplex. The parental strand is methylated with the newly synthesised mutated DNA unmethylated. Digestion with *DpnI* selectively digests the methylated strand, to leave only the mutated strand, which is then transformed into competent XL10 Gold bacteria.

The primers utilised for the site-directed mutagenesis are given in Table 2 below.

	Mutation	Direction	Sequence
PU.1 Consensus Mutagenesis	CC-TT	Forward	GCCTGGCGCACTCACT TTTT GCGTCCCGCCGC CCTCCGG
	CC-TT	Reverse	CCGGAGGGCGGCGGGACGC AAA GTGAGT GCGCCAGGC
	C-T	Forward	GCCTGGCGCACTCACT TTCC GCGTCCCGCCGC CCTCCGG
	C-T	Reverse	CCGGAGGGCGGCGGGACGC GGA GTGAGT GCGCCAGGC
Hypoxic Responsive Element Mutagenesis	Δ HRE1	Forward	CCTCTACGAATAACGAGCCTACTAGGG TGTA TGCTTTTACTGCTGCACTGAGG
	Δ HRE1	Reverse	CCTCAGTGCAGCAGTAAAAGC TACACC CCTA GTAGGCTCGTTATTCGTAGAGG
	Δ HRE2	Forward	GCTTTTACTGCTGCACTGAGG TACAAA ATG CGCGCAGGCACAACGAGAC
	Δ HRE2	Reverse	GTCTCGTTGTGCCTGCGCGC ATTTTGTAT CC TCAGTGCAGCAGTAAAAGC
	Δ HRE3	Forward	CGCCCCGGCGCGGGCTCGGG TACAC AGAG CCGGCGAGCGAGCAGC
	Δ HRE3	Reverse	GCTGCTCGCTCGCCGGCTCTG TGTA TCCCGA GCCCGCGCCGGGGCG

Table 2: Sequences of primers used for site-directed mutagenesis.

The reaction components and conditions for the mutagenesis reactions were as follows:

10X Reaction Buffer	5 μ l
10ng plasmid DNA	1 μ l
125ng forward primer	1 μ l
125ng reverse primer	1 μ l
dNTP mix (final concentration 0.2mM each dNTP)	1 μ l
QuikSolution	3 μ l
H ₂ O	37 μ l
<i>PfuUltra</i> (5Units)	1 μ l

	50 μ l

95°C	1min	} 18 cycles
95°C	1min	
60°C	50s	
68°C	1min/kb	
68°C	7min	

+1µl *DpnI* (20,000Units/ml)

37°C 60min

5µl of the reaction was then transformed into one aliquot of XL10 Gold competent cells, and resultant colonies screened by sequencing for correct plasmid mutations. All sequencing chromatograms appear in the Appendix.

2.2.12 Polymerase Chain Reaction (PCR)

PCR reactions were carried out using Phire hot start DNA Polymerase (NEB) in a 20µl total reaction volume. Reaction components and conditions were as follows:

H ₂ O	11.6µl
5X Reaction Buffer	4µl
10ng plasmid DNA	1µl
Forward primer (final concentration 0.2µM)	1µl
Reverse primer (final concentration 0.2µM)	1µl
dNTP (final concentration 0.2mM each dNTP)	1µl
<i>Phire DNA Polymerase</i> (10Units)	0.4µl

	20µl

98°C	2min	} 35 cycles
98°C	10s	
60°C	10s	
68°C	30s	
68°C	2min	

For amplification of PU.1 cDNA and incorporation of restriction endonuclease sites, primer sequences used were 5'CGCGAATTCCAGATGTTACAGGCGTGCAAATGGAAGGGTTTCCCCTCGTCCCCCTCCATC (forward) and 5'GCGGGATCCTCAGTGGGGCGGGTGGCGCCGCTCGGCCAGGCCCCGCGGCCAGCACTTCGC (reverse).

Successful PCR amplification was analysed by resolving the PCR reaction by agarose gel electrophoresis.

2.2.13 TA Cloning of PCR Products

TA cloning[®] was used to clone purified PCR products that contained a 3' adenosine overhang (introduced through the non-specific terminal transferase activity of Taq polymerase) into a pcDNA4/HisMax[®]-TOPO[®] plasmid vector (K864-20, Invitrogen, Carlsbad, USA), that possessed a 5' thymidine overhang. Reactions were performed in a final volume of 5µl, and contain 3.5µl of purified PCR product, 1µl of salt solution and 0.5µl of TOPO[®] vector. The reaction was incubated at room temperature for 30 minutes prior to transformation of 2µl of the reaction mixture containing ligated PCR insert/TOPO vector backbone TOP10 chemically competent cells. All sequencing chromatograms are included in the Appendix section.

2.2.14 Cell Culture Techniques

2.2.15 Cell Maintenance and Passaging of Adherent Cells

Adherent monolayer human cell lines were cultured in DMEM supplemented with 10% FCS and 1% penicillin/streptomycin and incubated in a humidified 37 °C 5% CO₂ incubator.

When cells reached 80% confluency (as determined through inspection on an inverted light microscope) they were passaged through trypsinisation. The cell media was removed and cells washed twice with room temperature equilibrated PBS. 1x trypsin-EDTA (2.5ml for a 75cm² flask, 5ml for a 225cm² flask) was added and the cells incubated at 37°C until all the cells had visibly detached (2-10 minutes depending on cell type). As fetal calf serum contains naturally occurring trypsin inhibitors, the trypsin was then inactivated by addition of D-MEM containing 10% FCS (v/v) that was equal to three times the volume of trypsin originally used. Cells were then homogeneously resuspended prior to appropriate dilution with D-MEM supplemented with 10% FCS (v/v) and 1% penicillin/streptomycin solution (v/v) into a new flask.

2.2.16 Cell Maintenance and Passaging of Suspension Cells

Suspension U937 cells were maintained in RPMI 1640 supplemented with 10% FCS and 1% penicillin/streptomycin and incubated in a humidified 37°C 5% CO₂ incubator.

Cells were passaged every 2-3 days as determined by the confluency and indication of the media colour changing from orange to yellow. One third of the volume of the cell suspension was added to 2 thirds the volume of new media in a new flask and mixed by gentle pipetting.

2.2.17 Cell Freezing

Cells (of a low passage) were trypsinised and resuspended in a final volume of 25ml media. Cells were then gently pelleted by centrifugation (500g, 5 minutes), resuspended in 25ml of ice cold PBS and re-pelleted. The washed cell pellet was then resuspended in freezing media (10% (v/v) DMSO in FCS) and transferred into 2ml cryovials. The cryovials were stored for 24 hours at -80°C and then transferred into liquid nitrogen for long term storage.

2.2.18 Cell Counting

Cells were manually counted using an Improved Neubauer Hemacytometer (AC1000, Hawksley & Sons Ltd, Lancing, UK). Cells were trypsinised and neutralised as described (section 2.41 and 2.42). 10µl of the cell suspension was pipetted into each chamber of the hemacytometer and cells in each of the 8 large 1mm corner squares counted using an inverted light microscope. Cells that lay on the top and left border of a square were included in the count, but cells lying on the bottom and right border were excluded. An average cell count per 1mm square was calculated, and as the volume of each square was 0.1mm³, the cell count was multiplied by 10⁴ to obtain the number of cells per ml of neutralized cell suspension.

2.2.19 Cell Seeding

Cells were seeded into sterile tissue culture plates or dishes according to the transfection reagent protocol. Typically, adherent cells were seeded 24 hours prior to transfection so that they were 50-70% confluent when transfected. For seeding of cells for endogenous experiments, cells were plated so that they would reach the required cell number/density as required by the protocol.

2.2.20 Hypoxic Treatment of Cells

Hypoxic treatment refers to the exposure of cells to 1% oxygen within a ProOx110 controller chamber (BioSpherix Ltd, New York, USA). The chamber was humidified and maintained at 37°C.

2.2.21 Transfection of DNA into Monolayer Adherent Cells

U2OS, HeLa and HEK 293 cells were transfected using GeneJuice Transfection Reagent (70967-6, Merck4Biosciences, Darmstadt, Germany). Briefly, cells were seeded 24 hours prior to transfection (typically 1.5 x 10⁶ cells per 10cm plate). The required amount of GeneJuice was mixed in Optimem and incubated for 10 minutes at room temperature. DNA was then added, mixed gently by pipetting, incubated for 45 minutes at room temperature and then added dropwise to cells. Cells were then incubated for 24-48 hours.

MDA-MB435 cells were transfected using FuGene (11815091001, Roche Applied Science, Germany) as per manufacturer's protocol. Briefly, cells were seeded 24 hours prior to transfection. The required volume of FuGene was mixed with Optimem, DNA added and mixed by pipetting, incubated for 15 minutes at room temperature and then added dropwise to the cells.

2.2.22 Transfection of siRNA into Monolayer Adherent Cells

Adherent cells were transfected with siRNA using the DharmaFECT[®] siRNA transfection reagent (Thermo Scientific Dharmacon[®], Lafayette, USA). 24 hours prior to transfection, cells were seeded at 5×10^4 cells per well of a 12 well plate in 0.5ml complete growth medium. siRNA from a 20mM stock solution was added to serum free Optimem to a final volume of 50 μ l, so that in 500 μ l the desired concentration of siRNA would be achieved. In a separate tube, 1 μ l of DharmaFECT[®] was mixed with 49 μ l of Optimem, and both tubes were incubated for 5minutes at room temperature. Both tubes were then combined, gently mixed by pipetting and incubated for a further 20 minutes. After 20 minutes, growth media from the cells was removed, the cells washed with PBS and 400 μ l of fresh media was added. The DharmaFECT/siRNA mixture was then added drop wise to the cells to a make a final volume of 500 μ l. The cells were then incubated for 24-48 hours prior to subsequent analysis.

2.2.23 Transfection of siRNA into Suspension Cells

siRNA targeted against PU.1, LIMD1, Ets-1 or a scrambled control sequence was electroporated into the human leukaemic monocytic lymphoma U937 cell line using the Amaxa Cell Line Nucleofector Kit V (Lonza VCA-1003) on a Nucleofector II electroporator (Lonza) utilising the U937 cell specific programme (W-001). Briefly, 2×10^6 U937 cells were used per well of knockdown, which were resuspended in 100 μ l of the supplied Nucleofector[®] solution and 160pmol of siRNA added and mixed by gentle pipetting. Cells were not stored in this solution for more than 10 minutes. The siRNA/cell suspension was transferred to a supplied cuvette and electroporated using the manufacturer supplied programme for U937 cells (#W-001, exact electroporation conditions are not supplied by the manufacturer). Immediately after electroporation, 400 μ l of pre-warmed media was added to the cell solution, and then gently pipetted into a well of a 12 well plate containing 1.5ml of pre-warmed media to give a final volume of 2ml. Cells were then incubated for 48hours in a 37°C/5% CO₂ prior to lysis and analysis of mRNA/protein.

2.2.24 DNA/RNA Analysis Techniques

2.2.25 Bioinformatic Analysis

As a reference point for referring to positions within the *LIMD1* promoter, the unconfirmed transcriptional start site (TSS) was assigned according to the NCBI reference sequence NM_014240.2. This corresponds to nucleotide 45636323 on the primary chromosome 3 ref assembly NC_000003.11 and is 49bp upstream from the AUG translation initiation codon.

2.2.26 CpG Island and Transcription Factor Binding Motif Analysis

The human *LIMD1* promoter, which was preliminarily designated as 2.5kbp upstream of the ATG translation initiation codon, was scrutinised using the Ensembl Genome Browser (<http://www.genome.ucsc.edu>) for the presence of CpG Islands, utilising the default software thresholds. The promoter sequences of other *LIMD1* expressing mammals were extracted from the Ensembl Genome Browser (<http://www.ensembl.org>). Sequence alignments throughout were performed using ClustalW2 (<http://www.ebi.ac.uk/Tools/msa/clustalw2>). The *in silico* screen for transcription factor binding motifs within the promoter was performed using the MatInspector software programme (<http://genomatix.de>) using the Matrix Family Library Version 8.1 and the default threshold values of 0.80 representing a good match and 1.0 representing a perfect match respectively.

2.2.27 Methylation Specific PCR

15ng of bisulphite treated DNA was amplified using primers specific for methylated and unmethylated regions within the CpG promoter of *LIMD1* to produce a 151bp product. Genomic DNA from *LIMD1* expressing U2OS cells and non *LIMD1* expressing MB435 cells were used as positive and negative controls respectively, as both cell lines had been characterised as being homogeneously hypo- and hyper-methylated respectively. The primers specific for the methylated sequence were 5' GTCGATTCGTCGTCGTTATC (forward) and 5' CGCTAAATCCTCCGCTACTT (reverse), and for the unmethylated sequence were 5' GTTGATTTGTTGTTGTTATT (forward) and 5' CACTAAATCCTCCACTACTT (reverse). Conditions for the MSP were 95°C for 5 minutes followed by 40 subsequent cycles of 95°C for 1 minute with a 1 minute annealing at 60.7°C for the methylated or 59°C for unmethylated primers and 1 minute at 70°C. The methylation status of the *RASSF1A* CpG promoter was determined using the previously characterised methylation specific primers 5' GGGTTTTGCGAGAGCGCG (forward) and 5' GCTAACAACGCGAACCG (reverse)

and the unmethylated specific primers 5' GGTTTTGTGAGAGTGTGTTTAG (forward) and 5' CACTAACAAACACAAACCAAAC (reverse) (Burbee et al., 2001). Conditions for the Rassf1a MSP were 95°C for 5 minutes with 40 subsequent cycles of 95°C for 1 minute, 60°C for 1 minute and 1 minute at 70°C. The MSP products were analysed by separation on a 1.5% Agarose gel.

2.2.28 Bisulphite Sequencing

Methylation of the CpG Island within the *LIMD1* promoter was analysed using bisulphite sequencing. Genomic DNA from lung tumour tissue and matched normal lung tissue from 48 patients was extracted and 500ng bisulphite treated using EZ DNA Methylation-Gold Kit (Zymo Research, Orange, CA, USA). 10ng of each treated DNA was amplified using the non-methylation discriminatory primers 5' GGYGYGGGTTYGGGAYGTGTAGAGTYGG (forward) and 5' CTAATAACTAACRACCCATTATCCRATAAC (reverse), corresponding to -787 to -648 of the *LIMD1* ATG. Conditions for the PCR were 94°C for 3 minutes followed by 40 subsequent cycles of 94°C for 15s, 61.5°C for 1minute and 72°C for 30s with a final elongation at 72°C for 2minutes. The 149bp products were purified by gel extraction (QIAquick Gel Extraction Kit, Qiagen) and sequenced using the same forward primer. Methylated cytosines are resistant to the initial bisulphite treatment, and are conserved after PCR, whereas unmethylated cytosines are converted to uracil and subsequently appear as thymine when sequenced. Unmethylated and methylated genomic DNA from *LIMD1* expressing U2OS and non-*LIMD1* expressing MDA-MB435 cells respectively were used as controls.

2.2.29 qRT-PCR Analysis

2.2.29.1 Lung Biopsy Samples

Total RNA was extracted from 100mg of 48 tumour and matched normal tissue pairs, DNase1 treated and 1µg used for cDNA synthesis as previously described. Primers and probes were designed using the Roche Universal Probe Library assay design software algorithm (<https://www.roche-applied-science.com/sis/rtPCR/upl/index.jsp>). The primers for *LIMD1* were 5'TTGTGGACATCTGATCATGGA (forward) and 5'AAACAGCCGGGTGGTAG (reverse) and for the housekeeping *GAPDH* 5'AGCCACATCGCTCAGACAC (forward) and 5'GCCCAATACGACCAAATCC (reverse), both utilising Probe #60. Each assay was carried out in triplicate with 200nM of primer and 100nM probe on an ABI 7000 machine, with a non template control on each plate. Determination of the Ct threshold was calculated automatically using the 7000 System Software (Applied Biosystems). mRNA levels were quantified through a

standard curve obtained from a representative serial dilution of 12 sample pairs and levels of *LIMD1* normalised to *GAPDH*. *LIMD1* levels were then normalised to 1 for each matched normal tissue, so levels in each tumour are relative to 1.

2.2.29.2 PU.1 and Hypoxic Responsive Gene mRNA Levels

qRT-PCR analysis was performed in collaboration with Dr Victoria James using the SYBR green method of amplicon detection, and analysis using the comparative Ct method ($2^{-[\Delta\Delta Ct]}$). The geometric mean of 2 housekeeping genes, β -tubulin and RPII was used for normalisation.

For PU.1 mRNA analysis primers utilised were PU.1 5'CAGGGGATCTGACCGACTC (forward) and 5'GCACCAGGTCTTCTGATGG (reverse), normalised to the β -tubulin housekeeper 5'ATACCTTGAGGCGAGCAAAA (forward) and 5'CTGATCACCTCCAGAACTTG (reverse).

2.2.305-Aza-2'-Deoxycytidine Treatment

MDA-MB435 and U2OS cells were seeded in 6 well plates at 1.5×10^5 cells/well. 4 hours after seeding, the DNA methylation inhibitor 5-Aza-2'-deoxycytidine was added to a final concentration of 100 μ M. The media with fresh drug was changed every 24 hours for 5 days before cell lysis with 5x SDS gel loading buffer for Western Blot analysis.

2.2.31 Protein-DNA Interaction Techniques

2.2.32 Mapping and hypoxic responsiveness of the *LIMD1* Promoter

The *LIMD1* promoter region was previously cloned into a pGL4.0 firefly luciferase vector and a series of internal deletions within the CpG Island created (Sharp et al., 2008). 50ng of the mutant promoter containing firefly luciferase was co-transfected along with 5ng of SV40 driven renilla luciferase (for normalisation) into U2OS in a 24 well plate. Transfected cells were harvested in 1x PLB 30 hours post transfection. Cells that were exposed to hypoxia were done so that the end point was 30 hours post transfection. The amount of luciferase was quantified using the Dual Luciferase Reporter Assay system.

2.2.33 Chromatin Immunoprecipitation

Chromatin immunoprecipitation was used to assay transcription factor binding to DNA. For endogenous ChIP 1×10^7 cells were used and for exogenously expressed transcription factors 6×10^6 cells were used. Cells were starved overnight in serum-free D-MEM, followed by 30 minute stimulation with 20% FCS/D-MEM (v/v). Formaldehyde was then added to the culture medium to a final concentration of 1% to cross-link protein to DNA and the cells incubated for

10 minutes at 37°C. Cross-linking was quenched by washing the cells twice with ice cold PBS supplemented with 0.125M glycine and the cells harvested in 1ml harvesting buffer (0.125M glycine, 1mM EDTA and protease inhibitors in PBS) and pelleted by centrifugation at 3,500g for 10 minutes at 4°C. The cell pellet was resuspended in 100µl of lysis buffer (50mM Tris-HCl pH8.0, 1% SDS, 10mM EDTA plus protease inhibitors) and incubated on ice for 10 minutes. 50µl of dilution buffer (20mM Tris-HCl pH8.0, 1% Triton X-100, 2mM EDTA, 150mM NaCl plus protease inhibitors) was added and the lysates sonicated on ice in 15 second pulses to shear the DNA to 200-600bp (the number of sonication pulses was empirically calculated in preliminary experiments and varied with cell type). Lysates were cleared of insoluble material by centrifugation at 13,000g for 10 minutes at 4°C. An input sample (5% of total lysate) was taken, the remaining soluble chromatin containing supernatant diluted to 1ml with dilution buffer and added to an already antibody conjugated IP matrix and incubated overnight at 4°C with rotation. The next morning the IP matrix beads were harvested by centrifugation at 4,000 g for 1 minute at 4°C and the beads washed 6x 1ml RIPA with 5 minute incubations at 4°C with rotation between washes. Bound protein-DNA complexes were eluted in 2x 75µl elution buffer (1%SDS, 0.1M NaHCO₃) for 15 minutes at room temperature with rotation. Cross links were then reversed for 6 hours at 65°C with NaCl (0.2M), followed by incubation with 20µg proteinase K, 40mM Tris-HCl pH6.5, 10mM EDTA. DNA was then purified using the Qiagen PCR purification kit.

2.2.34 Electrophoretic Mobility Shift Assay (EMSA)

80% confluent 10cm plates of HEK293T cells were starved overnight in serum-free D-MEM, followed by 30 minute stimulation with 20% FCS/D-MEM (v/v). Cells were then washed twice in ice cold PBS and scraped in 1ml hypotonic buffer supplemented with protease/phosphatase inhibitors. Cells were quickly pelleted (14,000g, 30secs, 4°C), cytosolic protein containing supernatant removed and the pellet resuspended in 150µl hypertonic buffer supplemented with protease/phosphatase inhibitors. The resuspended nuclear pellet was rotated at 4°C for 60min to ensure complete lysis prior to centrifugation at 13,000g for 20min to pellet the insoluble nuclear membrane and DNA. The supernatant containing nuclear proteins was then flash frozen in liquid N₂ and stored at -80°C. Oligonucleotides representing the wild type IR5 sequence (WT: 5' CTCACTTCCGCGTCCCGCCGC (forward) and 5' GCGGCGGGACGCGGAAGTGAG (reverse) or point mutated (MT) IR5 sequence (MT1: 5' CTCACTTTTTCGCGTCCCGCCGC (forward) and 5' GCGGCGGGACGCAAAAGTGAG (reverse); MT2: 5' CTCACGGCCGCGTCCCGCCGC (forward) and 5'

GCGGCGGGACGCGGCCGTGAG (reverse) were ³²P end labelled using T4 polynucleotide kinase. Single stranded forward oligo (10pmol), γ [³²P]-ATP (5mCi), T4 kinase buffer (1x, supplied with the T4 kinase) and T4 polynucleotide kinase (10Units, NEB M0201S) in a final reaction volume of 10 μ l were incubated for 1hour at 37°C, prior to inactivation of the enzyme at 65°C for 10minutes. 10pmol of the complimentary reverse oligo was added along with 90 μ l of annealing buffer (10 mM Tris-HCl pH 7.4; 50 mM NaCl; 0.1 mM EDTA pH 8.0). The solution was heated to 94°C for 1 minute and allowed to cool slowly (-2°C/minute) to 16°C to allow the oligos to anneal. The annealed oligos were then purified using the QIAquick Nucleotide removal kit (Qiagen #28304). A mix of 4 \times binding buffer (140 mM KCl, 18 mM MgCl₂, 12 mM spermidine), Poly dI/dC (26 μ g/ml final concentration), sheared Herring sperm (100 μ g/ml final concentration) and nuclear extract/recombinant protein was made up. The volume was made up with incubation buffer (10 mM HEPES, pH 7.8, 5% glycerol, 50 mM KCl, 1 mM EDTA, 1 mM DTT). Antibody or cold probe (either wt or containing point mutations) was added and the reaction incubated at room temperature for 1 h. Labelled probe was added and reactions incubated for a further 10 min at room temperature before loading onto a 5% polyacrylamide gel (0.5 \times TBE). Gels were dried and developed using a Fuji-film LAS-3000 phosphor-imager.

2.2.35 Protein-Protein Interaction Analysis Techniques

2.2.36 Recombinant protein purification

The expression plasmids, pGEX4T and pGEX6P (GE Healthcare), both encode a glutathione-s-transferase (GST) moiety, which upon expression of a sub-cloned cDNA, produces a N-terminal GST tag that is separated from the expressed protein by a recognition sequence for a specific protease. The plasmids contains a tac promoter (a fusion of the bacterial trp and lac operons), which allows for inducible expression in bacteria by isopropyl-beta-D-thiogalactoside (IPTG). When expressed in bacteria, the recombinant protein can be purified from other intracellular bacterial proteins by using sepharose beads with glutathione moieties attached. The GST tag on the recombinant protein will bind with high affinity to the glutathione and as such can be purified through isolation and extensive washing of the sepharose beads.

The pGEX4T vector has a thrombin protease recognition sequence and the pGEX6P vector has a PreScission protease recognition sequence between the GST tag and the protein. When immobilised onto glutathione sepharose, the

recombinant protein can be cleaved and eluted from the beads with thrombin (for pGEX4T) or PreScission protease (for pGEX6P), resulting in a highly purified recombinant protein. PreScission protease is itself a recombinant protease that also contains a GST moiety, and so during cleavage binds to the glutathione beads thus preventing contamination of the eluted protein.

Recombinant proteins were expressed using the pGEX4T-1 plasmid vector (27-4580-01, Amersham Biosciences, GE Healthcare, Buckinghamshire, UK) containing the required cDNA of interest. The plasmid was transformed into the BL21 (DE3) pLysS strain of *E.coli* and a single colony was used for a 5ml LB/ampicillin (100µg/ml) overnight starter culture, which was grown with vigorous shaking (220rpm) at 37°C. The next morning a new culture was inoculated 1/50 with the starter culture, still maintaining the same ampicillin concentration, and grown with vigorous shaking (220rpm) at 37°C for 3 hours. Protein production was then induced by the addition of 200µM IPTG and the cultures grown for a further 3 hours. The bacteria were then pelleted (15 minutes, 4,000rpm, 4°C) and resuspended in 1ml of ice cold PBS per 10ml of culture volume. To aid in lysis the resuspended pellets were then frozen and thawed. The thawed bacterial suspensions were then sonicated at 100% intensity on ice 3 x 15 seconds with 15 second intervals between sonications. The sonicated lysates were then cleared of insoluble lipids and DNA by centrifugation at 13,000rpm for 10 minutes at 4°C.

Glutathione Sepharose™ 4B beads (17-0756-01, Amersham Biosciences, GE Healthcare, Buckinghamshire, UK) have glutathione immobilised on sepharose beads. The high affinity of the glutathione-s-transferase tag on the recombinant protein for glutathione allows for the purification of the recombinant protein from the other bacterial proteins. For each purification 35µl of the glutathione beads were washed with 3 x 1ml ice cold PBS to remove the 20% ethanol they are preserved in. The required volume of bacterial lysate was added to the beads, and the volume made up to 1ml with ice cold PBS. To facilitate binding the beads were rotated for 30mins at 4°C. After 30 minutes the beads were harvested by centrifugation (3,000rpm, 1 minute, 4°C) and washed with 1ml RIPA buffer for 5 minutes with rotation in order to remove any non-specifically bound bacterial proteins. The wash was repeated twice more, and as much of the supernatant was removed as possible, leaving just the beads bound by the purified recombinant protein.

To analyse the amount of protein purified, 35µl of 5 x SDS buffer was added, the sample boiled for 5 minutes, and resolved by SDS PAGE. The resultant gel was then visualised by Coomassie staining. For pulldown assays the amount of different recombinant proteins bound to the glutathione beads was empirically equalised from the intensity of the bands.

2.2.37 Direct Binding Assay

pGEX4T-PHD2 and vector only and pGEX6T-LIMD1 and vector only were transformed into, expressed and purified from BL21(DE3) pLysS *E. Coli* as described above. Expression of recombinant PHD2 and LIMD1 was confirmed by immunoblotting with anti- PHD2 or LIMD1 antibodies. The pGEX6P vector contains a PreScission Protease (GE Healthcare) cleavage site between the GST tag and the sub cloned protein. PreScission protease is a recombinant protease that contains a GST tag and so when added to the immobilised and purified pGEX6P-LIMD1 (or vector only), it will cleave LIMD1 off the GST tag, and will also itself bind to the glutathione sepharose beads. This leaves purified LIMD1 eluted into the supernatant. Immobilised GST-LIMD1 from an original 5ml culture was equilibrated in 1ml of PreScission Protease Buffer for 5 minutes with rotation at 4°C. 10% of the sepharose beads were then taken as an input. 5 units of PreScission protease was added to the remaining beads and incubated overnight with rotation at 4°C. The following morning the supernatant containing the cleaved recombinant LIMD1 or vector only was removed and 10% taken as an input. 5 x SDS loading buffer were added to the cleaved sepharose beads to analyse the efficiency of cleavage. The cleaved LIMD1 or vector only was added to immobilised pGEX4T-PHD2 or vector only and incubated for 6 hours with rotation at 4°C. The supernatant containing any unbound protein was removed and the beads washed 3 x 1ml of PreScission Protease buffer prior to elution with 5 x SDS loading buffer and analysis by Western Blot.

2.2.38 Dephosphorylation Assay

U2OS, HeLa and HEK 293T cells were plated at 5×10^5 /well in a 6 well plate. 24 hours after seeding cells were exposed to 16 hours hypoxia prior to lysis by scraping in RIPA supplemented with MG132, protease and phosphatase inhibitors (Roche). Cleared lysates were added to 2.5µg of HIF1α or isotype control antibody conjugated to 10µl settled bed volume of IP matrix (Santa Cruz sc-45042). Immunoprecipitation of HIF1α was carried out for 4 hours at 4°C with rotation, followed by extensive washing with RIPA buffer (unsupplemented). Dephosphorylation was carried out in 50µl reaction volumes using 400Units of lambda protein phosphatase (NEB #P0753S) at 30°C for 60 minutes along with a

control reaction that omitted the enzyme. The reaction was stopped by addition of 20µl 5 x SDS buffer and HIF1α protein analysed by Western blot.

2.2.39 Immunoprecipitation (IP)

In vivo protein-protein interactions were assayed by immunoprecipitation. For endogenous IP cells were allowed to reach 80-90% confluency, for exogenously transfected protein interactions cells were transfected 48 hours before lysis. The immunoprecipitating antibody was firstly conjugated to IP matrix beads (mouse antibodies used sc-45042; rabbit antibodies used sc-45043, Santa Cruz Biotech, CA, USA). 40µl of the IP matrix slurry (25% v/v) was made up to 1 ml using ice cold PBS. Dependent upon antibody and abundance of antigen, 1-5µg of precipitating antibody was added and rotated overnight at 4°C. The conjugated antibody-IP matrix was then pelleted by centrifugation at 3,500rpm for 1 minute at 4°C. Cells were washed 3 times with ice cold PBS, then gently scraped to harvest in 1ml ice cold PBS. Cells were pelleted by centrifugation (10,000rpm for 1 minute at 4°C) and the resultant pellet lysed by addition of 1ml RIPA (supplemented with protease and phosphatase inhibitors) and rotated at 4°C for 20 minutes. The lysate was then cleared of insoluble cellular debris by centrifugation at 13,000rpm for 10 minutes at 4°C. 50µl of lysate was removed as input, and the remaining supernatant was added to the antibody-IP matrix beads and incubated at 4°C with rotation for 4-6 hours. The matrix was then washed 3-6 times in RIPA/PBS (50% v/v) with 5 minute rotation between washes. Bound proteins were then eluted with 35µl of 5 x SDS buffer and analysed by Western blot.

2.2.40 Western Blot Analysis

Proteins were resolved by SDS-PAGE, prior to semi-dry electro transfer on a TransBlot Semi Dry Transfer Cell (Biorad) at a constant 20volts for 1 hour. Following transfer, membranes were blocked in blocking buffer (5% Marvel milk powder in PBS-Tween (0.05% v/v)). The required primary antibody was diluted in blocking buffer and then incubated on the membrane overnight at 4 °C with gentle agitation. The next morning, membranes were washed 3 x 5mins in PBS-Tween to remove any unbound antibody, prior to incubation in secondary antibody (horse radish peroxidase (HRP) conjugated) diluted in blocking buffer for 1 hour at room temperature with gentle agitation. The membranes were again washed 3 x 5mins in PBS-Tween before incubation with an Enhanced Chemiluminescence Reagent (ECL) Western Blotting Detection Solution (0.1ml/cm² of membrane, Amersham™, GE Healthcare, UK) for 5 minutes to initiate a HRP-catalysed luminescent reaction. Excess ECL solution was drained

off, the membranes covered with a single piece of cling film and exposed to Chemiluminescent Detection Film (Roche Applied Science) for ten seconds up to one hour dependent upon the signal strength. The film was then hand developed in PQ Universal Paper Developer (Ilford, UK) and fixed in 2000RT fixer (Ilford) before being rinsed in water and allowed to air dry.

Chapter 3 Results: *LIMD1* transcription and promoter methylation in lung cancer

3.1 Introduction

Reduced *LIMD1* protein expression in lung tumours has been reported to be a result of genetic ablation, specifically chromosomal deletions and/or loss of heterozygosity (Sharp et al., 2008). Using lung adenocarcinomas (ADC) as a representative example, the percentage of tumours showing reduced protein expression is 79%, with 32% and 12% reductions due to *LIMD1* gene deletion and loss of heterozygosity respectively (Sharp et al., 2004; Sharp et al., 2008). This therefore leaves a deficit (35%) between the overall percentage protein loss in ADC (79%) and the percent loss that can be accounted for by genetic deletions (44%). This discrepancy in *LIMD1* loss therefore may be due to mechanisms that affect *LIMD1* transcription rather than genetic ablations.

The 5'-proximal promoter regions of transcribed genes contain binding motifs for multiple transcriptional regulatory proteins, some of which are ubiquitously expressed, some expressed in response to a stimuli and others in a tissue or cell type specific manner. To initiate the study of the *LIMD1* promoter, and as an aid for referring to positions within the promoter, the unconfirmed transcriptional start site (TSS) was assigned according to the NCBI reference sequence NM_014240.2. This corresponds to nucleotide 45636323 on the primary chromosome 3 ref assembly NC_000003.11 and is 49bp upstream from the AUG translation initiation codon.

3.2 The *LIMD1* Promoter contains a Single CpG Island

The *LIMD1* gene promoter spanning 2kb upstream from the translation start site was scrutinised using the UCSC Genome Browser to identify the presence of any CpG Islands (Figure 3.1). Only one CpG Island was identified within the promoter sequence, predicted as being 842bp long, with a G + C content of 65.3% and an observed/expected CpG ratio of 95%. This meets the criteria set by both Gardiner-Garden and Takai for the definition of a CpG Island (Gardiner-Garden and Frommer, 1987; Takai and Jones, 2002).

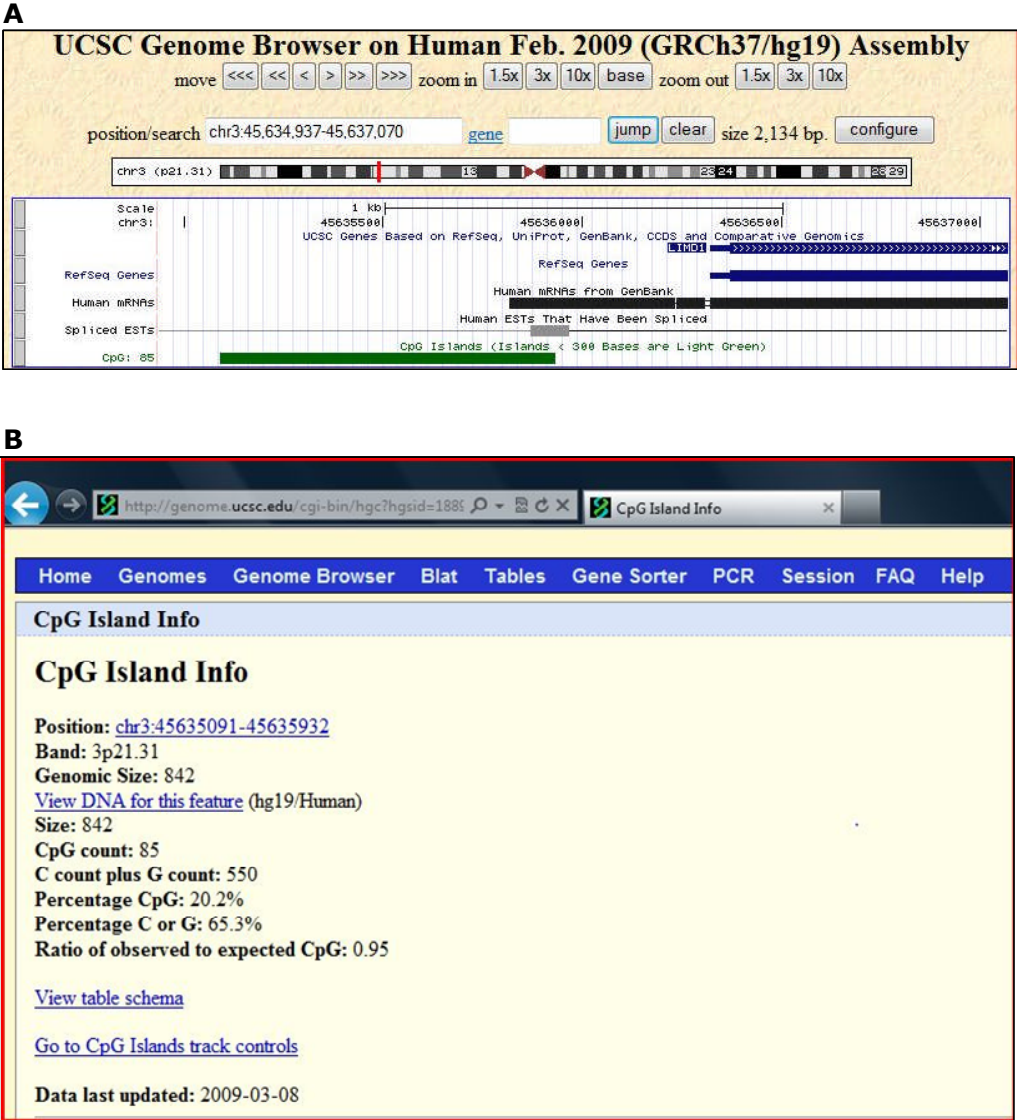


Figure 3.1: The *LIMD1* promoter contains a single CpG Island. The *LIMD1* genomic locus was scrutinised using the Ensembl Genome browser. Parameters were set to (A) visually identify any CpG Islands upstream of the AUG translation initiation codon. (B) Further scrutinisation of the details of the CpG Island revealed it spans 842 bases and contains 85 CpG dinucleotides.

The *LIMD1* promoter region spanning from -1990 relative to the TSS and up to the AUG *LIMD1* initiation codon (+50) was previously cloned into a pGL4.10 vector (Sharp et al., 2008). This allowed for the transcriptional activity of the promoter to be assayed indirectly through the transcription and translation of the luciferase gene under the control of the *LIMD1* promoter. A series of ten consecutive but discreet internal deletions ranging in size from 18 to 35bp were also created within the CpG Island (Sharp et al., 2008), which are schematically depicted in Figure 3.2A. The internal mutants were named 'internal deletion 1-10' (IΔ1-10), and when referring to the corresponding region that was deleted the nomenclature 'internal region 1-10' (IR1-10) is used.

3.2.1 The CpG Island within the *LIMD1* Promoter Contains Both Negative and Positive Regulatory Regions

By utilising the internal promoter deletions, the presence of any positive or negative regulatory regions within the CpG Island could be identified. If a region that harboured a consensus binding motif for a negative transcriptional regulator was removed, an increase in transcriptional activation would be observed, and vice versa for a positive regulator. To identify these regions, equal amounts (50ng) of the wild type and internal promoter deletion reporters were separately co-transfected with a renilla luciferase plasmid (for normalisation) into U2OS cells, along with the control vector only (VO) and resultant luciferase activity assayed 24hours post transfection.

The promoter internal deletion mutants exerted different effects on *LIMD1* promoter activity (Figure 3.2B). The IΔ2, 3, 7 and 10 mutants showed no statistically significant changes in transcriptional activity compared to wild type, showing that these regions (in the absence of specific external stimuli) in U2OS cells do not contain binding sites for major transcriptional (co)-activators or (co)-repressors. Two of the mutants, IΔ4 and 6, showed 50 and 100% increases in transcriptional activities compared to wild type respectively. This indicated these regions may contain binding sites for proteins that negatively regulate transcription. Conversely the IΔ1, 9 and 10 mutants all caused decreases in transcription of 60%, implicating these regions as containing binding sites for positive transcriptional regulators. The largest effect on transcription was seen with the IΔ5 deletion, which caused a 90% reduction in transcription.

The IΔ5 mutant showed the greatest reduction in transcription of 90%, which indicated that it may contain the binding motif or consensus for the protein(s) that were responsible for basal *LIMD1* transcription. Therefore this region was focused upon for subsequent analyses.

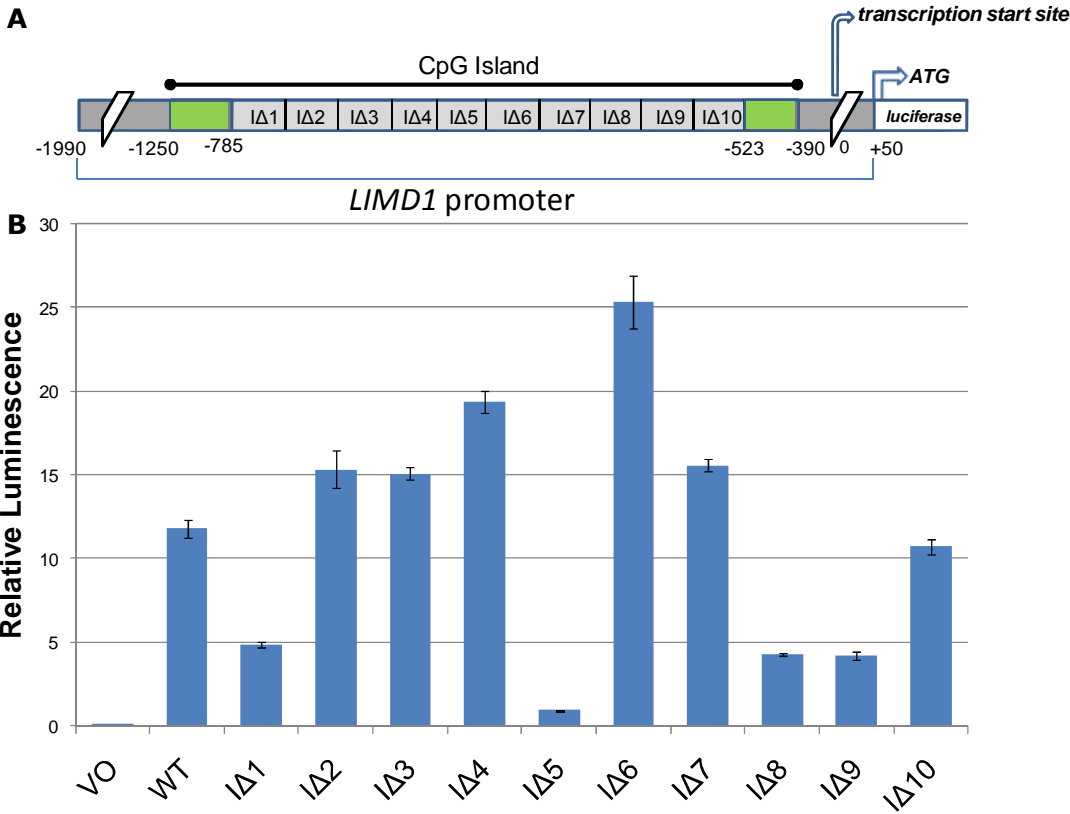


Figure 3.2: The *LIMD1* promoter contains positive and negative regulatory regions. (A) Schematic diagram showing the cloned *LIMD1* promoter in the pGL4 luciferase vector, with the CpG Island and ten internal deletions (IΔ1-10) indicated. Base pair numbering is relative to the transcriptional start site as assigned according to the NCBI reference sequence NM_014240.2 (nucleotide 45636323 on the primary chromosome 3 ref assembly NC_000003.11). (B) The indicated internal deletion mutants were co-transfected with a Renilla luciferase for normalisation into U2OS cells and resulting luciferase activity assayed 24 hours post transfection. Results shown as mean +/- 1 standard deviation; representative experiment of n=3.

3.3 Analysis of *LIMD1* Promoter Methylation

3.3.1 Identification of the Methylation Status of the *LIMD1* promoter in *LIMD1* expressing and non-expressing cell lines.

A common phenomenon that causes silencing of tumour suppressor genes in cancer is epigenetic silencing, which is a result of aberrant promoter hypermethylation (Esteller, 2007). Hypermethylation of promoters, specifically cytosine residues within CpG dinucleotides, inhibits transcription by blocking the binding of transcriptional activator proteins either directly via the methylated cytosine, or indirectly through chromatin remodelling facilitated by the recruitment of methyl binding proteins and histone remodelling proteins.

One of the cell lines maintained in the lab is the MDA-MB435 breast epithelial cell line, which does not express *LIMD1* protein or mRNA (Sharp et al., 2004) however PCR analysis of the genomic locus revealed that the gene, including promoter, introns and exons were all present and so loss of expression was not due to genetic deletions (data not shown). This therefore gave an indication that an epigenetic factor could be the reason for non-expression of *LIMD1*. To test this hypothesis, the methylation status of the promoter region, specifically IR5, was analysed to assess if there were any differences between *LIMD1* non-expressing MB435 cells and *LIMD1* expressing U2OS cells. Genomic DNA from both cell types was extracted and then treated with sodium bisulphite using an EZ DNA Methylation Gold kit (Zymo Research).

Sodium bisulphite deaminates unmethylated cytosines into uracil, whereas 5-methyl cytosines are resistant (Figure 3.3). The result of this is a different sequence of DNA dependent upon original methylation status and as such traditional PCR based methods can subsequently be utilised to assay the original methylation status of the DNA. In methylation specific PCR, specific primers that will only bind to cytosine rich (i.e. originally methylated) DNA, or thymine rich (i.e. originally unmethylated) DNA are used. If the DNA was originally methylated, only the methylation specific primers would produce an amplicon, whereas the unmethylated specific primers would not anneal to the different sequence and so will not produce an amplicon (Figure 3.3). These amplicons can then be ethidium bromide stained and visualised by agarose gel electrophoresis.

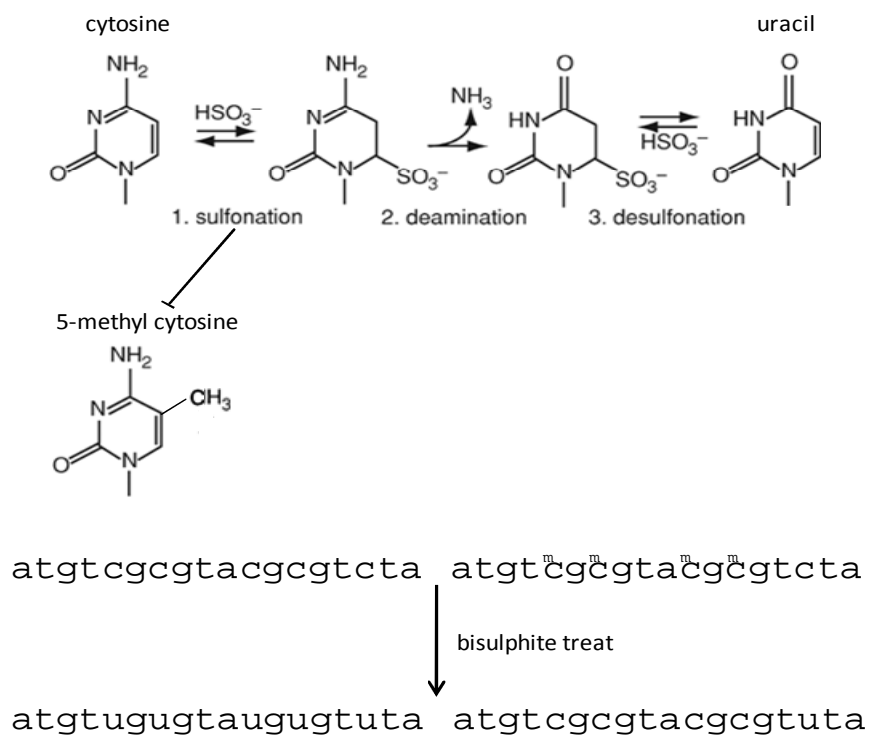


Figure 3.3: Sodium bisulphite can modify cytosine to uracil but not methyl-cytosine. Sulphonation followed by deamination and desulphonation of cytosine by sodium bisulphite results in formation of uracil, which during a subsequent PCR reaction leads to the incorporation of thymine in the amplicon as opposed to the original cytosine. 5-methyl cytosine however is resistant to bisulphite modification and so remains as cytosine after treatment. The differences in sequence following bisulphite treatment can be exploited for either restriction endonuclease or PCR/ sequencing analysis. Adapted from (Darst et al., 2010).

Primers were initially designed to amplify the region surrounding IR5 within the promoter. The design was such that the primers would anneal to the promoter region without discriminating against if it was initially methylated or not in order that they would produce an amplicon in both U2OS and MB435 cells.

The resultant amplicon from each cell line was gel excised, purified and sequenced using the same forward primer used for the PCR. The sequencing chromatograms revealed that the IR5 region (which harbours 4 CpG dinucleotides) of the LIMD1 promoter in the U2OS (LIMD1 expressing) cell line was unmethylated, whereas the same region within the MB435 (LIMD1 non-expressing) cell line was methylated (Figure 3.4). It was also noticed that the region surrounding IR5 was also methylated in the MB435 cells compared to U2OS. Thus at the genetic level the only difference between the promoters encompassing IR5 in U2OS and MB435 genomic DNA was the methylation

status, demonstrating that epigenetic silencing may be the cause for loss of LIMD1 expression in the MB435.

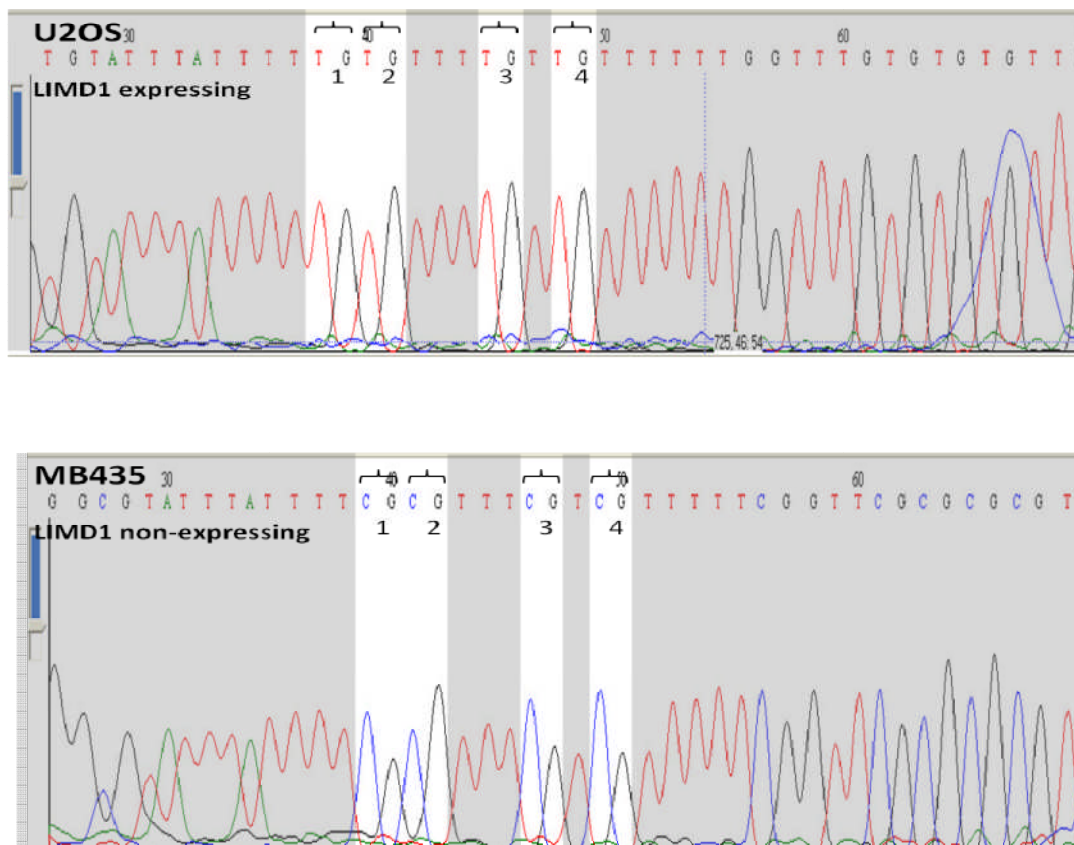


Figure 3.4: The IR5 region of the LIMD1 promoter is unmethylated in the LIMD1 expressing U2OS cell line, but methylated in the LIMD1 non-expressing MB435 cell line. Genomic DNA from U2OS and MB435 cells was extracted and bisulphite treated. Primers that incorporated the IR5 region of the LIMD1 promoter were used to amplify the DNA, and the resultant amplicon sequenced using the same forward primer. Scrutiny of the resultant sequence revealed the cytosines of the 4 CpG dinucleotides were all originally unmethylated as they have been converted to thymines following bisulphite treatment. The same cytosines within the MB435 cells were however methylated as they remain unaffected by the bisulphite treatment. Representative chromatogram from n=6.

3.3.2 Methylation within IR5 of the LIMD1 promoter increases in primary lung tumours compared to normal control tissue.

Tumour cell lines undergo changes in methylation of multiple CpG Islands during prolonged culturing when compared to primary malignancies (Meissner et al., 2008; Smiraglia et al., 2001). It was therefore important to assess if hypermethylation of the IR5 region in the MB435 cell line was a result of tissue culture passages or if such IR5 methylation could also be detected in the DNA of primary lung tumour samples when compared to matched normal adjacent

tissue controls. To investigate this, a cohort of 48 paired lung tumour tissue samples with matched normal tissue biopsies was examined.

To assess the methylation status of the promoter region, methylation specific PCR (MSP) analysis was employed. MSP utilises primers that are specifically designed to anneal to a region containing multiple CpG dinucleotides. Originally unmethylated CG dinucleotides following bisulphite treatment become TG, whereas originally methylated CpG remain as CG. Therefore by differentially designing the primer to anneal to TG as opposed to CG, differences in methylation can be detected by PCR.

The promoter of the characterised *Rassf1a* TSG has been reported to be methylated in lung tumours. Burbee *et al* reported 75% of lung cancer cell lines, 30% of primary NSCLC and 100% of SCLC cell lines had *Rassf1a* promoter methylation (Burbee *et al.*, 2001). Agathangelou *et al* and Dammann *et al* reported similar findings of methylation in 72% of SCLC and 35% of NSCLC primary and cell lines and 100% of SCLC and 38% of NSCLC respectively (Agathangelou *et al.*, 2001; Dammann *et al.*, 2000). Therefore to place the results obtained for the *LIMD1* promoter into perspective the methylation status of the characterised *Rassf1a* promoter was assayed alongside that of *LIMD1* in the same cohort of tumour and matched normal tissue samples. This firstly ensured that if the proportion of *Rassf1a* methylation matched published findings then the cohort could be considered a representative sample. Secondly, it would allow for any *LIMD1* methylation to be put into context by comparing against the results for *Rassf1a*. MSP primer sequences for *Rassf1a* were taken from Burbee *et al* (Burbee *et al.*, 2001).

3.3.3 Optimisation of methylation specific PCR (MSP)

To confirm the methylation specific primers could distinguish between DNA that was methylated or unmethylated the designed primers were initially used to amplify U2OS and MB435 genomic DNA. These two genomic DNA samples were chosen as the different methylation states had been identified by sequencing and the genomic DNA was from homogeneous cell populations, unlike primary tissue samples which could contain mixed cell populations.

The initial methylation specific PCR reaction using annealing temperatures of 55°C gave multiple non-specific banding. Furthermore, amplicons were produced by the unmethylated DNA specific primers in the MB435 (which should only

produce an amplicon with the methylated specific primers) showing a degree of non specific binding. Therefore the PCR was optimised by initially increasing the Mg^{2+} concentration and then carrying out a PCR using a temperature gradient of primer annealing temperatures from 48°C to 62°C. One feature of the primers that differs between the methylation specific and unmethylated specific primers is the CG content, with the latter having a lower CG content than the former because, as described following bisulphite treatment, methylated cytosines remain as cytosines, whilst unmethylated cytosines become thymines. This means the primers end up having different optimum annealing temperatures due to different GC contents.

The gradient PCR showed that at higher annealing temperatures, the non specific amplicons disappeared, to leave one specific amplicon (Figure 3.5). At 60.4°C the unmethylated specific primers (U) give a single amplicon with U2OS bisulphite treated DNA but no amplicon with the methylated MB435 treated DNA (Figure 3.5). At the slightly higher temperature of 62°C the methylation specific primers (M) give a single amplicon with the treated MB435 genomic DNA, but not with the U2OS treated DNA (Figure 3.5). The amplicons were then confirmed as being of the correct sequence by direct sequencing with the same forward primer (data not shown).

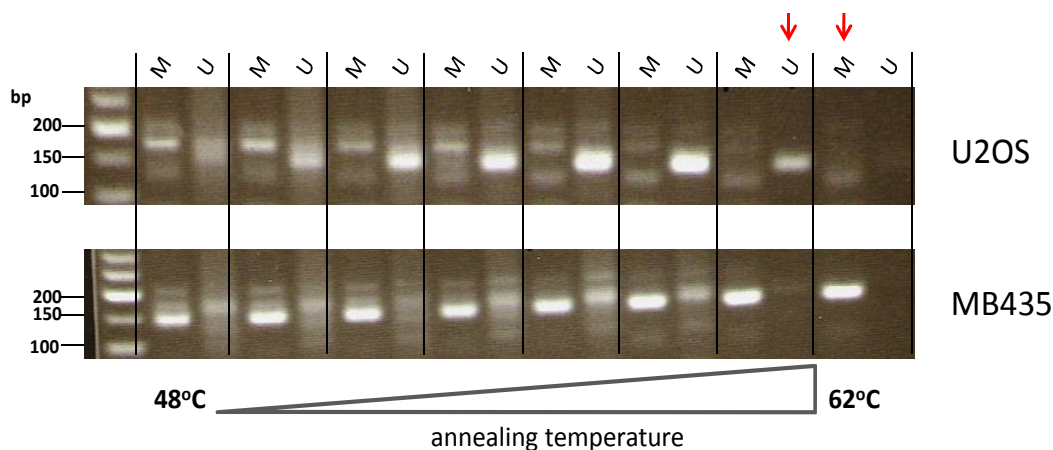


Figure 3.5: Optimisation of annealing temperatures of primers specific for methylated and unmethylated genomic DNA from U2OS and MB435 cells. Genomic DNA from LIMD1 expressing U2OS and non-expressing MDA-MB435 cells was extracted and bisulphite treated. PCR was performed on the treated DNA using primers that were specific and would only anneal to methylated (M) or unmethylated (U) DNA. In order to obtain a single specific amplified band with the methylated primers for MB435 and unmethylated primers for U2OS a temperature gradient PCR of annealing temperatures was carried out to find the optimal annealing temperature for each set of primers. The optimal annealing temperatures were 62°C for the methylated specific primers and 60.4°C for the unmethylated primers (indicated with red arrows).

3.3.4 MSP of Primary Lung Tissue and Matched Lung Tumours

Once the methylation specific primers and PCR reaction had been optimised and validated, the methylation status of IR5 from genomic DNA from matched normal and lung tumour tissues was assayed. Genomic DNA and RNA were extracted from the cohort of 48 lung tumour and matched normal tissues. The genomic DNA was then bisulphite treated as described for U2OS and MB435 genomic DNA.

Equal amounts of DNA (15ng) were used for each MSP, and for each reaction a water only PCR negative control (H₂O) and a positive control of U2OS or MB435 genomic DNA (+ve) were included. To ensure reproducibility of results, each PCR with controls was performed in two independent experiments. As the focus of the MSP was to assay methylation increases in tumour samples, only methylation specific primers were used. The hypothesis for this experiment was that the results for the normal tissue (which were assumed to be LIMD1 expressing) would mirror the results within the U2OS cells, that is the promoter would be unmethylated, whilst a proportion of the tumour tissue (in which ~70-80% would be expected not to express LIMD1 (Sharp et al., 2004; Sharp et al., 2008)) would mirror the MB435 cells and be methylated. A representative sample of normal (N) and matched tumour samples (T) following MSP is shown in Figure 3.6.

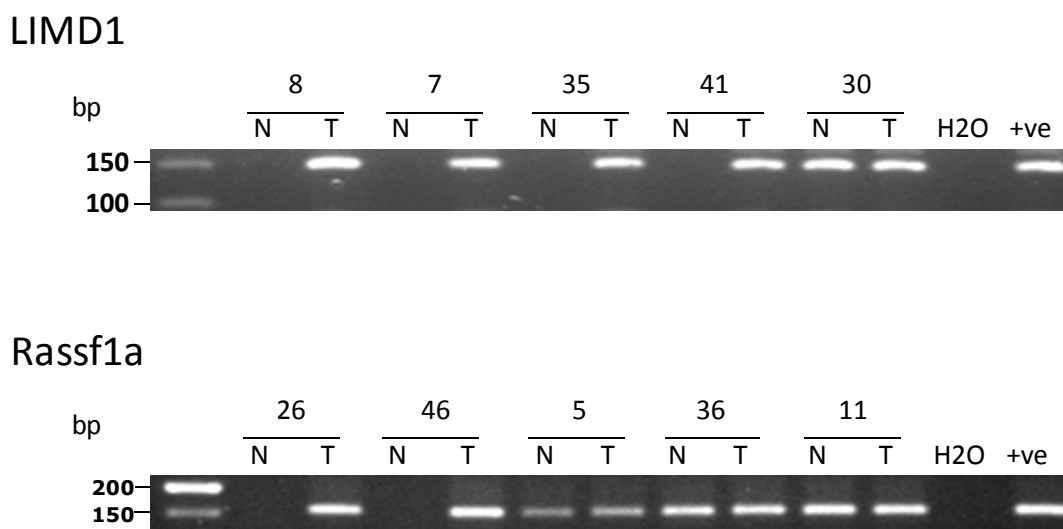


Figure 3.6: Representative methylation specific PCR results for the *LIMD1* and *Rassf1a* promoters. Genomic DNA was extracted from a cohort of 48 lung tumour and matched normal lung tissue samples and bisulphite treated. After bisulphite treatment, PCR utilising methylation specific primers was carried out to assess any change in methylation status of the (A) *LIMD1* and (B) *Rassf1a* promoters.

For nine of the *LIMD1* and three of the *Rassf1a* promoter analyses either the normal and/or tumour sample failed to give an amplicon, and as such were omitted from the comparative analysis. The results of the MSP for the *LIMD1* and *Rassf1a* promoters are summarised in Table 3 and Figure 3.7. The overall percentage changes in methylation changes of both the *LIMD1* and *Rassf1a* promoters were similar; 55-60% exhibited no change in methylation status and 20% showed an increase in methylation in the tumour tissue compared to the matched normal tissue. The surprising result, however, was ~20% showed a decrease in methylation from the matched normal to tumour tissue, which was counter intuitive as to what would be expected and indeed hypothesised.

No correlation was observed between tumour type and changes in methylation state of either promoter. Furthermore there was no positive or negative correlation between the two promoters; an increase or decrease in one did not correlate with an increase or decrease in the other. Out of the cohort of informative sample pairs, 9 tumours showed an increase in *LIMD1* promoter methylation with a different 9 tumours showing an increase in *Rassf1a* methylation when compared to the matched normal tissue. A decrease in *LIMD1*

methylation was observed in 7 tumours and *Rassf1a* methylation in a total of 8 tumours, with two tumours showing a common decrease in methylation of both promoters. There was no change in methylation between the normal and tumour tissue of the *LIMD1* promoter in 20 samples or of the *Rassf1a* promoter in 26 samples.

Sample No.	Tumour	Promoter Methylation Status		Sample No.	Tumour	Promoter Methylation Status	
		<i>LIMD1</i>	<i>RASSF1A</i>			<i>LIMD1</i>	<i>RASSF1A</i>
1	A	-	No change	25	A	Increase	Decrease
2	S	No change	No change	26	BC	No change	Increase
3	S	Decrease	Decrease	27	S	Decrease	No change
4	S	No change	Increase	28	A	Increase	No change
5	A	No change	No change	29	A	No change	No change
6	A	Increase	No change	30	S	No change	Decrease
7	A	Increase	Decrease	31	PC	Increase	No change
8	TC	Increase	Decrease	32	S	No change	No change
9	LCC	No change	No change	33	A	No change	No change
10	A	-	-	34	S	Decrease	Increase
11	A	No change	No change	35	S	Increase	Decrease
12	A	Decrease	Increase	36	LCC	No change	No change
13	A	No change	No change	37	S	No change	Increase
14	A	No change	No change	38	A	No change	Decrease
15	S	-	No change	39	A	No change	No change
16	A	Increase	No change	40	S	No change	No change
17	AC	-	No change	41	A	Increase	No change
18	A	-	No change	42	TC	Decrease	No change
19	A	-	No change	43	BC	Decrease	No change
20	S	-	Increase	44	TC	No change	Increase
21	A	-	-	45	A	No change	Increase
22	TC	-	-	46	S	No change	Increase
23	A	No change	-	47	AC	No change	No change
24	BC	Decrease	Decrease	48	TC	-	-
				Total	n=	36	43
					Increase	9	9
					Decrease	7	8
					No change	20	26

Table 3: Summary of methylation specific PCR (MSP) analysis of the *LIMD1* and *Rassf1a* promoters in a cohort of lung tumour and matched normal tissue.

Genomic DNA was extracted from a cohort of 48 lung tumour and matched normal tissue and bisulphite treated. The treated DNA was then subject to MSP with methylation specific primers for either the *LIMD1* promoter or the *Rassf1a* promoter. Also indicated is the tumour type. A, adenocarcinoma; S, squamous cell carcinoma; TC, typical carcinoid; AC, atypical carcinoid; BC, basaloid carcinoma; PC, pleomorphic carcinoma; LCC, large cell carcinoma.

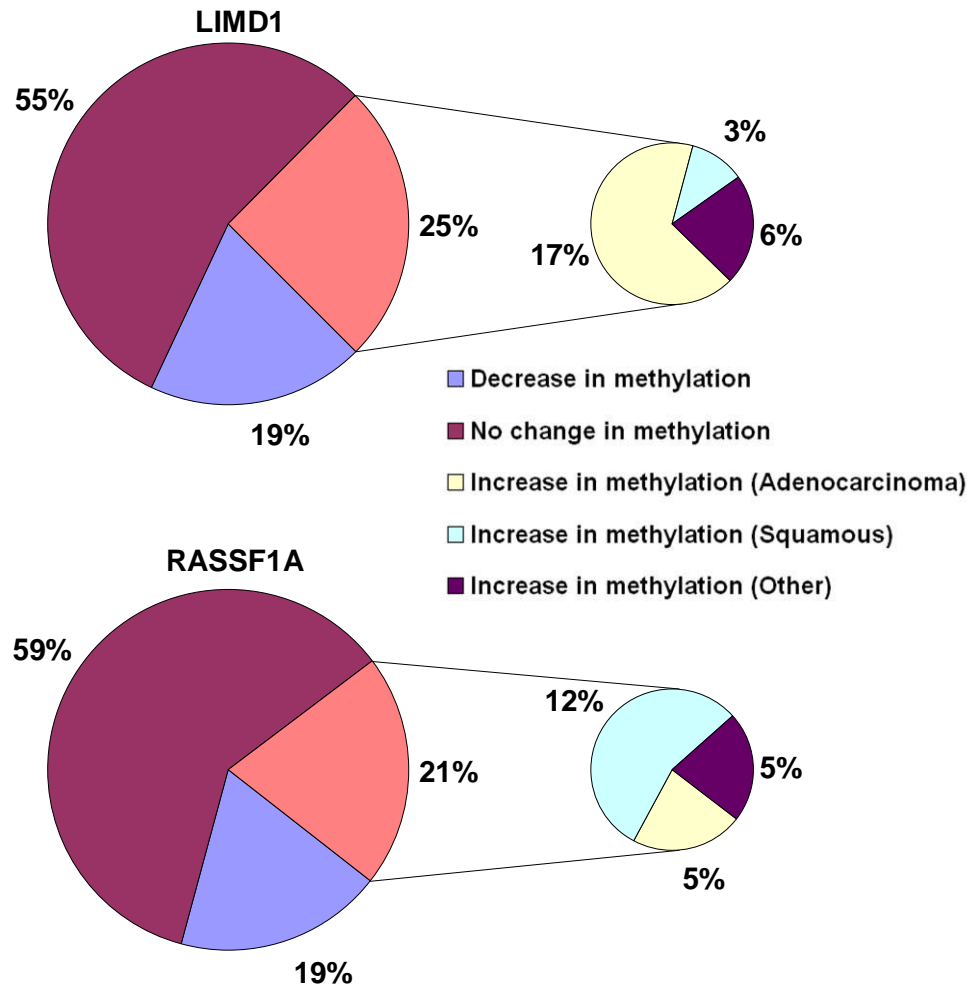


Figure 3.7: Summary of the changes in methylation status of the LIMD1 and RASSF1A promoters in lung tumour tissue as compared to matched normal tissue as analysed by methylation specific PCR. Genomic DNA was extracted from a cohort of 48 lung tumour and matched normal tissue and bisulphite treated. The treated DNA was then subject to MSP with methylation specific primers for either the LIMD1 promoter or the RASSF1A promoter.

The results from the MSP analysis gave an indication that there were changes in methylation status of both the *LIMD1* and *Rassf1a* promoters between normal and tumour tissue. However 19% of samples showed that the promoters of both genes were methylated in normal tissue and hypomethylated in the tumour samples. Due to these unexpected findings, no clear conclusions could be drawn about changes in methylation between normal and tumour tissue. Methylation specific PCR as an analytical tool does have disadvantages, the main one being that *only* the methylation status of the CpG dinucleotides within the primer sequences can be quantified as being methylated or not. The regions in between the forward and reverse primers remain uncharacterised. Furthermore it is possible for primers to anneal with a base pair mismatch, so one CpG within the primer could be methylated and the others unmethylated, yet the primer could still be able to anneal and give a false positive amplicon.

A better methodology for assaying specific methylation of DNA is to sequence the bisulphite treated DNA (bisulphite sequencing). With sequencing, primers that anneal to the DNA irrespective of methylation status can be used, and the purity/extent of methylation can be visualised by examining the resultant sequenced chromatogram. Therefore bisulphite sequencing of the *LIMD1* and *Rassf1a* promoters were performed using the same cohort of bisulphite treated genomic DNA.

3.3.5 Optimisation of Bisulphite Sequencing the *LIMD1* Promoter

For bisulphite sequencing, primers were designed so that they would (a) only anneal to bisulphite treated DNA, (b) anneal to the DNA irrespective of methylation status and (c) produce an amplicon of suitable size to be directly sequenced without having to first sub-clone into a vector which would significantly increase the cost of the assay. These primer specifications would allow for an amplicon to be produced and sequenced without the possible contamination of DNA that hadn't been bisulphite treated (the bisulphite reaction converts 99% of DNA as quoted by the manufacturer's protocol). It also removes any bias of primers annealing more efficiently to either methylated or unmethylated DNA, and after successful amplification would allow for simple preparation of samples for sequencing as the amplicon would only have to be gel purified and quantified.

To optimise the conditions for PCR and sequencing, genomic DNA from U2OS, HeLa (*LIMD1* expressing) and MDA-MB435 cells (*LIMD1* non-expressing) was extracted. Again, using cultured cell lines ensured a homogeneous cell

population. Using just one set of methylation indiscriminatory primers, PCR reactions were carried out on the extracted genomic DNA both pre and post bisulphite treatment. Only the genomic DNA which had been bisulphite treated produced an amplicon of the correct size (147bp) (Figure 3.8). To ensure the amplicon corresponded to the correct section of genomic DNA, the amplicon was gel extracted, purified and sequenced. In agreement with the previous findings, the MDA-MB435 amplicon was found to be methylated and the U2OS and HeLa amplicons unmethylated (data not shown).

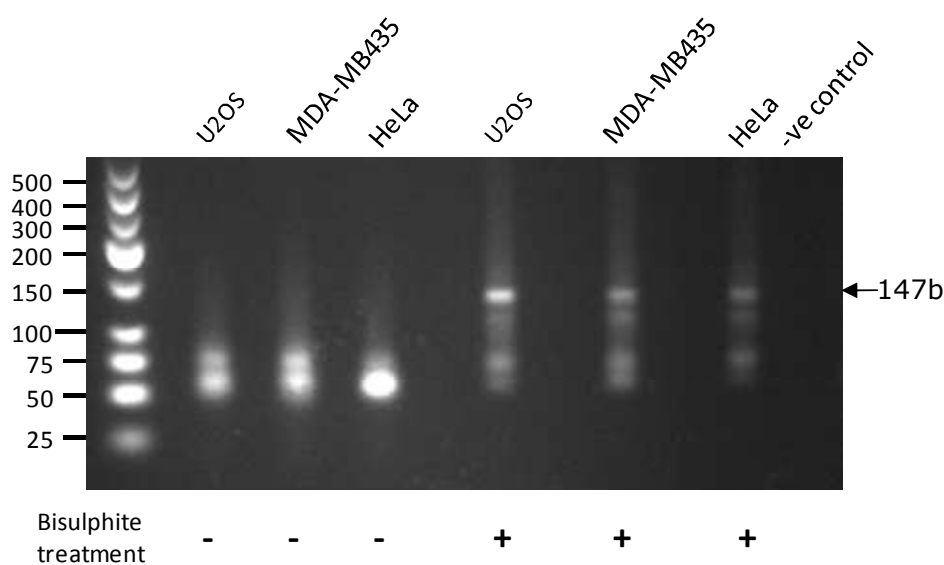


Figure 3.8: PCR amplicons of the correct size are only obtained from genomic DNA that has been bisulphite treated. Genomic DNA was extracted from U2OS, MDA-MB435 and HeLa cells and bisulphite treated. PCR was then carried out using bisulphite treated specific but methylation in-discriminatory primers. No amplicon of the correct (147bp) size was obtained with untreated genomic DNA (-), however after bisulphite sequencing (+) specific amplicons were obtained. To confirm the sequence specificity of the amplicons, the amplicons were gel excised and sequenced.

3.3.6 Bisulphite Sequencing of the IR5 Region within the *LIMD1* Promoter identified Aberrant Methylation in Primary Lung Tumours

Once the specificity of the bisulphite specific primers had been confirmed, the bisulphite treated genomic DNA from the cohort of lung and matched normal tissue was bisulphite sequenced. Due to the number of samples (48x2=96 plus controls) that had to be manually processed, the PCR reactions and gel purifications were carried out in batches of 20 samples. As internal controls for each batch of samples, U2OS and MDA-MB435 bisulphite DNA was included and sequenced to ensure reproducible results were obtained.

Due to the high costs involved in sequencing and the predominant interest in the IR5 region (Figure 3.2), only the methylation status of this region was examined. The sequence of IR5 is 5'-CTCACTTCCGCGTCCCGCCGC, containing 4 CpG dinucleotides (underlined) and it was the methylation status of these that were scrutinised. When the sequencing results were received, the sequence text file for each was scrutinised alongside the chromatogram to be confident any miscalled bases by the sequence analyser software were not included as false positive results. Furthermore, for some samples a mixed signal peak for a cytosine base was obtained, which the sequencing text file alone did not identify.

It has been observed that primary tumour cells from biopsies potentially contain mixed cell populations, for example from infiltrating blood lymphocytes or chromosomal loss of heterozygosity in some cells. The result of this is a sample that contains genomic DNA with potentially different extents of methylation, which following bisulphite sequencing gives rise to a mixed C/T chromatogram peak for a single cytosine within a CpG dinucleotide. Therefore to distinguish between a single C or T peak and a mixed C/T peak, nomenclature from previously published papers was used (Beedanagari et al., 2010; Mishra et al., 2010). The nomenclature is as follows; a cytosine residue was considered to be fully methylated if on the chromatogram trace there was only a single cytosine peak, it was considered to be partially methylated if a mixed overlapping C and T peak for a single cytosine was observed, and unmethylated if the trace was exclusively T. An example of the partial and full methylation observed is demonstrated in Figure 3.9 taken from the chromatograms of tumour samples 30 and 16.

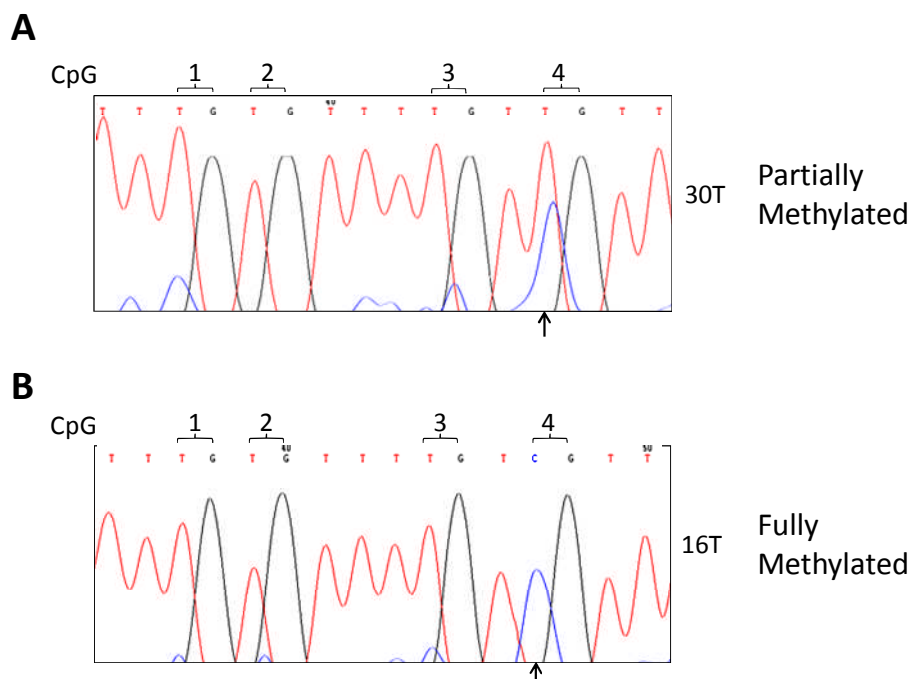


Figure 3.9: Representative sequencing chromatograms demonstrating partial and full methylation. Bisulphite treated genomic DNA was amplified by PCR using methylation indiscriminatory primers and the resultant amplicon sequenced using the same forward primer. Shown are two chromatograms from tumour samples 30 and 16 in order to illustrate a mixed peak of C and T representing partial methylation and then a single peak showing full methylation respectively, as indicated by the arrows. The 4 CpG dinucleotides within the IR5 region are numbered 1-4.

Thirty eight out of the 48 matched samples gave a PCR amplicon and/or sequencing data for both the tumour and matched normal tissue. The results of the bisulphite sequencing are shown in Figure 3.10. Samples where data was not obtained are shaded in grey, unmethylated cytosines are shaded yellow, partially methylated cytosines are orange and fully methylated cytosines are red. Of all the normal tissue samples, only 3 showed a partial methylation (samples 19, 23 and 24) exclusively at the 4th CpG. In the tumour samples 9 showed full methylation (samples 9, 16, 19, 24-28 and 32) and one partial methylation (sample 30), again exclusively of the 4th CpG. Sample 26 in addition to being methylated at position 4, was the only sample to show methylation at an additional CpG. Out of the three normal tissue samples that exhibited partial methylation, samples 19 and 24 showed a further increase in methylation in the corresponding tumour sample. No amplicon was obtained for the matched tumour of the other partially methylated sample (sample 23). Samples 10, 22 and 48 gave no amplicon in either the normal or tumour tissue, possibly indicating these were subject to large chromosomal gene deletion.

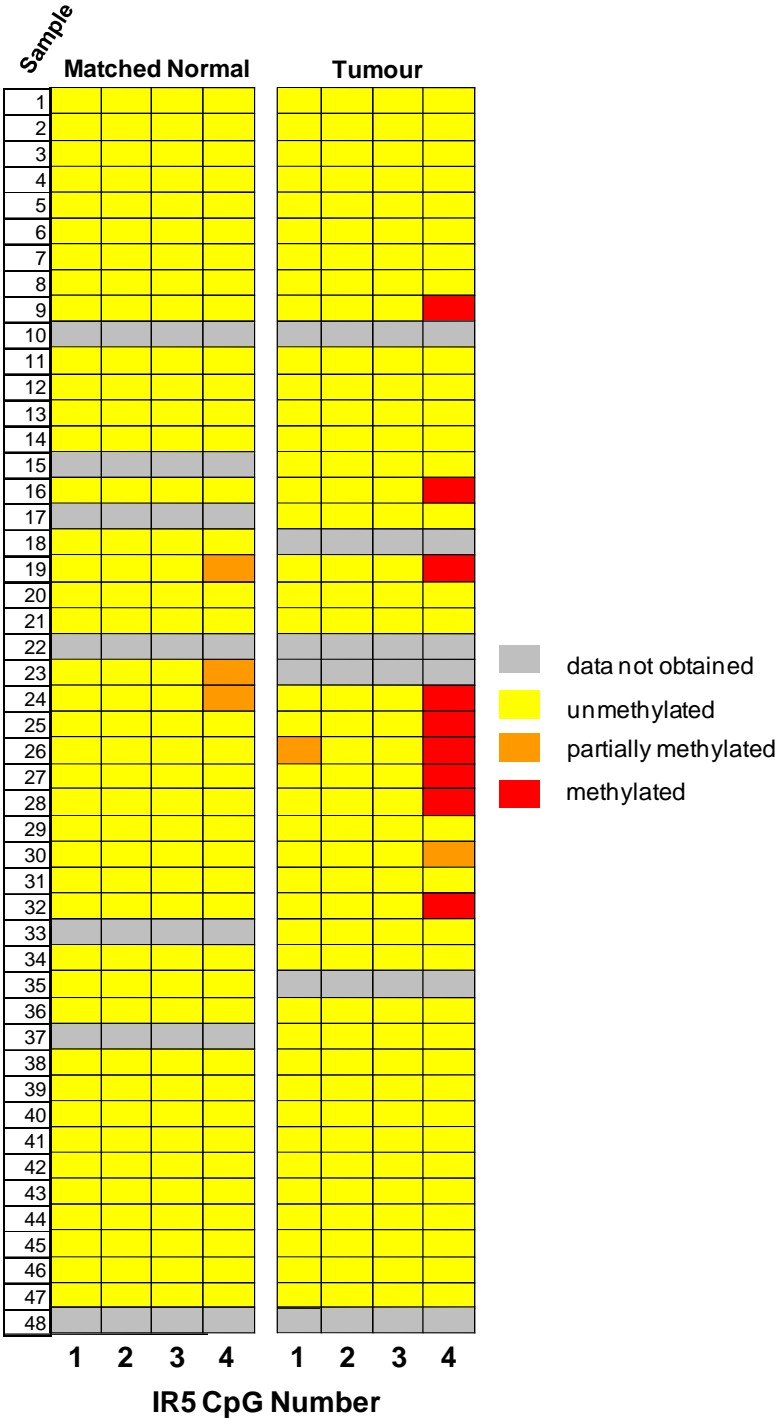


Figure 3.10: Summary of the methylation status of the individual cytosine residues of the CpG dinucleotides within the IR5 region of the LIMD1 promoter in lung tumours and matched normal tissue. Genomic DNA was extracted from a cohort of 48 lung tumour and matched normal tissue and bisulphite treated. A region encompassing IR5 was then amplified using methylation non-discriminatory primers. The amplicon was then gel extracted and purified and sequenced using the same forward primer used for amplification. Each of the 4 CpG dinucleotides within IR5 are identified (1-4) and colour coded according to the methylation status; red- methylated, orange- partially methylated, yellow- unmethylated and grey- no data was obtainable for that sample. Only 3 of the normal lung tissue samples showed partial methylation at the 4th CpG dinucleotide, whereas 9 showed full and 1 partial methylation in the tumour samples.

In summary, 21% (8/39) of the matched samples showed tumour specific methylation compared to the matched normal tissue and a further 5% (2/39) showed an increase in methylation in the tumour tissue compared to the normal matched control. 74% (28/38) of samples showed no evidence of methylation within IR5 in either the normal or tumour tissue. Chromatograms for the samples where methylation was observed are included in the Appendix (Figure 8.3)

3.4 *LIMD1* and *Rassf1a* mRNA Expression is Reduced in the Majority of Primary Lung Tumours Examined

In addition to genomic DNA, RNA was also extracted from the cohort of lung and matched normal tissue in order that qRT-PCR analysis of mRNA expression could be performed. cDNA was synthesised from the extracted RNA and *LIMD1* mRNA expression quantified to detect any differences in expression between lung tumour and matched normal tissue. *Rassf1a* mRNA expression was also quantified for the same reasons as was done for the MSP analysis.

The tumour mRNA levels of both genes showed a wide variation, with samples having decreased, unchanged and increased amounts of expression when compared to their matched normal tissue (Figure 3.11). For *LIMD1* mRNA expression levels, approximately 20% of tumours had no significant change in mRNA expression, 50% of tumours showed an 80% or greater loss of expression and a further 10% of tumours showed an increased expression. Similar changes were also observed for *Rassf1a* mRNA expression; approximately 12% had no change in expression levels, 50% showed an 80% or greater loss of expression and 12% had an increase in expression.

Of the tumours analysed, similar changes in expression of both *LIMD1* and *Rassf1a* mRNA within the same sample were observed. Sample 16 showed no significant changes in expression of either gene between normal and tumour tissue. Samples 1, 3 and 43 showed a 50% reduction in mRNA of both genes in the tumour samples, whilst samples 4, 28, 32 and 36 had no mRNA detected in the tumour samples at all. Conversely, sample 10 showed an increase in both gene expressions in the tumour sample.

Out of the nine tumour samples that exhibited evidence of *LIMD1* methylation (Figure 3.10), three showed greater than 50% decreases in mRNA expression. Three samples had tumours that failed to generate a significantly analysable CT value by qRT-PCR, putatively indicating that the gene is not expressed at all in these samples. Interestingly two of these three samples (28 and 32) gave the

same result when *Rassf1a* mRNA was assayed. Due to the close proximity of the *LIMD1* and *Rassf1a* genes, this could implicate within these tumours a large 3p chromosomal alteration may have occurred.

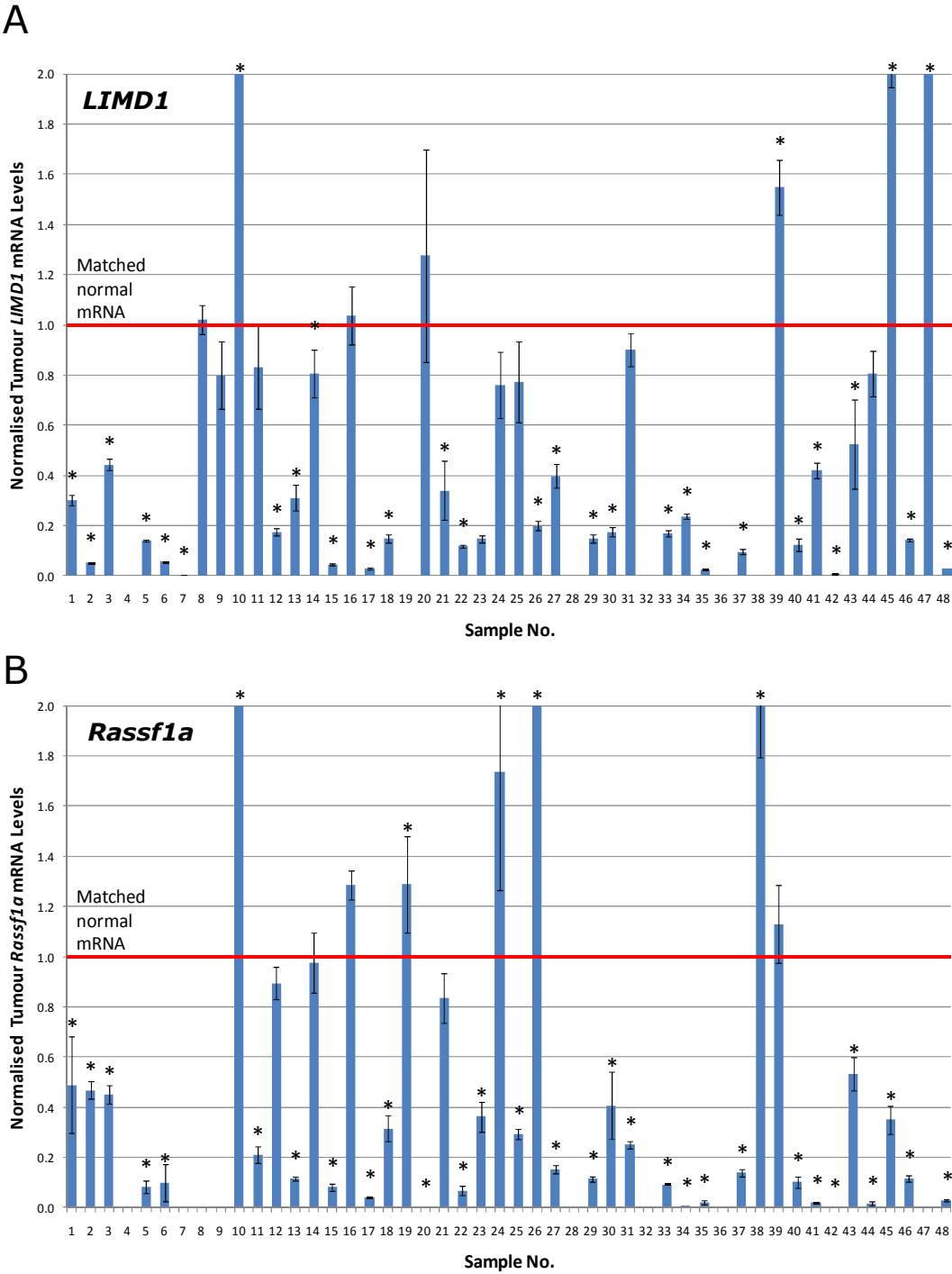


Figure 3.11: qRT-PCR analysis for *LIMD1* and *Rassf1a* mRNA expression in lung tumours when normalised to mRNA expression levels in matched normal lung tissue. RNA was extracted from a cohort of 48 lung tumours and matched normal tissue and cDNA synthesised. qRT-PCR was used to assay levels of (A) *LIMD1* and (B) *Rassf1a* mRNA and normalised to levels of the housekeeper *GAPDH* mRNA. Levels of *LIMD1/Rassf1a* mRNA in normal tissue was then normalised to 1 (bold red line), so the values displayed on the histogram are tumour mRNA levels as a proportion of normal tissue mRNA levels. * $p < 0.05$. Comparable data not obtained for *LIMD1* samples 4, 19, 28, 32, 36 and 38 and for *Rassf1a* samples 4, 7, 8, 9, 28, 32, 36, 47.

3.5 Epigenetic Silencing of LIMD1

Multiple tumour suppressor genes have been found to undergo promoter methylation in cancers that cause them to become silenced. 5-Aza-2'-deoxycytidine is a potent DNA methylation inhibitor that as a cytosine analogue when incorporated into DNA during replication covalently binds to the methylation maintenance methyltransferase Dnmt1. This reduces the available free pool of Dnmt1 available to maintain the methylation pattern during mitosis, as well as resulting in DNA repair, replacing potential methyl cytosines with cytosine (Egger et al., 2004). As maintenance of the methylation pattern is inhibited this ultimately causes DNA hypomethylation, and the re-expression of genes. As methylation within the lung tumours examined in this study was observed (Figure 3.10) in addition to the MB435 cell line (which does not express LIMD1 despite having an intact gene; Figure 3.4), the possibility of *LIMD1* gene silencing by methylation was further investigated.

3.5.1 Optimisation of 5-azacytidine Treatment

Extensive studies on DNA methylation have revealed that different cell types and genes respond to different concentrations of 5-azacytidine. Therefore a titration of concentrations and time points of treatment with 5-azacytidine was carried out on the MB435 cell line. Cells were treated with 5, 10, 20, 40, 60 or 100 μ M 5-azacytidine for either 3 or 5 days. Expression of LIMD1 was analysed by Western blot and hypomethylation of IR5 confirmed by sequencing using the same primers as in Figure 3.4 (data not shown). After cells had been treated for 3 days, in all concentrations of 5-azacytidine, no LIMD1 expression was detected. However, after 5 days of treatment with media changes every day with fresh drug, LIMD1 expression was observed by Western blot at 40 μ M concentrations of the drug and above (Figure 3.12). As a positive control for the Western blot, lysate from LIMD1 expressing U2OS cells was used.

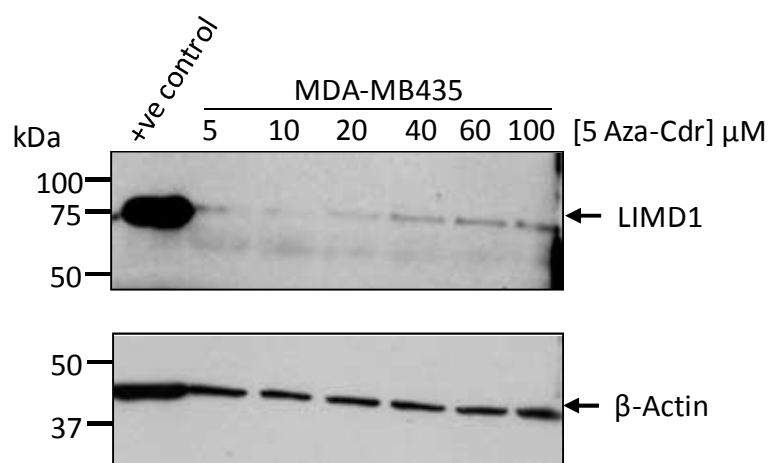


Figure 3.12: Optimisation of the concentration of the DNA methylation inhibitor drug 5-Aza-2'-deoxycytidine needed to restore LIMD1 expression in the MDA-MB435 cell line. MDA-MB435 cells were treated with differing concentrations of 5-Aza-Cdr from 5 to 100μM for 5 days. Cells were then lysed and LIMD1 expression analysed by Western blot with β-actin as a loading control and U2OS cell lysate as a positive control for LIMD1 expression. LIMD1 expression increases with increasing concentrations of the drug.

The highest expression of LIMD1 was observed at the higher concentrations of 5-azacytidine (>40μM). MB435 cells were therefore subsequently treated for 5 days with 100μM azacytidine (with new drug containing media changed every 24hours). In addition to having untreated MB435 cells as a control, U2OS cells were also treated with 5-azacytidine.

3.5.2 LIMD1 is Epigenetically Silenced in the non-LIMD1 Expressing MDA-MB435 Cell Line

Treatment of LIMD1 expressing U2OS cells with 100μM 5-deoxycytidine had no significant changes on LIMD1 expression when compared to untreated cells (Figure 3.13). However, treatment of the non-LIMD1 expressing MDA-MB435 cells with 5-azacytidine caused LIMD1 expression (Figure 3.13). As a confirmation that the expression was due to promoter hypomethylation, genomic DNA was extracted and IR5 bisulphite sequenced (data not shown). The sequencing result confirmed that following 5-azacytidine treatment, the region of the promoter analysed was hypomethylated in the MDA-MB435 cell line, whilst the promoter in U2OS cells maintained its hypomethylated state. Therefore, in the MB435 cell line, LIMD1 is epigenetically silenced.

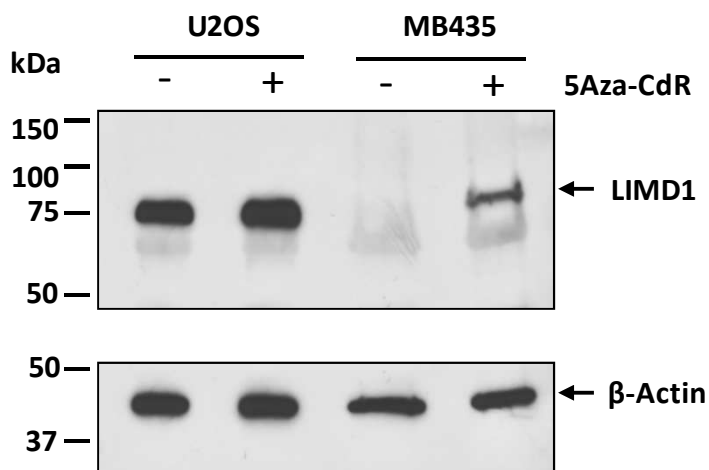


Figure 3.13: Treatment of the non *LIMD1* expressing MDA-MB435 cells with the methylation inhibitor drug 5-Aza 2-deoxycytidine restores expression of *LIMD1*. *LIMD1* expressing U2OS and non *LIMD1* expressing MDA-MB435 cells were treated with 100 μ M 5Aza-Cdr for 5 days. Cells were then lysed and *LIMD1* expression analysed by Western blot. Treatment of MDA-MB435 cells with 5Aza-Cdr resulted in *LIMD1* expression.

3.6 Summary

Within the CpG Island in the *LIMD1* promoter (Figure 3.1) a small 21bp region (IR5) was been identified as being critical for transcription, as deletion of this region reduced transcriptional activation by 90% (Figure 3.2). Within the *LIMD1* expressing U2OS cell line, cytosine bases within CpG dinucleotides within the IR5 region are unmethylated; however in the MDA-MB435 cell line that does not express *LIMD1* the bases are methylated (Figure 3.4). In a cohort of lung tumours with matched normal tissue this same region also had evidence of methylation in the tumour tissue, specifically at the fourth CpG dinucleotide (Figure 3.10). qRT-PCR analysis of the same lung tumour cohort revealed the presence of methylation correlated with a reduction in *LIMD1* mRNA levels, and the reduction in mRNA levels overall was similar to that of another well characterised 3p21.3 tumour suppressor gene *Rassf1a* (Figure 3.11). Furthermore, treatment of the MDA-MB435 cell line with the potent DNA methylation inhibitor, 5-azacytidine, caused demethylation of IR5 within the *LIMD1* promoter and expression of *LIMD1* protein (Figure 3.13), thus demonstrating *LIMD1*, like other characterised tumour suppressor genes, undergoes epigenetic silencing.

**Chapter 4 Results: Identification of PU.1 as a Major
Transcriptional Activator of *LIMD1***

4.1 Introduction

The 21bp IR5 region within the CpG Island of the *LIMD1* promoter is critical for transcriptional activation; deletion of IR5 resulted in a 90% decrease in transcription (Figure 3.2) and methylation of this region contributes to epigenetic silencing of *LIMD1* (Figure 3.13). It was therefore hypothesised that the reduction in transcription was indicative that IR5 contained a binding motif for one or more critical transcriptional activators. The identity of such a factor(s) was therefore the aim of this chapter of investigation.

4.1.1 IR5 within the *LIMD1* Promoter is Perfectly Conserved Between Different Mammalian Species

Species which diverged many millions of years ago, for example humans and mice ca.75 million years ago, will have undergone evolutionary mutations and selections, causing diversity in genomic sequences and resultant phenotypes. However, genes and regulatory elements involved in expression of proteins essential for cellular survival (e.g. TSG) and fertility (e.g. enzymes involved in gametogenesis) remain conserved; a mutation that is either fatal or renders the species infertile by definition is not inherited and as such these sequences remain conserved (Boffelli et al., 2004). As such, homology of nucleotide sequences between species has been used as a tool for identifying both genes and enhancers whose protein product has a pivotal function in the survival of an organism (Pennacchio and Rubin, 2001).

The *LIMD1* promoter sequences from 13 different *LIMD1* expressing mammalian species were extracted from the Ensembl Genome Browser and aligned using the multiple sequence alignment tool ClustalW. Initial attempts to simultaneously align 2.5kb upstream of the ATG initiation codon between 13 different mammals proved problematic due to a large number of small conserved stretches of nucleotides causing mis-alignments. To overcome this problem, 200 base pair regions that encompassed 100bp both 5' and 3' to IR5 were aligned and scrutinised for areas of homology (Figure 4.1). IR5 and a core region of IR7 were perfectly conserved between all the mammalian genomes examined. Interestingly IR6 was also highly (>80%) conserved between 8 of the species examined. As deletion of IR7 did not result in a significant change in transcriptional activity of the promoter, no further analysis of this region was performed.

nucleotide discrepancies between the query sequence and the database of known sequences.

To avoid the possibility of disrupting a putative consensus sequence by selectively only analysing IR5 or the immediate surrounding regions, the entire cloned promoter was analysed in the *in silico* search. From this analysis, three transcription factors received a perfect match score of 1.0, including the well characterised basal Transcription Factor II B (TFIIB), which makes up part of the RNA Polymerase II Preinitiation Complex. As the promoter deletion analysis hypothesised that IR5 may contain an important transcription factor binding site, this region was then selectively scrutinised. This revealed a potential binding consensus for the human and murine Ets factor Spi1/PU.1, which obtained a score of 0.989. IR5 contained a matched consensus of gcGGAAgt on the anti-sense strand at base pair position -673 to -670 relative to the predicted TSS (Figure 4.2). As the algorithm screened the *LIMD1* promoter in a 5' to 3' direction, the start, end and anchor positions for each transcription factor are distance from the 5' end of the promoter, which itself is at base -1990 relative to the TSS. The positions of the binding sites relative to the TSS can therefore be calculated by subtracting 1990 from the stated positions (i.e. $1320-1990=-670$). The putative PU.1 binding site within IR5 has been annotated onto Figure 4.1. The *in silico* analysis was the first indication that the transcription factor PU.1 may bind to the *LIMD1* promoter within IR5 and so could be responsible for the major transcriptional activation. However, as the Ets family of proteins bind to a very similar core sequence of GGAA (Hsu et al., 2004), there was a probability that another Ets factor may also bind this element. The raw data for DNA motif analysis within the *LIMD1* promoter is available at <http://www.sciencedirect.com/science/article/pii/S0014579311001669>.

Matrix Family	Detailed Family Information	Matrix	Start position	End position	Anchor position	Strand	Core sim.	Matrix sim.	Sequence
V\$E2FF	E2F-myc activator/cell cycle regulator	V\$E2F.03	1257	1273	1265	+	0.81	0.855	cgcggGCTCgggacgtg
V\$HIF	Hypoxia inducible factor, bHLH/PAS protein family	V\$HRE.01	1262	1278	1270	+	1	0.931	gctcgggaCGTgacagag
V\$CREB	cAMP-responsive element binding proteins	V\$ATF6.02	1261	1281	1271	+	1	0.896	ggctcggGACGtgacagccg
V\$AP1R	MAF and AP1 related factors	V\$MAFA.01	1269	1289	1279	+	0.905	0.942	acgTGCAgagccggcagcga
V\$NRSF	Neuron-restrictive silencer factor	V\$NRSF.01	1284	1314	1299	+	1	0.737	gagcgAGCAgcaggactcgc
V\$ZF5F	ZF5 POZ domain zinc finger	V\$ZF5.01	1306	1316	1311	-	1	0.952	gagtGCGCcg
V\$ETSF	Human and murine ETS1 factors	V\$SPI1_PU1	1310	1330	1320	-	1	0.989	cgggacgcGGAgtgagtcgc
V\$SP1F	GC-Box factors SP1/GC	V\$SP2.01	1322	1336	1329	-	1	0.849	gggcgccgGGACgcg
V\$SP1F	GC-Box factors SP1/GC	V\$SP1.03	1325	1339	1332	-	1	0.918	ggaGGGCggcgggac
V\$CTCF	CTCF and BORIS gene family, transcriptional regulators with 11 highly conserved zinc finger domains	V\$CTCF.02	1323	1349	1336	-	0.75	0.699	cgcgcggggccggaggcgGGCGgga
V\$STAF	Selenocysteine tRNA activating factor	V\$ZNF76_143.0	1330	1352	1341	+	0.81	0.77	gccgCCTCccggcccgccgcgc
V\$NRF1	Nuclear respiratory factor 1	V\$NRF1.01	1337	1353	1345	-	1	0.839	ggcGCGCgcccggccgga
V\$NRF1	Nuclear respiratory factor 1	V\$NRF1.01	1338	1354	1346	+	0.75	0.797	ccgGCCCGcgcgcgccc
V\$NRF1	Nuclear respiratory factor 1	V\$NRF1.01	1339	1355	1347	-	1	0.789	tcgGCGCgcccggccg
V\$ZF5F	ZF5 POZ domain zinc finger	V\$ZF5.01	1342	1352	1347	-	1	0.967	gcgcGCGCggg
V\$HESF	Vertebrate homologues of enhancer of split complex	V\$HES1.01	1341	1355	1348	-	0.944	0.948	tcggcgcGCGCgggc

Figure 4.2: *In silico* analysis of the *LIMD1* promoter for transcription factor binding sites. The cloned sequence of the *LIMD1* promoter was scrutinised for transcription factor binding sites using the MatInspector transcription factor binding software. Analysis around the IR5 region identified Spi1/PU.1 as having a high matrix similarity score of 0.989 (where 0.8 is classed as a good match and 1.00 is a perfect match).

4.2.1 Mutation of the DNA Consensus for Ets Factor Binding within IR5 Reduces *LIMD1* Promoter Driven Transcription

In silico analysis is a fast and simple method of identifying potential DNA binding proteins for a specific consensus. However, as it is based on an algorithm and is purely computational, when applied to an uncharacterised promoter it does not prove the protein-DNA interaction occurs *in vivo*. To ascertain if the predicted interaction occurs, *in vitro* and *in vivo* experiments were performed. It was initially hypothesised that if PU.1 were to bind the predicted motif, mutation of the consensus should abrogate any interaction between PU.1 and the *LIMD1* promoter, and thus result in a significant decrease in transcriptional activity, comparable to that seen with $\Delta 5$ (Figure 3.2).

Site directed mutagenesis was performed to mutate the putative PU.1/Ets consensus from TTCC to TTTT ('CC→TT') and confirmed by sequencing. Since the *LIMD1*-luciferase plasmid was ~8kb, it was not feasible to sequence check the whole plasmid for other mutations that may have been introduced through PCR amplification, although a proof reading *Pfu* was used in the PCR reactions. Therefore the mutation was reverse mutated back to the wild type consensus ('TT→CC') to check the resultant luciferase values returned to that of the wild type promoter, ruling out any unseen mutations that may have given a false

positive result. As an additional control, a further downstream cytosine (still within IR5) was mutated and then reverted back to wild type ('C→T' and 'T→C' respectively) (Figure 4.3A). This cytosine corresponded to the commonly methylated cytosine in the primary lung tumours (Figure 3.10). These new promoter mutated plasmids were co-transfected with a Renilla luciferase normalisation vector into U2OS cells, and luciferase activity assayed after 24 hours. In addition to the new mutations, the IΔ5 promoter mutation was also transfected as a control for loss of transcriptional activity.

Mutation of the putative PU.1 consensus ('CC→TT') reduced *LIMD1* promoter driven transcription by over 90% (Figure 4.3B). This was comparable to that seen with the IΔ5 promoter deletion. The specificity in reduction in transcription was confirmed as reversion of the mutation back to wild type restored luciferase levels to that of the wild type promoter. Furthermore, mutating the downstream cytosine resulted in luciferase values that were not significantly different to that of the wild type promoter.

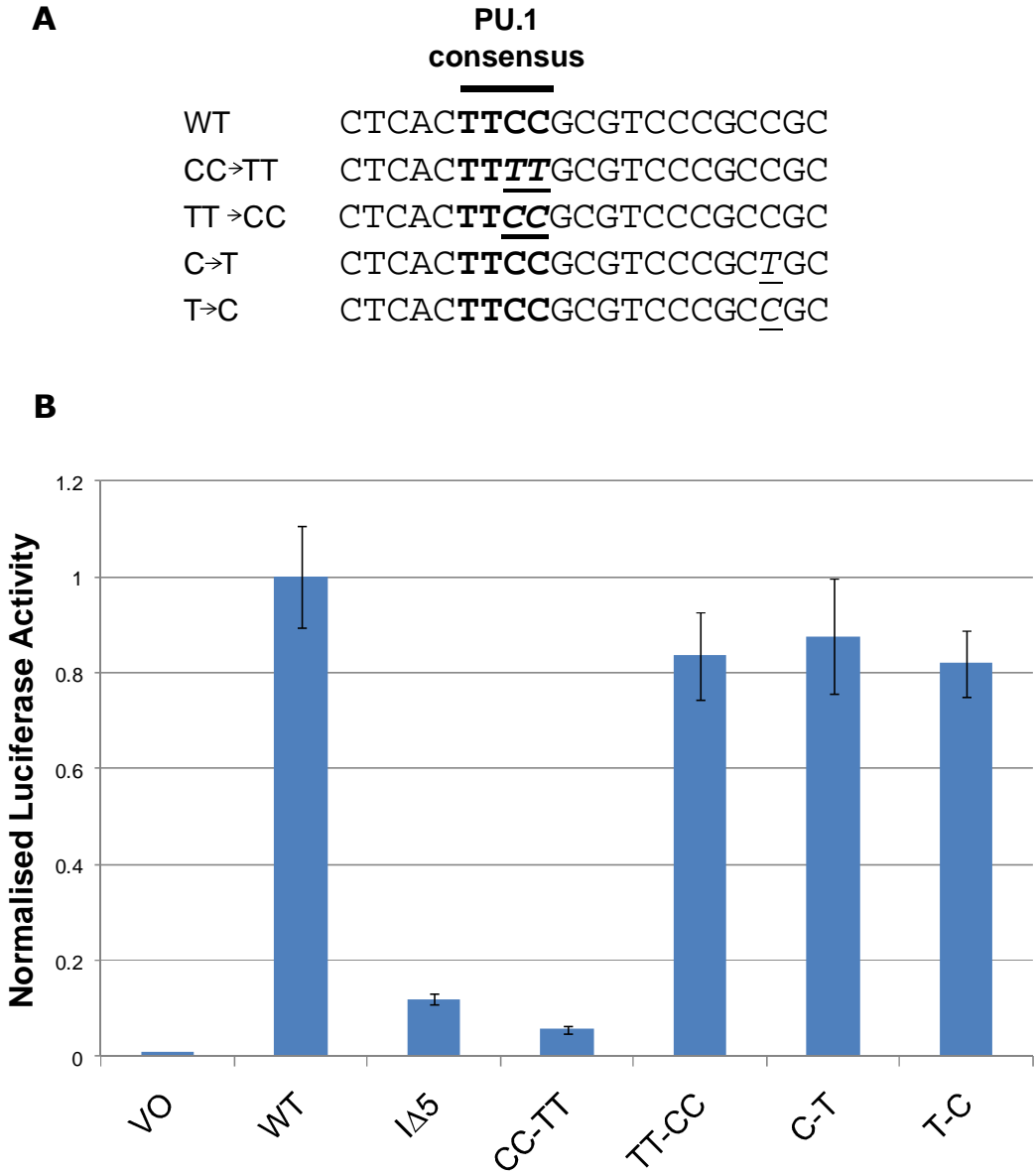


Figure 4.3: Mutagenesis of the putative PU.1 motif reduces transcriptional activity by 90%. (A) The PU.1 consensus (bold) within the full length LIMD1 promoter was mutated using site directed mutagenesis from TTCC to TTTT (CC-TT; underlined). As a control a separate C to T point mutant was created (C-T; underlined). Both mutant consensus plasmids were reverse mutagenised back to the wild type sequence as a control. (B) 50ng of the mutated plasmids, along with the wild type and IA5 promoter plasmids were co-transfected with 5ng of Renilla luciferase into U2OS cells and resultant luciferase activity assayed 24hours post transfection. Mutation of the putative PU.1 consensus reduced transcriptional activity by 90%, comparable to the reduction seen with the IA5 mutant.

4.3 Identification of PU.1 Binding to the *LIMD1* Promoter and Activating Transcription

4.3.1 Sub-cloning of PU.1 into pcDNA4 His/Max TOPO and pCMV-HA Vectors

Luciferase assays with the PU.1 consensus mutations provided the first *in vivo* evidence to suggest PU.1/Ets factor binding to the *LIMD1* promoter. In order to investigate the identity of the protein that bound to the Ets consensus, *in vivo* chromatin immunoprecipitation (ChIP) and *in vitro* electrophoretic mobility shift assays (EMSA) were performed. These assays use antibodies targeted against a specific protein, in this investigation PU.1, to analyse the presence of the protein bound to the IR5 region of the *LIMD1* promoter, and both techniques will be discussed fully later on. To facilitate the ChIP and EMSA analysis, PU.1 cDNA was subcloned into two expression vectors to allow for ectopic over expression; pcDNA4 His/Max TOPO which encodes an Xpress and hexa-His epitope, and pCMV-HA, which encodes a HA epitope onto the N terminal of the expressed protein.

Human PU.1 cDNA was a kind gift from A. Rizzino (University of Nebraska Medical Centre). Prior to sub-cloning of the cDNA, it was sequenced using primers against the T7 promoter within the plasmid. Upon analysis of the sequence, nucleic acid codons for the first four N terminal amino acids were found to be omitted, and the sequence started with an alternative internal ATG codon.

PCR primers were designed to incorporate the 4 missing codons, as well as 5' *EcoR1* and a 3' *BamH1* restriction enzyme sites to facilitate the downstream sub-cloning of PU.1. Due to the long length of the primers, a gradient PCR was carried out to determine the optimal annealing temperature using the high fidelity hot start Phire (NEB) polymerase (Figure 4.4A). The correct sized amplicon (816bp as obtained from Ref Seq NM_001080547.1) was generated with all annealing temperatures from 52.0 to 64.0°C, the lower temperatures gave a stronger more intense band than at higher annealing temperatures when visualised under UV light with ethidium bromide staining, however this was also accompanied by more smearing on the gel (Figure 4.4A). The PCR was therefore repeated using a compromise annealing temperature of 57.1°C. After the PCR had completed 35 cycles, one Unit of Taq Polymerase was added for ten minutes at 70°C. The reason for this is that the high fidelity hot start Phire polymerase does not possess the ability to add the 3' dA overhangs which were needed for

the subsequent topoisomerase mediated TA cloning into the pcDNA4 His/Max TOPO vector. The subsequent amplicon was purified and extracted from an agarose gel and TA cloned into the pcDNA4 His/Max TOPO vector. The cloning reaction was transformed into TOP10[®] chemically competent cells, and colonies screened to check for successful ligation by single digestion with *EcoR1* to excise the PU.1 cDNA. Two of the selected colonies contained an insert of the correct size and was confirmed as PU.1 cDNA by sequencing (Figure 4.4B and C).

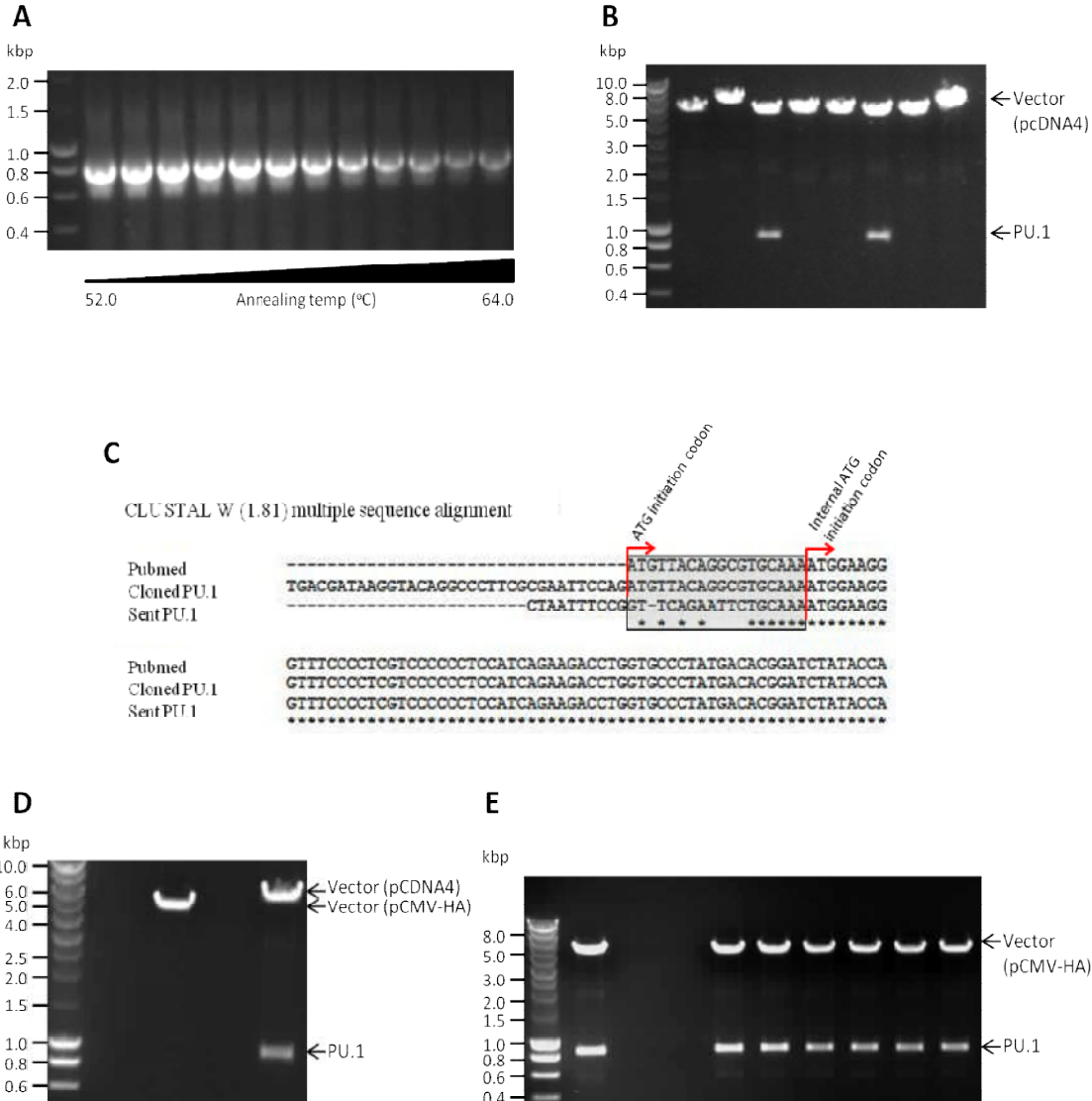


Figure 4.4: The introduction of four N-terminal amino acids and sub-cloning of PU.1. (A) Primers to incorporate the first four N terminal amino acids of PU.1 to match the NCBI sequence, as well as 5' *EcoR1* and 3' *BamH1* sites were used to PCR PU.1 using a gradient of annealing temperatures. The amplicon was gel excised and purified and TA cloned into the pcDNA4 His/Max TOPO vector and 8 colonies selected. (B) Transformants were screened by digestion of the plasmids after miniprep purification revealing 2 contained the PU.1 insert. (C) Sequencing of the newly cloned pcDNA4-PU.1 confirmed the PU.1 insert was both in frame and contained the extra four N terminal amino acids compared to the gifted cDNA. (D) Digestion of pcDNA4-PU.1 and pCMV-HA vector only with *EcoR1* and *BamH1* allowed the PU.1 insert to be cut and pasted in to the HA vector. (E) Transformation of the ligated HA-PU.1 followed by digestion with *EcoR1* and *BamH1* revealed the sub cloning had been successful.

The PU.1 cDNA was then subcloned into a pCMV-HA vector, which incorporates a HA epitope tag onto the N terminus of the subcloned protein. PU.1 cDNA was excised from the newly created pcDNA4-PU.1 plasmid using the incorporated *EcoRI* and *BamHI* flanking restriction sites and ligated into the similarly cut pCMV-HA vector (Figure 4.4D). Again colonies were selected after transformation of the ligation and positive clones identified by restriction digest and sequencing (Figure 4.4E).

4.3.1.1 PU.1 binds to the *LIMD1* Promoter *in vivo* as demonstrated by Chromatin Immunoprecipitation Assays

To identify if PU.1 was able to directly bind IR5, a chromatin immunoprecipitation (ChIP) assay was employed. ChIP is a method for assaying protein-DNA interactions. In the assay, formaldehyde is used to crosslink protein to DNA in cells (i.e transcription factors to the DNA promoters of genes) so that any interactions (which may be transient) are stabilised throughout the experiment. The nuclei are then extracted and the genomic DNA is sheared, followed by subsequent immunoprecipitation of the transcription factor of interest and analysis of any co-immunoprecipitated DNA by PCR and/or sequencing.

For ChIP analysis, pcDNA4-PU.1 or pcDNA4-vector only (VO, as a control) were transfected into HEK 293T cells. After formaldehyde crosslinking genomic DNA was sheared by sonication to 200-500bp in length. The number of sonications had to be empirically optimised for each cell type in order to generate fragments of the correct size; too few sonications would produce larger DNA fragments whilst too many sonications would produce much smaller DNA fragments. The optimum number of sonications for the HEK 293T cells was 4 x 15s (Figure 4.5).

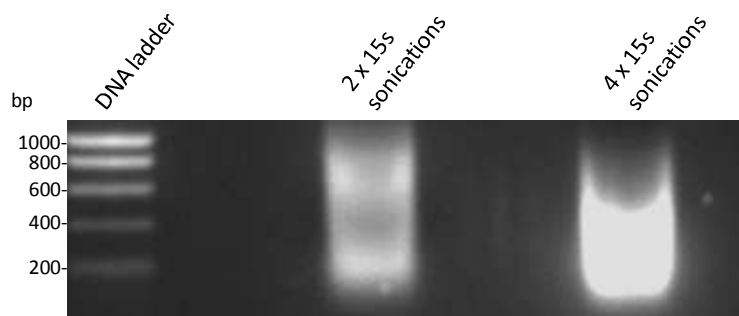


Figure 4.5: Optimisation of HEK 293T genomic DNA shearing for subsequent ChIP analysis. HEK 293T cells were treated with formaldehyde to crosslink protein to DNA prior to lysis by sonication. For accurate ChIP analysis, the optimal genomic DNA fragment length is 200-500bp, which is achieved through differential amounts of sonication followed by analysis by visualisation on an ethidium bromide stained 1% agarose gel. 4 x 15s pulses of sonication produce the correct sized fragments (4 x 15s sonications), whereas less sonications (2 x 15s) produce a longer smear of genomic DNA on the gel representing larger DNA fragments due to insufficient sonication.

The pcDNA4 vector encompasses an Xpress[®] epitope tag onto the subcloned DNA, and so the ectopically expressed PU.1 or the VO were immunoprecipitated with an anti-Xpress antibody. Protein immunoprecipitation was confirmed by Western blot (Figure 4.6A). As a positive control for the ChIP assay, primers for the previously characterised *CD11b* promoter to which PU.1 binds (Brugnoli et al., 2009) were used alongside primers to encompass IR5 of the *LIMD1* promoter. When PU.1 was immunoprecipitated, both the *CD11b* and *LIMD1* promoter regions that encompass the PU.1 binding motif were co-immunoprecipitated, as detected by PCR (Figure 4.6). These regions were not detected when the VO was precipitated, showing that ectopic PU.1 specifically binds to the *LIMD1* promoter *in vivo* in HEK 293T cells.

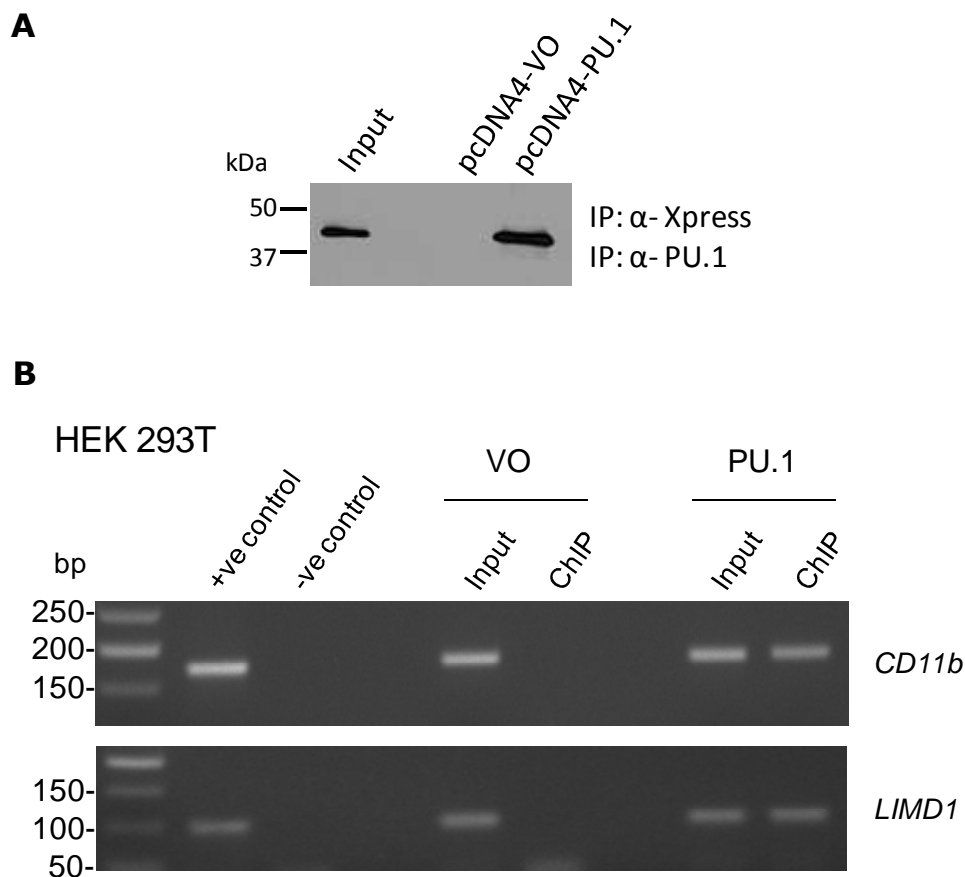


Figure 4.6: Exogenous PU.1 binds to the LIMD1 promoter in HEK 293T cells. pcDNA4-PU.1 or vector only (VO) was transfected into HEK 293T cells. 48 hours post transfection cells were serum starved overnight, then stimulated with 20% FCS before protein and DNA were crosslinked and DNA was sheared by sonication. (A) PU.1 or control VO were immunoprecipitated with 2.5 μ g of anti-Xpress and confirmed by Western blot probed with anti-PU.1. (B) Co-immunoprecipitated DNA was purified and analysed by PCR utilising primers for the previously characterised *CD11b* promoter as a positive control along with primers encompassing the PU.1 motif within the *LIMD1* promoter.

To then ascertain the relevance of ectopically expressed PU.1 bound to the LIMD1 promoter the interaction between endogenous PU.1 and the *LIMD1* promoter was assayed. As PU.1 is expressed at high levels in haematopoietic derived cell lineages, the U937 histiocytic lymphoma cell line was assayed for endogenous expression of both PU.1 and LIMD1 protein. Total cell lysate from U937 cells was Western blotted and probed with anti-PU.1 and anti-LIMD1 antibodies. This analysis showed both proteins were expressed (Figure 4.7A) and as such was a suitable cell line for endogenous ChIP analysis.

For ChIP analysis, endogenous PU.1 was immunoprecipitated from U937 cell nuclei with an anti-PU.1 rabbit polyclonal antibody. As a matched isotype control for antibody specificity, IgG from a non-immunised rabbit was used.

Following immunoprecipitation, PU.1 specifically co-immunoprecipitated a region spanning the PU.1 binding motif within IR5 of the *LIMD1* promoter (Figure 4.7B). The *CD11b* promoter was used as a positive control (Brugnoli et al., 2009). This result was consistent with the result from the ChIP assay with exogenously expressed PU.1 in HEK 293T cells (Figure 4.6). As a further control for specificity of the assay, primers incorporating a region of the *LIMD1* promoter further upstream from the PU.1 motif (US *LIMD1*) were also included. No amplicon for this region was detected from the co-immunoprecipitated DNA, and neither were any amplicons detected following precipitation with the isotype control antibody, indicating endogenous PU.1 specifically binds to the *LIMD1* promoter *in vivo*.

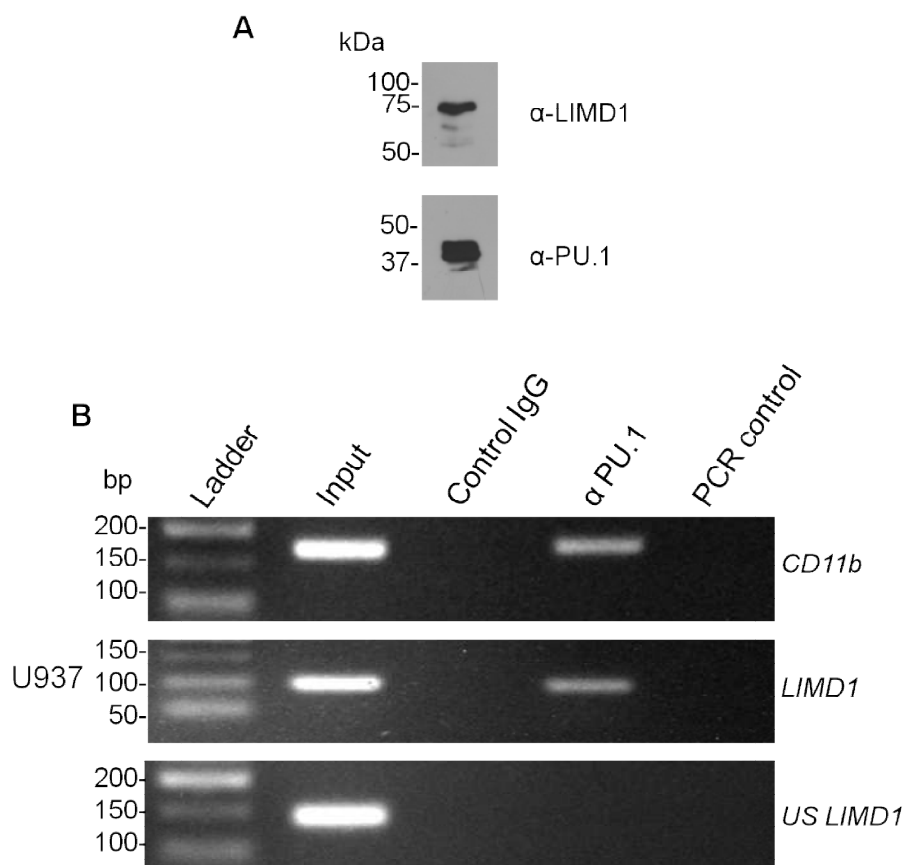


Figure 4.7: Endogenous PU.1 binds to the *LIMD1* promoter that encompasses the PU.1 motif *in vivo*. (A) U937 human monocytic leukemic cells express both endogenous LIMD1 and PU.1 as detected by Western blot. (B) U937 cells were stimulated with 20% FCS following 24 hour serum starvation. Protein and DNA were then crosslinked with formaldehyde, nuclei extracted and DNA sheared by sonication. PU.1 was immunoprecipitated with an anti-PU.1 or control IgG antibody and co-immunoprecipitated DNA purified and PCR analysed. Primers encompassing the *CD11b* and *LIMD1* promoter encompassing IR5 yielded amplicons, however no amplicon was produced using primers for further upstream of IR5 (*US LIMD1*), showing endogenous PU.1 associates with the *LIMD1* promoter *in vivo*.

4.3.2 PU.1 binds the IR5 region of the *LIMD1* Promoter *in vitro* as demonstrated by Electrophoretic Mobility Shift Assay

To further verify PU.1 binding to the *LIMD1* promoter, *in vitro* electrophoretic mobility shift assays (EMSA) were also performed. HEK 293T cells were transfected with pCMV-HA-PU.1 48 hours prior to nuclear extraction and lysis. Nuclear extracts were then incubated with a ³²P-labelled oligo probe that had the identical 21bp sequence of IR5. If PU.1 bound specifically to the probe, then a protein-DNA complex would form and migrate slower on a non-denaturing gel than the probe or PU.1 protein alone, and is known as a band shift. To identify if the band shift contained PU.1 rather than a different nuclear protein complex, addition of an anti-PU.1 antibody to the reaction would result in an even larger antibody-PU.1-³²P-oligo complex and would be retarded on a gel even further. This is known as a super-shift. Any band shifts are visualised using autoradiography on a phosphorimager.

Upon addition of HEK 293T HA-PU.1 transfected nuclear lysate to the ³²P-labelled oligo probe, 3 distinct band shifts are observed, corresponding to the formation of protein-DNA complexes (Figure 4.8A lane 3). One of these bands is commonly observed following addition of nuclear extract both in the presence and absence of PU.1 (Figure 4.8A lanes 2 and 3). This band is unlikely to be PU.1 as HEK 293T cells do not express PU.1 at levels detectable by Western blot and so could not be an endogenous PU.1 complex. Upon addition of either α-PU.1 or α-HA antibodies, a supershift was observed. The intensity of the original band shift significantly diminished (denoted by the arrow) and a new band of higher molecular weight in the gel is observed (Figure 4.8A lanes 4 and 7). This indicated the complex specifically contained PU.1. As a control for specificity of PU.1 binding, antibodies against the Ets transcription factor family members Ets-1 or Elk-1, or another transcription factor STAT3 were used. None of these antibodies gave a supershift (Figure 4.8A lanes 5, 6 and 8), demonstrating the band shift complex that formed contained PU.1, further strengthening the evidence that PU.1 binds to the *LIMD1* promoter.

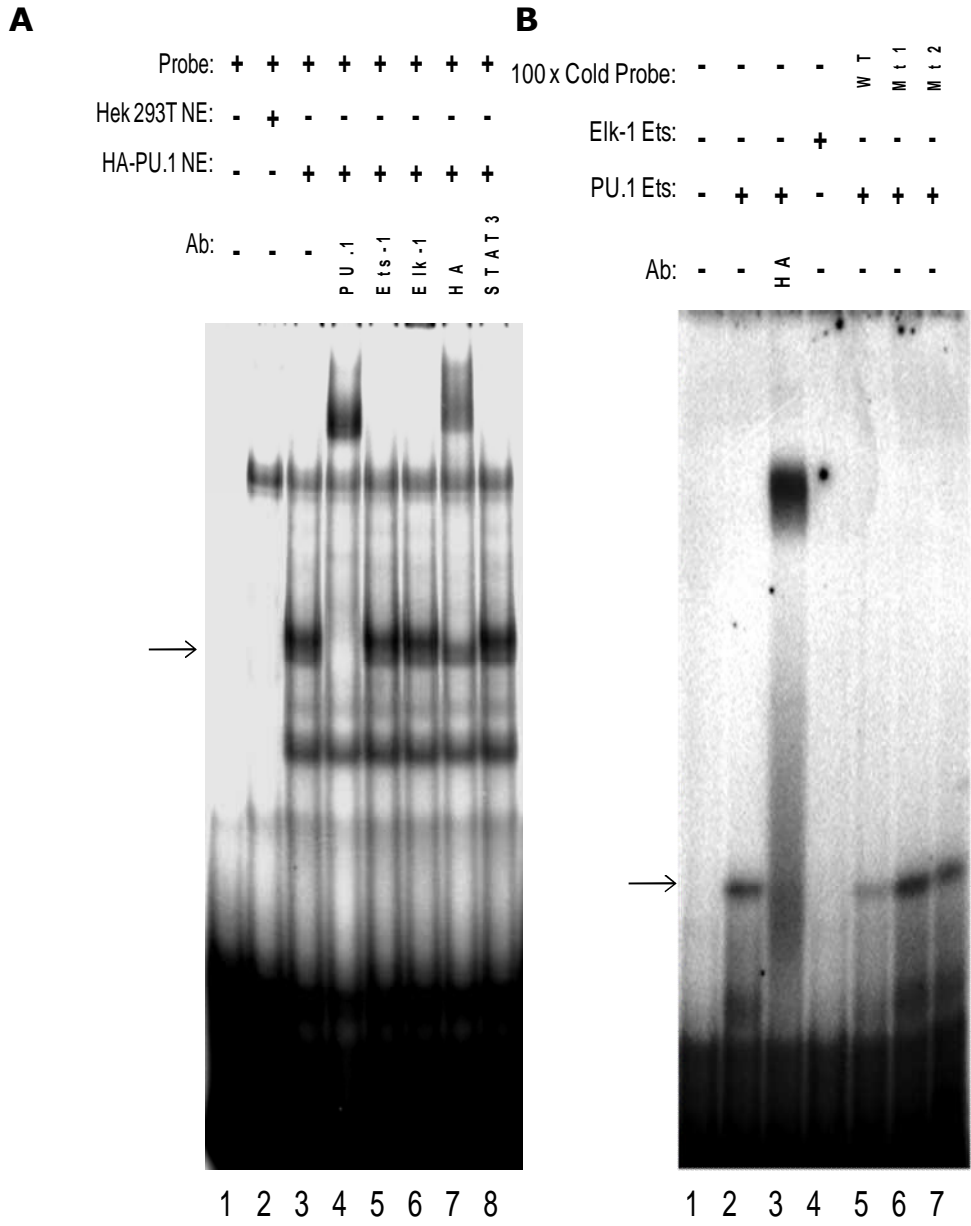


Figure 4.8: PU.1 specifically binds to the wild type but not mutated IR5 consensus. (A) HA-PU.1 was expressed in HEK 293T cells and nuclear extracts were incubated with a ³²P labelled oligonucleotide probe with sequence identical to that of IR5, resulting in a band shift. Upon addition of either an anti-PU.1 or anti-HA antibody a supershift is observed, but not with addition of control Ets-1, Elk-1 or STAT3 antibodies. (B) Recombinant Ets domain of PU.1 was incubated with the same ³²P labelled oligo probe, resulting in a band shift. No band shift is seen with the recombinant Ets domain of Ets-1. Upon addition of a 100 fold excess of cold unlabelled probe the band shift is out competed. A 100 fold excess of cold probe where the PU.1 consensus has been mutated does not compete out PU.1 binding and so the band shift remains. EMSA experiments were kindly performed by Professor. P. E. Shaw.

4.3.3 The Ets-domain alone of PU.1 binds to the *LIMD1* Promoter

The Ets family of transcription factors exhibit a diverse range of functions, and are able to specifically bind to highly homologous DNA sequences, with as little as one base pair selecting for one transcription factor over another (Verger and Duterrque-Coquillaud, 2002). To show the specificity of PU.1's Ets domain alone as the critical protein domain responsible for binding to the *LIMD1* promoter, the PU.1 Ets domain was sub-cloned into a pQE60 vector, which when transformed into *E. Coli* produced recombinant glutathione-s-transferase (GST) and hexa-His tagged PU.1 Ets domain. A further EMSA experiment was then performed with the recombinant Ets domains used in place of nuclear extract. The Ets-domain of Elk-1 had previously been cloned into the same vector and so was used as a negative control. When recombinant PU.1 Ets domain was added to a radio-labelled IR5 oligo probe, a band shift was observed, followed by a supershift upon addition of α -HA antibody (Figure 4.8B lanes 2 and 3). This corroborated the previous results observed with HA-PU.1 transfected HEK 293T nuclear extract. Addition of the Ets domain of Elk-1 did not cause a band shift (Figure 4.8B lane 4), showing the specificity for the Ets domain of PU.1 in binding the *LIMD1* promoter.

Previous mutational analysis of the PU.1 consensus resulted in a 90% decrease in transcriptional activation from the promoter (Figure 4.3), which was hypothesised to be due to inhibition of PU.1 binding. To prove if mutation of the consensus did inhibit PU.1 binding, a further EMSA using the recombinant Ets domains of PU.1 was carried out in a competition assay. When a 100 fold excess of cold unlabelled IR5 oligo probe (compared to labelled probe) was added to the assay, it was able to compete for binding to the PU.1 Ets domain, resulting in a significant decrease in intensity of the band shift (Figure 4.8B lanes 2 and 5). However, when a 100 fold excess of cold oligo containing a mutated PU.1 binding consensus was added instead (mt1 and mt2), this was unable to compete for PU.1 binding and so did not affect band shift intensity (Figure 4.8B lanes 2, 6 and 7). These data therefore support the initial reporter and ChIP assay findings that PU.1 binds to the predicted PU.1 binding motif within the *LIMD1* promoter, and mutation of the consensus abrogates PU.1 binding and reduces transcription accordingly.

4.3.4 siRNA Mediated Depletion of PU.1 reduces LIMD1 Protein Levels

ChIP and EMSA analyses of the *LIMD1* promoter (Figure 4.6, Figure 4.7 and Figure 4.8) demonstrated that PU.1 was able to bind to the *LIMD1* promoter specifically at the PU.1 binding motif within IR5, and mutation of the consensus abrogates this binding. In order to assess the physiological significance of this interaction we reasoned that if PU.1 was a major transcriptional activator of *LIMD1* expression through binding to its promoter, loss of endogenous PU.1 protein should cause a loss of endogenous LIMD1 protein expression.

siRNA mediated gene silencing was therefore used to deplete endogenous PU.1 protein. For continuity with the endogenous ChIP assay (Figure 4.7B), endogenous PU.1 depletion was carried out using U937 cells. U937 cells are a suspension cell line that are difficult to transfect with either siRNA or DNA (Martinet et al., 2003; Stroh et al., 2010). This compared to other monolayer adherent cell lines within the lab (U2OS, HEK-293T, HeLa and MDA-MB435) that were easy to transfect with both siRNA and DNA. Initially siRNA knockdown was attempted with the standard laboratory siRNA transfection reagent Dharmafect 1 (Thermo Fisher). However, even at siRNA concentrations at up to 300nM, knockdown of PU.1 was unsuccessful.

Another siRNA transfection reagent, Interferin (Polyplus Transfection) was tested for ability to transfect the U937 cells. Transfection of high concentrations of siRNA with this reagent proved unreliable due to low transfection efficiency, however this was still more efficient than the Dharmafect 1 reagent. To check that the transfection difficulties were due to cell type and not siRNA degradation or a non-optimum sequence target, siRNA targeted against LIMD1 and using Interferin was transfected into U2OS and HeLa cells alongside U937, utilising the same mastermix of siRNA and reagent. Significant protein knockdown of LIMD1 was achieved in both the U2OS and HeLa cell lines (as quantified by Western blot), however no significant knockdown was achieved in the U937 cells (Figure 4.9). This further confirmed that it was the U937 cells rather than the siRNA or transfection reagent that was the problem. Electroporation had been reported as being a successful way of transfecting monocytic cell lines, as limited DNA trafficking in these cells prevents nuclear delivery of DNA through traditional lipid based transfection reagents (Martinet et al., 2003; Stroh et al., 2010).

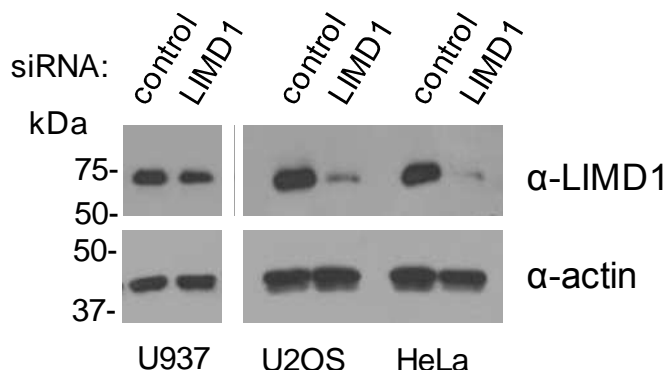


Figure 4.9: Optimisation of siRNA transfection into U937 cells with a lipid based transfection reagent. U937, U2OS and HeLa cells were transfected with 100nM LIMD1 or scrambled control siRNA using Interferin siRNA transfection reagent. 48 hours post transfection cells were lysed in RIPA buffer supplemented with protease inhibitors and LIMD1 protein levels assayed by Western blot, with actin as a loading control. In U2OS and HeLa cells significant depletion of endogenous LIMD1 was observed, however in U937 cells no significant knockdown was observed. As depletion of LIMD1 was observed in U2OS and HeLa cells, this indicated that the U937 cell line, rather than the siRNA and/or the transfection reagent was the reason why protein depletion was not being achieved.

Using electroporation, 160pmol of siRNA oligo duplexes were electroporated into a suspension of 1×10^6 cells, which successfully resulted in a significant knockdown of PU.1 as detected by Western blot. siRNA depletion of endogenous PU.1 in U937 cells caused a reduction in endogenous LIMD1 protein levels as detected by Western blot (Figure 4.10A). As a control, siRNA depletion of Ets family member Ets-1 had no effect on LIMD1 protein levels when compared to the scrambled control, showing the reduction in LIMD1 was specific for PU.1 depletion. As a confirmation of the specificity of the siRNAs used in the experiment, PU.1 mRNA levels were quantified following each of the siRNA knockdowns (Figure 4.10B). Only the PU.1 directed siRNA caused a decrease in PU.1 mRNA, ruling out any off target affects of the siRNA.

As the initial reporter assays were carried out in U2OS cells, the same siRNA depletion experiment was also carried out in this cell line, where PU.1 levels were detectable only by qRT-PCR and not Western Blot. siRNA depletion of PU.1 resulted in significantly reduced LIMD1 protein levels, almost as much as direct LIMD1 targeted siRNA depletion (Figure 4.10C). Again as a control, siRNA depletion of Elk-1 did not cause a decrease in LIMD1 protein levels. As with the

results obtained from the U937 cells, qRT-PCR analysis of PU.1 mRNA levels indicated only PU.1 directed siRNA caused a decrease (~70%) in PU.1 mRNA levels (Figure 4.10D). Of note was a decrease in Elk-1 levels following LIMD1 depletion (Figure 4.10C), possibly implicating LIMD1 as a regulatory protein of Elk-1 expression. This effect was seen to a lesser extent with PU.1 knockdown; however, this can most probably be attributed to reduced LIMD1 protein levels as a result of PU.1 knockdown.

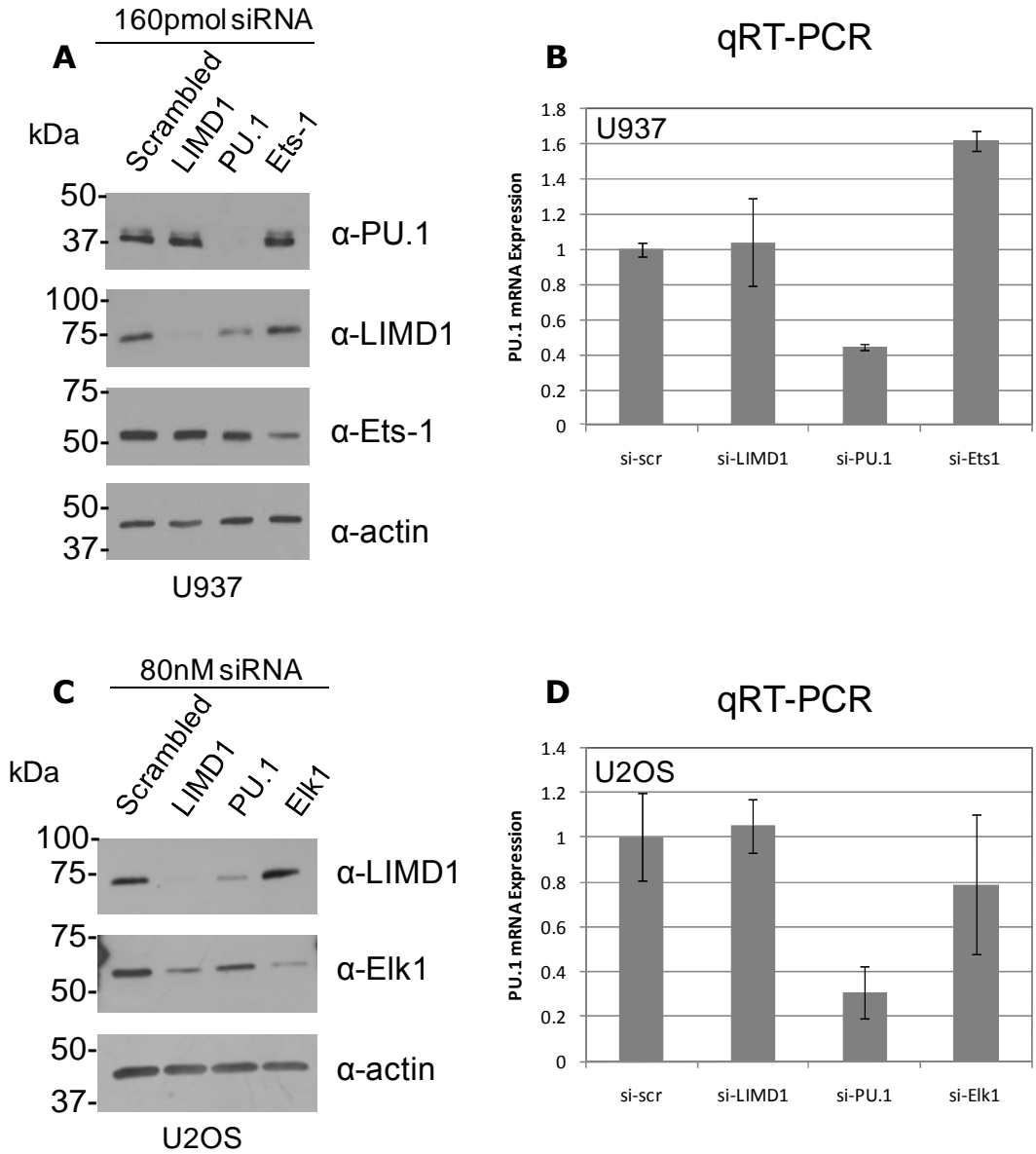


Figure 4.10: Depletion of endogenous PU.1 protein significantly reduces endogenous LIMD1 protein levels. (A) siRNA targeted against LIMD1, PU.1, Ets-1 or scrambled control were transfected into U937 cells and protein knockdown assayed by Western blot. siRNA depletion of PU.1 protein resulted in a significant decrease in endogenous LIMD1 protein levels. (B) As a control for siRNA specificity, PU.1 mRNA levels for each siRNA knockdown were quantified by qRT-PCR, confirming only PU.1 targeted siRNA negatively affects PU.1 mRNA. (C) siRNA targeted against LIMD1, PU.1, Elk-1 or scrambled control were transfected into U2OS cells and protein knockdown assayed by Western blot. siRNA targeted against PU.1 again significantly reduced LIMD1 protein levels, comparable to the reduction seen. (D) Due to the low levels of PU.1 in U2OS, PU.1 knockdown was quantified by qRT-PCR, along with PU.1 mRNA levels following transfection of the other targeting siRNAs. qRT-PCR analysis was kindly performed by Dr. V. James.

4.4 Summary

In this chapter, sequence alignment of the IR5 region within the *LIMD1* promoter of LIMD1 expressing mammals identified the transcriptionally critical IR5 region is perfectly conserved between all species examined (Figure 4.1). *In silico* analysis revealed a potential PU.1 binding site within IR5 (Figure 4.2), that when mutated, resulted in a 90% decrease in transcriptional activity from the promoter, similar to deletion of the whole IR5 (Figure 4.3). ChIP analysis showed that both exogenous and endogenous PU.1 binds to the *LIMD1* promoter *in vivo* (Figure 4.6 and Figure 4.7), which also corroborated with both full length and Ets domain only of PU.1 being able to bind to the IR5 consensus in EMSA assays *in vitro* (Figure 4.8). Furthermore, mutation of the PU.1 consensus prevented PU.1 binding (Figure 4.8B). The physiological relevance of PU.1 binding to the *LIMD1* promoter was then confirmed by siRNA mediated depletion of endogenous PU.1. This resulted in a significant reduction in LIMD1 protein levels (Figure 4.10). Therefore, it can be concluded that PU.1 is a major transcriptional activator of *LIMD1* gene transcription.

Chapter 5 Results: LIMD1 as a Regulator of the Hypoxic Response

5.1 Introduction

The intracellular response to low oxygen tensions is mediated by the protein HIF1 α . In normoxia (20% oxygen), HIF1 α is hydroxylated by the active proline hydroxylase PHD2, whose activity is rate limited by the availability of oxygen. Following hydroxylation of prolines 402 and 564 by PHD2, hydroxyl HIF1 α is recognised by the VHL component of the VCB E3 ubiquitin ligase complex, which causes its ubiquitylation and subsequent 26S proteasome mediated degradation. However, under hypoxic conditions, the low oxygen tension is rate limiting for PHD2 activity and as such is no longer active. Therefore HIF1 α escapes hydroxylation, and so recognition and ubiquitination by VHL cannot occur. The net result is an increase in HIF1 α protein levels, due to increased protein stability. Stabilised HIF1 α is then phosphorylated and dimerises with HIF1 β in the nucleus to form the HIF1 transcription factor, which binds to hypoxic responsive elements (HREs) within the 5' proximal promoter region of selected genes, and enhances transcription through recruitment of p300/CBP. Preliminary data identified over-expressed PHD2 and VHL as binding to LIMD1. Furthermore PHD2 and the VHL containing VCB complex are both upregulated in hypoxia through the presence of a HRE within their promoters. The *in silico* transcription factor binding screen that identified the PU.1 binding motif also identified three putative HRE elements within the *LIMD1* promoter; therefore it was hypothesised that *LIMD1*, like PHD2 and VHL, may also be responsive to hypoxia.

5.2 The *LIMD1* Promoter is Responsive to Hypoxia

5.2.1 *LIMD1* Promoter Driven Transcription Increases Following Hypoxic Exposure

To investigate if the *LIMD1* promoter was responsive to hypoxia, the same pGL4-*LIMD1* promoter or vector only reporter plasmids used in the previous promoter analysis (Figure 3.2) were transfected into U2OS cells and placed into hypoxia for 0, 4, 8 or 24 hours. Cells were lysed in 1 x Passive Lysis Buffer and luciferase activity assayed. Renilla luciferase values were normalised to firefly values, and then for each time point the vector only values were normalised to 1. As an internal control for the hypoxic response in each experiment, additional triplicate wells of U2OS were transfected with a luciferase plasmid that contained

5x synthetic hypoxic responsive elements (HRE) within its promoter. As levels of active HIF1 α increased in hypoxia, this would increase the binding of HIF1 to the HREs within the luciferase promoter, which would increase the levels of luciferase transcript and protein produced. This thus gives an indirect quantification of the intracellular hypoxic response.

The *LIMD1* promoter showed an increase in luciferase activity at 8 and 24 hours hypoxia (1% O₂), with the 24 hours time-point showing the most significant increase of activity (2 fold) when compared to the normoxic (20% O₂) values (Figure 5.1A). For analysis of the luciferase values in hypoxia, the corresponding vector only time points were all normalised to 1, allowing the hypoxic *LIMD1* promoter values to be directly comparable between each time point. The hypoxic response (i.e. increased HIF1 α protein levels) was confirmed by an increase in the HRE driven luciferase internal control (Figure 5.1B).

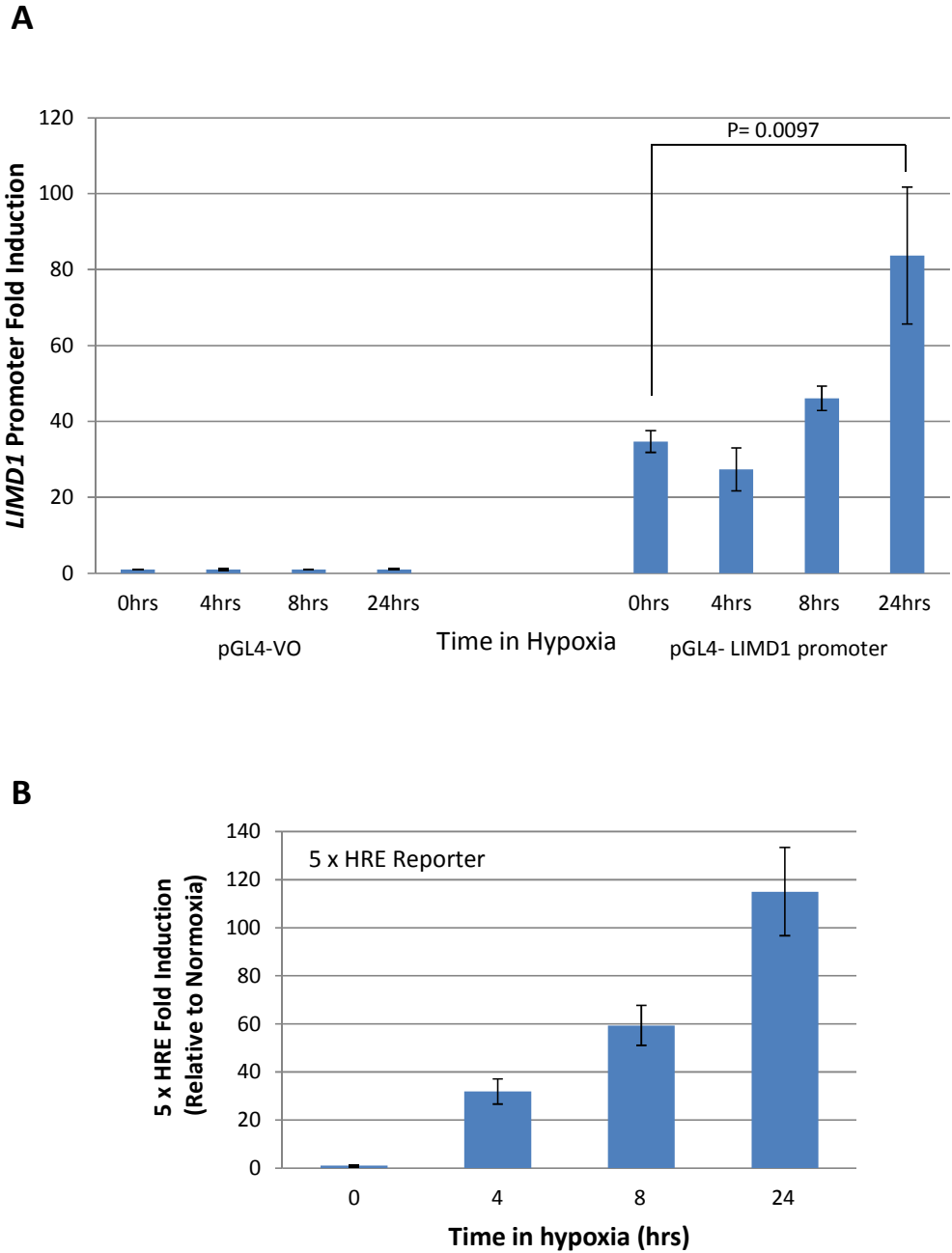


Figure 5.1: Hypoxia causes an increase in *LIMD1* promoter driven transcription. (A) *LIMD1* promoter driven firefly luciferase or firefly luciferase alone vector was co-transfected along with a renilla luciferase vector for normalisation into U2OS cells. Transfected cells were exposed to hypoxia (1% O₂) for 0, 4, 8 or 24 hours and the resultant luciferase protein assayed. *LIMD1* promoter driven transcription was normalised to the vector only values. After 24 hours hypoxia, a 2 fold increase in transcription is observed. (B) A synthetic 5x hypoxic responsive element (HRE) driven renilla luciferase was concurrently transfected into U2OS cells that were exposed to the same hypoxic time course as in (A). The increase in resultant luciferase over the time course confirms an increase in hypoxic HIF1 α protein induction.

5.2.2 LIMD1 Protein Levels Increase Following Prolonged Hypoxic Exposure

To confirm that the increase in synthetic luciferase mirrored a physiological increase in LIMD1 protein total U2OS cell lysates were assayed by Western blot following 24hours hypoxia, as this was the time point with the largest increase in promoter driven transcription (Figure 5.1A). In order to observe modest inductions in protein, the amount of lysate loaded onto the gel was titrated. This was to ensure that when the blots were developed, the signal intensity was such that the band intensity was semi-quantitative of the amount of protein on the gel.

Following hypoxic exposure, a modest but significant increase in LIMD1 protein was observed when lower amounts (2 and 4 μ l) of protein were loaded onto the gel (Figure 5.2). As a control, PHD2 which is characterised as being up-regulated in hypoxia, was also blotted as a control, and showed a clear increase in hypoxia. β -actin was used as a control for equal loading of cell number. Of note are the slightly higher amounts of actin observed in the normoxic samples, indicating a higher cell number, which further supports the hypoxic dependent increase in LIMD1 and PHD2 protein levels observed.

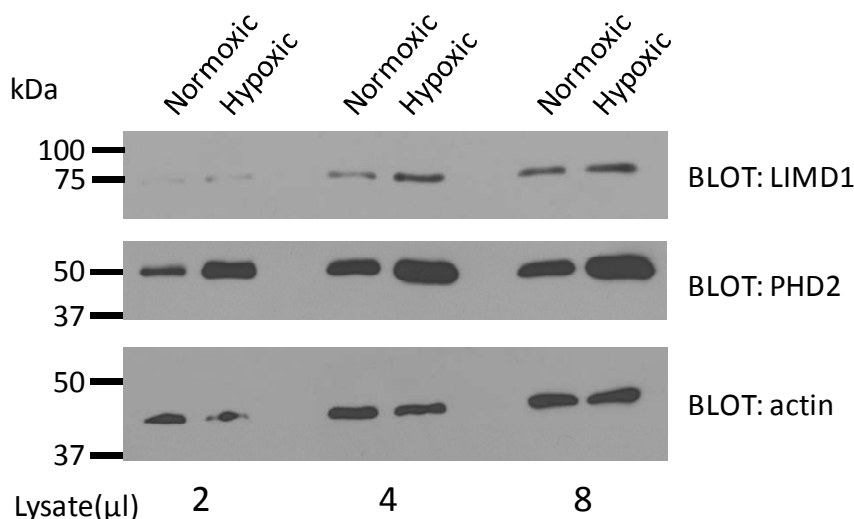


Figure 5.2: Hypoxic exposure increases LIMD1 protein levels. U2OS cells were exposed to 24hours hypoxia prior to lysis and protein analysis by immunoblotting. In order to visualise any differences in normoxic and hypoxic protein levels differing amounts of lysate were loaded onto the gel (2 μ l to 8 μ l) in order to capture band intensities whilst they were in the quantitative stage. LIMD1 protein shows a modest increase in hypoxia (2 μ l and 4 μ l lanes), as does the previously characterised PHD2. β -actin was utilised as a loading control.

5.3 Characterisation of the Hypoxic Responsive Element in the *LIMD1* Promoter

5.3.1 The IR3 Region of the *LIMD1* Promoter is required for Hypoxic Responsiveness.

This initial reporter experiment demonstrated that the *LIMD1* promoter shows increased transcriptional activity in hypoxia (Figure 5.1). To map the precise region of the promoter responsible for this, the ten internal CpG Island deletion mutants that were described previously (Figure 3.2) were again utilised. The ten deletion mutants were transfected in U2OS cells, and the cells exposed to either normoxia or 24 hours hypoxia prior to lysis as previously described. The luciferase values were then double normalised. Firstly the values for the vector only plasmids were normalised to one, and then the normoxic values for each mutant were normalised to one. This resulted in clearer visualisation of the data, as the hypoxic values represented the fold induction in transcriptional up-regulation of the promoter in hypoxia compared to normoxia. Again the induction of hypoxia was confirmed by using the HRE driven luciferase plasmid internal control (data not shown).

The ten internal deletion mutants exhibited the same pattern of increases and decreases in transcriptional activity that were observed in the initial promoter analysis experiment (Figure 3.2 and Figure 5.3A). This pattern was mirrored when cells were exposed to hypoxia. The wild type promoter exhibited a 3.5 fold induction in activity in hypoxia (Figure 5.3), which was slightly higher than the fold inductions seen previously. However the internal control HRE driven luciferase plasmid also had a higher induction in hypoxia than in previous experiments, which validates the hypoxic promoter inductions observed. The *LIMD1* promoter mutants exhibited a 2-3 fold increase in promoter activity, even the I Δ 5 mutant that exhibited a 90% repression in normoxia showed increased transcriptional activity following hypoxic exposure. The only exception was the I Δ 3 mutant. The I Δ 3 mutant showed no significant increase in transcription following hypoxic induction, indicating this region most probably contained a functional HRE.

To more clearly assess the hypoxic inductions observed, for each deletion mutant, the luciferase values (that had already been normalised to the renilla values) were normalised to their respective matched normoxic value. The result of this was the value for normoxia was 1.0, and the hypoxic value was then the fold induction in transcription (Figure 5.3B). This allowed for clearer analysis of

the hypoxic response, showing the IΔ3 mutant had no significant increase in transcription in hypoxia.

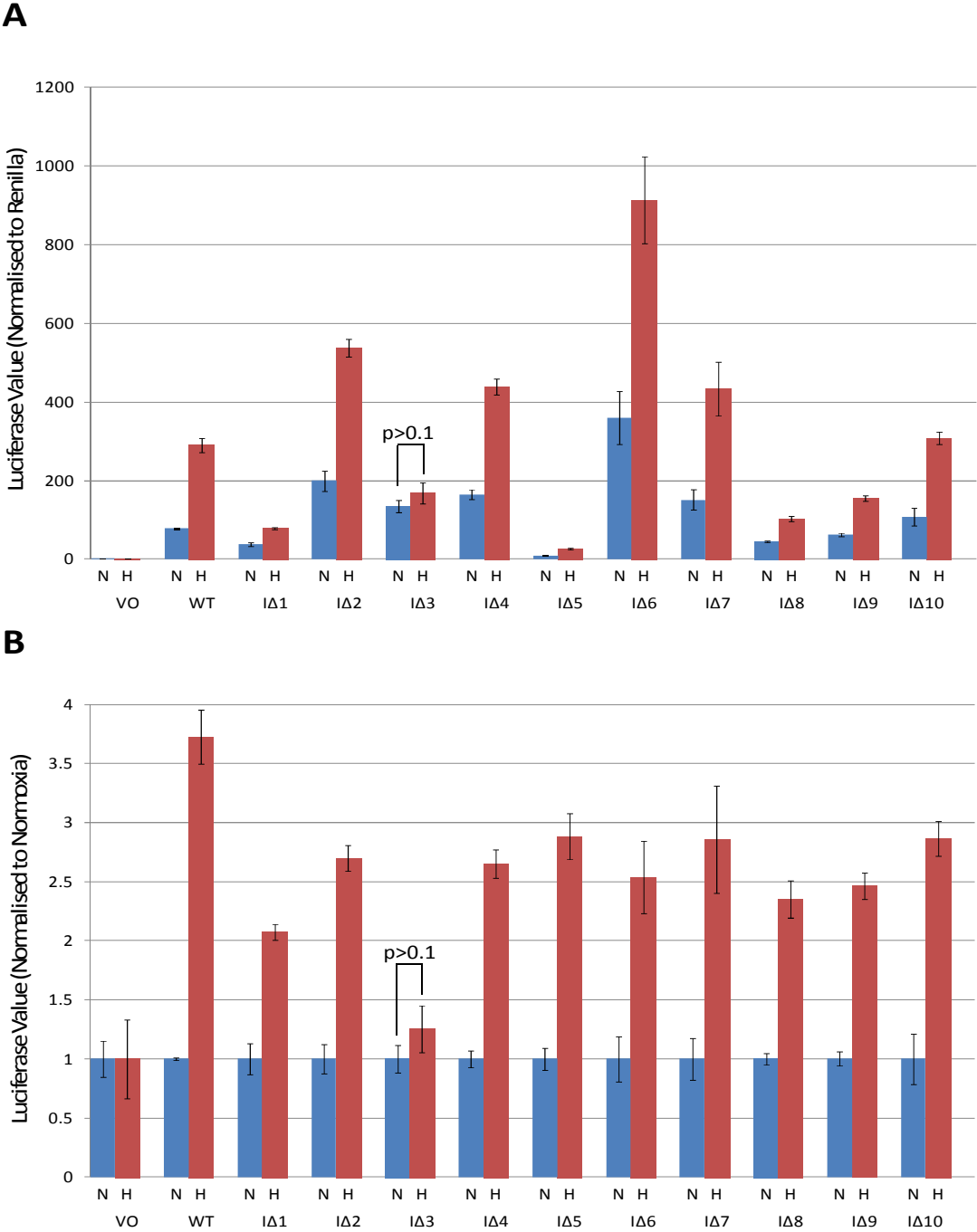


Figure 5.3: Deletion of internal region 3 (IR3) abolishes the hypoxic responsiveness of the LIMD1 promoter. Ten consecutive internal deletions within the LIMD1 promoter were co-transfected with a renilla normalisation plasmid into U2OS and exposed to either 20% (N; normoxia) or 1% oxygen (H; hypoxia) for 24 hours. Cells were then lysed and resultant luciferase protein assayed, with firefly values normalised to renilla values. Luciferase values were double normalised (A) firstly to vector only values to account for differential basal transcriptional activities under different oxygen tensions and then to (B) the normoxic value so that the hypoxic value represented the fold induction in transcription. Deletion of the IΔ3 region abolished the increase in transcriptional activity in hypoxia observed with the wild type promoter, indicating this region as containing a functional HRE.

5.3.2 Mutagenesis of the HRE or HIF1 α Depletion Abolishes the Hypoxic Response of the *LIMD1* Promoter

The hypoxic promoter analysis thus far had been carried out blind with respect to comparing the result to the *in silico* promoter screening. Experimentally the HRE within *LIMD1* had been narrowed to IR3; this agreed exactly with one of the matches in the *in silico* screen, which also predicted a HRE element within IR3. The other two potential HRE elements predicted were 5' to the CpG Island. However, as the Δ 3 deletion ablated the hypoxic responsiveness of the promoter (Figure 5.3), this implicated the *in silico* identified non-CpG Island HREs as being a false positive result.

To confirm the HRE within IR3 was functional and responsible for the increased promoter activity in hypoxia, site directed mutagenesis was used to mutate the HRE motif from CGTG to TACA. As the *in silico* analysis identified a total of three potential HREs, for completeness, the other two predicted HREs were also mutated in the same way. The HRE mutant plasmids were named delta (Δ) HRE1, HRE2 and HRE3 in the order they appeared from the 5' end of the promoter. Therefore Δ HRE1 and 2 were the putative non-functional response elements that were outside the CpG Island, and Δ HRE3 was within IR3 in the CpG Island. Similar to the hypothesis with PU.1 binding to the promoter, it was hypothesised that if HIF1 α was binding to a HRE within the promoter region, then mutation of the consensus should prevent the binding interaction, and as such prevent the hypoxic response of the promoter.

In conjunction with the promoter HRE mutational analysis, another technique to confirm the hypoxic response would be to deplete HIF1 α , the major hypoxic responsive transcriptional enhancer. HIF1 α is only active in hypoxia due to proteasomal degradation under normoxic conditions as previously described. Therefore depletion of HIF1 α should ablate any differences in transcriptional activation as a result of hypoxia. Plasmids encoding shRNA targeted against HIF1 α or a negative control drosophila HIF1 α (sh-HIF1 α or sh-drosHIF1 α respectively) were transfected into U2OS cells 24 hours prior to transfection with the mutated HRE promoter constructs (Δ HRE1-3). Cells were then exposed to either normoxia or 24 hours hypoxia prior to lysis and analysis of luciferase (Figure 5.4).

The wild type, Δ HRE1 and Δ HRE2 *LIMD1* promoter constructs all exhibited a 2 fold increase in transcriptional activation in hypoxia with the control shRNA, showing that in U2OS cells there is no functional HRE at HRE1 or 2 (Figure 5.4).

However, the Δ HRE3 promoter construct had no hypoxic induction, which agreed with the hypothesis that this was the functional HRE within the CpG Island of the *LIMD1* promoter. shRNA mediated depletion of endogenous HIF1 α resulted in ablation of the hypoxic response as neither the wild type or HRE *LIMD1* promoter mutants showed a significant induction following hypoxic exposure (Figure 5.4). Of note, Δ HRE3 showed a significant decrease in transcriptional activity in hypoxia, an observation that at present cannot be explained. In sum however, these data show that the hypoxic responsiveness of the *LIMD1* promoter is mediated by HIF1 α , and requires the HRE within IR3.

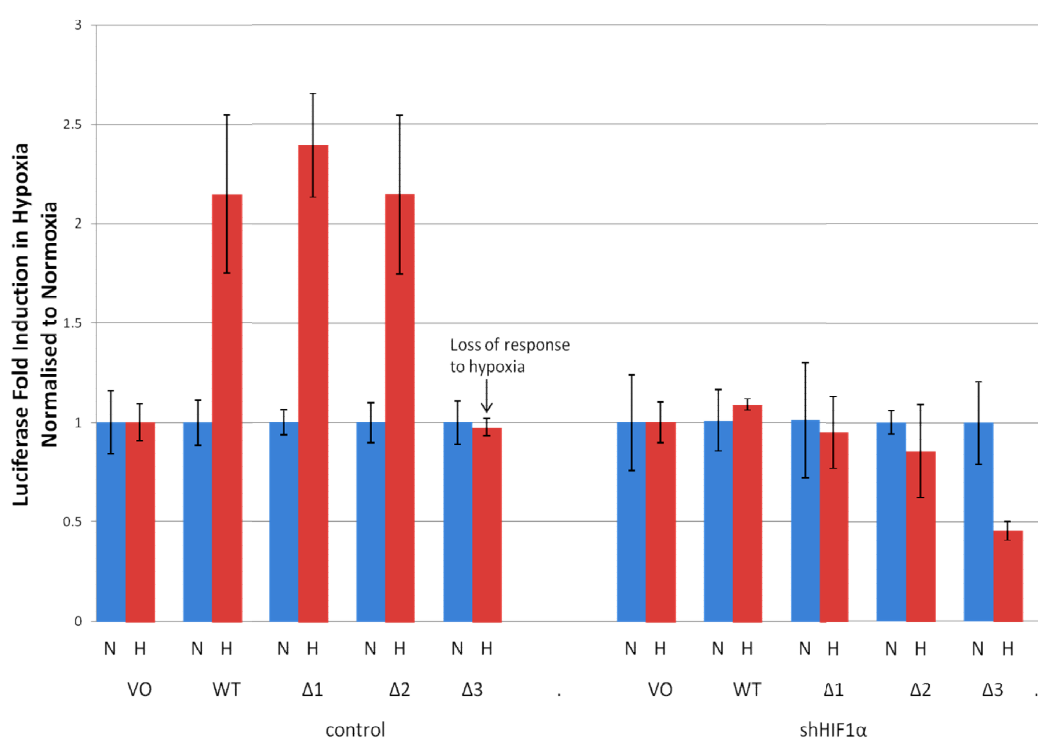


Figure 5.4: shRNA knockdown of HIF1 α or mutation of the HIF1 α binding consensus ablates the hypoxic response of the *LIMD1* promoter. Plasmids containing sequences to produce shRNA against control drosophila HIF1 α or human HIF1 α were transfected into U2OS cells 24 hours prior to transfection with the 3 indicated internal promoter HRE mutations. Cells were then exposed to hypoxia for 24 hours and lysed as previously described. Luciferase values were double normalised so that the normoxic values were 1 and the hypoxic value represented the fold induction of transcription under hypoxia. Knockdown of HIF1 α ablated the hypoxic response associated with both the wild type and mutant plasmids. Mutation of the HRE within IR3 (Δ HRE3) also ablated the hypoxic response with the control or HIF1 α knockdown, showing both HIF1 α and the HRE within IR3 are critical for the hypoxic response. N, normoxia; H, hypoxia.

5.3.3 Depletion of Endogenous HIF1 α Significantly Reduces Endogenous LIMD1 Protein.

To demonstrate the physiological significance of the hypoxic responsive element within the *LIMD1* promoter, the effect of depleting HIF1 α on endogenous LIMD1 protein expression within U2OS cells was examined. It was hypothesised that if HIF1 α activity was the main requirement for the hypoxic responsiveness of the *LIMD1* promoter then depletion of HIF1 α should prevent an increase in LIMD1 proteins levels in hypoxia.

To test this hypothesis, endogenous HIF1 α was depleted from U2OS cells using shRNA and LIMD1 protein levels assayed by Western blot following either normoxic or hypoxic exposure. Again as a negative control shRNA against *Drosophila* HIF1 α was included. 24 hours post transfection cells were exposed to 1% oxygen for 24hours, and then lysed in RIPA supplemented with protease inhibitors and MG132 (a potent inhibitor of the 26S proteasome, used to prevent degradation of HIF1 α following cell lysis). Expression levels of HIF1 α and LIMD1 protein were then quantified by Western blot, with β actin used as a loading control.

Knockdown of HIF1 α in hypoxia resulted in a reduction in LIMD1 protein levels when compared to the control *drosophila* HIF1 α depleted cell extracts (Figure 5.5). These data support the reporter assay data (Figure 5.1) showing that *LIMD1* driven transcription is up regulated in hypoxia and the HRE mutation experiments which suggested HIF1 α mediates the hypoxic response of the *LIMD1* promoter (Figure 5.4). The shRNA experiment also showed that a depletion of the low levels of HIF1 α in normoxia, also resulted in a decrease in LIMD1 protein (Figure 5.5).

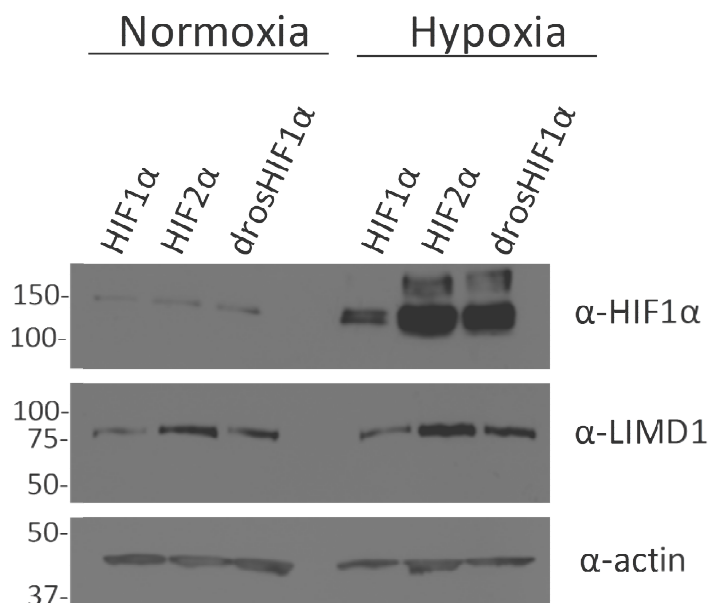


Figure 5.5: shRNA knockdown of HIF1 α significantly reduces endogenous LIMD1 protein levels. shRNA directed against human HIF1 α , HIF2 α or drosophila HIF1 α were transfected into U2OS cells. 32 hours post transfection cells were exposed to hypoxia for 16 hours, prior to lysis in RIPA buffer. Proteins were detected by Western blot analysis with monoclonal anti HIF1 α , LIMD1 and actin antibodies. Representative blot from 3 independent experiments.

The results obtained from the promoter mutational analysis and shRNA knockdown experiments indicated the hypoxic responsiveness and transcription of LIMD1 is dependent upon HIF1 α . To further the physiological relevance of these observations, reciprocal experiments were then performed to investigate the role of increased LIMD1 protein expression in low intracellular oxygen tensions (hypoxia).

5.4 The role of LIMD1 in Regulation of the Hypoxic Response

Preliminary studies within our laboratory identified LIMD1 as being intimately involved in the negative regulation of HIF1 α and therefore the hypoxic response. Co-immunoprecipitation experiments using over-expressed PHD2, VHL and LIMD1 have implicated these three proteins to be part of the same complex, with LIMD1 bridging and enhancing the interaction between PHD2 and VHL (Figure 1.26). However, it remained to be elucidated if LIMD1 binding to PHD2 or VHL was direct and if the preliminary ectopic expression data mirrored a true endogenous interaction.

5.4.1 LIMD1 Binds Directly to PHD2 *in vitro*

In order to address if LIMD1 directly bound to PHD2, an *in vitro* direct binding assay using recombinant LIMD1 and recombinant PHD2 was performed. pGEX4T-PHD2 and pGEX6P-LIMD1 were transformed separately into the pLysS strain of BL21 *E.coli*, and expression of the recombinant proteins induced with 0.5mM IPTG. pGEX6P-LIMD1 was purified onto glutathione beads and eluted with PreScission protease, with the extent of purification assayed by Western blot (Figure 5.6). GST-LIMD1 is 100kDa in size (GST=25kDa, LIMD1=75kDa); following cleavage a band of 75kDa is observed in the supernatant (Figure 5.6 middle lane), showing successful cleavage of GST-LIMD1. The lower banding represents shorter fragments of LIMD1 that arise from degradation of the full length GST-LIMD1. To confirm loss of recombinant LIMD1 from the glutathione sepharose beads, following cleavage the beads were also subject to Western blot. Fifty times more beads were loaded onto the gel post cleavage than pre-cleavage, yet the intensity of bands is still significantly less than the input, confirming successful recombinant LIMD1 cleavage (Figure 5.6 lanes 1 and 3).

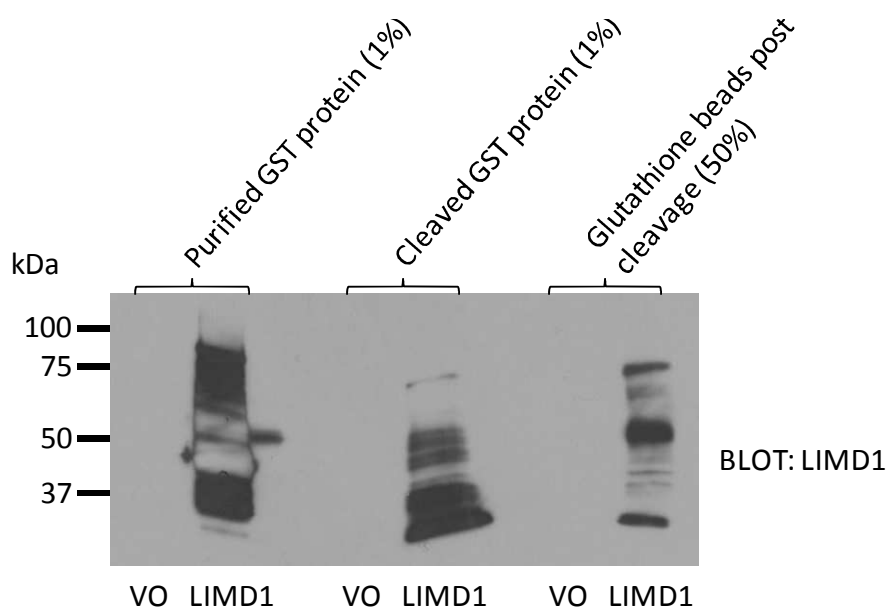


Figure 5.6: Recombinant pGEX6P-LIMD1 can be expressed, purified and cleaved from glutathione sepharose. pGEX6P-LIMD1 or vector only was transformed into BL21 pLysS *E.Coli* and protein expression induced by IPTG. Bacteria were lysed by sonication and recombinant GST-LIMD1 or vector only purified onto glutathione sepharose. The protein was cleaved from the glutathione-s-transferase tag using PreScission protease. Successful cleavage was detected by resolving the indicated cleaved supernatants or reduced glutathione sepharose by SDS PAGE and immunoblotting with anti-LIMD1. Recombinant LIMD1 was successfully purified onto glutathione sepharose ('Purified GST protein (1%)'), then eluted following cleavage with PreScission protease ('Cleaved GST Protein (1%)'), leaving only a small amount of uncleaved protein on the beads ('Glutathione beads post cleavage (50%)', note 50% more beads in lane 3 than lane 1).

pGEX4T-PHD2 (GST=25kDa, PHD2=50kDa) was expressed and purified onto glutathione beads (but not eluted), and expression confirmed by Western blot with an anti-PHD2 antibody (Figure 5.7A). The purified and cleaved recombinant LIMD1 was then incubated with the purified and immobilised PHD2, and following washing of the beads any bound protein was eluted with SDS sample buffer and analysed by Western blot. Recombinant purified and cleaved LIMD1 specifically bound to the purified and immobilised recombinant GST-PHD2 (Figure 5.7B), thus demonstrating LIMD1 directly interacts with PHD2.

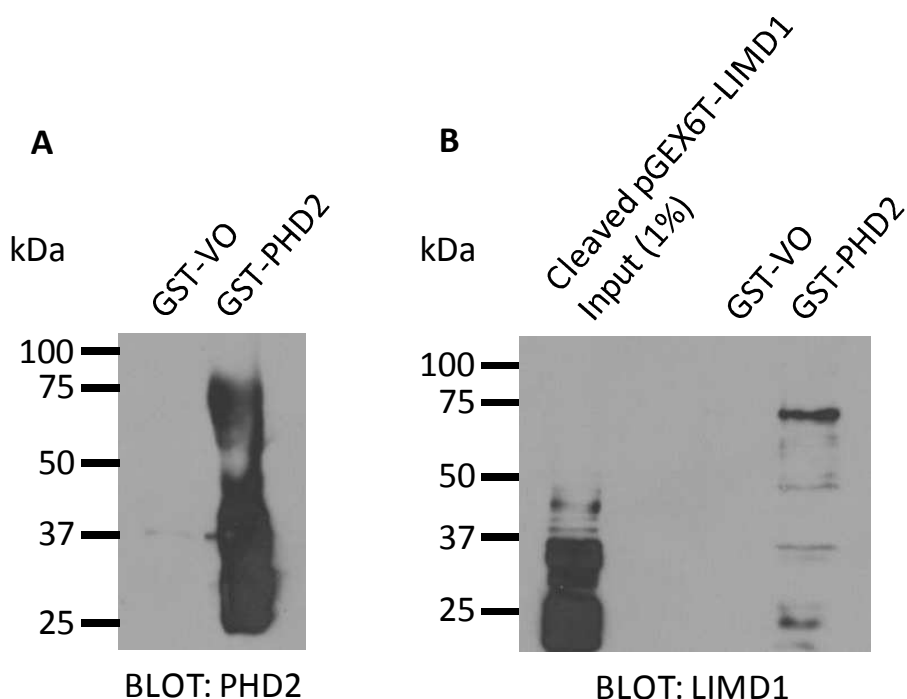


Figure 5.7: Recombinant LIMD1 directly binds to recombinant PHD2. (A) Recombinant GST-PHD2 or vector only was bound and purified onto glutathione sepharose 4B. (B) Recombinant LIMD1 was purified onto glutathione sepharose, and cleaved from the GST moiety using an on bead digest with PreScission protease. Eluted LIMD1 was added to GST-PHD2 or vector only from (A), incubated for 6 hours, washed and proteins eluted from the glutathione beads with SDS sample buffer. Eluted proteins were analysed by immunoblotting. Recombinant LIMD1 was found to directly bind to recombinant PHD2 *in vitro*.

5.4.2 LIMD1 interacts Endogenously with PHD2, VHL and VCB Complex Proteins

The direct binding assay indicated that PHD2 and LIMD1 were able to interact *in vitro* and preliminary over-expression data identified that PHD2, VHL and LIMD1 all interact. However for physiological relevance it was critical to demonstrate that this interaction occurred endogenously. Therefore, *in vivo* endogenous immunoprecipitations were performed next.

5.4.3 Optimisation of Endogenous Co-immunoprecipitations Methods

Endogenous immunoprecipitations required significant optimisation in order to obtain robust evidence of an *in vivo* interaction. Initially, immunoprecipitations were performed with antibodies against LIMD1, PHD2 and VHL. Dependent upon the epitope binding region, binding of an antibody to its target protein can disrupt endogenous protein-protein binding, and so the three different antibodies were used to avoid this issue.

As the majority of the work regarding LIMD1 and its role in hypoxic regulation had been performed in U2OS cells, these cells were again used for the initial immunoprecipitations. To obtain complete cell lysis, cells were lysed in RIPA buffer, which contains the denaturing agent SDS, the detergent NP40 and a physiological concentration of NaCl (150mM), making it a stringent buffer. Initial immunoprecipitations were performed in RIPA, followed by 4 washes of the IP-bead matrix, again with RIPA. These results indicated that the anti-LIMD1 and VHL antibodies were able to successfully immunoprecipitate their target protein (Figure 5.8A and B).

PHD2 is 48kDa in size, and due to cross reactivity of the secondary antibody with the immunoprecipitating PHD2 IgG heavy chain (molecular weight 50kDa) it was difficult to distinguish between PHD2 and the IgG heavy chain via Western blot (Figure 5.8C). Therefore until optimisation of the immunoprecipitations had been fully carried out, immunoprecipitation with this antibody was omitted.

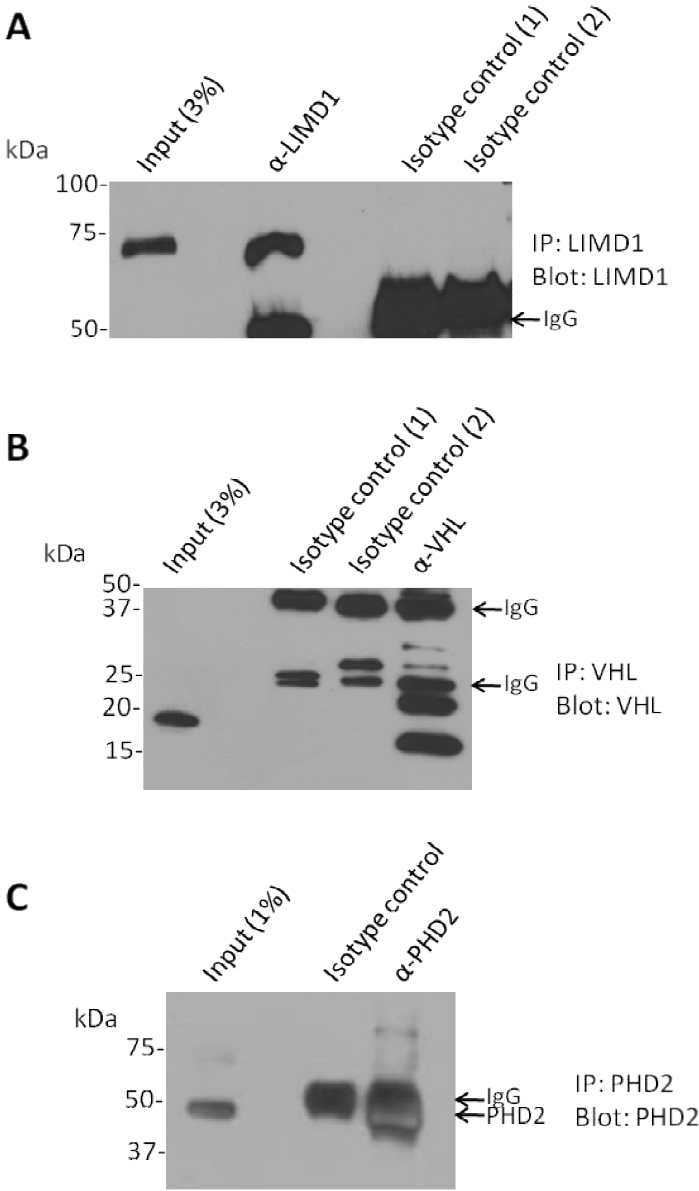


Figure 5.8: α-LIMD1, VHL and PHD2 antibodies are able to successfully immunoprecipitate their target proteins. For each immunoprecipitation, a confluent 15cm plate of U2OS cells were lysed in RIPA buffer supplemented with protease and phosphatase inhibitors and incubated overnight with antibody pre-conjugated to the IP matrix (Santa Cruz). Antibody-IP matrices were washed 4 times in RIPA, prior to elution of bound proteins with 5 x SDS buffer and analysis by Western blot. (A) α-LIMD1 and (B) α-VHL antibodies were immunoprecipitated LIMD1 and VHL proteins respectively, with specificity of the antibodies confirmed with α-GFP (isotype control 1) and α-cortactin (isotype control 2) control antibodies. (C) Cross reactivity of the secondary antibody with the α-PHD2 IgG heavy chain (50kDa) obscures the potentially immunoprecipitated PHD2 band (48kDa). Therefore immunoprecipitation of PHD2 could not be confirmed.

For the first experiments, the standard lab protocol was to carry out 4 x 5min washes of the IP matrix using RIPA buffer following incubation of the antibody and lysates. However, following this the co-immunoprecipitated proteins were only detectable as faint bands (Figure 5.9A). Furthermore, with the LIMD1 antibody, the amount of precipitated and co-immunoprecipitated protein was substantially less than with the VHL antibody (Figure 5.9A). Therefore, for optimisation purposes only immunoprecipitation with the VHL antibody was pursued.

Non-specific binding to the isotype control antibody was the major problem incurred with the immunoprecipitation experiments. To optimise this, the length of time the antibody was incubated with the cellular lysates was reduced from overnight (16-20 hours) to 4 hours, which significantly reduced the non specific binding (Figure 5.9B).

To further eliminate non-specific binding, whilst maintaining specific co-immunoprecipitation, the buffer for washing of the IP-bead matrix, along with the number of times the IP matrix was washed following incubation was optimised by carrying out a titration of between 2 and 6 washes. The level of co-immunoprecipitated protein was high at 2 washes and systematically decreased as the number of washes increased. However, with fewer washes the level of non-specific binding to the isotype control increased. The optimal point for these two parameters was 3 washes. Furthermore, instead of using pure RIPA for the washes, a wash buffer of 50/50 PBS/RIPA was used to reduce the stringency of the washes; this helped eliminate binding of proteins to the isotype control whilst concurrently being the correct stringency so that the degree of co-immunoprecipitated proteins were maintained with the specific α -VHL IP complex.

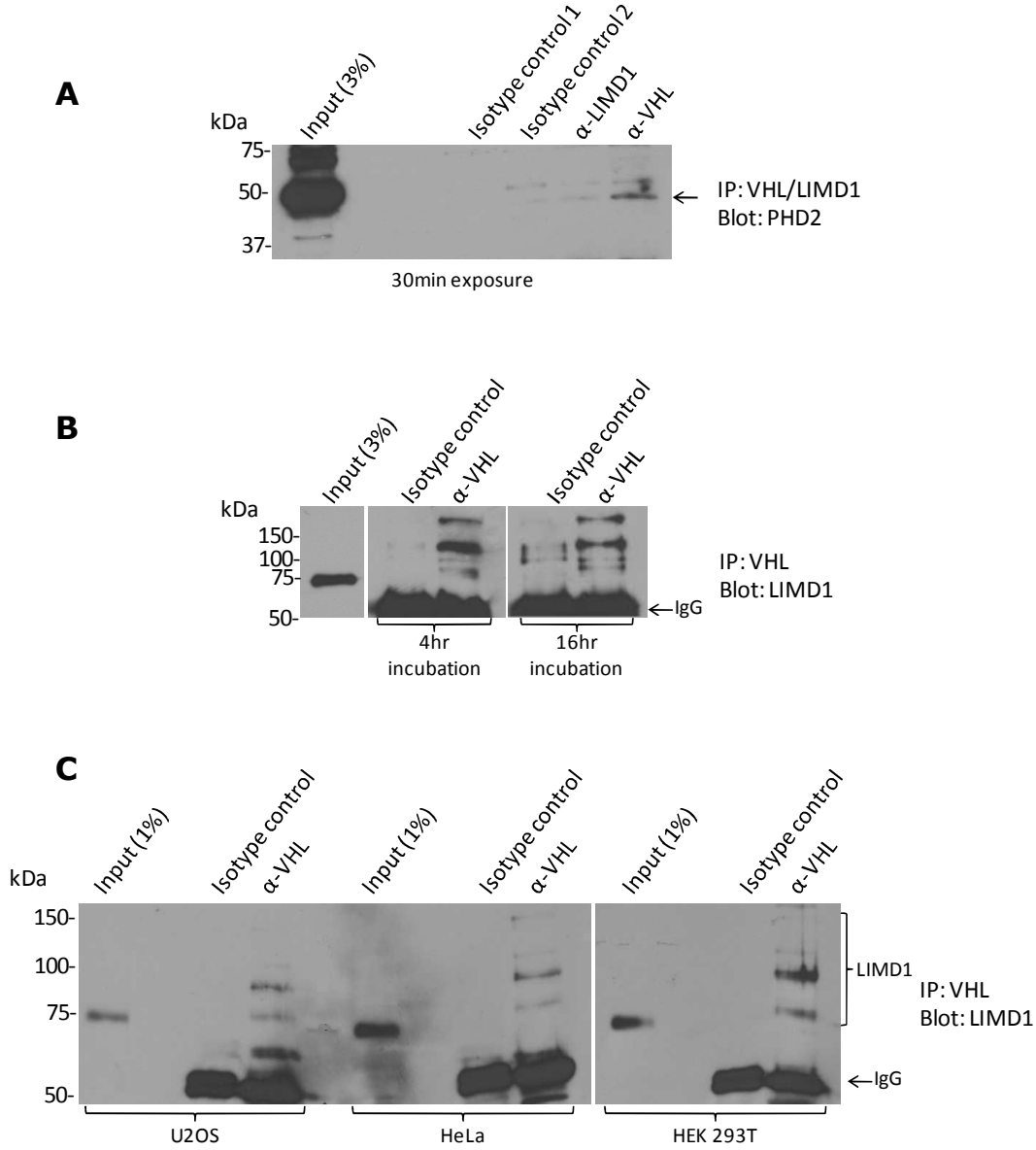


Figure 5.9: Optimisation of endogenous immunoprecipitations. (A) Following initial overnight immunoprecipitation with anti-LIMD1, VHL and isotype control (1, α-GFP; 2, α-cortactin) antibodies where the IP matrix was washed 6 times, only low levels of co-immunoprecipitated PHD2 protein was detected after a long exposure Western blot. Furthermore, co-immunoprecipitated protein with the VHL antibody was significantly greater than that observed with the LIMD1 antibody. (B) Reduction of the incubation time between the antibody and cell lysate from 16hr to 4hr resulted in a significant decrease in non specific binding of protein to the control (α-GFP) antibody. (C) To establish if cell number was a limiting factor in the experiment, HeLa and HEK293T cells were used as they have a greater cell number per area when confluent compared to U2OS cells. Immunoprecipitation of VHL resulted in co-immunoprecipitation of LIMD1 in all three lines tested; however, larger amounts of input and co-immunoprecipitated proteins were observed in the HeLa and HEK293T lysates.

For immunoprecipitations, U2OS cells from a confluent 15cm plate were used. Contact inhibition in this cell line meant that the cell density achievable in a confluent 15cm plate of U2OS was less than that of other cell lines. To establish if cell number (i.e. amount of protein) was limiting the immunoprecipitations, 2 other well established cell lines within the lab, HeLa and HEK293T, were used in the immunoprecipitations as in a 15cm plate format, a greater cell number/density could be achieved compared to U2OS. The higher cell number was reflected by greater protein input levels (as detected by Western blotting 1% of the total cell lysate), and subsequently greater levels of co-immunoprecipitated protein (Figure 5.9C).

The final step of optimisation was to increase the amount of antibody used in the immunoprecipitation from 4µg to 5µg. So far the other possibly limiting steps (antibody, number of washes, wash buffer and cell number) had been optimised. Increasing the amount of immunoprecipitating antibody made the significant difference in these experiments; the amount of co-immunoprecipitated protein was substantially increased. This implied that the lower amount of immunoprecipitating antibody in the initial experiments was the limiting factor and not sufficient to precipitate all of the available endogenous complexes.

5.4.4 Endogenous VHL, LIMD1 and PHD2 Co-Immunoprecipitate *In Vivo*.

Immunoprecipitation of endogenous VHL from HEK 293T cells using 5µg of anti-VHL antibody, resulted in co-immunoprecipitation of endogenous LIMD1 and PHD2, demonstrating their association in an endogenous *in vivo* complex (Figure 5.10). In addition to having the isotype antibody as a control, two proteins that are part of the VCB complex and bind VHL, elongin B and cullin 2, also co-immunoprecipitated, further corroborating the specificity and integrity of the endogenous complex *in vivo*.

When VHL was immunoprecipitated, there are five bands of different molecular weights between ~19 and 35kDa observed. However, in the input lane, only two molecular weights are observed, which correspond to the characterised p19 and p25 isoforms. The other bands are of unknown origin; multiple VHL banding has been previously identified (Liu et al., 2011), but the identity of the modification was unknown. Similarly, following co-immunoprecipitation of LIMD1, as well as a molecular weight band of 75kDa that corresponds to what is observed in the input, three additional higher molecular weight bands are also observed that correspond to a modified LIMD1. However, as both LIMD1 and VHL are part of a

concentrated ubiquitin ligase complex, and VHL itself becomes ubiquitylated (Liu et al., 2011), it could be speculated that these extra forms could represent ubiquitylated VHL or LIMD1.

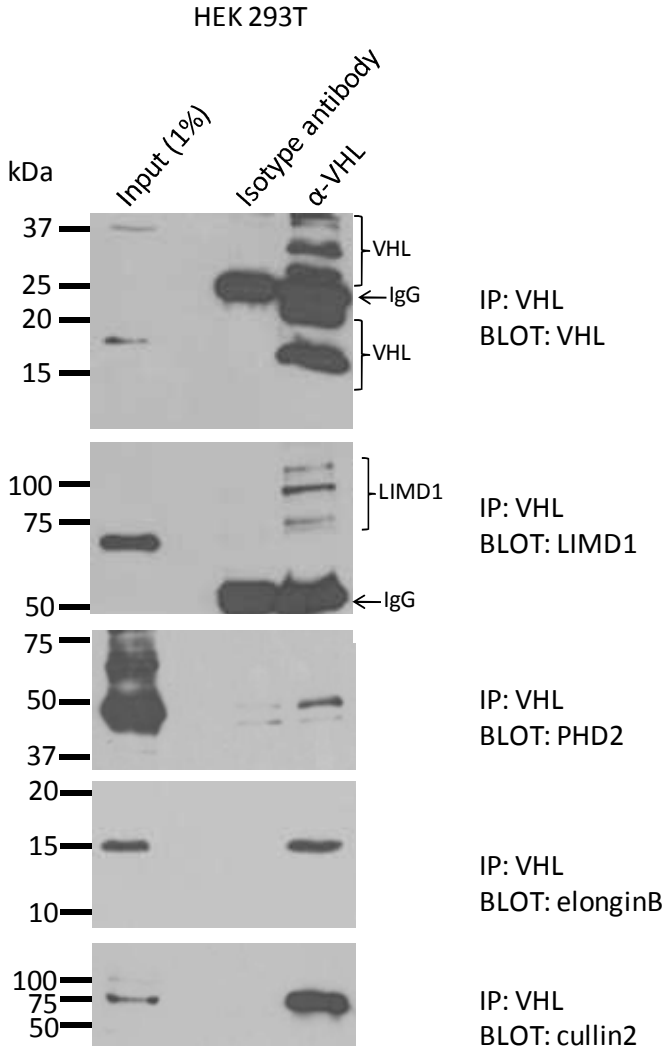


Figure 5.10: Co-immunoprecipitation of LIMD1, PHD2, elongin B and cullin 2 when VHL is immunoprecipitated. A confluent 15cm plate of HEK 293T cells were lysed and the clarified lysate was added to 5µg of anti-VHL or anti-GFP (used as an isotype control as both antibodies are IgG_{k1}) antibody conjugated to 35µl of IP matrix beads. After 4 hours incubation at 4°C with rotation, the beads were washed three times and eluted in 5 x SDS loading buffer and co-immunoprecipitated proteins analysed by Western blot.

The same protocol was then repeated for endogenous co-immunoprecipitations using HeLa and U2OS cell extracts. By comparing the intensity of the input bands between the different cell lysates (Figure 5.10 and Figure 5.11), it can be seen that there was substantially more protein in the HEK 293T cell lysate than in U2OS or HeLa lysates. However, LIMD1 still co-immunoprecipitated in both these cell lines. Elongin B and cullin 2 also co-immunoprecipitated with VHL in the HeLa cell line. However, due to the lower protein concentration in the U2OS lysate cullin 2 or Elongin B could not be detected by Western blot in the input or co-immunoprecipitated samples (data not shown).

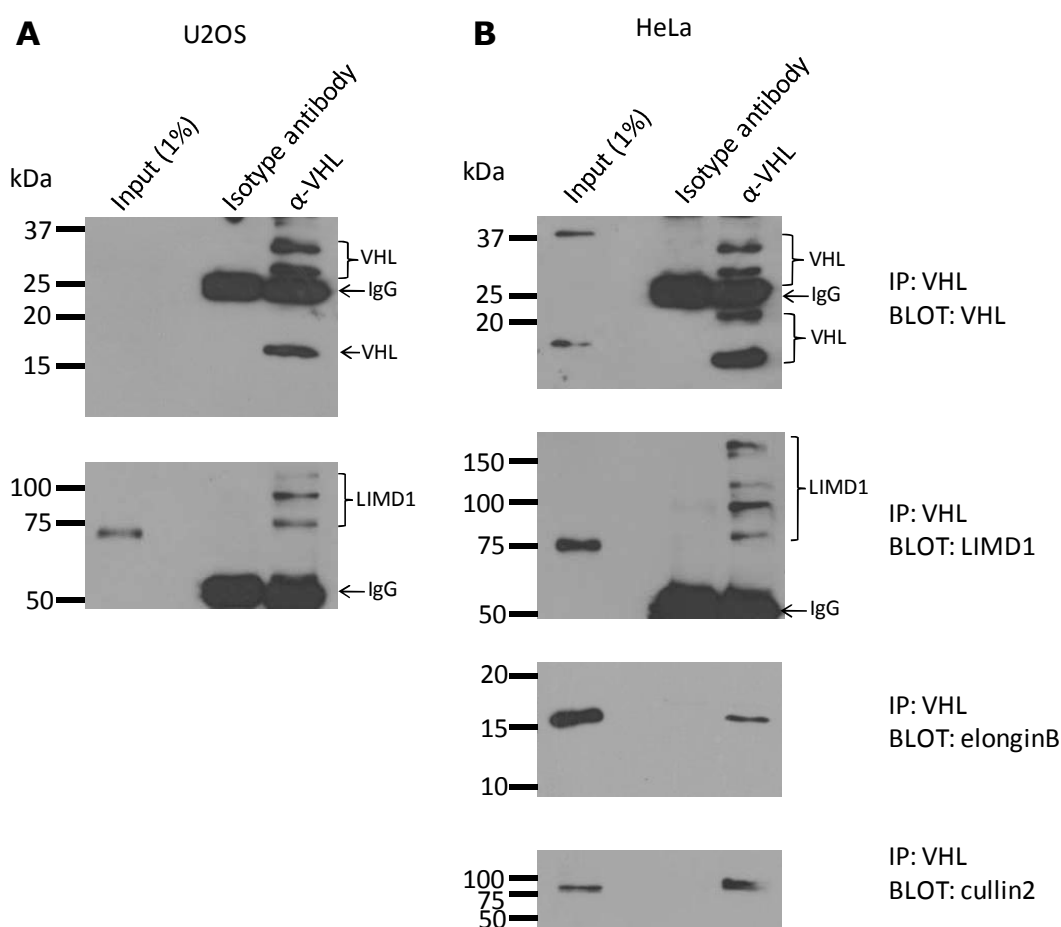


Figure 5.11 LIMD1 co-immunoprecipitates with VHL in U2OS and HeLa cell lines.

A confluent 15cm plate of HeLa or U2OS cells were lysed and the clarified lysate was added to 5 μ g of anti-VHL or anti-GFP (used as an isotype control as both antibodies are IgG clones) antibody conjugated to 35 μ l of IP matrix beads. After 4 hours incubation at 4 $^{\circ}$ C with rotation, the beads were washed three times and eluted in 5 x SDS loading buffer and co-immunoprecipitated proteins analysed by Western blot. (A) LIMD1 specifically co-immunoprecipitates with VHL in U2OS cells and (B) in HeLa cells, where elongin B and cullin2 also co-immunoprecipitate.

The endogenous immunoprecipitations were then repeated using a PHD2 antibody for the immunoprecipitation. In order to overcome the problems previously described regarding cross reactivity of the secondary anti-rabbit antibody with the anti-PHD2 IgG heavy chain (Figure 5.8C) a mouse monoclonal PHD2 antibody was purchased. Immunoprecipitations were carried out with the mouse monoclonal PHD2 antibody, and Western blot analysis with the rabbit polyclonal antibody, thus eliminating the cross-reactivity issue. This modification to the protocol allowed clear visualisation of immunoprecipitated PHD2 with co-immunoprecipitation of LIMD1 in all the cell lines analysed; HEK 293T, HeLa and U2OS (Figure 5.12).

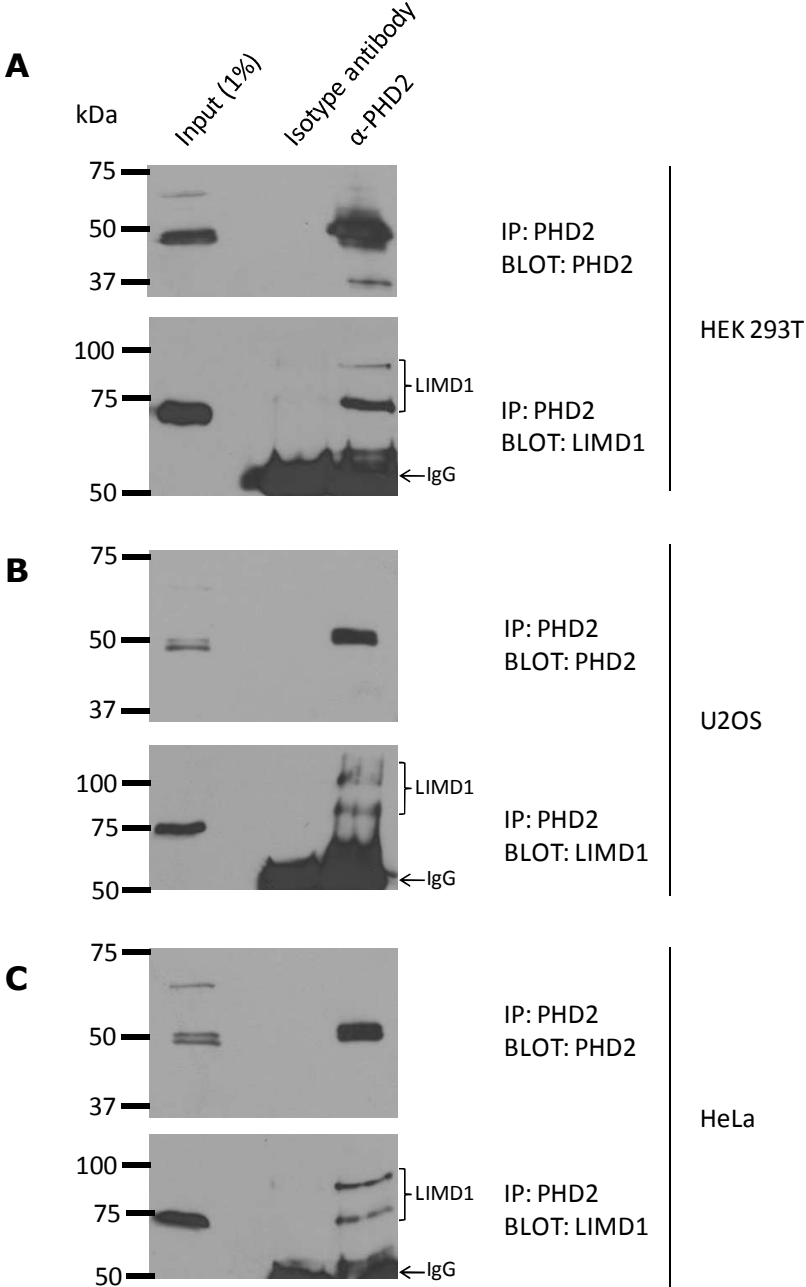


Figure 5.12: Endogenous co-immunoprecipitation of LIMD1 with PHD2. A confluent 15cm plate of HEK-293T, U2OS and HeLa cells were lysed and added to 5µg of anti-PHD2 or anti-GFP (used as an isotype control as both antibodies shared the same IgG) antibody conjugated to 35µl of IP matrix beads. After 4 hours incubation at 4°C with rotation, the beads were washed three times and eluted in 5 x SDS loading buffer. Immunoprecipitation of PHD2 and co-immunoprecipitation of LIMD1 was analysed using Western blot with rabbit polyclonal anti-PHD2 and monoclonal anti-LIMD1 in (A) HEK 293-T, (B) U2OS and (C) HeLa cells.

As a final confirmation for specificity and integrity of the immunoprecipitation experiments, reactivity of the immunoprecipitating antibody alone with the antibodies used for Western blot analysis was assayed. The α -VHL, PHD2 and LIMD1 monoclonal antibodies were conjugated to the IP matrix beads and incubated overnight, as was done for the actual immunoprecipitation experiments. The antibodies were then eluted from the beads using 5 x SDS buffer and analysed by Western blot with α -LIMD1 and VHL antibodies (Figure 5.13).

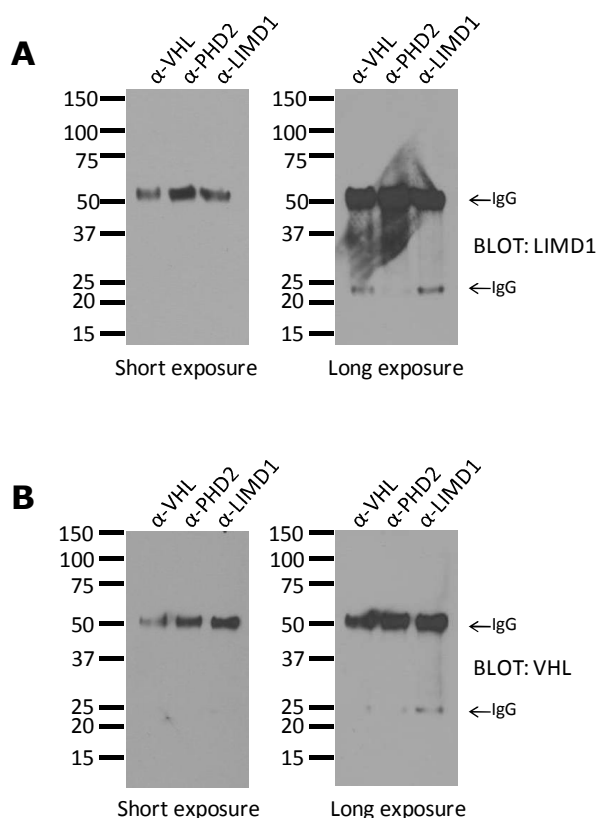


Figure 5.13: The α -VHL, LIMD1 and PHD2 monoclonal antibodies do not produce any non-IgG bands on a Western blot when probed with VHL or LIMD1 antibodies. To confirm specificity of the bands observed following Western blot of the immunoprecipitation experiments, α -VHL, PHD2 and LIMD1 antibodies were conjugated overnight to IP matrix beads, eluted with 5 x SDS loading buffer and analysed by Western blot. Cross reactivity of the α -mouse secondary antibody causes the appearance of the IgG heavy (50kDa) and light (25kDa) chains on a Western blot when probed with (A) α -LIMD1 or (B) α -VHL antibodies. No other bands are observed, even after a long exposure, showing the bands observed following the immunoprecipitation experiments are from specific in vivo protein-protein interactions.

Following Western blot analysis, cross reactivity of the mouse monoclonal immunoprecipitating antibody with the α -mouse secondary antibody produced bands on the blots that corresponded to the IgG heavy (50kDa) and light (25kDa) chains (Figure 5.13). No other bands were observed, even after a long 30minute exposure. Therefore, it can be concluded that the bands observed following the endogenous immunoprecipitation experiments are specific, and as such reinforces the integrity of the identified *in vivo* endogenous interactions.

5.4.5 LIMD1 Protein Loss Inhibits Adaptation to Chronic Hypoxia

Under exposure to a reduced oxygen tension, the level of HIF1 α protein increases due to decreased PHD2 activity that prevents hydroxylation of HIF1 α and subsequent recognition and ubiquitylation by VHL. The increase in protein continues until approximately 24 hours post hypoxia, during a phase known as acute hypoxia. After the initial 24 hours, cells enter a period of prolonged oxygen starvation known as chronic hypoxia, where the cell begins to adapt to the hypoxic conditions and is characterised by a decrease in levels of HIF1 α protein. Adaptation to hypoxia is critical, as HIF1 α promotes the expression of angiogenic and proliferative genes, as well as growth factors that induce signal-transduction pathways that promote cell survival and so to avoid cellular transformation and uncontrollable proliferation, the levels of HIF1 α and associated genes must be attenuated (Semenza, 2003).

PHD2 is the proline hydroxylase within cells that has the greatest activity towards HIF1 α , where it facilitates proline hydroxylation of HIF1 α whilst utilising O₂ as a substrate. Thus under hypoxic conditions where O₂ is limiting, hydroxylation of HIF1 α does not occur and so the protein is stabilised as it is not recognised by VHL, ubiquitinated or degraded. Contradictory to this central dogma of HIF1 α regulation, a number of publications have demonstrated that PHD2 is still active under hypoxic conditions. siRNA mediated depletion of PHD2 in hypoxia has been shown to cause an increase in levels of HIF1 α in hypoxia, implicating PHD2 to still be active under these conditions. Furthermore, the promoter of PHD2 contains a HRE and as such under hypoxia an increase in protein levels is observed. To date the reason for this is not fully understood, however it is generally postulated that the increased levels are to pre-empt the cells for rapid degradation of HIF1 α should they become re-oxygenised in order to ablate the hypoxic response. The increase in levels of PHD2 in hypoxia is one of the major caveats in the understanding of HIF1 α biology.

Both PHD2 and LIMD1 are involved in the degradation pathway for HIF1 α . LIMD1 directly binds to PHD2 (Figure 5.7), forming a complex with VHL (Figure 5.10 and Figure 5.11) and contains a HRE in its promoter causing its up-regulation in hypoxia (Figure 5.1). It was therefore hypothesised that if LIMD1 was a true component of the HIF1 α degradation pathway, depletion of LIMD1 would cause a stabilisation of HIF1 α protein, similar to the described effects of PHD2 depletion.

To assay this, siRNA mediated depletion of LIMD1 was carried out in U2OS cells, which were then exposed to up to 72 hours hypoxia. As controls scrambled or PHD2 siRNA were transfected in parallel, along with a combination of LIMD1 and PHD2 siRNA. Cells were then lysed in 1 x Passive Lysis Buffer (Promega) supplemented with 10 μ M MG132 and levels of HIF1 α , LIMD1, PHD2 and actin (as a control for equalised loading) in the lysates were assayed by Western blot (Figure 5.14).

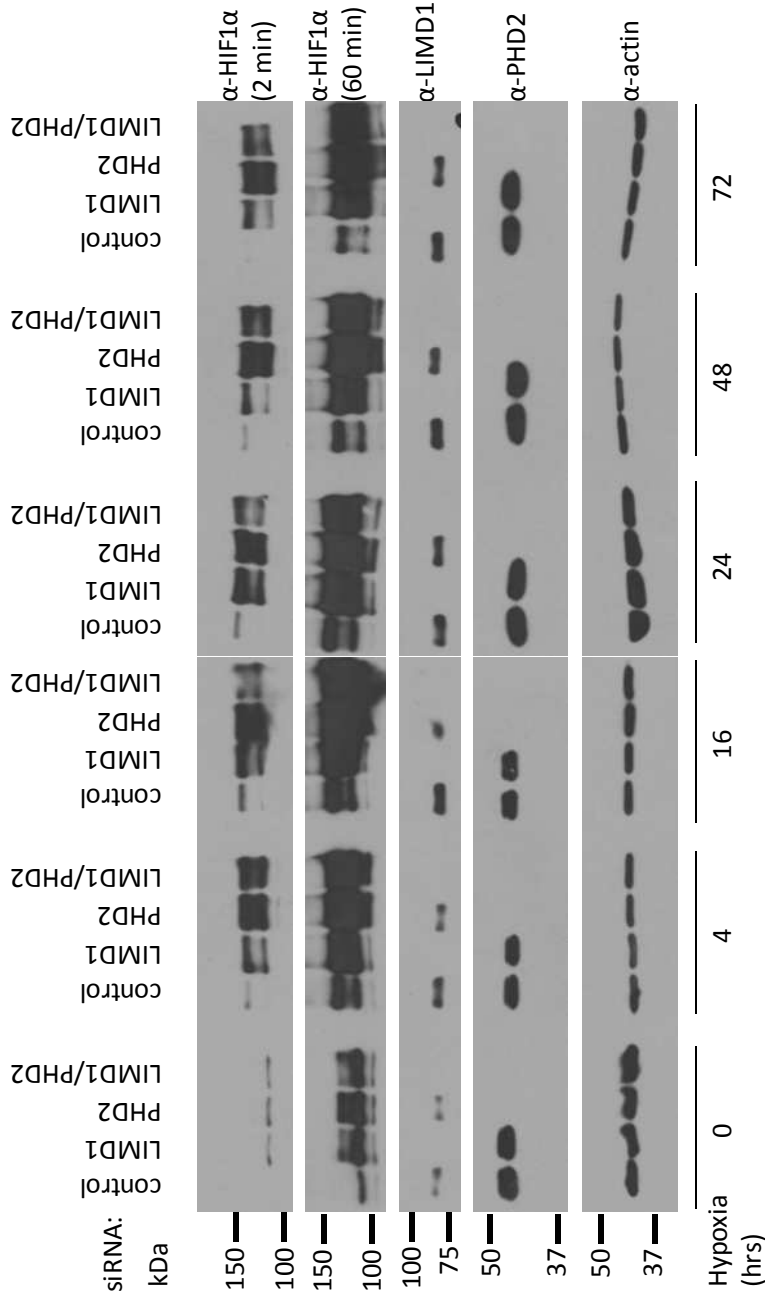


Figure 5.14: siRNA mediated depletion of LIMD1, PHD2 or combined LIMD1 and PHD2 knockdown increases HIF1α protein levels in normoxia, acute and chronic hypoxia. siRNA was used to deplete either endogenous LIMD1, PHD2, or both LIMD1 and PHD2, alongside a scrambled control in U2OS cells. Cells were then exposed to hypoxia for 0, 4, 16, 24, 48 or 72 hours, lysed in Passive Lysis Buffer (Promega) supplemented with 10μM MG132 and resultant protein levels assayed by immunoblotting. Depletion of LIMD1 and PHD2 proteins both independently or together resulted in an increase in HIF1α protein levels at all time points assayed showing LIMD1 (and PHD2) are critical for regulation of HIF1α independent of oxygen tension.

In normoxia, following treatment with the control siRNA, only very low levels of HIF1 α are present due to its rapid PHD2/VHL mediated degradation. The levels of HIF1 α then increase through exposure to 4 and 16 hours hypoxia (due to inactive PHD2), with no further increase seen after 24 hours. After 48 and 72 hours the levels of HIF1 α then significantly reduce (Figure 5.14, control lanes). This trend follows the published and described level of expression through normoxia, acute and chronic hypoxia (Stiehl et al., 2006).

When LIMD1 protein is depleted, an increase in HIF1 α protein is seen in normoxia, as previously identified and described in the preliminary data (Figure 1.27). In hypoxia, the increase in HIF1 α protein level is significantly exaggerated through to 24 hours when compared to the control siRNA. As cells enter chronic hypoxia, HIF1 α protein levels decrease but are still significantly higher than in the control. Overall, loss of LIMD1 had a stabilising effect on HIF1 α , and this was independent of oxygen tension; i.e. loss of LIMD1 inhibits the adaptive response to hypoxia.

Depletion of PHD2 resulted in an even greater stabilisation and increase in levels of HIF1 α than with LIMD1 depletion. The increase in HIF1 α from normoxia to 16/24 hours hypoxia is seen in the same manner as with the control or LIMD1 knockdown. However no decrease is observed in chronic hypoxia. A possible explanation for this could be that because the majority of HIF1 α degradation by the proteasome is dependent upon the initial hydroxylation of HIF1 α ; ablation of this initial step (through siRNA depletion of PHD2) inhibits all the further downstream processes that culminate in degradation of HIF1 α ; therefore PHD2 loss has a more potent stabilisation effect of HIF1 α than LIMD1 loss does.

Upon combined depletion of LIMD1 and PHD2, the observed increase in HIF1 α protein levels are between those seen with LIMD1 and PHD2 knockdown alone, and still significantly higher than the protein levels in the scrambled control. The levels of HIF1 α do not appear to be cumulative of LIMD1 knockdown combined with PHD2 knockdown, but neither was it as great an increase as with just PHD2 alone. The reason for this is unknown, but one possible explanation could be that depletion of both proteins simultaneously could induce LIMD1 and PHD2 independent HIF1 α degradation pathways to become active, allowing for some degradation of HIF1 α to occur.

Overall these data show that LIMD1 loss, like loss of PHD2, causes an increase in normoxic and hypoxic HIF1 α protein levels, and inhibits the cellular adaptation to chronic hypoxia through inhibition of HIF1 α degradation.

5.5 HIF1 α is Post Translationally Modified by Phosphorylation

After performing the siRNA depletion and time course experiment (Figure 5.14), HIF1 α was observed as two different motilities on the gel, often appearing as a doublet (easily observed in the short exposure of the anti-HIF1 α Western blot, indicated by arrows). Furthermore, in normoxia the predominant form was the lower molecular weight band, whereas in hypoxia the predominant form was the higher molecular weight form.

Published investigations into HIF1 α function identified HIF1 α becomes phosphorylated and this directly effects its transcriptional activity. Unphosphorylated HIF1 α is transcriptionally inactive, however when phosphorylated, it is able to dimerise with HIF1 β and become transcriptionally active (Wang and Semenza, 1993a; Berra et al., 2000). The different phosphorylated forms of HIF1 α were identified as resolving with different motilities on a gel. It was therefore hypothesised that the differences observed in HIF1 α motility (Figure 5.14) were also due to phosphorylation; in normoxia, HIF1 α is transcriptionally inactive, so is therefore unphosphorylated and runs at a lower molecular weight. However in hypoxia, where HIF1 α is required to be active, it becomes phosphorylated and so runs at a higher molecular weight.

To investigate the differences in motilities and prove this may be due to phosphorylation it was hypothesised that treatment of the higher motility form of HIF1 α with a phosphatase should result in the appearance of the lower motility form. As the higher molecular weight form was only significantly observed after cells had been exposed to hypoxia, with levels peaking by 16-24 hours, duplicate wells of U2OS were exposed to hypoxia overnight prior to lysis in RIPA buffer supplemented with protease inhibitors and MG132 to prevent degradation of HIF1 α (following reoxygenation of the cell lysate by atmospheric oxygen). One of the duplicate wells was lysed with the lysis buffer also supplemented with phosphatase inhibitors as a control. 50 Units of shrimp alkaline phosphatase were added to the lysates, and incubated for 60 minutes at 37°C. HIF1 α protein was then analysed by Western blot (Figure 5.15).

In agreement with the initial observation of the different molecular weights of HIF1 α in normoxia and hypoxia (Figure 5.14), in normoxic U2OS cell lysates HIF1 α was observed as a single lower molecular weight band. After exposure to 24 hours hypoxia, HIF1 α was observed as a doublet with the higher molecular weight form appearing slightly more prominent (Figure 5.15, indicated by arrow heads). Following SAP treatment however, there was no change in motility of

HIF1 α compared to the untreated lysate in either normoxic or hypoxic cell lysates. This result did not correspond to the hypothesis that the molecular weight differences were due to phosphorylation, as SAP treatment should have resulted in dephosphorylation with only the lower molecular weight HIF1 α being observed on a Western blot.

It was reasoned, however, that this could be a false negative result for two reasons. Firstly the amount of phosphorylated proteins in total cell lysate would have been huge, and so as such the amount of SAP could have been rate limiting in order to dephosphorylate all the phospho-proteins. Secondly, SAP is not a specific protein phosphatase; it is a generic phosphatase that is most commonly used to dephosphorylate the 5' base of a DNA vector or insert during routine cloning and as such may not be the optimal phosphatase to use against proteins.

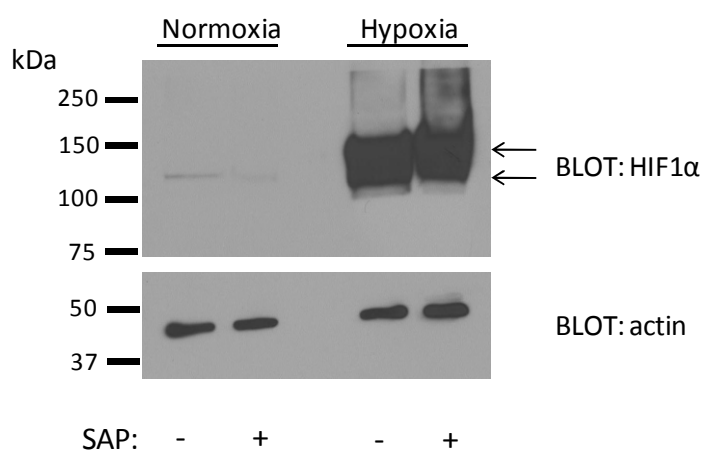


Figure 5.15: Treatment of normoxic or hypoxic cell lysates with shrimp alkaline phosphatase does not affect motility of HIF1 α . U2OS cells were exposed to hypoxia for 24 hours prior to lysis in RIPA buffer supplemented with protease inhibitors and the 26S proteasome inhibitor MG132. 50 units of shrimp alkaline phosphatase (SAP) were added and lysates incubated for 60 minutes at 37°C. Analysis of resultant HIF1 α protein levels by Western blot showed the lower molecular weight HIF1 α in normoxia and the higher molecular weight in hypoxia. SAP treatment did not affect the molecular weight of HIF1 α in either oxygen tension.

To overcome these problems HIF1 α was purified from total cellular lysate by immunoprecipitation with anti-HIF1 α antibody. The immunoprecipitation was carried out in the presence of protease, phosphatase inhibitors and MG132 to preserve the amount and phosphorylation state of any HIF1 α . The phosphatase inhibitors were then removed from the IP by extensive washing with unsupplemented RIPA, and successful immunoprecipitation confirmed by Western blot. Immunoprecipitations were carried out using hypoxic U2OS, HEK 293T and HeLa cell lysates. This was for continuity with the endogenous IPs (Figure 5.10 and Figure 5.11) and to assess if any possible phosphorylation was cell type specific. Lambda protein phosphatase, which is a specific protein phosphatase, was incubated with the purified HIF1 α and incubated for 60 minutes at 30°C and subsequent HIF1 α protein analysed by Western blot (Figure 5.16).

HIF1 α was expressed in the hypoxic extracts of all 3 cell lines tested (Figure 5.16 Input lane). Upon close inspection of the input blot a doublet band is visible in all the cell lines, albeit slightly obscured by the more prominent higher motility form. As a control for specificity of the immunoprecipitation, an isotype control antibody was used. Immunoprecipitation of HIF1 α without subsequent lambda phosphatase treatment from HeLa and U2OS cells resulted in immunoprecipitation of both the higher and lower molecular weight forms, whereas 293T cells solely gave the higher form (Figure 5.16). Following phosphatase treatment, the higher motility band disappeared from all three cell lines, leaving the lower molecular weight form (Figure 5.16, indicated by arrow heads).

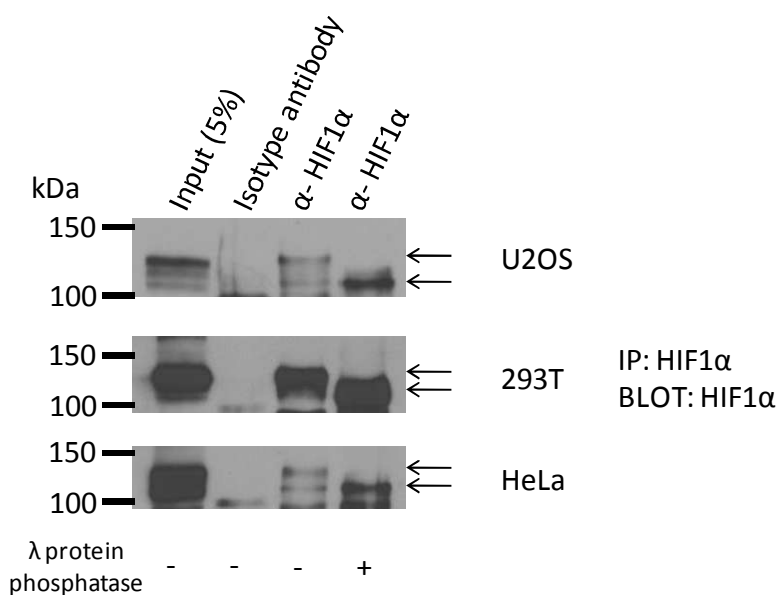


Figure 5.16: HIF1α is predominantly phosphorylated in hypoxia and unphosphorylated in normoxia. Hypoxic (16hours) cell extracts from U2OS, HEK 293T and HeLa cells were immunoprecipitated with an anti-HIF1α antibody in the presence of MG132, protease and phosphatase inhibitors so as to maintain phosphorylation status and quantity of protein under normoxic immunoprecipitation conditions. Immunoprecipitations were extensively washed with unsupplemented wash buffer before incubation with lambda protein phosphatase and HIF1α protein levels assayed by Western blot.

5.5.1 Phosphorylation of HIF1α Affects Transcription of HRE Containing Genes

The phosphatase assay data indicated the difference in the two molecular weight forms of HIF1α were due to phosphorylation, as phosphatase treatment is able to convert the higher form to the lower form. In normoxia the majority of HIF1α that is present is of the lower molecular weight, meaning it is unphosphorylated and so transcriptionally inactive (Figure 5.14). It was therefore hypothesised that the increase in stability caused by depletion of LIMD1 and/or PHD2 would not have any significant effects upon transcription of hypoxic responsive genes in normoxia. However, in hypoxia where the stabilisation is of the predominantly higher molecular weight phosphorylated form, it would be predicted that loss of LIMD1 and or PHD2 would have the most significant increase on downstream hypoxic gene transcription.

To test the hypothesis, siRNA mediated depletion of LIMD1 was performed in HEK293T cells and resultant mRNA levels of HIF1 driven hypoxic responsive genes assayed. These comprised of *BNIP3* (a mitochondrial stress sensor), *JMJD1A* (transcriptional regulator), *WSB1* (protein degradation pathway), *ALDOC* (glucose metabolism), *Endoglin* (endothelium glycoprotein), *ERO1L* (oxidative protein folding), *HK1* (glucose metabolism) and *MXI1* (transcriptional repressor). As controls, scrambled or PHD2 siRNA was also included. Following knockdown, cells were exposed to 24 hours hypoxia and RNA levels of a selection of HIF responsive genes were quantified (Figure 5.17). qRT-PCR analysis was kindly performed by Dr. Victoria James.

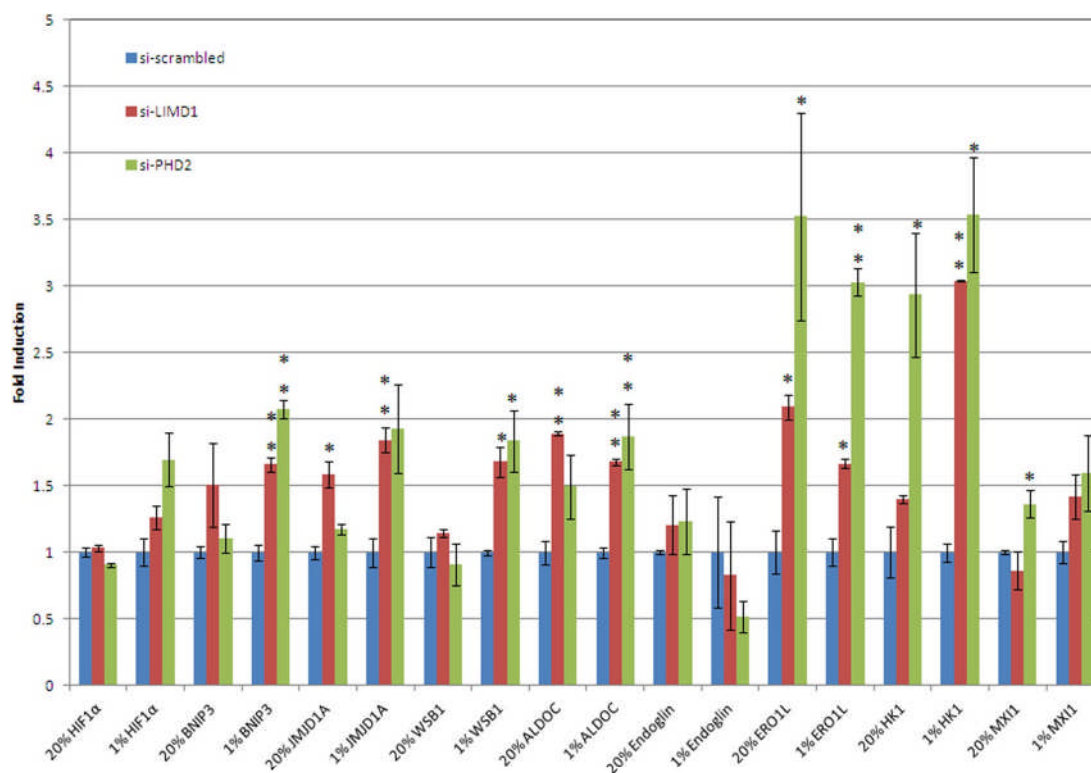


Figure 5.17: mRNA levels of HIF-1 responsive genes following LIMD1, PHD2 or control scrambled siRNA depletion. HEK293 cells were depleted of LIMD1 or PHD2 by siRNA, prior to exposure to 24 hours normoxia (20%) or hypoxia (1%). RNA was then extracted and mRNA levels of a selection of HIF-1 responsive genes quantified. Data are mean \pm SEM, n=3 independent experiments *P<0.005, **P<0.05. BNIP3, BCL2/adenovirus E1B 19kDa interacting protein 3; VEGF, vascular endothelial growth factor A; WSB1, WD repeat and SOCS box containing 1; ALDOC, aldolase C, fructose-bisphosphate; ERO1L, Endoplasmic reticulum oxidoreductin-1-like; HK1, hexokinase 1; MXI1, MAX-interacting protein 1. qRT-PCR analysis was kindly performed by Dr. Victoria James.

As hypothesised, following LIMD1 depletion, increases in mRNA transcription were only observed in hypoxia and not normoxia for *WSB1*, *HK1* and *MXI1*. Similar observations were also observed following PHD2 depletion for *BNIP3*, *JMJD1A* and *WSB1*, implicating the importance of HIF1 α phosphorylation for transcriptional activation, regardless of increased protein levels caused by LIMD1 or PHD2 depletion in normoxia.

Differences were also observed between the responsiveness of the same gene following depletion of LIMD1 or PHD2. In normoxia, *HK1* mRNA was not significantly affected by LIMD1 depletion; however PHD2 depletion increased *HK1* mRNA levels three fold. In hypoxia, where LIMD1 depletion caused an increase in mRNA levels compared to normoxia, PHD2 depletion caused an increase compared to the scrambled control, but was not significantly more than observed in normoxia. The converse result was observed with *JMJD1A*; LIMD1 depletion caused an increase in mRNA levels in both oxygen tensions, whereas PHD2 depletion only caused an increase in hypoxia. These data therefore suggest that the responsiveness of some genes may be cell type specific, with the interactions with other endogenous proteins and pathways also possibly affecting mRNA levels.

5.6 Summary

Under low oxygen tensions, *LIMD1* promoter driven transcription (Figure 5.1) and LIMD1 protein (Figure 5.5) are both up-regulated by HIF1 α , due to the presence of a functional HRE within IR3 of the CpG Island (Figure 5.3). At a molecular level, LIMD1 directly binds to the major oxygen sensor PHD2 (Figure 5.7), and forms an endogenous *in vivo* complex with PHD2, VHL, cul2 and elongin B (Figure 5.10, Figure 5.11 and Figure 5.12) that was hypothesised to participate in degradation of HIF1 α . Depletion of LIMD1, which would disrupt the degradation complex, caused a stabilisation of HIF1 α under normoxic, acute hypoxic and chronic hypoxic conditions (Figure 5.14) showing that LIMD1 is critical for regulation of HIF1 α and adaptation to chronic hypoxia. In normoxia, the stabilisation of HIF1 α is of the unphosphorylated, transcriptionally inactive form, whereas in hypoxia it is predominantly of the phosphorylated, transcriptionally active form (Figure 5.16), and this is implicated through qRT-PCR analysis of HIF1 responsive genes following LIMD1 depletion in normoxia and hypoxia (Figure 5.17).

Chapter 6 Discussion

6.1 *LIMD1* Gene Transcription and Promoter Methylation

To date, *LIMD1* protein and gene loss has been demonstrated in lung, breast and head and neck squamous cell carcinomas (HNSCC) and has been correlated with poor prognosis and a decrease in survival from time of diagnosis (Sharp et al., 2004; Sharp et al., 2008; Spendlove et al., 2008; Ghosh et al., 2008). Specifically in lung cancer, *LIMD1* protein loss has been identified in up to 79% of tumours, however the reasons for loss of expression had not been fully elucidated. Gene deletion and loss of heterozygosity has been identified as a cause of loss of *LIMD1* protein expression in 44% of lung tumours (Sharp et al., 2008), leaving 30% of tumours with unexplained mechanisms of *LIMD1* loss. This therefore implicated other mechanisms must account for *LIMD1* gene silencing. Lung cancer is the second most common form of cancer in developed countries; in the USA in 2010 it accounted for 15% of all new cancer cases, and it has the highest mortality rate (30%) of all cancers (Jemal et al., 2010). Therefore, identification of any other factors that result in *LIMD1* loss could have significant clinical implications and initial investigations performed in this thesis focused upon identification of these mechanisms.

6.1.1 The *LIMD1* Promoter is Methylated in the Non-*LIMD1* expressing MDA-MB435 Cell Line

As many characterised TSG have been shown to undergo epigenetic silencing through promoter CpG Island hypermethylation, it was postulated that this could also be a cause of *LIMD1* silencing. Using the Ensembl Genome Browser a single 860bp CpG Island was identified within the promoter spanning -1250 to -390 relative to the predicted transcription start site (TSS) (Figure 3.1).

In an independent preliminary study, Huggins *et al* also analysed the promoter for the presence of any CpG Islands (Huggins and Andrulis, 2008). They took a region of the *LIMD1* promoter spanning 10kb upstream from the translation initiation codon and performed analysis using the European Bioinformatics Institute CpG Island finder. They reported the identification of 3 small CpG Islands very close together that spanned a 1.2kb region of the promoter that ended at -400 relative to the TSS. Although using the Ensembl Genome Browser only one CpG Island was identified, both programmes identified the CpG Islands in the same promoter region (-1250 to -390 and -1600 to -400), thus the findings of Huggins *et al* corroborate the results of this investigation. The single large CpG Island identified in this study, compared to being split into three smaller islands by Huggins *et al* can most likely be explained due to the different algorithms used by both software programmes; however both results abide by

the Gardiner-Garden and Takai CpG Island definitions (Gardiner-Garden and Frommer, 1987; Takai and Jones, 2002).

Analysis of the *LIMD1* promoter using mutational analysis identified IR5 as being critically important for transcriptional activity as deletion of this region decreased transcription by 90% (Figure 3.2). For initial investigations, the osteosarcoma U2OS and breast epithelial MDA-MB435 cell lines, which had previously been characterised as *LIMD1* mRNA and protein expressing and non-expressing respectively were used. The *LIMD1* promoter and gene (including intron/exon boundaries) were present in both lines as confirmed by PCR (Sharp *et al*, unpublished data), however DNA sequencing of bisulphite treated genomic DNA from both cell lines revealed that genomic DNA from U2OS was unmethylated, whilst genomic DNA from MDA-MB435 cells was methylated (Figure 3.4). Concurrent experimentation using methylation specific restriction analysis also identified methylation within the *LIMD1* promoter, mapped to within the region spanning -885 to -373 (Huggins and Andrulis, 2008). IR5 is within this large region, and corresponds to bases -678 to -658. The sequence of IR5 (CTCACTCCGCGTCCCGCCGC) does not contain any endonuclease restriction sites for pairs of methylation sensitive and insensitive isochizomers. Therefore, similar methylation specific restriction analysis could not be performed specifically on this region.

6.1.2 The *LIMD1* Promoter is Methylated in Primary Lung Tumours

To assess the relevance of methylation within IR5 identified in the cultured cell lines and correlate it to primary tumours, a cohort of 48 matched normal and tumour lung tissues were used. Following bisulphite treatment of genomic DNA, the region surrounding IR5 was analysed using methylation specific PCR (MSP). MSP was initially chosen as after the initial bisulphite treatment, samples could be quickly and easily analysed using standard PCR. Furthermore, as genomic DNA from U2OS and MDA-MB435 cells had previously been characterised as being unmethylated and methylated respectively, they were able to serve as ideal internal controls. Analysis of the *LIMD1* and *Rassf1a* promoters by MSP gave the unexpected result of some tumours becoming hypomethylated compared to the matched normal tissue (Figure 3.7). Mixed methylation status and tumour hypomethylation has been reported at the *Rassf1a* promoter in prostate carcinomas (Florl *et al.*, 2004), however in lung tumours the *Rassf1a* gene promoter is accepted as becoming hypermethylated when compared to matched normal tissue (Burbee *et al.*, 2001; Dammann *et al.*, 2005; Pfeifer and Dammann, 2005). Furthermore, the primers used for the *Rassf1a* MSP had been

previously published where hypomethylation of tumour samples was not observed. Therefore consideration had to be given to the results obtained.

More recent investigations into promoter methylation within non small cell lung cancers have shown that some TSG are methylated even in normal tissues, including LSAMP and OPCML that were methylated in 55-88% of normal and cancer tissues as well as BRCA1 and p14^{ARF} which were methylated in less than 8% of samples. *Rassf1a* was included in the analysis and showed methylation in 8% of normal and 40% of tumour samples (Zhang et al., 2011b). Therefore it may be possible that the observations obtained with the MSP could be correct with respect to normal methylation of *Rassf1a* or *LIMD1*, however weaknesses in MSP methodology also need to be considered.

MSP is considered a simple qualitative method of methylation analysis, which due to the presence of different intensity bands, with some barely detectable, can be subjective, especially when only low level methylation is present. Furthermore, altering the number of PCR cycles can change the intensity or cause the appearance/disappearance of amplicons, again introducing a very subjective method of analysis. The annealing of the methylation specific primer is dependent upon the uniformed hypo or hyper methylation within the primer annealing region, and so if there is a variation in methylation within this region, factors such as mis-match base pairing within the primer can result in false positive results. Furthermore, any variation of the methylation status within the amplified region between the forward and reverse primers is not assayed unless subsequent sequencing analysis is performed.

The mixed results obtained with the MSP could also originate from the biopsy samples. *LIMD1* expression within the blood associated cell lineages has not been investigated, so any infiltrating lymphocytes or other cells would introduce non-lung tissue derived genomic DNA that may be normally methylated or unmethylated. Unpublished observations from immunohistochemical studies have identified lymphocytes as expressing high levels of *LIMD1* (Dr T.V. Sharp unpublished data). As the tissue samples were obtained by biopsy, it is possible that infiltrating lymphocytes, or indeed contamination of tumour samples with adjacent normal tissue, could produce artefactual results. Assuming that normal tissue/lymphocytes express *LIMD1* and contain hypomethylated promoters, contamination of potentially hypermethylated tumour cells with these could produce a false observation of hypomethylation. Furthermore, it has been reported in some renal carcinoma cell lines and renal cell carcinoma somatic

hybrids, which contain up to 5-6 copies of chromosome 3 per cell, differentially methylated alleles of *Rassf1a* were present inside the same cell (Dreijerink et al., 2001). As such, this could also be the case for a proportion of the lung tissue/tumour samples. Chromosome number analysis was not performed on the cohort used within this thesis. Therefore, the possibility of aberrant chromosome number increases could also contribute to the unexpected MSP result. Epigenetic silencing of genes within normal tissue has been demonstrated (Shen et al., 2007; Futscher et al., 2002), and so any blood lineages that have *LIMD1* silenced, could achieve this through promoter methylation and thus introduce a false hypermethylated tissue genotype.

To avoid any possible artefactual results that may be introduced through experimental procedure, technique or analysis, the *LIMD1* promoter was re-analysed using bisulphite sequencing, which allows for methylation analysis at the single base pair level (Figure 3.10) and omits any weaknesses in the methodology associated with MSP. In contrast to the MSP results, no tumour hypomethylation was observed. Mixed chromatogram peaks (referred to as 'partially methylated' within Chapter 3) were observed in some of the samples. However, as the included U2OS/MDA-MB435 homogeneous cell population controls did not produce any mixed peaks, this confirmed the biopsy samples as harbouring heterogeneously methylated cell populations, and that the mixed peaks were not introduced through experimental procedure.

26% of matched sample pairs showed aberrant tumour methylation at the penultimate CpG dinucleotide within IR5, with one of these tumour samples also having partial methylation at another CpG dinucleotide. The reason for why predominantly only one CpG became methylated in the tumour samples is unclear, however due to the specificity of the methylation a common, unknown, mechanism may be responsible for this.

6.1.3 *LIMD1* mRNA Expression is Down-Regulated in Lung Tumours

LIMD1 mRNA expression was down-regulated in 70% of the tumours analysed (Figure 3.11); this corroborates well with immunohistochemical studies where 75-79% of lung tumours showed decreased expression of *LIMD1* protein (Sharp et al., 2008) and in the first study of *LIMD1* mRNA expression in lung tumours where 100% of the small cohort of samples showed mRNA down-regulation (Sharp et al., 2004).

In the analysis presented in this study (Figure 3.11), 12.5% of the samples failed to generate Ct values for *LIMD1* mRNA in the tumour samples, implying

that 3p *LIMD1* gene deletion could have occurred; in total 4 out of 48 samples did not express either *LIMD1* or *Rassf1a* mRNA, which implies larger scale gene deletion could have occurred that caused the silencing of a cluster of 3p21.3 tumour suppressor genes. Out of the samples that exhibited methylation, as 2 of these showed no change in mRNA expression levels in the tumour compared to the normal tissue, no definitive correlation between methylation and mRNA expression could be drawn. This is the same conclusion obtained by Huggins *et al* from primary breast tumours (Huggins and Andrulis, 2008).

6.1.4 *LIMD1* is Epigenetically Silenced in MDA-MB435 Cells

The re-expression of *LIMD1* protein in MDA-MB435 cells following treatment with 5'-Aza-2'-deoxycytidine showed that *LIMD1* was epigenetically silenced. This was confirmed through sequencing of the promoter, which identified that following treatment, the promoter became hypomethylated (Figure 3.13).

Increased methylation was observed within IR5 within the human lung tumour samples assayed, however it may not be concluded if this alone causes silencing of the *LIMD1* gene. Firstly, as described, only one of the CpG dinucleotides within IR5 became methylated in the tumour samples and secondly only a small, yet transcriptionally critical, region of the promoter was analysed by sequencing. It is therefore not known if this is sufficient to instigate silencing of *LIMD1* expression and it cannot be ruled out that other regions of the promoter (within the CpG) Island may have also been hypermethylated in the tumours and contribute to silencing of *LIMD1*. As the MB435 cell line is of breast epithelial origin, it is possible that epigenetic silencing of *LIMD1* may be more applicable in breast cancers, and this may be a future area of investigation.

5'-Aza-2'-deoxycytidine is a cytosine analogue that is incorporated into DNA during replication and is resistant to methylation. Experimentally it has been shown to cause the re-expression of multiple tumour suppressor genes including *Rassf1a* (Shen *et al.*, 2008) and *BRCA1* (Magdinier *et al.*, 2000). Clinically, 5'-Aza-2'-deoxycytidine is administered to patients suffering from myelodysplastic syndrome, acute myeloid leukaemia and chronic myelogenous leukaemia (Kantarjian *et al.*, 2003; Kantarjian *et al.*, 2006). Furthermore, 5-Aza-2'-deoxycytidine treatment both with and without the HDAC inhibitor depsipeptide, exerted anti-neoplastic effects on the MDA-MB435 and MB-231 breast cancer cell lines (Primeau *et al.*, 2003; Gagnon *et al.*, 2003). In these investigations it has been demonstrated that *LIMD1* is re-expressed in MB435 cells following 5-Aza-2'-deoxycytidine treatment, and through *LIMD1*'s associated tumour suppressive

properties, may be a factor that contributes to the anti-neoplastic properties observed. LIMD1 expression is reduced in breast cancer, where reduced expression correlates with decreased survival (Spendlove et al., 2008) as well as in lung and HNSCC (Sharp et al., 2008; Spendlove et al., 2008). Therefore, there could be a clinical interest in expanding this research to assess if re-expression of LIMD1 could be achieved in patients.

Epigenetic silencing of *LIMD1* is evident as a possible cause of silencing within tumours. However, from the results in the primary lung tumours, it is unlikely that this could account for the 30% shortfall in unexplained mechanisms of LIMD1 protein loss that have been reported. Therefore, further investigations were performed on the promoter to address how transcription of *LIMD1* is controlled. Uncovering the mechanistic detail of this regulation could provide further insights to gene silencing, as deregulation of a controlling transcription factor would also result in deregulation of *LIMD1* transcription.

6.2 Identification of PU.1 as a Major Transcriptional Activator of *LIMD1*

The IR5 region was identified as being critical for transcriptional activity of the *LIMD1* promoter, however the reasons for why this region was so critical were unknown. The decrease in transcription from the $\Delta 5$ mutant could have been due to steric interference between transcriptional regulator proteins as a result of the deletion of the 21bp of DNA. However, this was thought to be unlikely as when the set of ten internal deletion mutants were examined together, a range of increases, decreases and no changes in transcriptional activities were observed, suggesting that the individual deletions were specific in abrogating protein-DNA interactions. As deletion of IR5 resulted in the greatest (90%) decrease in transcription, it was hypothesised that the region probably contained a binding site for a critical transcription factor. Furthermore, CpG methylation within this region also supported this hypothesis.

6.2.1 IR5 is Perfectly Conserved between *LIMD1* Expressing Species and Harbours an Ets Family Member/PU.1 Binding Motif

Comparative genomic analysis identified that the IR5 region was perfectly conserved between 13 *LIMD1* expressing mammals (Figure 4.1), which was indicative of it containing a binding motif critical for survival of a species (Boffelli et al., 2004; Pennacchio and Rubin, 2001). *In silico* screening of the promoter for transcription factor binding motifs identified a putative Ets transcription factor family member binding motif within IR5 (Figure 4.2), that through ChIP, EMSA and siRNA depletion experiments was confirmed as being PU.1 (Figure 4.7, Figure 4.8, Figure 4.10).

PU.1 was initially identified as binding to the core sequence 5'-GAGGAA (Klemsz et al., 1990), however variations within the preceding and following bases around the GGAA motif have since been identified; recent ChIP-Seq analysis of PU.1 binding in macrophages and B-cells revealed the core binding motif for PU.1 (GGAA) is commonly preceded by G/C then A/C, and followed by, in the majority of sequenced motifs, GTG (Heinz et al., 2010). This gives rise to a generalised consensus G/C-A/C-GGAA-GTG, which matches the IR5 sequence of GCGGAAGTG. Other genes under PU.1 control have homology to the IR5 sequence, including secretory interleukin-1 receptor antagonist (*IL-1Ra*) which has the consensus GCGGAAATA (Smith, Jr. et al., 1998), and Toll-like receptor 4 (*TLR4*) has the consensus GAGGAAGTG (Rehli et al., 2000). These additional

experimentally verified PU.1 binding motifs therefore corroborate the identification of PU.1 binding the *LIMD1* promoter and activating its transcription.

The initial internal promoter deletion experiments were performed in U2OS cells, a cell line which by Western blot does not express PU.1 (Brown et al., 2011). Furthermore, the same experiments were also performed in MDA-MB435 breast epithelial and A549 lung epithelial cell lines (data not presented), where the *IA5* deletion also resulted in similar significant decreases in transcriptional activity. These cells are also considered PU.1 negative, and so consequently it is believed another transcription factor must also activate transcription from the same region of the promoter. Point mutagenesis of the core Ets binding motif GGAA in U2OS cells alone (Figure 4.3) resulted in the same significant decrease in transcription as observed with the whole *IA5* deletion. Therefore it is highly probable that in non-haematopoietic derived lineages, another Ets factor may replace PU.1 as an activator of *LIMD1* expression. From the Ets family member controls used throughout Chapter 4, the family members Elk-1 and Ets-1 do not appear to affect *LIMD1* promoter transcription or associate with the promoter both *in vitro* and *in vivo*.

As little as one flanking DNA base, or amino acid residue surrounding the protein Ets domain is enough to provide specificity for Ets protein binding and gene activation (Verger and Duterque-Coquillaud, 2002), with multiple factors also being known to bind to the same single motif within a promoter. For example, the platelet factor 4 (PF4) gene contains multiple Ets factor binding motifs; Ets1 binds to one motif to activate transcription, whilst three different Ets factors, FLI-1, ELF-1, and GABP, compete for binding to another site during megakaryocytic differentiation to regulate stage specific gene expression (Okada et al., 2011). It is still not fully understood how different factors can bind to the same motif, yet are also able to distinguish between almost identical sequences. The similarity in sequence specificity of the Ets family proteins is illustrated in Figure 6.1 (Hollenhorst et al., 2007). Expression profiles of 27 human Ets genes in 16 tissue samples and 7 cell lines revealed that in each sample at least 16 Ets members were expressed, with 14 showing ubiquitous expression (which was defined as being expressed in a least 22/23 samples) (Hollenhorst et al., 2004). It is thought however that stage/tissue specific changes in Ets family expression, interaction with other Ets factors and transcriptional co-activator/repressor proteins help facilitate the binding specificity (Hollenhorst et al., 2007). Genetic redundancy of an Ets factor is unlikely to be a contributing factor, as deletion of

each Ets member results in unique phenotypic consequences, summarised in (Hollenhorst et al., 2004). Therefore with respect to *LIMD1* expression, it may be that several other Ets factors activate (or repress) its transcription.

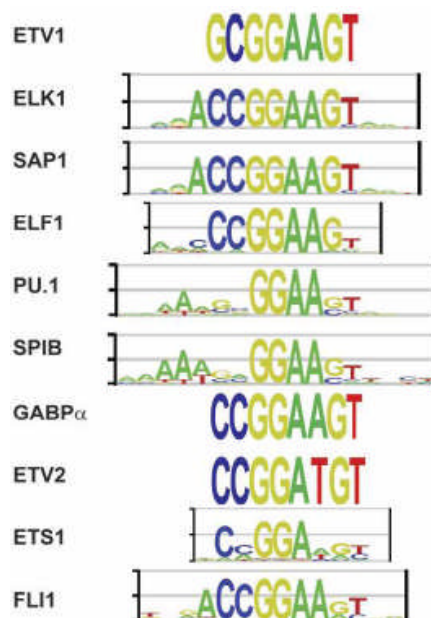


Figure 6.1: The ETS transcription factor family bind to very similar DNA sequences. Binding consensus sequences for the indicated Ets proteins were analysed through *in vitro* screening (the SELEX method), with the height of each base directly proportional to the frequency of which it is found. The Ets proteins bind to highly homologous sequences, and the precise mechanisms for site discrimination are not fully understood given that over half of Ets factors appear to be ubiquitously expressed (Hollenhorst et al., 2007).

6.2.2 The *LIMD1* Promoter Contains a putative Second PU.1 Binding Site

As well as being a transcriptional activator, PU.1 has also been associated with gene silencing. Over-expression of PU.1 causes silencing of the tumour suppressor c-myc in murine erythroleukaemia (MEL) cells through formation of a transcriptional repressor complex that includes the proteins mSin3A and HDAC1 (Kihara-Negishi et al., 2001). In undifferentiated MEL cells, PU.1 is associated with the MeCP2 co-repressor and mSin3A/HDAC1 at both a synthetic PU.1 motif containing reporter vector and at the β globin gene and repressed transcription. However, following differentiation the complex was removed from the β globin gene and the gene expressed (Suzuki et al., 2003). PU.1 also associates with the DNA methyl transferases 3a and b (Dnmt3a/b) and over-expression induced methylation within, and subsequent silencing of the p16INK4A tumour suppressor gene (Suzuki et al., 2006).

LIMD1 itself is epigenetically silenced through promoter methylation in the MDA-MB435 breast cancer cell line, with promoter methylation also evident in 26% of human lung tumours when compared to normal matched lung tissue (Sharp et al., 2008; Huggins and Andrulis, 2008). In light of the possible dual function of PU.1, the role of PU.1 during *LIMD1*-loss associated transformation remains to be elucidated. *In silico* screening of the promoter identified a second putative Ets domain/PU.1 binding site at -120 relative to the TSS. As point mutation of the PU.1 motif within IR5 (Fig. 2B) resulted in a 90% decrease in transcription, it is likely that the second PU.1 site is not involved in transcriptional activation. However, during transformation it could act as a site for PU.1 binding, subsequent Dnmt3a/b mediated CpG promoter methylation and ultimately loss of *LIMD1* expression through epigenetic silencing (Figure 6.2). It would be interesting to assess, if under specific stimuli, PU.1 does indeed associate with the second putative binding site, and if so does it induce methylation and epigenetic silencing of *LIMD1*.

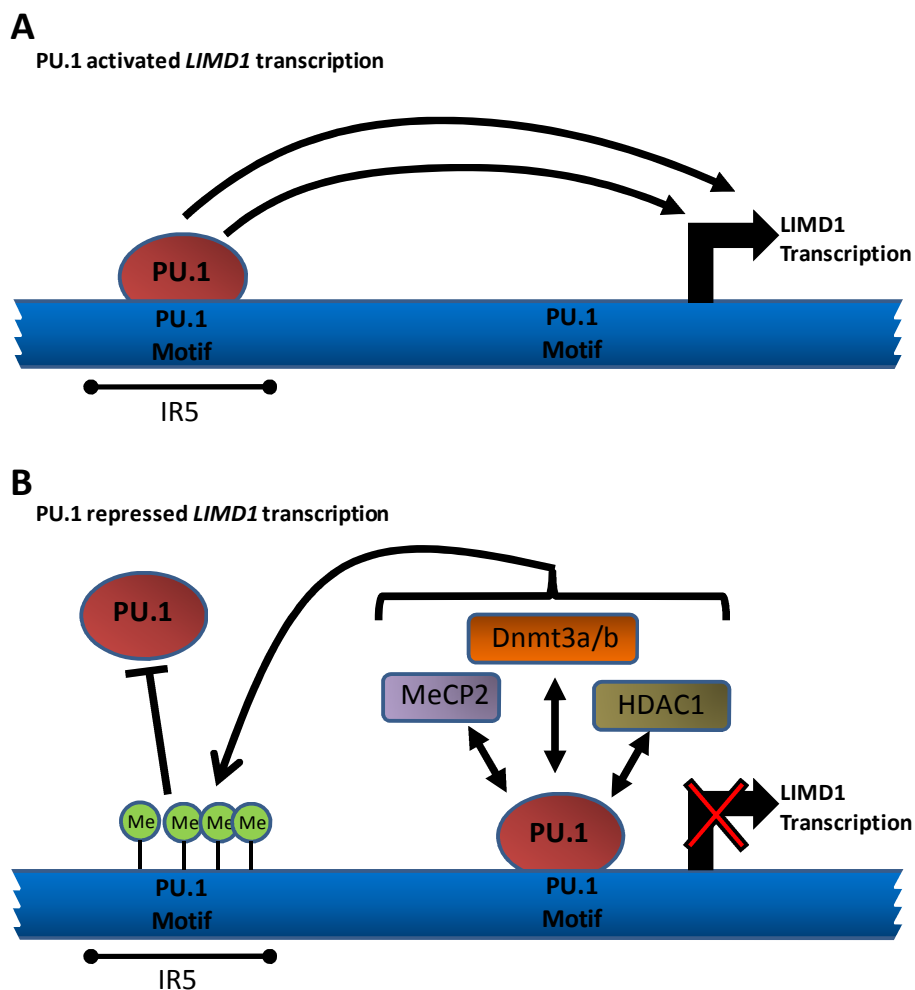


Figure 6.2: Schematic representation of the possible role of PU.1 as a transcriptional repressor of *LIMD1* expression. (A) In this thesis PU.1 has been identified as a major transcriptional activator of *LIMD1* expression, and *LIMD1* is not expressed when the promoter is methylated. (B) However PU.1 has been observed to associate with the transcriptional repressors MeCP2, HDAC1 and Dnmt3a/b, and repress transcription through CpG methylation and the formation of a heterochromatin structure. The *LIMD1* promoter contains a second PU.1 binding motif that is not required for transcriptional activation, however during transformation it could act as a functional binding site for PU.1, leading to promoter CpG methylation and histone deacetylation, causing a repression of *LIMD1* transcription.

6.3 Additional (Unconfirmed) Features of the *LIMD1* Promoter

The *in silico* analysis of the *LIMD1* promoter also identified other common promoter related features that could be directly related to transcriptional control of the *LIMD1* gene. As this was not within the scope of this thesis, these sites were not examined experimentally; however their identification and possible implications will still be discussed.

6.3.1.1 SP1 Binding Sites

The transcription factor Sp1 binds to GC boxes and can activate transcription (Briggs et al., 1986). Sp1 binding can be abrogated by methylation (Clark et al., 1997), specifically exemplified within the extracellular superoxide dismutase and p21 gene promoters in lung cancer cell lines (Zelko et al., 2008; Zhu et al., 2003). 17 potential Sp1/GC boxes were identified within the *LIMD1* promoter, with all but three located within the CpG Island. It has not been determined if Sp1 contributes to *LIMD1* expression, however if so then *LIMD1* promoter methylation could prevent Sp1 binding and reduce gene expression accordingly.

6.3.1.2 TFIIB Recognition Element

A BRE (TFIIB recognition element) was also identified with a perfect match score of 1.0 within IR1 of the CpG Island. The function of BRE elements is not fully understood, however these elements can have both positive (Lagrange et al., 1998) and negative (Evans et al., 2001) effects upon transcription.

6.3.1.3 Initiator Elements/TATA Boxes

Two Inrs (initiator elements) were identified, both 5' proximal to the CpG Island as were two putative TATA boxes 305bp and 155bp upstream of the NCBI predicted transcriptional start site. Experimentally, as these have not been confirmed, it is not possible to ascertain if the *LIMD1* promoter is a TATA containing or TATA-less promoter. The TSS used within these investigations was the unconfirmed NCBI assigned start site; as CpG Island containing genes often do not possess just a single discreet start site but multiple sites spread over up to 100bp (Stamatoyannopoulos, 2010), it is plausible that one or both of the predicted TATA boxes could be functional and may indeed give rise a undefined small range of transcriptional start sites.

So far within the investigations discussed, the main focus has been upon *LIMD1* transcriptional control specifically surrounding IR5, and how this regulates *LIMD1* gene expression. The results obtained identified *LIMD1* expression becoming down-regulated through epigenetic silencing, as well as PU.1, and potentially one or more other Ets factors as activators of *LIMD1* gene expression. The concluding part of the discussion will now switch focus from gene expression control to a novel tumour suppressive function of *LIMD1*; as a negative regulator of the hypoxic response.

6.4 LIMD1 is a Regulator of the Hypoxic Response

6.4.1 LIMD1 driven Transcription and Protein Levels are increased in Hypoxia

Protein levels of PHD2, VHL and the SAG component of the VBC E3 ubiquitin ligase complex are increased in hypoxia due to the presence of a HRE within their promoters (Marxsen et al., 2004; Tan et al., 2008; Liu et al., 2011) and this facilitates HIF1 α degradation in hypoxia. Investigations identified that transcription from the *LIMD1* promoter is also upregulated in hypoxia (Figure 5.1), reaching a maximal level after 24 hours and that this was dependent upon HIF1 α (Figure 5.4). The binding site for HIF1 α was mapped to within IR3 of the CpG Island (Figure 5.3), which corroborated with the HIF1 binding site identified in the *in silico* screen for transcription factor binding motifs.

LIMD1 protein levels also modestly increased in hypoxia (Figure 5.2), with depletion of HIF1 α in hypoxia causing a significant decrease in *LIMD1* protein levels (Figure 5.5). Interestingly, depletion of HIF1 α in normoxia also caused a decrease in *LIMD1* protein. This was surprising, as in normoxia, due to the rapid PHD2 mediated degradation of HIF1 α and active FIH which hydroxylates Asn803 preventing association with the p300/CBP transcriptional co-activator, there is relatively very little active HIF1 α able to form the active HIF1 transcription factor. However, studies with a HIF1 inducible reporter vector in association with depletion of endogenous HIF1 α have identified there is a basal level of normoxic HIF1 driven transcription in cells (Dayan et al., 2006), therefore indicating HIF1 α expression is critical for both normoxic and hypoxic *LIMD1* expression.

Investigations into HIF1 α binding sites in the human genome using ChIP-seq and ChIP-chip analysis identified that outside the core RCGTG binding motif, no extended sequence preferences for HIF1 binding were identified, except at the R

position, adenine was observed at a 3:1 preference over guanine (Xia et al., 2009; Schodel et al., 2011). Over 50% of observed HRE elements were identified as within gene promoter regions, with over 90% of HIF-1 binding in hypoxia associated with genes that were actively expressed under normoxic conditions (as determined by RNA PolII binding or the presence of tri-methylated H3K4) (Xia and Kung, 2009). This data corroborates with the HRE identified within the promoter (consensus ggaCGTGcag) and normoxic transcription of *LIMD1*.

There are a reported 2.5×10^6 occurrences of the RCGTG motif within the human genome (Xia et al., 2009). Only a minority of these (<1%) were identified by either ChIP-seq/chip study as being bound by HIF1/2 α , therefore showing a large redundancy in motifs; however this could be due to differing chromatin accessibility as assayed through DNase1 hypersensitivity experiments (Schodel et al., 2011). The initial *in silico* identification of 3 putative HIF binding sites within the promoter, of which only one proved to be functionally active (Figure 5.4) therefore demonstrates the importance of wet laboratory experimental confirmation of transcription factor binding so as to avoid any false positive results. This was also demonstrated with the identification of two PU.1 binding sites within the *LIMD1* promoter.

6.4.2 HIF1 α Modulates *LIMD1* Transcription but is not a Major Transcriptional Activator

The basal level of transcription from the *LIMD1* promoter is only modulated by HIF1, as the basal level of transcription is controlled by PU.1/other Ets factor, and this is illustrated by the IR5 deletion. In hypoxia, HIF1 up-regulates *LIMD1* transcription 2-3 fold (Figure 5.1). Following deletion of IR5, which abrogates PU.1 binding, in normoxia transcription was repressed by ~90%. However, in hypoxia with the same deletion there was a slight de-repression in the reduction in transcription observed in normoxia (Figure 5.3), even though PU.1 was still unable to bind. Compared to the wild type promoter in hypoxia, this equated to an 80% reduction in transcription. As the I Δ 5 mutant still contained a functional HRE, this de-repression can be explained by the binding of HIF1 to the reporter plasmid, which provided a 2-fold enhancement in promoter driven transcription. This therefore demonstrates that HIF1 solely acts to enhance *LIMD1* transcription, whereas the major transcriptional activation from the promoter is still provided by PU.1, even under hypoxic conditions.

6.4.3 Promoter Methylation may Prevent Transcription Factor Binding to the *LIMD1* Promoter

It has been demonstrated that methylation of transcription factor DNA binding motifs, including those for Sp1 and ETS transcription factors, prevents transcription factor binding (Rozenberg et al., 2008). It has yet to be fully proven if methylation of the Ets motif prevents PU.1 binding and thus a reduction in *LIMD1* transcription. Within the cohort of lung tissue and tumour samples there was no evidence of methylation within the PU.1 motif. However, in the epigenetically silenced MDA-MB435 cell line the entire IR5 was methylated, and following 5-azacytidine treatment, became unmethylated and *LIMD1* re-expressed. This could therefore support the hypothesis of methylation blocking transcription factor binding. Methylation of one or more residues could also cause the association of methyl CpG binding domain (MBD) proteins, which in turn would recruit HDACs and other chromatin structure modifying proteins to enhance the formation of a transcriptionally inactive heterochromatin conformation, thus indirectly blocking transcription (Dillon and Festenstein, 2002).

More recently it has been demonstrated that the PHD3 promoter is methylated in a selection of transformed cells, including MB435 cells, and that this methylation abrogates the normal hypoxic up-regulation of the protein (Place et al., 2011). Furthermore, non-methylated HREs are critical for hypoxic, HIF1 α mediated, upregulation of erythropoietin and HIF1 α itself (Wenger et al., 1998; Koslowski et al., 2011). It could therefore be postulated that if the *LIMD1* promoter, which encompasses the HRE within IR3 was methylated, then this could also abrogate the hypoxic up-regulation of *LIMD1* and loss of the adaptive response in chronic hypoxia.

6.4.4 *LIMD1* Forms an Endogenous Complex with PHD2 and VHL/VCB Complex Proteins

Preliminary data obtained in the Sharp laboratory using protein over-expression studies identified *LIMD1* as binding to both the proline hydroxylase (PHD) and the von Hippel-Lindau (VHL) proteins, both of which are required for degradation of HIF1 α , predominantly under high oxygen tensions. To ensure that the over-expression binding data between *LIMD1*/PHD2/VHL was a true reflection of an interaction *in vivo*, extensive endogenous immunoprecipitation studies were performed (Figure 5.10, Figure 5.11 and Figure 5.12). These investigations

revealed that within the 3 distinct cell lines investigated (HEK 293T, HeLa and U2OS), endogenous LIMD1 interacted with endogenous PHD2 and VHL, along with elonginB and cullin2 that form part of the VCB E3 ubiquitin ligase complex. This data therefore demonstrated that the formation of the complex was physiologically true and occurs endogenously *in vivo*. Furthermore it was not cell type specific and thus these results help present a new fundamental mechanism of HIF1 α regulation, that could have major clinical implications.

6.4.5 LIMD1 Loss Reduces the Efficiency of HIF1 α Degradation and Inhibits Adaptation to Chronic Hypoxia

Levels of HIF1 α protein have been widely reported to decrease following prolonged (chronic) exposure to hypoxia, and as in normoxia, are surprisingly dependent upon the PHDs and VHL (Ginouves et al., 2008). This has been attributed primarily to a hypoxic increase in PHD2 protein levels, which compensates for its decreased (oxygen dependent) activity (Stiehl et al., 2006; Ginouves et al., 2008). Furthermore, hypoxic upregulation of pyruvate dehydrogenase 1 kinase, which phosphorylates and causes inactivation of pyruvate dehydrogenase, inhibits the mitochondrial TCA cycle. This reduces mitochondrial oxygen consumption and allows for redistribution of molecular oxygen within the cell, thus causing a relative increase in intracellular oxygen tension and allowing for increased PHD activity (Kim et al., 2006; Papandreou et al., 2006). In addition, nitric oxide (NO) or other inhibitors of mitochondrial respiration also prevent stabilisation of HIF1 α in hypoxia (Hagen et al., 2003). Therefore, this allows for hydroxylation of HIF1 α , followed by subsequent VHL mediated ubiquitylation/degradation.

LIMD1 was identified as forming an endogenous complex with VHL and PHD2, as well as being up-regulated in hypoxia. Therefore the effect of LIMD1 depletion in hypoxia was investigated. In normoxia, preliminary data identified that LIMD1 loss caused an increase in HIF1 α protein stability, presumably through abrogation of the LIMD1/VHL/PHD2 complex. siRNA mediated depletion of LIMD1 inhibited degradation of HIF1 α in up to 72 hours hypoxia, which was the longest time point assayed. In the control samples, the levels of HIF1 α peaked by 16 hours, and then proceeded to decline after 24 hours and were expressed at almost normoxic levels after 72 hours, which corroborated with other published observations of HIF1 α in chronic hypoxia. As a positive control, PHD2 depletion was performed alongside, and as reported by Stiehl *et al*, also inhibited HIF1 α

degradation (Stiehl et al., 2006). This therefore demonstrated that loss of LIMD1 significantly reduces degradation of HIF1 α in hypoxia, and ultimately inhibits the intracellular adaptation to hypoxia.

HIF1 α over-expression is commonly found in many cancers and is often associated with increased proliferation and metastases. Therefore appropriate control of HIF1 α expression is required to allow for proper control of cell growth and proliferation. In a widespread study of HIF1 α expression in normal and primary cancers, 69 (53%) of 131 primary malignant tumours had HIF1 α over-expression; this included prostate, breast, lung, colon, pancreas, brain, gastric, ovarian, and renal cell carcinomas, mesothelioma, and melanoma (Zhong et al., 1999). In the lung adenocarcinoma cell line CL1 and the gastric cancer cell line SC-M1, over-expression of HIF1 α resulted in increased invasiveness of cells in an *in vitro* invasiveness assay (Shyu et al., 2007). In a cohort of breast tumours, 69% of breast metastases had HIF1 α over-expressed compared to only 29% of primary breast cancers (Zhong et al., 1999). Furthermore, in human prostate cancer cell lines, elevated HIF1 α protein was observed which is associated with increased cell growth and metastatic potential (Zhong et al., 1998). LIMD1 loss has been demonstrated in lung, breast and HNSCC (Sharp et al., 2008; Spendlove et al., 2008; Ghosh et al., 2010). Therefore it could be postulated that in cancers where LIMD1 is lost, HIF1 α protein levels would be increased, leading to the aforementioned increases in cellular proliferation and metastasis. It is likely that this therefore represents one mechanism of LIMD1 mediated tumour suppressive activity, and a future line of investigation.

6.4.6 LIMD1 Expression does not Effect HIF1 α Phosphorylation

In hypoxia, HIF1 α becomes phosphorylated, which facilitates dimerisation with HIF1 β to form the active HIF1 transcription factor that can enhance transcription of HRE containing genes (Zagorska and Dulak, 2004; Semenza, 2003). Whilst performing the described investigations within this thesis, it was observed on Western blots that under normoxia and hypoxia, HIF1 α appeared to migrate at two different molecular weights. In normoxia HIF1 α was at a lower molecular weight than in hypoxia, where an additional, more prominent higher molecular weight band was observed. Therefore further analyses were performed to assess if the different forms of HIF1 α observed correlated with its different phosphorylation state. Treatment of purified hypoxic HIF1 α with lambda phosphatase confirmed the different molecular weight observed was due to phosphorylation (Figure 5.16).

LIMD1 or PHD2 depletion inhibited HIF1 α degradation and therefore increased the stability and levels of HIF1 α protein. In normoxia, the stabilisation predominantly resulted in an increase in the lower molecular weight form of HIF1 α , whereas in hypoxia it was predominantly the higher molecular weight phosphorylated form that was observed (Figure 5.14). This therefore indicated that loss of LIMD1 or PHD2 did not affect the ability of HIF1 α to become phosphorylated, indicating that LIMD1 specifically targets HIF1 α for degradation rather than regulating any pathways that converge on its phosphorylation and activity. Furthermore, as the dephosphorylation experiments were also performed in three different cell lines (U2OS, HEK293 and HeLa), this further validated the findings as not being cell type specific, thus corroborating a new universal role of LIMD1 in regulation of HIF1 α protein expression.

6.4.7 Loss of LIMD1 Expression Affects HIF-1 Driven Gene Expression

qRT-PCR analysis of a panel of HIF1 responsive genes following hypoxic exposure with and without LIMD1 depletion identified differences between normoxic and hypoxic mRNA levels (Figure 5.17). LIMD1 depletion, which resulted in an increase in HIF1 α protein levels, gave increased gene expression of *BNIP3*, *WSB1*, *HK1* and *MXI1* in hypoxia, but not in normoxia, presumably due to HIF1 α being phosphorylated (transcriptionally active) predominantly in hypoxia, despite the significant increase in normoxic protein levels following LIMD1 depletion. Similar results were also observed with PHD2 depletion as a control.

Some hypoxic responsive genes, however, showed a variation in response to 24 hours hypoxia, including *Endoglin*, which showed no hypoxic induction, and *ERO1L*, which was up-regulated in both normoxia and hypoxia following LIMD1 or PHD2 depletion. Hypoxic induction of these genes have been previously been reported; 24 hours hypoxia resulted in an 8-fold increase in Endoglin expression in the monocytic U937 cell line, but only 1.3-fold in the endothelial HMEC-1 cell line (Sanchez-Elsner et al., 2002). In MEF cells, ERO1L expression was increased equally by either hypoxia, or the PHD2 inhibitor DFO in normoxia (Saletta et al., 2010). An independent micro-array analysis of 6 cell lines identified large variations in the number of genes up-regulated by hypoxic exposure; 486 genes in monocytes compared to 2119 in HeLa cells (Benita et al., 2009). The unresponsiveness of some HIF1 responsive genes despite increased levels of HIF1 α protein have also been observed in studies on the minichromosome maintenance (MCM) proteins, which are DNA helicase proteins that bind to HIF1 α and enhance its proline hydroxylation/degradation and inhibition of its

transactivation domain (Hubbi et al., 2011; Semenza, 2011). shRNA mediated knockdown of MCM3 resulted in an increase in synthetic HRE driven luciferase transcription in normoxia in 293 cells, however under the same oxygen tension in the same cell line, mRNA levels of the endogenous *VEGF* or *Glut3* HRE containing genes were not affected following MCM3 depletion (Hubbi et al., 2011).

Therefore, there are strong implications that some genes may exhibit hypoxic responses that are cell type specific, and may be dependent upon interactions with endogenous cell specific proteins. With respect to LIMD1 depletion, these variations will only be fully elucidated as the role of LIMD1 and the hypoxic response in a range of cell types is investigated.

6.4.8 LIMD1 forms a Negative Regulatory Pathway of HIF1 α Degradation

Data within this thesis has demonstrated LIMD1 is a critical component of an endogenous complex containing PHD2 and VHL that is required for degradation of HIF1 α under both high and low oxygen tensions. Furthermore, like PHD2 and SAG within the VHL complex, *LIMD1* transcription and protein expression is up-regulated in hypoxia through the presence of a HRE within its promoter.

This data can therefore be integrated into a proposed revised model of HIF1 α degradation. In normoxia, LIMD1 forms a complex with PHD2 and VHL/VCB proteins, which facilitates the oxygen dependent hydroxylation of Pro402/564, ubiquitination and subsequent degradation of HIF1 α by the 26S proteasome. Concurrent to this, degradation of HIF1 α can also occur in the absence of LIMD1, as well as also in the absence of PHD2, however these LIMD1 independent mechanisms are not fully understood and are thought to provide a less efficient pathway for HIF1 α degradation (Yee et al., 2008). Furthermore, FIH hydroxylates Asn802 within HIF1 α , preventing association with the transcriptional activator p300/CBP. However, as HIF1 α regulation exists in equilibrium, there is still a low basal level of un-degraded, transcriptionally active HIF1 α in normoxia, which contributes to the transcription of some HRE containing genes (Dayan et al., 2006), and this now includes LIMD1.

In hypoxic conditions, low oxygen concentrations means PHD2 activity is significantly reduced. This therefore ablates PHD2 mediated hydroxylation of HIF1 α , and is thus unable to be recognised by VHL and escapes degradation. Similarly, FIH activity is also significantly reduced, and so Asn802 remains un-hydroxylated, which along with phosphorylation of stabilised HIF1 α protein,

facilitates dimerisation with HIF1 β , to form the active HIF1 transcription factor. HIF1 then binds to HREs, where association with the p300/CBP transcriptional co-activator enhances transcription of these genes to allow adaptation to hypoxic conditions.

However, PHD2, SAG and LIMD1 all contain HRE elements within their promoters, which cause an upregulation of their expression in hypoxia. This allows for formation of the same complex identified in normoxia. Increased PHD2 protein levels coupled with increased oxygen availability from inhibition of mitochondrial respiration, allows for PHD2 hydroxylation of HIF1 α , followed by VHL recognition and proteasomal degradation. Thus, a negative feedback loop is formed. Again, LIMD1 and PHD2 independent mechanisms of degradation also exist, however as described for normoxia, these are not fully elucidated but appear to be less efficient. The net result is HIF1 α degradation increases the longer cells are exposed to hypoxia, giving rise to the characterised down-regulation of HIF1 α protein levels in chronic hypoxia.

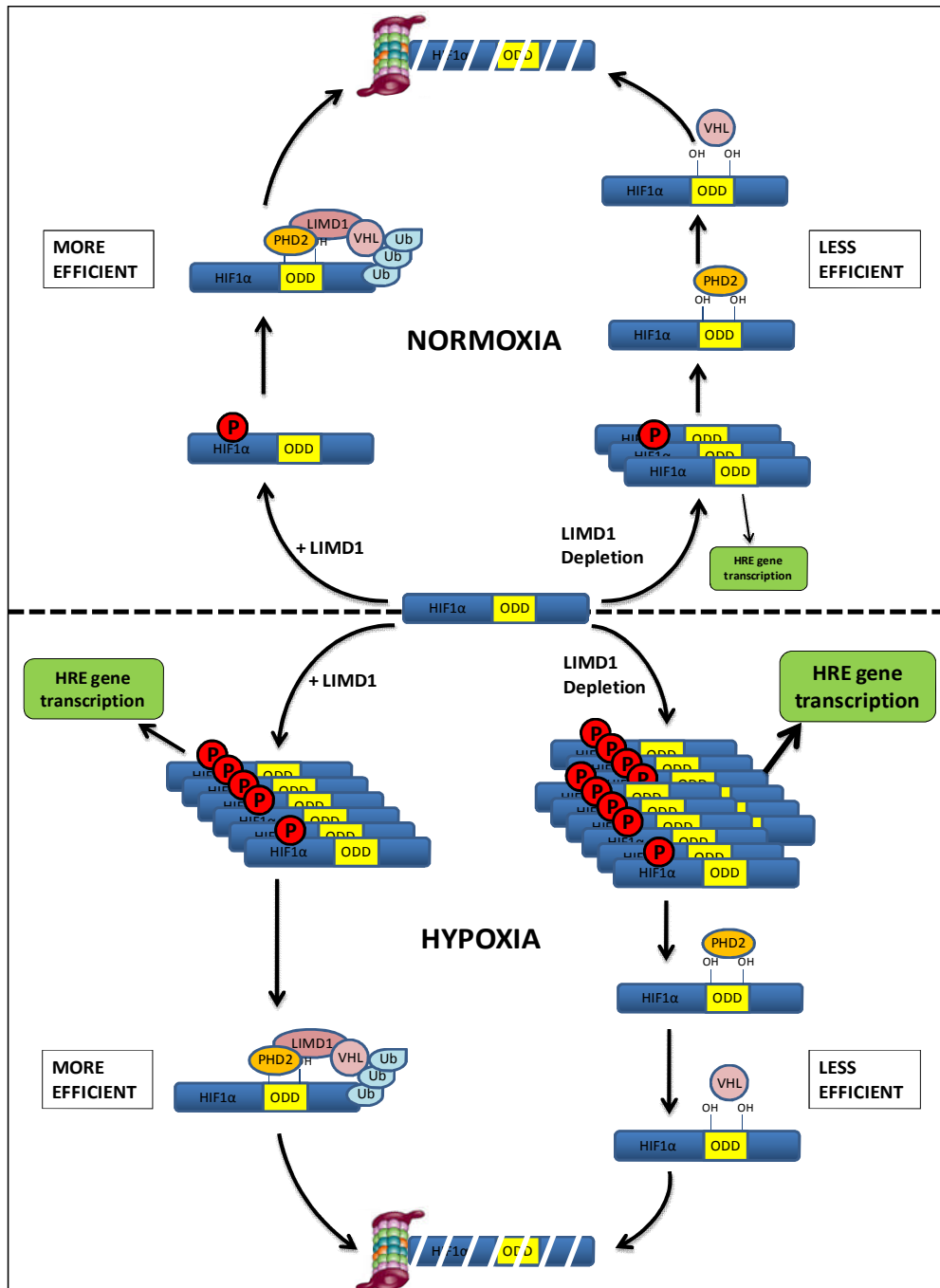


Figure 6.3: Proposed updated mechanism of HIF1 α degradation. LIMD1 forms a complex with PHD2 and VHL to facilitate degradation of HIF1 α . In normoxia, the high oxygen tension facilitates high PHD2 activity, causing hydroxylation of Pro402/564 that allows for VHL recognition/ubiquitination and degradation of HIF1 α . HIF1 α is also degraded when LIMD1 is lost, however this process is less efficient, resulting in an accumulation of a small pool of un-degraded HIF1 α that is able to form the transcriptionally active HIF-1 to provide a low basal level of HIF driven transcription. In hypoxia, low oxygen tensions significantly inhibit PHD2 activity, causing the stabilisation of HIF1 α and transcription of HRE containing genes to allow cellular adaptation to hypoxia. Hypoxic up-regulation of LIMD1 facilitates the formation of an active PHD2 and VHL complex, resulting in degradation and a decrease in HIF1 α levels. When LIMD1 is depleted, degradation of HIF1 α is inhibited, resulting in an exaggerated accumulation of HIF1 α protein that gives a further increase in HRE gene transcription.

Chapter 7 Future Work

7.1 Future Work

This chapter will put a future perspective onto the novel findings presented within this thesis, highlighting areas of particular significance and interest to future work within the group.

7.1.1 Methylation Analysis of the Full *LIMD1* Promoter and Gene

Within this thesis only a relatively small, but yet transcriptionally critical, region of the *LIMD1* promoter was assayed for CpG methylation. It would, however, be of interest to analyse the whole of the CpG Island within the promoter. From the initial promoter mapping using the deletion mutants (Figure 3.2), other regions within the CpG Island are also critical for transcription; IR1, 8 and 9 all gave reductions in transcription of over 50% when deleted. Therefore it is possible that methylation of these regions may also reduce *LIMD1* promoter driven transcription. Furthermore, different experimental techniques could be used to provide a quantitative rather than qualitative analysis of methylation.

Following PCR of bisulphite treated DNA, the subsequent amplicon could be sub-cloned into a vector, transformed into competent bacteria and individual colonies sequenced. As each colony would have originated from a single dsDNA fragment within the amplicon, only single peaks would have been observed. From sequencing large numbers of colonies, the proportion of methylated to unmethylated individual residues could be quantified. In a similar manner, pyrosequencing, which indirectly detects pyrophosphate release from incorporated nucleotides through a parallel luciferase/luminescence assay, would allow for quantification of methylated to unmethylated cytosines. Compared to MSP, pyrosequencing is more sensitive and accurate with single base pair resolution, as confirmed through comparative studies (Lee et al., 2008) and allows for exact quantification of methylation.

There has in the past few years been increasing interest towards methylation within intragenic regions of genes (i.e. within regions 3' to the ATG translation initiation codon). Methylation of intragenic DNA does not prevent transcription of genes; for example the intronic imprinting centre on the maternal allele for the imprinted murine *Igf2r* gene is methylated as are the p16^{INK4A} and p14^{ARF} genes and these are all expressed regardless of intragenic methylation (Lorincz et al., 2004). Early studies using stably expressed plasmids with differential methylation patterns (introduced *in vitro*) identified that promoter methylation alone only reduced transcription by 50%, however methylation of either the

coding region alone or of the whole plasmid reduced transcription by up to ten and two hundred fold respectively (Hsieh, 1997). Lorincz *et al* utilised a Cre/loxP based recombinase mediated cassette exchange (RMCE) system to integrate an *in vitro* methylated or unmethylated GFP gene into mouse erythroleukaemic cells (Lorincz *et al.*, 2004). This analysis revealed that intragenic methylation reduced GFP expression by ~40% but did not affect RNA Pol II binding to the 5' promoter region. Binding of Pol II to the intragenic methylated region however was reduced by half, which correlated with the same reduction in mRNA levels when compared to the unmethylated control (Lorincz *et al.*, 2004). In the unmethylated GFP region higher levels of covalently modified di- and tri-methylated Lys4 and acetylated Lys 4 and 9 on histone H3 (modifications associated with active promoters/genes) were observed when compared to the methylated gene, overall suggesting intragenic methylation reduces the efficiency of elongation but not initiation (Lorincz *et al.*, 2004; Appanah *et al.*, 2007). A more recent genome wide analysis revealed that methylation that extends into the first exon of a gene correlates highly with reduced expression, even more significantly than promoter methylation, whilst further downstream methylation towards the 3' end of a gene had little effect on expression (Brenet *et al.*, 2011). Therefore, with the increasing evidence of more than promoter methylation being critical for gene silencing, it would be of importance to assess the entire *LIMD1* gene.

Point mutation of the PU.1/Ets consensus reduced *LIMD1* promoter driven transcription by 90% (Figure 4.3). Therefore, in a clinical setting, sequencing of this motif would be indicative of *LIMD1* expression, even if the remaining *LIMD1* gene appeared non-mutated. As already discussed, this would also be indicative of downstream HIF1 α protein levels and miRNA silencing efficacy.

7.1.2 The Identification of PU.1 as an Activator of *LIMD1* Transcription May Imply a Hematopoietic Lineage Related Function of *LIMD1*

PU.1 expression is associated almost exclusively to the haematopoietic lineages, and it was for this reason endogenous protein studies were performed in the U937 human leukemic monocyte lymphoma cell line. To date, *LIMD1* protein expression or function has not been studied in hematopoietic derived cell lineages. The only exception being in this study, where *LIMD1* has been demonstrated to be expressed in U937 cells, in a PU.1 dependent manner. It would therefore be of future interest to examine expression of *LIMD1* in

hematopoietic derived lineages. From the evidence presented, it could be postulated that LIMD1 expression would mirror PU.1 expression, and as such it may be expected that expression would be high in early myeloid lineages and low/absent from the lymphoid lineages (Gallant and Gilkeson, 2006). However, the interplay of other Ets factors could alter this prediction.

PU.1 loss is a characteristic occurrence in acute myeloid leukaemia, with as little as a 20% loss in expression causing an increase in pre-leukaemic cells (Metcalf et al., 2006; Stirewalt, 2004). This would therefore raise the possibility that if LIMD1 is expressed in early myeloid lineages, PU.1 loss would also cause LIMD1 loss. This could result in a double hit for the cell; PU.1 loss would block differentiation of cells through decreased myeloid cell maturation (Dahl and Simon, 2003) and LIMD1 loss would contribute to transformation through its elucidated mechanisms, namely loss of repression of E2F driven transcription, reduced microRNA silencing, and increased HIF1 α protein expression (Sharp et al., 2004; James et al., 2010).

3p deletions are rare in haematological malignancies, with deletions reported in only 2.9% of AML, 1% of chronic myeloid leukaemias, 1.5% of acute lymphoblastic leukaemias and 1.1% of non-Hodgkin's lymphomas, with most deletions happening in association with other genetic alterations, e.g. t(9;22) translocations and deletions (Angeloni, 2007). Therefore, LIMD1 loss, if applicable in these malignancies, is likely to be indirect, potentially through PU.1 loss. This is in contrast to lung cancers, where almost half of tumours that exhibit loss of LIMD1 expression can be accounted for by chromosomal alterations (Sharp et al., 2008).

Several components of the micro RNA silencing machinery are frequently deregulated in cancers. TRBP is down-regulated due to genetic frame shift mutations in sporadic and hereditary colorectal carcinomas and cell lines with microsatellite instability, which also causes decreased levels of Dicer and mature miRNAs. Re-introduction of TRBP into these cell lines re-establishes miRNA processing and inhibits tumour growth (Melo et al., 2009). In a cohort of hepatocellular carcinomas, Dicer was found to be down-regulated in tumour tissue when compared to normal tissue (Wu et al., 2010). In NSCLC, patients with lower expression levels of *Dicer* had a significantly reduced 5 year survival rate when compared to tumours with higher levels of expression (~30% compared to ~80% respectively) (Karube et al., 2005). In ovarian cancer reduced expression of *Dicer* and *Drosha* mRNA correlated with reduced patient

survival rates (~2.5 years compared to 7-9 years for low and high expression respectively) (Merritt et al., 2008). In colorectal cancer, over expression of Dicer correlates with a decreased patient survival and progression free survival (Faber et al., 2011) and Dicer is also overexpressed atypical adenomatous hyperplasias, bronchioloalveolar carcinomas and subsequent adenocarcinomas (Chiose et al., 2007). In gastric and colorectal cancers, AGO2 and GW182 are susceptible to mutations that cause loss of expression in cancers with high microsatellite instability that reduce their expression (Kim et al., 2010b).

The loss of functional microRNA mediated silencing components is also observed in hematopoietic derived malignancies. In a proportion of multiple myelomas, AGO2 is over expressed, and shRNA mediated knockdown of AGO2 is able to induce apoptosis in H929, OCI-My5 and HL-60 myeloma cell lines as well as reduce the expression of genes involved in myeloid leukaemia development (Naoghare et al., 2011; Zhou et al., 2010). DGCR8 is observed to be down-regulated in T-cell lines and along with TRBP up-regulated in B cell malignancies (Lawrie et al., 2009). Drosha is upregulated approximately 10 fold in B cell lines when compared to normal B cells, PACT is upregulated in T cell lines and Dicer down-regulated in both B and T cell lines (Lawrie et al., 2009). In a cohort of patients suffering from primary T cell lymphomas, patients with no Dicer expression (60%) had a higher mean survival time than patients that expressed Dicer (Valencak et al., 2011). As previously described, PU.1 loss is associated with leukaemic transformation; therefore, any resultant loss of LIMD1 protein expression would also reduce miRNA mediated gene silencing, and could mimic the observations of loss of expression of other miRNA effector proteins.

Using ChIPseq, expression of miR-146a, 342, 338 and 155 that are all involved in myeloid progenitor maturation, were found to be dependent on PU.1 (Ghani et al., 2011). PU.1 also activates expression of the miR23a cluster (encoding miR23a, 27a and 24-2) that promotes myeloid over lymphoid lineage development from hematopoietic progenitor cells (Kong et al., 2010). *In vivo* it has been demonstrated that over-expression of LIMD1 enhances miRNA silencing (James et al., 2010). Thus, as PU.1 activates transcription of *LIMD1* as well as multiple microRNAs, it could be postulated that PU.1 may have a two-pronged effect with regards to facilitating miRNA induced silencing. PU.1 induces specific miRNA expression, and the efficacy of the silencing dictated by these miRNAs is then also increased through increased PU.1 mediated expression of LIMD1.

7.1.3 PU.1 and LIMD1 are Both Critical Regulators of Osteoclast Differentiation

A functional miRNA mediated gene silencing pathway is also required for osteoclastogenesis; loss of the miRNA-silencing associated proteins DGCR8, Dicer1 and Ago2 impairs osteoclast differentiation and function (Sugatani and Hruska, 2009). LIMD1 is an important component of miRNA mediated silencing (James et al., 2010) and as previously described, during RANK-L mediated osteoclast differentiation, Limd1 protein levels are up-regulated, and positively regulate osteoclast differentiation (Feng and Longmore, 2005; Feng et al., 2007). Therefore, loss of LIMD1 expression may impair osteoclast differentiation through both reduced miRNA silencing efficacy and reduced sequestosome/AP-1 activation, and this will now be elaborated upon.

PU.1 is an essential transcription factor in osteoclastogenesis, with PU.1^{-/-} mice lacking osteoclasts and suffering from osteopetrosis (Tondravi et al., 1997). miR-223 is a critical PU.1 driven miRNA for osteoclast differentiation; siRNA mediated knockdown of miR-223 allows for osteoclast development, whereas over-expression of precursor miR-223 blocked development (Sugatani and Hruska, 2007; Fukao et al., 2007). M-CSFR is expressed in osteoclast precursors, again controlled by PU.1, and is essential for osteoclast differentiation (Karsenty and Wagner, 2002). Nuclear factor 1-A (NF1-A) negatively controls expression of M-CSFR, and is not detectable in osteoclast precursors that have a functional miRNA silencing pathway; conversely in AGO2, DGCR8 or Dicer siRNA mediated knockout cells, levels of NFI-A were elevated (Sugatani and Hruska, 2009). Elevated NFI-A levels reduce M-CSFR and PU.1 protein expression and suppress osteoclast formation/bone resorption. Therefore, for osteoclast development, down-expression of NFI-A protein through a functional miRNA silencing pathway is required (Sugatani and Hruska, 2009).

From the published literature and findings within this thesis, a PU.1/LIMD1 mediated mechanism of osteoclast differentiation may be postulated. Following binding of RANK-L to RANK on the osteoclast precursor, trimerisation of the receptor leads to activation of TRAF6, which through the sequestosome causes activation of the transcription factors NFκB and AP-1, leading to increased transcription of PU.1. The increased level of PU.1 protein then leads to increased transcription of *LIMD1* (Foxler et al., 2011) and *pri-miR-223* (Fukao et al., 2007). Increased LIMD1 protein expression then facilitates the formation of the sequestosome and activation of AP-1 (Feng and Longmore, 2005; Feng et al.,

2007). Furthermore, it also enhances miRNA mediated silencing (James et al., 2010), which increases the efficacy of silencing of *NFI-A* through the PU.1 driven miR-223. This decreases the amount of NFI-A protein, leading to increased amounts of M-CSFR and PU.1, further driving a feed forward mechanism to enhance osteoclast differentiation (Figure 7.1). This postulated model may be a direction for future investigations that expands upon the initial investigations into the role of *Limd1* in osteoclastogenesis (Feng et al., 2007).

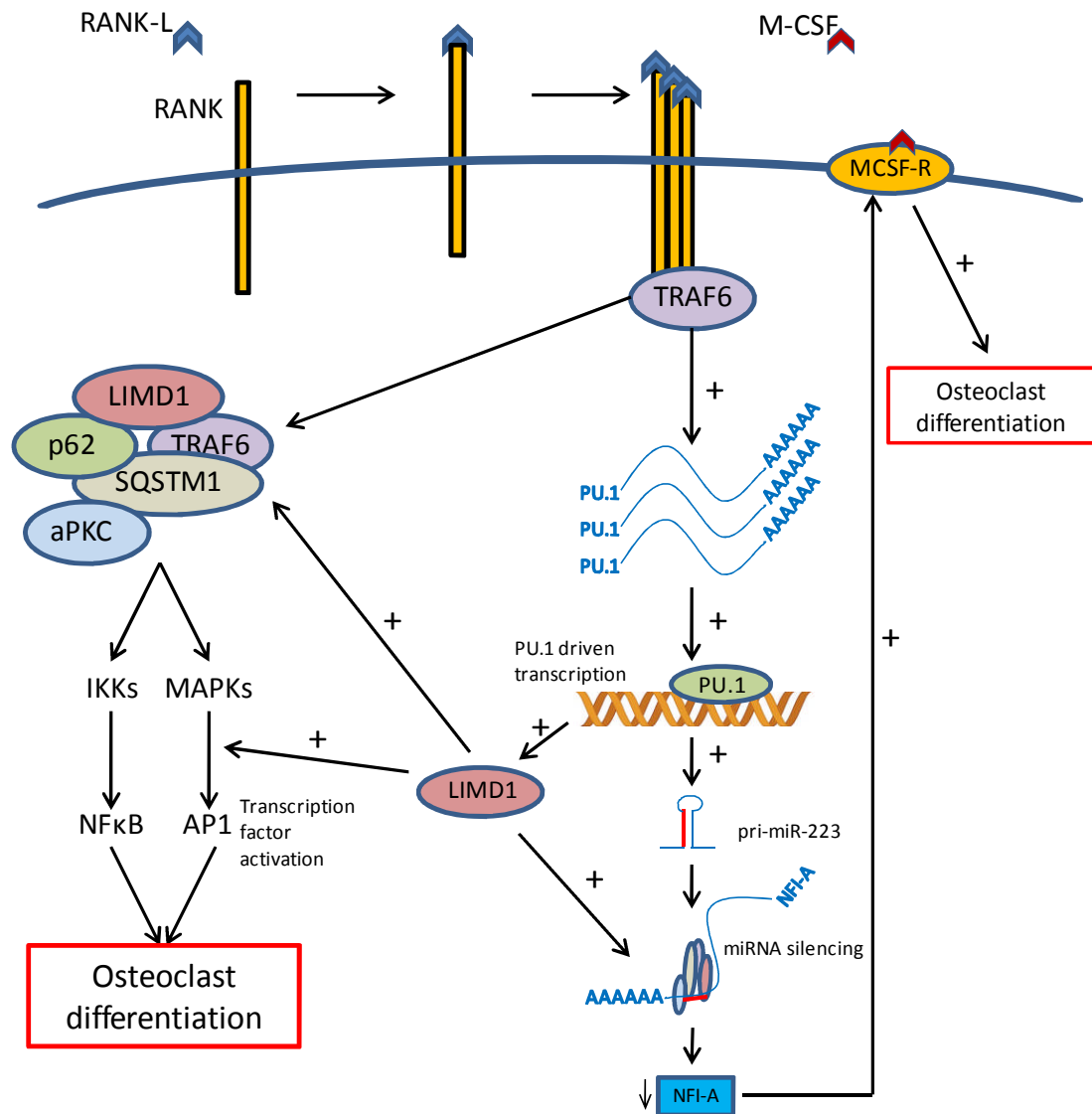


Figure 7.1: Proposed model of PU.1 and LIMD1 co-operation to enhance osteoclast differentiation. Trimerisation and activation of the RANK receptor is facilitated through binding of RANK-L on the surface of the osteoclast precursor. This leads to TRAF6 association with the sequestosome complex of proteins, which ultimately leads to NFκB and AP1 transcription factor activation and the expression of genes to promote osteoclast differentiation. Furthermore, PU.1 transcription and protein levels are also up-regulated; this leads to up-regulation of PU.1 specific miRNAs, including miR-223, as well as LIMD1. Increased LIMD1 expression enhances sequestosome formation and activation of AP1, positively influencing osteoclast differentiation. Furthermore, LIMD1 would also enhance the efficacy of PU.1 specific driven miRNA silencing. Specifically this would lead to decreased translation and expression of NFIa, a negative regulator of osteoclast differentiation. This would further increase PU.1 expression and M-CSFR, which upon M-CSF binding would further promote osteoclast differentiation.

7.1.4 Loss of LIMD1 Expression May Initiate Cell Transformation and Growth through Pathways Involving PU.1 or HIF1 α

HIF1 α contributes to the differentiation of acute myeloid leukemia cells. Induction of HIF1 α in myeloid leukemic U937 cells, either through hypoxia or chemically induced hypoxia, resulted in leukemic cell growth arrest and granulocytic differentiation. This occurs via HIF1 α transcriptional activity-independent mechanisms as depletion of endogenous HIF1 β (which would disrupt HIF1 activity) did not abrogate differentiation (Song et al., 2008). Again, from the findings presented, de-regulation of LIMD1 protein expression, either directly or indirectly through PU.1 protein de-regulation, would disrupt HIF1 α protein expression and could thus contribute to AML.

Cancer stem cells (CSC) are a subset of cells found within cancers that are able to self-renew and differentiate and are responsible for initiating and maintaining tumour growth and metastases (Gao, 2008; Gupta et al., 2009). The first identification of the existence of these cells was in acute myeloid leukaemia (Lapidot et al., 1994), and since then CSCs have been identified in brain, breast, ovarian, prostate and pancreatic cancers as well as melanomas and multiple myelomas.

HIF1 α signalling was observed to be activated in human AML and mouse lymphoma stem cells under normoxic conditions (Wang et al., 2011). In colony forming unit (cfu) experiments, depletion of endogenous HIF1 α , or inhibition with its inhibitor echinomycin within the stem cells, abrogated the ability of CSCs to form colonies and in mice eradicated transplanted human AML or lymphoma. Similarly, reduced VHL protein levels were also required for CSC function, thus further implicating the importance of HIF1 α for CSC in haematological malignancies (Wang et al., 2011). PU.1 loss is characteristic of leukemic transformation (Metcalf et al., 2006; Stirewalt, 2004), and as already discussed could lead to a decrease in LIMD1 expression. The PU.1-LIMD1 mechanics could then be applicable to the function of HIF1 α within CSCs; loss of LIMD1 expression would lead to a stabilisation and increased activity of HIF1 α , thus allowing for CSC function and tumour growth. This is an exciting possibility that adds an extra level of complexity to the formation of haematological malignancies, with the question raised of PU.1 loss as an initiating or contributing factor in the activation of CSCs.

7.2 Final Conclusions

In conclusion, the data presented in this thesis identifies *LIMD1* as being epigenetically silenced, with evidence of aberrant promoter methylation demonstrated in primary human lung tumours, providing a possible further explanation for *LIMD1* protein loss in cancer distinct from that of large genomic deletions or LOH. Furthermore, PU.1 and HIF1 α were identified as being two activating transcription factors of *LIMD1* transcription, with the former giving rise to the possibility of undiscovered haematological functions of *LIMD1*. HIF1 α enhances *LIMD1* transcription and protein expression in hypoxia, contributing to a negative regulatory pathway for HIF1 α regulation and allowing cellular adaptation to chronic hypoxia. PU.1 and HIF1 α are both deregulated in a range of cancers, and as such this work forms a platform for further investigations to elucidate novel tumour suppressive properties of *LIMD1* as a potential clinical target for novel drug design/treatment.

Chapter 8 Appendix

8.1.2 The LIMD1 Promoter Showing the Relative Positions of the confirmed PU.1 and HIF1 α Binding Sites

```

CAGGCACTTG GCATACAGAT ATGGTCAAAT GGAGTGGGAA ACCTACCACC CAACCAAACA -1930
AAAAAAAAACG CATGTTAACC AACAAATAAA TAATTATAAA TAGTTATCAG AACTGAGCAG -1870
GAAGTAAAGA GGGTGTGAA AAAGAACAAC AGGAACCACT CTGAGGAGGC CTCTAAGAGG -1810
AGGTGACTTC AGCAGGGATG GGAAAGATGA GCCACTCAGT TTAGGGGCAA GCTCTGGGCA -1750
GACACCAGGA AGCTCCTGCA GCTAGAGTGC AGGGAGGGAG GGAAGATCCC TAGATCTGGC -1690
CCAGAAGGCT GCGGCAAGGG GCCGATTCA ATTTAATTCT GGGGTAAGCA CTGAGGATTT -1630
AGGTAGAGAA GTGTCTGTTC TAGTATTGTC CTTAGGATCA CGATGGCTGT AGTGTGGGAA -1570
ATGAAACCTC TCCAGGATCG CCTGGGAAC TGTATAGGGA GTCCCGGGCC ATGCGGGGGC -1510
GCCAAGGAGT CAGGCCTGGT GTCCCTGCAG CCGCGGGAT CCACTTGCAG ATGGGTCCCT -1450
CTACGAATAA CGAGCCTACT AGGGCACGTG CTTTACTGC TGCCTGAGG ACGTAAAATG -1390
CGCGCAGGCA CAACGAGACT TTCTCTTTT TCGCTCTTTC AGAGGGCCCG GGCTCCCATC -1330
TACGCTTTGC TGTTACGTT GGCATGTTG GCATTTCCC CTCTCTGCCT CAGTCTCCC -1270
ACCTGTCAA GAGGACGGT GGCCAGCCAT GGGTGACAG CCCGTGCGCC TCTCCAATAG -1210
                                ⓄCpG Island start
TGCACCTCGG GCAAGCCGGG CGGCGGGCAC AGCCTGGACG GTGCCGGCCT CGAGAGGCAC -1150
AAAGGGCTGG CTTTCCACCG GGGAACTGA GGCAGTGGAG CGAGGAGCGG CGTCCCTCGAA -1090
AGTCCCTCGCA AACTCCAGC GCCTGTGTTG GGCCCATGCA GGCTACCCAG GCCGCCCGTC -1030
TCCGAGCGGA GGACCCGCC CAGCGCTGCC AGGGCGGGG CCGGGCTGAG GACCCGAGGC -970
TGGAAGGGAG GTCGGAGCAC CCAATTCGGT CCAGGACTCG CAGGGGGCGG CAGTGGCGGC -910
GGCGAAGTCC CGTGCAGTCC CAGTGTAGA GCGTGGGACG GACTTGTGGG GCACCCCTCG -850
GTGTTCTCCA GCCAGGCCTG GGGCAGGAG GCCAGCCAC GCTGCCGGT GCAGGCCTGC -790
CCCTGGGCGC CCGCCCGCGC GCCGTCCCG CCCCTCGGC GCCCCTCCG CCCC GGCGCGC -730
GGCTCGGGAC GTGCAGAGCC GCGAGCGAG CAGCAGGGAC TCGCCTGGC GCACTCACTT -670
                                ⓄHIF1 $\alpha$  binding site
CCGCGTCCCG CCGCCCTCCG GCCCGCGCGC GCCGATCCG CGCCGCCATC GGACAATGGG -610
ⓄPU.1 binding site
CCGCCAGCCC CAGCTGCCGT GAACTTCCTG CCGTGCTCG GCCGCCGTG CGTCCCGGAC -550
GGCGTTCTTG CCAGGCGCCG GCCGGATCG CAGTCCGGG GAAGCAGCGG AGGACCCAGC -490
GCCTGGAACG TACCTGCGCC TCAGCCGCC CGCGTTGCT CCGGCCGAC TCGCGGCCTC -430
GGCGCCCTCC CGGCCGATTC AGCTTACCC GGCCAGTCG GCTGCTGCCT TGCTGTGAGT -370
                                ⓄCpG Island end
TTCCGTGTTT GGTTCCTAA GGAGGATGT ATTTACTTT TTTGCTGTTT TCTTTTCT -310
TTTATAATTT GAAGAGGAGA AAAGAACTCC GCTGAGCAGG CCCGGGACCG CGAAGTGCCA -250
CCAGTACCC CAACAAGGAC GTCTCCAGGG GAAAGGGAGT TGGAAGCAA CTTGGTCCAG -190
CTGGCGTTGA GGTCTCAACT TCGGCTGGAC TCTAAATCC TGGGGTCATG CCCTTCACGC -130
TAGGCAGGTG GAAGTCTTTA CTTGTAAGT GCCGACTTG AGCCCCGACC CTTCGCCAGC -70
ATCTCCCCGC TGCCCTCAAC ACACACACAC ACACACACAC ACACACACAC ACACACACAC -10
ACACACACAC ACACACACAC ACACGGCACC TGGGCTAGGC CCGGACACCT GTCTGCAGCA +50
                                ⓄTranscription start site
TGATAAGTA TGACGACCTG GCCTGGAGG CCAGTAAATT CATCGAGGAC CTGAACATG +110
ⓄTranslation start site

```

Figure 8.2: The LIMD1 promoter annotated with the transcription factor binding sites identified within this thesis. Shown is the sequence of the LIMD1 promoter with the identified binding sites of the transcription factors PU.1 and HIF1 α . The CpG Island is also identified in green, along with the unconfirmed transcriptional start site and the translational start site.

8.1.3 Sequencing Chromatograms of Primary Lung Tumours that Exhibited a Change in Methylation of IR5 Compared to Matched Normal Lung Tissue

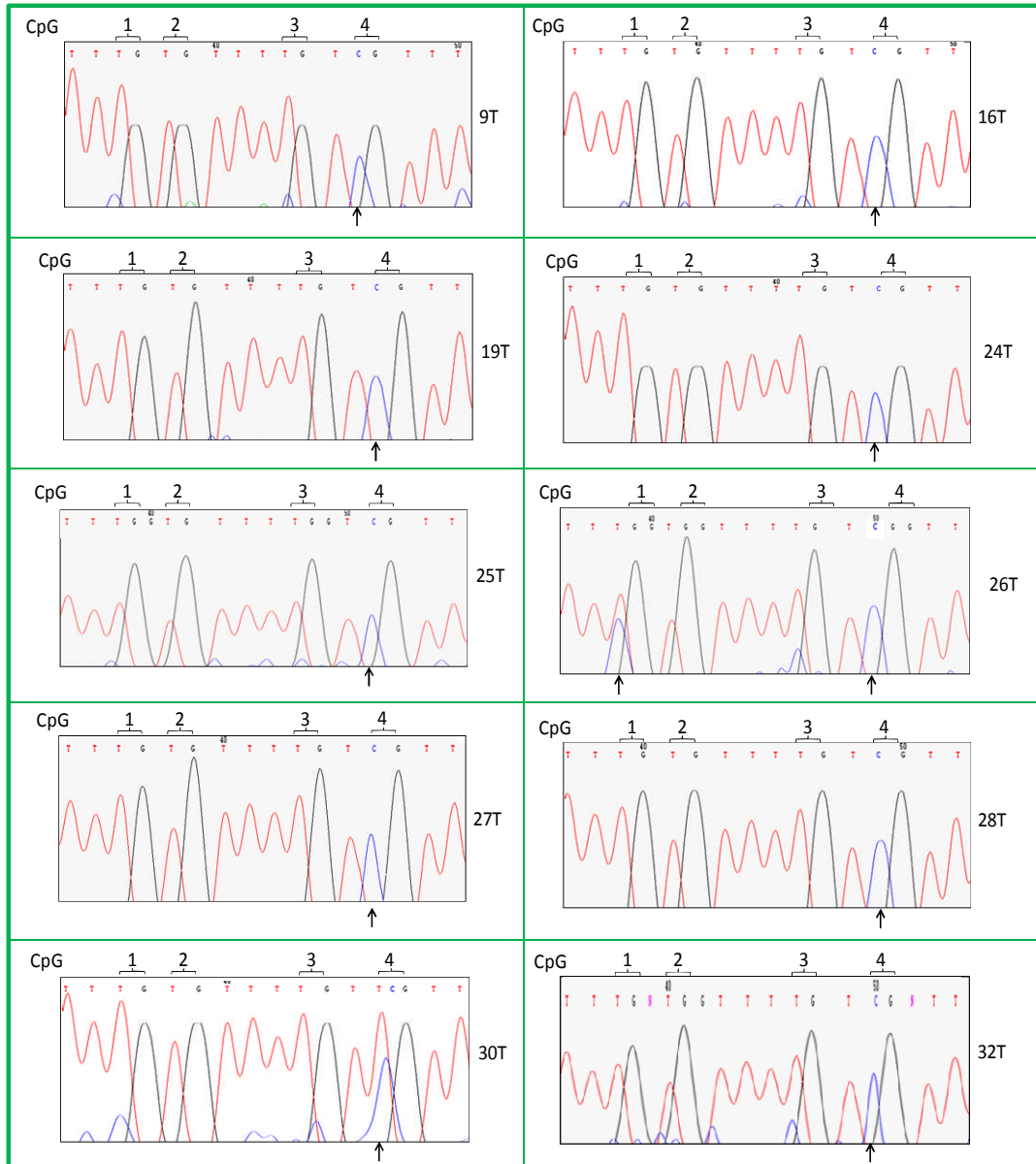
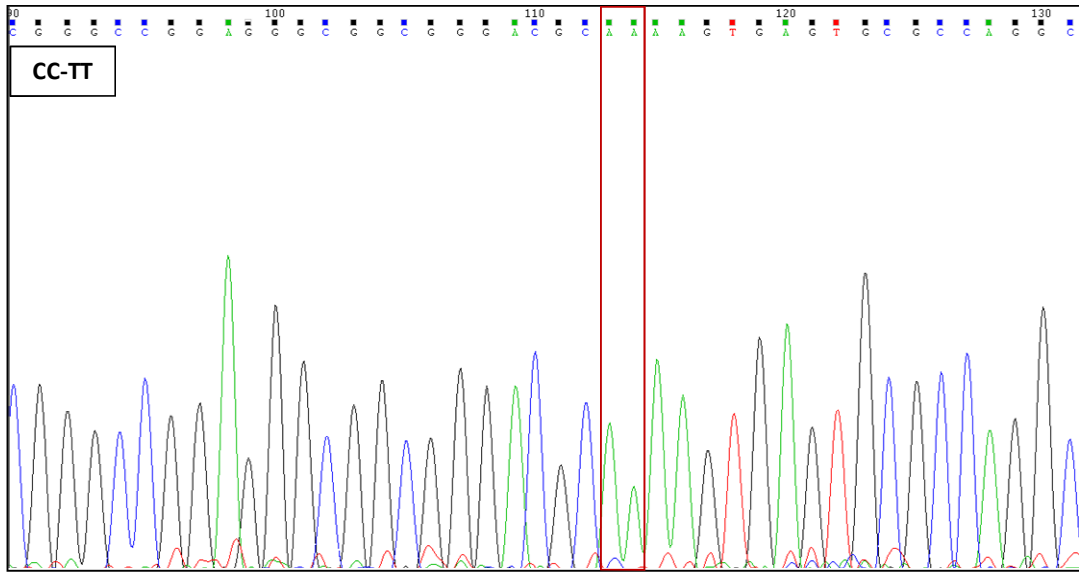


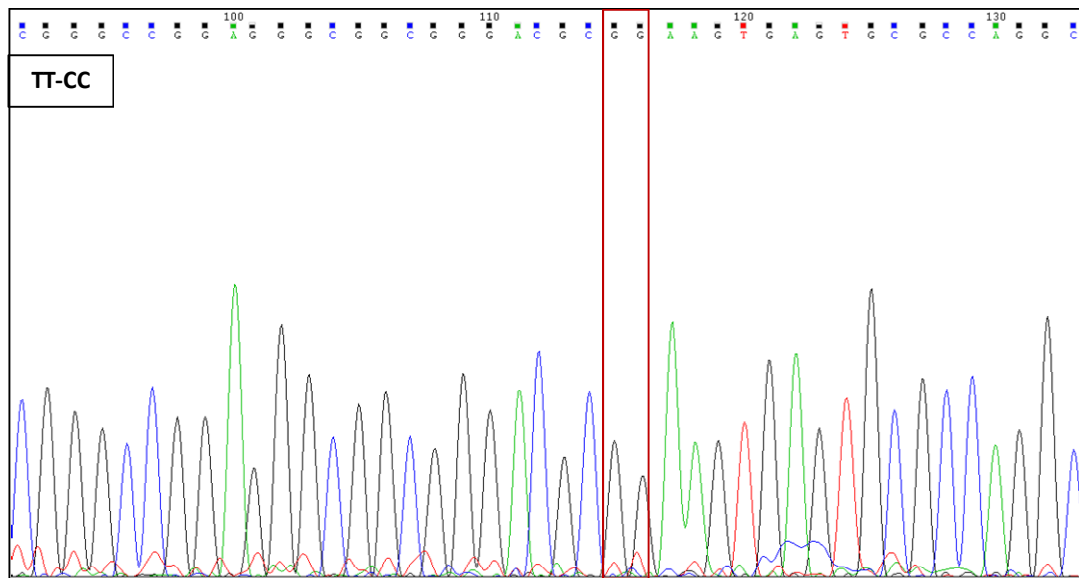
Figure 8.3 Sequencing chromatograms of primary lung tumour samples that exhibited increased promoter hypermethylation when compared to matched normal lung tissue. Genomic DNA was extracted from a cohort of primary lung tumours and matched normal tissue and IR5 bisulphite sequenced. Displayed is the sequencing chromatograms from the tumour samples that displayed hypermethylation compared to the matched control tissue. The four CpG dinucleotides within IR5 are indicated, along with the respective tumour sample number.

8.1.4 Sequencing Chromatograms of Point Mutations Created Within and Downstream of the PU.1 Binding Motif

A



B



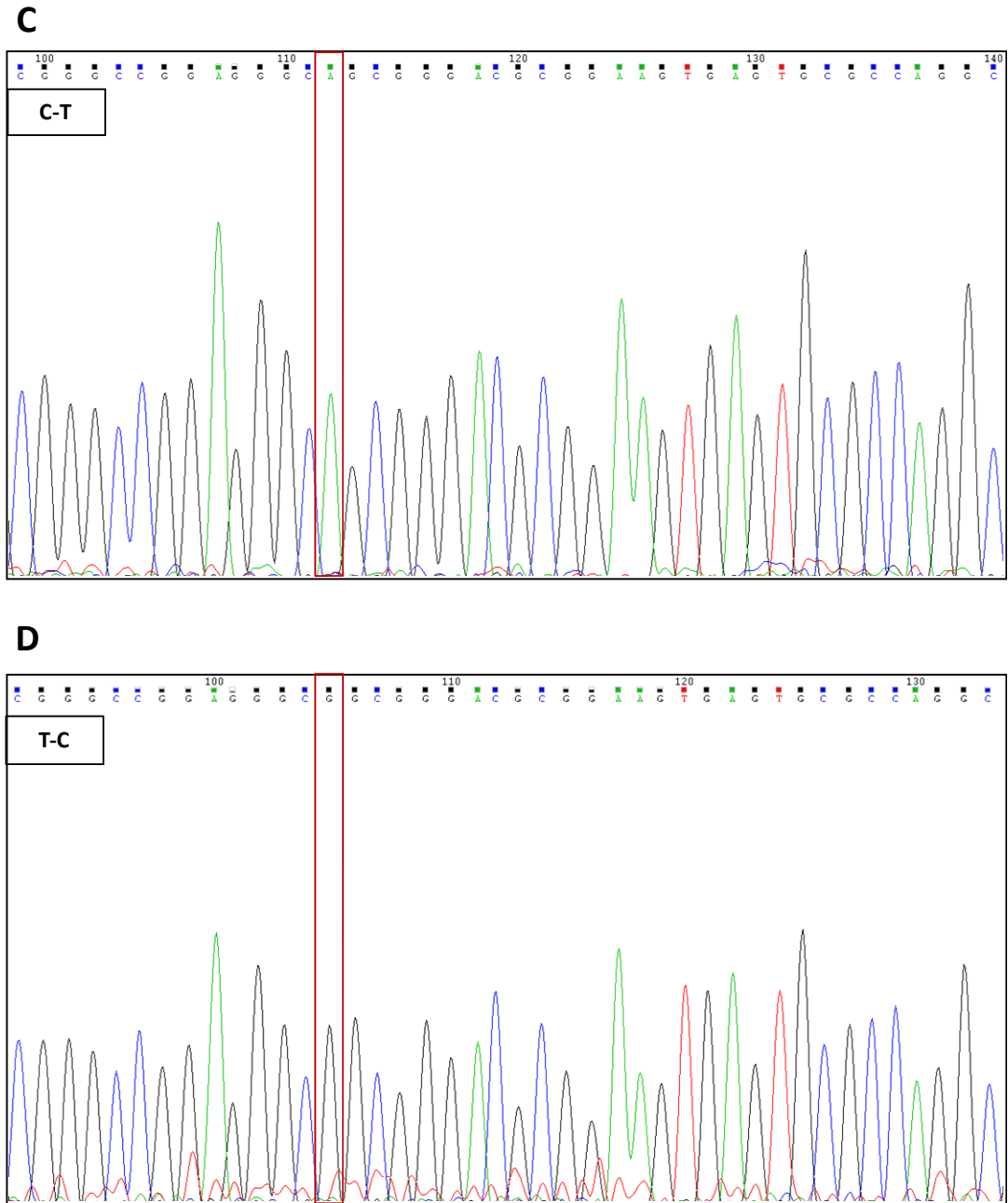


Figure 8.4: Sequencing chromatograms of the LIMD1 promoter following site directed mutagenesis of the putative PU.1 binding motif and control downstream base. In silico scrutinisation of the LIMD1 promoter for transcription factor binding motif identified a putative binding motif for the transcription factor PU.1. Site directed mutagenesis was used to mutate the motif from TTCC to TTTT along with a downstream cytosine as a control. The mutations were then reverse-mutated back to the wild-type sequence. The mutations were sequenced to confirm their identity using a reverse downstream primer, resulting in a chromatogram of the anti-sense strand read 5' to 3'. Shown are the chromatograms with the mutations identified. (A) CC-TT mutation and (B) TT-CC reversion back to wild type sequence of the PU.1 motif. (A) C-T mutation and (B) T-C reversion back to wild type sequence of a downstream cytosine as a control.

8.1.5 Sequencing chromatogram of PU.1 cDNA Sub-cloned into pcDNA4 His/Max TOPO Vector

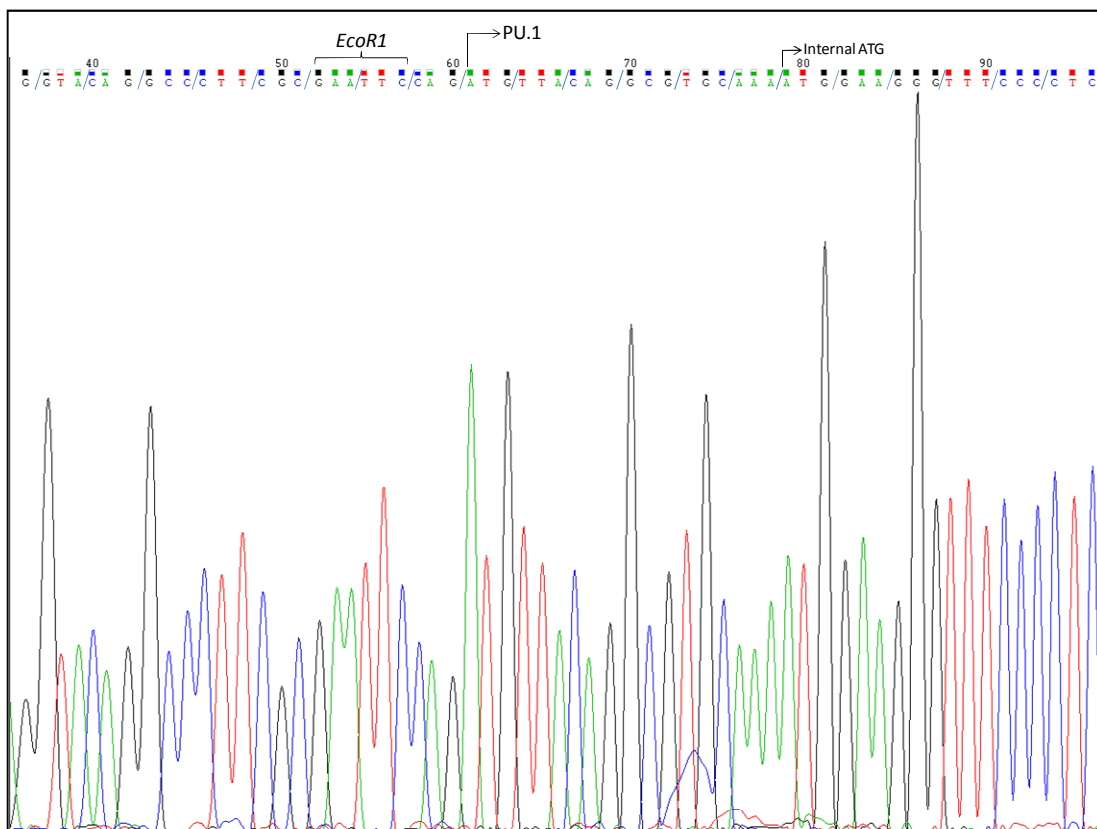
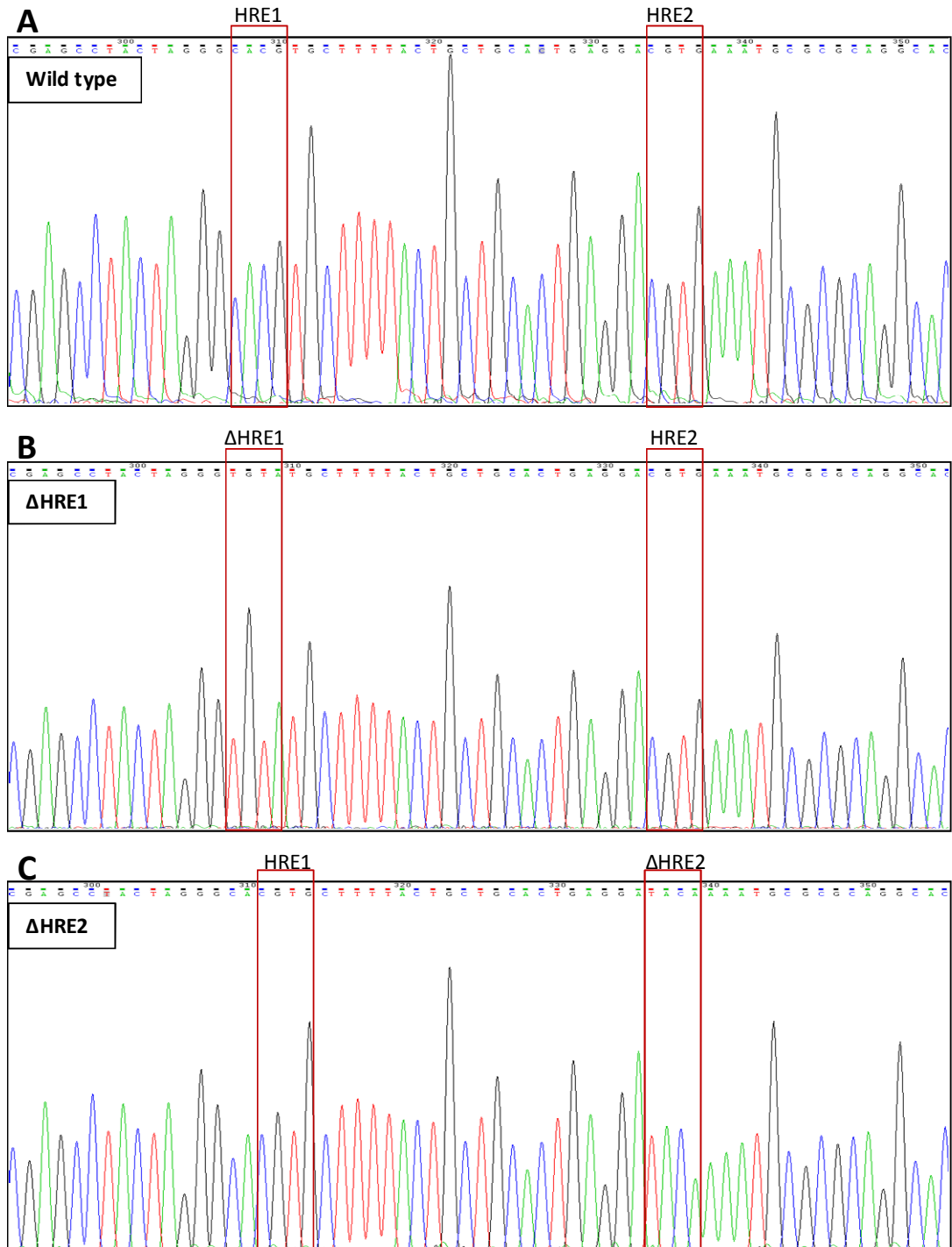


Figure 8.5: Sequencing chromatogram of pcDNA4-PU.1. PU.1 cDNA was amplified from cDNA kindly donated by A. Rizzino using primers to incorporate a 5' *EcoRI* and a 3' BamH1 restriction endonuclease site. The PCR product was then ligated into a linear pcDNA His/Max TOPO vector (Invitrogen) and the resultant plasmid sequenced with a T7 forward primer to ensure the PU.1 cDNA was of the correct sequence and was in-frame.

8.1.6 Sequencing Chromatograms of Point Mutations Created Within the putative Hypoxic Response Elements within the *LIMD1* Promoter



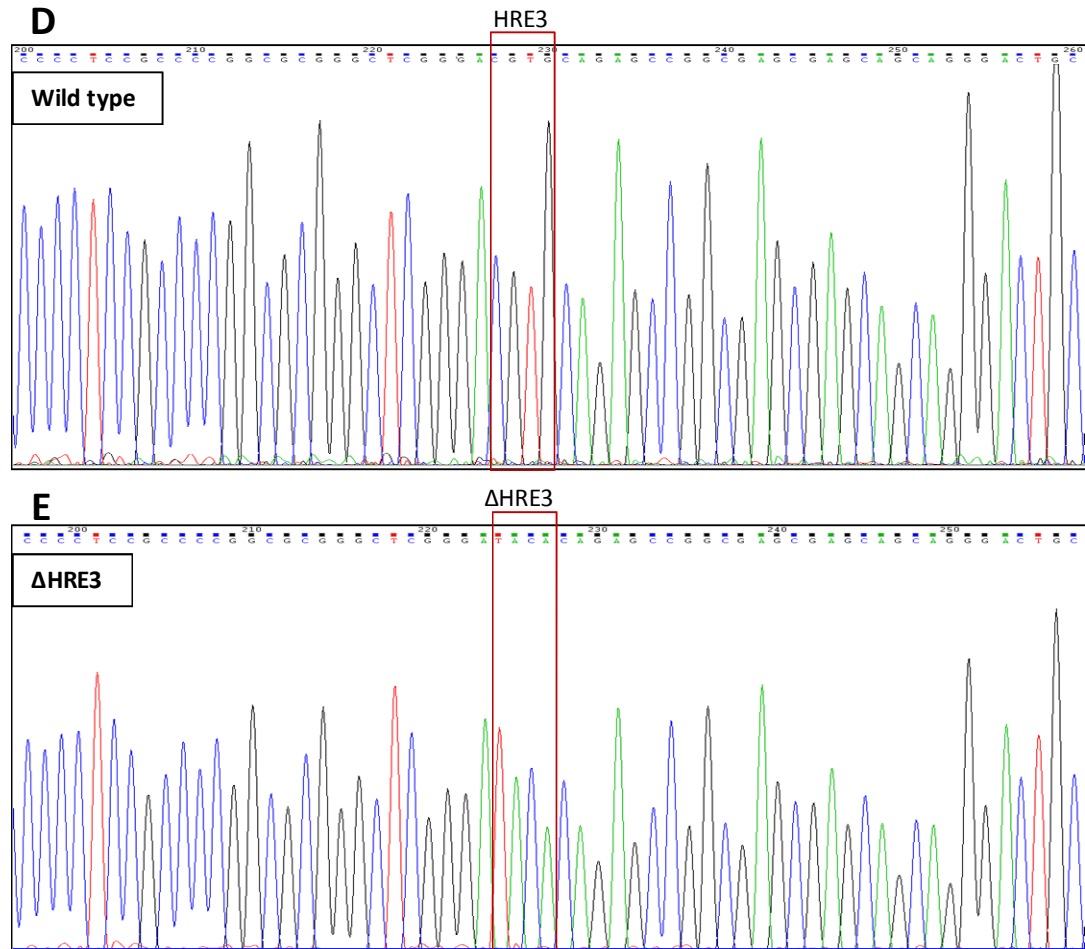


Figure 8.6: Sequencing chromatograms of the LIMD1 promoter following site directed mutagenesis of the three putative hypoxic response elements. In silico scrutinisation of the LIMD1 promoter for transcription factor binding motifs identified three putative HREs. The wild type promoter showed an increased activity in hypoxia compared to normoxia, so to identify the HRE responsible, site directed mutagenesis was used to sequentially mutate each HRE. (A) and (D) Sequencing of the wild type promoter identified the 3 HRE elements with each sequentially mutated (B) Δ HRE1, (C) Δ HRE2 and (E) Δ HRE3.

Chapter 9 Reference

Reference List

- Agathangelou,A., Honorio,S., Macartney,D.P., Martinez,A., Dallol,A., Rader,J., Fullwood,P., Chauhan,A., Walker,R., Shaw,J.A., Hosoe,S., Lerman,M.I., Minna,J.D., Maher,E.R., and Latif,F. (2001). Methylation associated inactivation of RASSF1A from region 3p21.3 in lung, breast and ovarian tumours. *Oncogene* 20, 1509-1518.
- Akazawa,H., Kudoh,S., Mochizuki,N., Takekoshi,N., Takano,H., Nagai,T., and Komuro,I. (2004). A novel LIM protein Cal promotes cardiac differentiation by association with CSX/NKX2-5. *J. Cell Biol.* 164, 395-405.
- Amsellem,V., Kryzskze,M.H., Hervy,M., Subra,F., Athman,R., Leh,H., Brachet-Ducos,C., and Auclair,C. (2005). The actin cytoskeleton-associated protein zyxin acts as a tumor suppressor in Ewing tumor cells. *Exp. Cell Res.* 304, 443-456.
- Angeloni,D. (2007). Molecular analysis of deletions in human chromosome 3p21 and the role of resident cancer genes in disease. *Brief. Funct. Genomic. Proteomic.* 6, 19-39.
- Appanah,R., Dickerson,D.R., Goyal,P., Groudine,M., and Lorincz,M.C. (2007). An unmethylated 3' promoter-proximal region is required for efficient transcription initiation. *PLoS. Genet.* 3, e27.
- Aprelikova,O., Chandramouli,G.V., Wood,M., Vasselli,J.R., Riss,J., Maranchie,J.K., Linehan,W.M., and Barrett,J.C. (2004). Regulation of HIF prolyl hydroxylases by hypoxia-inducible factors. *J. Cell Biochem.* 92, 491-501.
- Arany,Z., Huang,L.E., Eckner,R., Bhattacharya,S., Jiang,C., Goldberg,M.A., Bunn,H.F., and Livingston,D.M. (1996). An essential role for p300/CBP in the cellular response to hypoxia. *Proc. Natl. Acad. Sci. U. S. A* 93, 12969-12973.
- Ayyanathan,K., Peng,H., Hou,Z., Fredericks,W.J., Goyal,R.K., Langer,E.M., Longmore,G.D., and Rauscher,F.J., III (2007). The Ajuba LIM domain protein is a corepressor for SNAG domain mediated repression and participates in nucleocytoplasmic shuttling. *Cancer Res.* 67, 9097-9106.
- Battle,E., Sancho,E., Franci,C., Dominguez,D., Monfar,M., Baulida,J., and Garcia De,H.A. (2000). The transcription factor snail is a repressor of E-cadherin gene expression in epithelial tumour cells. *Nat. Cell Biol.* 2, 84-89.
- Baumann,M., Pontiller,J., and Ernst,W. (2010). Structure and basal transcription complex of RNA polymerase II core promoters in the mammalian genome: an overview. *Mol. Biotechnol.* 45, 241-247.
- Baylin,S.B., Fearon,E.R., Vogelstein,B., de,B.A., Sharkis,S.J., Burke,P.J., Staal,S.P., and Nelkin,B.D. (1987). Hypermethylation of the 5' region of the calcitonin gene is a property of human lymphoid and acute myeloid malignancies. *Blood* 70, 412-417.
- Beckerle,M.C. (1986). Identification of a new protein localized at sites of cell-substrate adhesion. *J. Cell Biol.* 103, 1679-1687.

- Beedanagari,S.R., Taylor,R.T., Bui,P., Wang,F., Nickerson,D.W., and Hankinson,O. (2010). Role of epigenetic mechanisms in differential regulation of the dioxin-inducible human CYP1A1 and CYP1B1 genes. *Mol. Pharmacol.* *78*, 608-616.
- Benedict,W.F., Murphree,A.L., Banerjee,A., Spina,C.A., Sparkes,M.C., and Sparkes,R.S. (1983). Patient with 13 chromosome deletion: evidence that the retinoblastoma gene is a recessive cancer gene. *Science* *219*, 973-975.
- Benita,Y., Kikuchi,H., Smith,A.D., Zhang,M.Q., Chung,D.C., and Xavier,R.J. (2009). An integrative genomics approach identifies Hypoxia Inducible Factor-1 (HIF-1)-target genes that form the core response to hypoxia. *Nucleic Acids Res.* *37*, 4587-4602.
- Berra,E., Milanini,J., Richard,D.E., Le,G.M., Vinals,F., Gothie,E., Roux,D., Pages,G., and Pouyssegur,J. (2000). Signaling angiogenesis via p42/p44 MAP kinase and hypoxia. *Biochem. Pharmacol.* *60*, 1171-1178.
- Bestor,T., Laudano,A., Mattaliano,R., and Ingram,V. (1988). Cloning and sequencing of a cDNA encoding DNA methyltransferase of mouse cells. The carboxyl-terminal domain of the mammalian enzymes is related to bacterial restriction methyltransferases. *J. Mol. Biol.* *203*, 971-983.
- Bestor,T.H. and Ingram,V.M. (1983). Two DNA methyltransferases from murine erythroleukemia cells: purification, sequence specificity, and mode of interaction with DNA. *Proc. Natl. Acad. Sci. U. S. A* *80*, 5559-5563.
- Bird,A. (2007). Perceptions of epigenetics. *Nature* *447*, 396-398.
- Bird,A., Taggart,M., Frommer,M., Miller,O.J., and Macleod,D. (1985). A fraction of the mouse genome that is derived from islands of nonmethylated, CpG-rich DNA. *Cell* *40*, 91-99.
- Bird,A.P. (1980). DNA methylation and the frequency of CpG in animal DNA. *Nucleic Acids Res.* *8*, 1499-1504.
- Bird,A.P. and Taggart,M.H. (1980). Variable patterns of total DNA and rDNA methylation in animals. *Nucleic Acids Res.* *8*, 1485-1497.
- Boffelli,D., Nobrega,M.A., and Rubin,E.M. (2004). Comparative genomics at the vertebrate extremes. *Nat. Rev. Genet.* *5*, 456-465.
- Boggs,B.A., Cheung,P., Heard,E., Spector,D.L., Chinault,A.C., and Allis,C.D. (2002). Differentially methylated forms of histone H3 show unique association patterns with inactive human X chromosomes. *Nat. Genet.* *30*, 73-76.
- Boyle,W.J., Simonet,W.S., and Lacey,D.L. (2003). Osteoclast differentiation and activation. *Nature* *423*, 337-342.
- Brandeis,M., Frank,D., Keshet,I., Siegfried,Z., Mendelsohn,M., Nemes,A., Temper,V., Razin,A., and Cedar,H. (1994). Sp1 elements protect a CpG island from de novo methylation. *Nature* *371*, 435-438.

- Brenet,F., Moh,M., Funk,P., Feierstein,E., Viale,A.J., Socci,N.D., and Scandura,J.M. (2011). DNA methylation of the first exon is tightly linked to transcriptional silencing. *PLoS. One.* 6, e14524.
- Briggs,M.R., Kadonaga,J.T., Bell,S.P., and Tjian,R. (1986). Purification and biochemical characterization of the promoter-specific transcription factor, Sp1. *Science* 234, 47-52.
- Brown,N.L., Fannon,R., Bulman,R.A., Fannon,P., Moody,J., Bouffler,S.D., and Badie,C. (2011). Sfp1/PU.1 mutations in mouse radiation-induced acute myeloid leukaemias affect mRNA and protein abundance and associate with disrupted transcription. *Leuk. Res.* 35, 126-132.
- Brugnoli,F., Lambertini,E., Varin-Blank,N., Piva,R., Marchisio,M., Grassilli,S., Miscia,S., Capitani,S., and Bertagnolo,V. (2009). Vav1 and PU.1 are recruited to the CD11b promoter in APL-derived promyelocytes: Role of Vav1 in modulating PU.1-containing complexes during ATRA-induced differentiation. *Exp. Cell Res.*
- Bruick,R.K. and McKnight,S.L. (2001). A conserved family of prolyl-4-hydroxylases that modify HIF. *Science* 294, 1337-1340.
- Burbee,D.G., Forgacs,E., Zochbauer-Muller,S., Shivakumar,L., Fong,K., Gao,B., Randle,D., Kondo,M., Virmani,A., Bader,S., Sekido,Y., Latif,F., Milchgrub,S., Toyooka,S., Gazdar,A.F., Lerman,M.I., Zbarovsky,E., White,M., and Minna,J.D. (2001). Epigenetic inactivation of RASSF1A in lung and breast cancers and malignant phenotype suppression. *J. Natl. Cancer Inst.* 93, 691-699.
- Burke,T.W. and Kadonaga,J.T. (1997). The downstream core promoter element, DPE, is conserved from *Drosophila* to humans and is recognized by TAFII60 of *Drosophila*. *Genes Dev.* 11, 3020-3031.
- Burley,S.K. and Roeder,R.G. (1996). Biochemistry and structural biology of transcription factor IID (TFIID). *Annu. Rev. Biochem.* 65, 769-799.
- Buschhausen,G., Graessmann,M., and Graessmann,A. (1985). Inhibition of herpes simplex thymidine kinase gene expression by DNA methylation is an indirect effect. *Nucleic Acids Res.* 13, 5503-5513.
- Butler,J.E. and Kadonaga,J.T. (2002). The RNA polymerase II core promoter: a key component in the regulation of gene expression. *Genes Dev.* 16, 2583-2592.
- Campbell,P.M., Bovenzi,V., and Szyf,M. (2004). Methylated DNA-binding protein 2 antisense inhibitors suppress tumourigenesis of human cancer cell lines in vitro and in vivo. *Carcinogenesis* 25, 499-507.
- Carcamo,J., Buckbinder,L., and Reinberg,D. (1991). The initiator directs the assembly of a transcription factor IID-dependent transcription complex. *Proc. Natl. Acad. Sci. U. S. A* 88, 8052-8056.
- Carcamo,J., Lobos,S., Merino,A., Buckbinder,L., Weinmann,R., Natarajan,V., and Reinberg,D. (1989). Factors involved in specific transcription by mammalian RNA polymerase II. Role of factors IID and MLTF in transcription from the adenovirus major late and IVa2 promoters. *J. Biol. Chem.* 264, 7704-7714.

- Carey, J.O., Posekany, K.J., deVente, J.E., Pettit, G.R., and Ways, D.K. (1996). Phorbol ester-stimulated phosphorylation of PU.1: association with leukemic cell growth inhibition. *Blood* *87*, 4316-4324.
- Carninci, P., Sandelin, A., Lenhard, B., Katayama, S., Shimokawa, K., Ponjavic, J., Semple, C.A., Taylor, M.S., Engstrom, P.G., Frith, M.C., Forrest, A.R., Alkema, W.B., Tan, S.L., Plessy, C., Kodzius, R., Ravasi, T., Kasukawa, T., Fukuda, S., Kanamori-Katayama, M., Kitazume, Y., Kawaji, H., Kai, C., Nakamura, M., Konno, H., Nakano, K., Mottagui-Tabar, S., Arner, P., Chesi, A., Gustincich, S., Persichetti, F., Suzuki, H., Grimmond, S.M., Wells, C.A., Orlando, V., Wahlestedt, C., Liu, E.T., Harbers, M., Kawai, J., Bajic, V.B., Hume, D.A., and Hayashizaki, Y. (2006). Genome-wide analysis of mammalian promoter architecture and evolution. *Nat. Genet.* *38*, 626-635.
- Carrero, P., Okamoto, K., Coumailleau, P., O'Brien, S., Tanaka, H., and Poellinger, L. (2000). Redox-regulated recruitment of the transcriptional coactivators CREB-binding protein and SRC-1 to hypoxia-inducible factor 1 α . *Mol. Cell Biol.* *20*, 402-415.
- Chakrabarti, S.R. and Nucifora, G. (1999). The leukemia-associated gene TEL encodes a transcription repressor which associates with SMRT and mSin3A. *Biochem. Biophys. Res. Commun.* *264*, 871-877.
- Chalkley, G.E. and Verrijzer, C.P. (1999). DNA binding site selection by RNA polymerase II TAFs: a TAF(II)250-TAF(II)150 complex recognizes the initiator. *EMBO J.* *18*, 4835-4845.
- Chan, D.A., Sutphin, P.D., Yen, S.E., and Giaccia, A.J. (2005). Coordinate regulation of the oxygen-dependent degradation domains of hypoxia-inducible factor 1 α . *Mol. Cell Biol.* *25*, 6415-6426.
- Chastre, E., Abdessamad, M., Kruglov, A., Bruyneel, E., Bracke, M., Di, G.Y., Beckerle, M.C., van, R.F., and Kotelevets, L. (2009). TRIP6, a novel molecular partner of the MAGI-1 scaffolding molecule, promotes invasiveness. *FASEB J.* *23*, 916-928.
- Chendrimada, T.P., Gregory, R.I., Kumaraswamy, E., Norman, J., Cooch, N., Nishikura, K., and Shiekhattar, R. (2005). TRBP recruits the Dicer complex to Ago2 for microRNA processing and gene silencing. *Nature* *436*, 740-744.
- Chiosea, S., Jelezcova, E., Chandran, U., Luo, J., Mantha, G., Sobol, R.W., and Dacic, S. (2007). Overexpression of Dicer in precursor lesions of lung adenocarcinoma. *Cancer Res.* *67*, 2345-2350.
- Choy, J.S., Wei, S., Lee, J.Y., Tan, S., Chu, S., and Lee, T.H. (2010). DNA methylation increases nucleosome compaction and rigidity. *J. Am. Chem. Soc.* *132*, 1782-1783.
- Clark, S.J., Harrison, J., and Molloy, P.L. (1997). Sp1 binding is inhibited by (m)Cp(m)CpG methylation. *Gene* *195*, 67-71.
- Comb, M. and Goodman, H.M. (1990). CpG methylation inhibits proenkephalin gene expression and binding of the transcription factor AP-2. *Nucleic Acids Res.* *18*, 3975-3982.
- Cook, W.D., McCaw, B.J., Herring, C., John, D.L., Foote, S.J., Nutt, S.L., and Adams, J.M. (2004). PU.1 is a suppressor of myeloid leukemia, inactivated in mice by gene deletion and mutation of its DNA binding domain. *Blood* *104*, 3437-3444.

- Cooper,D.N., Taggart,M.H., and Bird,A.P. (1983). Unmethylated domains in vertebrate DNA. *Nucleic Acids Res.* *11*, 647-658.
- Corey,S.J., Minden,M.D., Barber,D.L., Kantarjian,H., Wang,J.C., and Schimmer,A.D. (2007). Myelodysplastic syndromes: the complexity of stem-cell diseases. *Nat. Rev. Cancer* *7*, 118-129.
- Costello,J.F., Fruhwald,M.C., Smiraglia,D.J., Rush,L.J., Robertson,G.P., Gao,X., Wright,F.A., Feramisco,J.D., Peltomaki,P., Lang,J.C., Schuller,D.E., Yu,L., Bloomfield,C.D., Caligiuri,M.A., Yates,A., Nishikawa,R., Su,H.H., Petrelli,N.J., Zhang,X., O'Dorisio,M.S., Held,W.A., Cavenee,W.K., and Plass,C. (2000). Aberrant CpG-island methylation has non-random and tumour-type-specific patterns. *Nat. Genet.* *24*, 132-138.
- Cougot,N., Babajko,S., and Seraphin,B. (2004). Cytoplasmic foci are sites of mRNA decay in human cells. *J. Cell Biol.* *165*, 31-40.
- Crawford,A.W. and Beckerle,M.C. (1991). Purification and characterization of zyxin, an 82,000-dalton component of adherens junctions. *J. Biol. Chem.* *266*, 5847-5853.
- Cundy,T. and Bolland,M. (2008). Paget disease of bone. *Trends Endocrinol. Metab* *19*, 246-253.
- Dahl,R. and Simon,M.C. (2003). The importance of PU.1 concentration in hematopoietic lineage commitment and maturation. *Blood Cells Mol. Dis.* *31*, 229-233.
- Dammann,R., Li,C., Yoon,J.H., Chin,P.L., Bates,S., and Pfeifer,G.P. (2000). Epigenetic inactivation of a RAS association domain family protein from the lung tumour suppressor locus 3p21.3. *Nat. Genet.* *25*, 315-319.
- Dammann,R., Schagdarsurengin,U., Seidel,C., Strunnikova,M., Rastetter,M., Baier,K., and Pfeifer,G.P. (2005). The tumor suppressor RASSF1A in human carcinogenesis: an update. *Histol. Histopathol.* *20*, 645-663.
- Darst,R.P., Pardo,C.E., Ai,L., Brown,K.D., and Kladde,M.P. (2010). Bisulfite sequencing of DNA. *Curr. Protoc. Mol. Biol.* *Chapter 7*, Unit-17.
- Das,T.M., Feng,Y., Jagannathan,R., Seppa,M.J., Skeath,J.B., and Longmore,G.D. (2010). Ajuba LIM proteins are negative regulators of the Hippo signaling pathway. *Curr. Biol.* *20*, 657-662.
- Davis,B.N. and Hata,A. (2010). microRNA in Cancer---The involvement of aberrant microRNA biogenesis regulatory pathways. *Genes Cancer* *1*, 1100-1114.
- Dawid,I.B., Breen,J.J., and Toyama,R. (1998). LIM domains: multiple roles as adapters and functional modifiers in protein interactions. *Trends Genet.* *14*, 156-162.
- Dayan,F., Roux,D., Brahimi-Horn,M.C., Pouyssegur,J., and Mazure,N.M. (2006). The oxygen sensor factor-inhibiting hypoxia-inducible factor-1 controls expression of distinct genes through the bifunctional transcriptional character of hypoxia-inducible factor-1alpha. *Cancer Res.* *66*, 3688-3698.

- de, B.A., Nelkin, B.D., Silverman, A., Ehrlich, G., Poiesz, B., and Baylin, S.B. (1988). The short arm of chromosome 11 is a "hot spot" for hypermethylation in human neoplasia. *Proc. Natl. Acad. Sci. U. S. A* *85*, 5693-5697.
- De, S. (2011). Somatic mosaicism in healthy human tissues. *Trends Genet.* *27*, 217-223.
- Deng, S., Calin, G.A., Croce, C.M., Coukos, G., and Zhang, L. (2008). Mechanisms of microRNA deregulation in human cancer. *Cell Cycle* *7*, 2643-2646.
- Deng, W. and Roberts, S.G. (2005). A core promoter element downstream of the TATA box that is recognized by TFIIB. *Genes Dev.* *19*, 2418-2423.
- Deng, W. and Roberts, S.G. (2006). Core promoter elements recognized by transcription factor IIB. *Biochem. Soc. Trans.* *34*, 1051-1053.
- Denli, A.M., Tops, B.B., Plasterk, R.H., Ketting, R.F., and Hannon, G.J. (2004). Processing of primary microRNAs by the Microprocessor complex. *Nature* *432*, 231-235.
- Dillon, N. and Festenstein, R. (2002). Unravelling heterochromatin: competition between positive and negative factors regulates accessibility. *Trends Genet.* *18*, 252-258.
- Dong, Z., Venkatachalam, M.A., Wang, J., Patel, Y., Saikumar, P., Semenza, G.L., Force, T., and Nishiyama, J. (2001). Up-regulation of apoptosis inhibitory protein IAP-2 by hypoxia. Hif-1-independent mechanisms. *J. Biol. Chem.* *276*, 18702-18709.
- Drees, B.E., Andrews, K.M., and Beckerle, M.C. (1999). Molecular dissection of zyxin function reveals its involvement in cell motility. *J. Cell Biol.* *147*, 1549-1560.
- Dreijerink, K., Braga, E., Kuzmin, I., Geil, L., Duh, F.M., Angeloni, D., Zbar, B., Lerman, M.I., Stanbridge, E.J., Minna, J.D., Protopopov, A., Li, J., Kashuba, V., Klein, G., and Zabarovsky, E.R. (2001). The candidate tumor suppressor gene, RASSF1A, from human chromosome 3p21.3 is involved in kidney tumorigenesis. *Proc. Natl. Acad. Sci. U. S. A* *98*, 7504-7509.
- Dynan, W.S., Saffer, J.D., Lee, W.S., and Tjian, R. (1985). Transcription factor Sp1 recognizes promoter sequences from the monkey genome that are simian virus 40 promoter. *Proc. Natl. Acad. Sci. U. S. A* *82*, 4915-4919.
- Dynan, W.S. and Tjian, R. (1983). The promoter-specific transcription factor Sp1 binds to upstream sequences in the SV40 early promoter. *Cell* *35*, 79-87.
- Ebert, B.L. and Bunn, H.F. (1998). Regulation of transcription by hypoxia requires a multiprotein complex that includes hypoxia-inducible factor 1, an adjacent transcription factor, and p300/CREB binding protein. *Mol. Cell Biol.* *18*, 4089-4096.
- Egger, G., Liang, G., Aparicio, A., and Jones, P.A. (2004). Epigenetics in human disease and prospects for epigenetic therapy. *Nature* *429*, 457-463.
- Ehrlich, M., Gama-Sosa, M.A., Huang, L.H., Midgett, R.M., Kuo, K.C., McCune, R.A., and Gehrke, C. (1982). Amount and distribution of 5-methylcytosine in human DNA from different types of tissues of cells. *Nucleic Acids Res.* *10*, 2709-2721.
- Ehrlich, M. and Wang, R.Y. (1981). 5-Methylcytosine in eukaryotic DNA. *Science* *212*, 1350-1357.

- Eisenbeis,C.F., Singh,H., and Storb,U. (1995). Pip, a novel IRF family member, is a lymphoid-specific, PU.1-dependent transcriptional activator. *Genes Dev.* *9*, 1377-1387.
- Epstein,A.C., Gleadle,J.M., McNeill,L.A., Hewitson,K.S., O'Rourke,J., Mole,D.R., Mukherji,M., Metzen,E., Wilson,M.I., Dhanda,A., Tian,Y.M., Masson,N., Hamilton,D.L., Jaakkola,P., Barstead,R., Hodgkin,J., Maxwell,P.H., Pugh,C.W., Schofield,C.J., and Ratcliffe,P.J. (2001). C. elegans EGL-9 and mammalian homologs define a family of dioxygenases that regulate HIF by prolyl hydroxylation. *Cell* *107*, 43-54.
- Eriksen,E.F. (2010). Cellular mechanisms of bone remodeling. *Rev. Endocr. Metab Disord.* *11*, 219-227.
- Esteller,M. (2007). Epigenetic gene silencing in cancer: the DNA hypermethylome. *Hum. Mol. Genet.* *16 Spec No 1*, R50-R59.
- Esteve,P.O., Chin,H.G., and Pradhan,S. (2007). Molecular mechanisms of transactivation and doxorubicin-mediated repression of survivin gene in cancer cells. *J. Biol. Chem.* *282*, 2615-2625.
- Eulalio,A., Behm-Ansmant,I., Schweizer,D., and Izaurralde,E. (2007). P-body formation is a consequence, not the cause, of RNA-mediated gene silencing. *Mol. Cell Biol.* *27*, 3970-3981.
- Eulalio,A., Huntzinger,E., and Izaurralde,E. (2008). Getting to the root of miRNA-mediated gene silencing. *Cell* *132*, 9-14.
- Evans,R., Fairley,J.A., and Roberts,S.G. (2001). Activator-mediated disruption of sequence-specific DNA contacts by the general transcription factor TFIIB. *Genes Dev.* *15*, 2945-2949.
- Eystathioy,T., Chan,E.K., Tenenbaum,S.A., Keene,J.D., Griffith,K., and Fritzler,M.J. (2002). A phosphorylated cytoplasmic autoantigen, GW182, associates with a unique population of human mRNAs within novel cytoplasmic speckles. *Mol. Biol. Cell* *13*, 1338-1351.
- Faber,C., Horst,D., Hlubek,F., and Kirchner,T. (2011). Overexpression of Dicer predicts poor survival in colorectal cancer. *Eur. J. Cancer.*
- Feng,Y. and Longmore,G.D. (2005). The LIM protein Ajuba influences interleukin-1-induced NF-kappaB activation by affecting the assembly and activity of the protein kinase Czeta/p62/TRAF6 signaling complex. *Mol. Cell Biol.* *25*, 4010-4022.
- Feng,Y., Zhao,H., Luderer,H.F., Epple,H., Faccio,R., Ross,F.P., Teitelbaum,S.L., and Longmore,G.D. (2007). The LIM protein, Limd1, regulates AP-1 activation through an interaction with Traf6 to influence osteoclast development. *J Biol. Chem.* *282*, 39-48.
- Filipowicz,W., Bhattacharyya,S.N., and Sonenberg,N. (2008). Mechanisms of post-transcriptional regulation by microRNAs: are the answers in sight? *Nat. Rev. Genet.* *9*, 102-114.
- Flori,A.R., Steinhoff,C., Muller,M., Seifert,H.H., Hader,C., Engers,R., Ackermann,R., and Schulz,W.A. (2004). Coordinate hypermethylation at specific genes in prostate carcinoma precedes LINE-1 hypomethylation. *Br. J. Cancer* *91*, 985-994.

- Forsythe, J.A., Jiang, B.H., Iyer, N.V., Agani, F., Leung, S.W., Koos, R.D., and Semenza, G.L. (1996). Activation of vascular endothelial growth factor gene transcription by hypoxia-inducible factor 1. *Mol. Cell Biol.* *16*, 4604-4613.
- Foxler, D.E., James, V., Shelton, S.J., Vallim, T.Q., Shaw, P.E., and Sharp, T.V. (2011). PU.1 is a major transcriptional activator of the tumour suppressor gene LIMD1. *FEBS Lett.* *585*, 1089-1096.
- Fradelizi, J., Noireaux, V., Plastino, J., Menichi, B., Louvard, D., Sykes, C., Golsteyn, R.M., and Friederich, E. (2001). ActA and human zyxin harbour Arp2/3-independent actin-polymerization activity. *Nat. Cell Biol.* *3*, 699-707.
- Fraley, S.I., Feng, Y., Krishnamurthy, R., Kim, D.H., Celedon, A., Longmore, G.D., and Wirtz, D. (2010). A distinctive role for focal adhesion proteins in three-dimensional cell motility. *Nat. Cell Biol.* *12*, 598-604.
- Freyd, G., Kim, S.K., and Horvitz, H.R. (1990). Novel cysteine-rich motif and homeodomain in the product of the *Caenorhabditis elegans* cell lineage gene *lin-11*. *Nature* *344*, 876-879.
- Fujita, N., Shimotake, N., Ohki, I., Chiba, T., Saya, H., Shirakawa, M., and Nakao, M. (2000). Mechanism of transcriptional regulation by methyl-CpG binding protein MBD1. *Mol. Cell Biol.* *20*, 5107-5118.
- Fujita, N., Watanabe, S., Ichimura, T., Tsuruzoe, S., Shinkai, Y., Tachibana, M., Chiba, T., and Nakao, M. (2003). Methyl-CpG binding domain 1 (MBD1) interacts with the Suv39h1-HP1 heterochromatic complex for DNA methylation-based transcriptional repression. *J. Biol. Chem.* *278*, 24132-24138.
- Fukao, T., Fukuda, Y., Kiga, K., Sharif, J., Hino, K., Enomoto, Y., Kawamura, A., Nakamura, K., Takeuchi, T., and Tanabe, M. (2007). An evolutionarily conserved mechanism for microRNA-223 expression revealed by microRNA gene profiling. *Cell* *129*, 617-631.
- Fuks, F., Hurd, P.J., Wolf, D., Nan, X., Bird, A.P., and Kouzarides, T. (2003). The methyl-CpG-binding protein MeCP2 links DNA methylation to histone methylation. *J. Biol. Chem.* *278*, 4035-4040.
- Futscher, B.W., Oshiro, M.M., Wozniak, R.J., Holtan, N., Hanigan, C.L., Duan, H., and Domann, F.E. (2002). Role for DNA methylation in the control of cell type specific maspin expression. *Nat. Genet.* *31*, 175-179.
- Gaber, T., Dziurla, R., Tripmacher, R., Burmester, G.R., and Buttgereit, F. (2005). Hypoxia inducible factor (HIF) in rheumatology: low O₂! See what HIF can do! *Ann. Rheum. Dis.* *64*, 971-980.
- Gagnon, J., Shaker, S., Primeau, M., Hurtubise, A., and Momparler, R.L. (2003). Interaction of 5-aza-2'-deoxycytidine and depsipeptide on antineoplastic activity and activation of 14-3-3sigma, E-cadherin and tissue inhibitor of metalloproteinase 3 expression in human breast carcinoma cells. *Anticancer Drugs* *14*, 193-202.
- Gallant, S. and Gilkeson, G. (2006). ETS transcription factors and regulation of immunity. *Arch. Immunol. Ther. Exp. (Warsz.)* *54*, 149-163.

- Gama-Sosa, M.A., Slagel, V.A., Trewyn, R.W., Oxenhandler, R., Kuo, K.C., Gehrke, C.W., and Ehrlich, M. (1983). The 5-methylcytosine content of DNA from human tumors. *Nucleic Acids Res.* *11*, 6883-6894.
- Gao, J.X. (2008). Cancer stem cells: the lessons from pre-cancerous stem cells. *J. Cell Mol. Med.* *12*, 67-96.
- Garcia-Ramirez, M., Rocchini, C., and Ausio, J. (1995). Modulation of chromatin folding by histone acetylation. *J. Biol. Chem.* *270*, 17923-17928.
- Gardiner-Garden, M. and Frommer, M. (1987). CpG islands in vertebrate genomes. *J. Mol. Biol.* *196*, 261-282.
- Garnis, C., Baldwin, C., Zhang, L., Rosin, M.P., and Lam, W.L. (2003). Use of complete coverage array comparative genomic hybridization to define copy number alterations on chromosome 3p in oral squamous cell carcinomas. *Cancer Res.* *63*, 8582-8585.
- Gershenzon, N.I. and Ioshikhes, I.P. (2005). Synergy of human Pol II core promoter elements revealed by statistical sequence analysis. *Bioinformatics.* *21*, 1295-1300.
- Ghani, S., Riemke, P., Schonheit, J., Lenze, D., Stumm, J., Hoogenkamp, M., Lagendijk, A., Heinz, S., Bonifer, C., Bakkers, J., Abdelilah-Seyfried, S., Hummel, M., and Rosenbauer, F. (2011). Macrophage development from HSCs requires PU.1-coordinated microRNA expression. *Blood* *118*, 2275-2284.
- Ghosh, S., Ghosh, A., Maiti, G.P., Alam, N., Roy, A., Roy, B., Roychoudhury, S., and Panda, C.K. (2008). Alterations of 3p21.31 tumor suppressor genes in head and neck squamous cell carcinoma: Correlation with progression and prognosis. *Int. J Cancer* *123*, 2594-2604.
- Ghosh, S., Ghosh, A., Maiti, G.P., Mukherjee, N., Dutta, S., Roy, A., Roychoudhury, S., and Panda, C.K. (2010). LIMD1 is more frequently altered than RB1 in head and neck squamous cell carcinoma: clinical and prognostic implications. *Mol. Cancer* *9*, 58.
- Gidoni, D., Kadonaga, J.T., Barrera-Saldana, H., Takahashi, K., Chambon, P., and Tjian, R. (1985). Bidirectional SV40 transcription mediated by tandem Sp1 binding interactions. *Science* *230*, 511-517.
- Ginouves, A., Ilc, K., Macias, N., Pouyssegur, J., and Berra, E. (2008). PHDs overactivation during chronic hypoxia "desensitizes" HIF α and protects cells from necrosis. *Proc. Natl. Acad. Sci. U. S. A* *105*, 4745-4750.
- Goelz, S.E., Vogelstein, B., Hamilton, S.R., and Feinberg, A.P. (1985). Hypomethylation of DNA from benign and malignant human colon neoplasms. *Science* *228*, 187-190.
- Goldberg, M.A., Dunning, S.P., and Bunn, H.F. (1988). Regulation of the erythropoietin gene: evidence that the oxygen sensor is a heme protein. *Science* *242*, 1412-1415.
- Goll, M.G., Kirpekar, F., Maggert, K.A., Yoder, J.A., Hsieh, C.L., Zhang, X., Golic, K.G., Jacobsen, S.E., and Bestor, T.H. (2006). Methylation of tRNA^{Asp} by the DNA methyltransferase homolog Dnmt2. *Science* *311*, 395-398.

- Gottardi,C.J., Wong,E., and Gumbiner,B.M. (2001). E-cadherin suppresses cellular transformation by inhibiting beta-catenin signaling in an adhesion-independent manner. *J. Cell Biol.* *153*, 1049-1060.
- Goyal,R.K., Lin,P., Kanungo,J., Payne,A.S., Muslin,A.J., and Longmore,G.D. (1999). Ajuba, a novel LIM protein, interacts with Grb2, augments mitogen-activated protein kinase activity in fibroblasts, and promotes meiotic maturation of *Xenopus* oocytes in a Grb2- and Ras-dependent manner. *Mol. Cell Biol.* *19*, 4379-4389.
- Gradin,K., McGuire,J., Wenger,R.H., Kvietikova,I., fhitelaw,M.L., Toftgard,R., Tora,L., Gassmann,M., and Poellinger,L. (1996). Functional interference between hypoxia and dioxin signal transduction pathways: competition for recruitment of the Arnt transcription factor. *Mol. Cell Biol.* *16*, 5221-5231.
- Grana,X., Garriga,J., and Mayol,X. (1998). Role of the retinoblastoma protein family, pRB, p107 and p130 in the negative control of cell growth. *Oncogene* *17*, 3365-3383.
- Graven,K.K., Yu,Q., Pan,D., Roncarati,J.S., and Farber,H.W. (1999). Identification of an oxygen responsive enhancer element in the glyceraldehyde-3-phosphate dehydrogenase gene. *Biochim. Biophys. Acta* *1447*, 208-218.
- Greenblatt,J. (1991). Roles of TFIID in transcriptional initiation by RNA polymerase II. *Cell* *66*, 1067-1070.
- Greijer,A.E. and van der Wall,E. (2004). The role of hypoxia inducible factor 1 (HIF-1) in hypoxia induced apoptosis. *J. Clin. Pathol.* *57*, 1009-1014.
- Gross,S.A., Zheng,J.H., Le,A.T., Kerzic,P.J., and Irons,R.D. (2006). PU.1 phosphorylation correlates with hydroquinone-induced alterations in myeloid differentiation and cytokine-dependent clonogenic response in human CD34(+) hematopoietic progenitor cells. *Cell Biol. Toxicol.* *22*, 229-241.
- Grummt,I. (2003). Life on a planet of its own: regulation of RNA polymerase I transcription in the nucleolus. *Genes Dev.* *17*, 1691-1702.
- Guo,B., Sallis,R.E., Greenall,A., Petit,M.M., Jansen,E., Young,L., Van de Ven,W.J., and Sharrocks,A.D. (2006). The LIM domain protein LPP is a coactivator for the ETS domain transcription factor PEA3. *Mol. Cell Biol.* *26*, 4529-4538.
- Guo,K., Searfoss,G., Krolikowski,D., Pagnoni,M., Franks,C., Clark,K., Yu,K.T., Jaye,M., and Ivashchenko,Y. (2001). Hypoxia induces the expression of the pro-apoptotic gene BNIP3. *Cell Death. Differ.* *8*, 367-376.
- Gupta,P.B., Chaffer,C.L., and Weinberg,R.A. (2009). Cancer stem cells: mirage or reality? *Nat. Med.* *15*, 1010-1012.
- Hagen,T., Taylor,C.T., Lam,F., and Moncada,S. (2003). Redistribution of intracellular oxygen in hypoxia by nitric oxide: effect on HIF1alpha. *Science* *302*, 1975-1978.
- Hagg,M. and Wennstrom,S. (2005). Activation of hypoxia-induced transcription in normoxia. *Exp. Cell Res.* *306*, 180-191.

- Hamdorf,M., Berger,A., Schule,S., Reinhardt,J., and Flory,E. (2011). PKCdelta-induced PU.1 phosphorylation promotes hematopoietic stem cell differentiation to dendritic cells. *Stem Cells* 29, 297-306.
- Han,J., Lee,Y., Yeom,K.H., Kim,Y.K., Jin,H., and Kim,V.N. (2004). The Drosha-DGCR8 complex in primary microRNA processing. *Genes Dev.* 18, 3016-3027.
- Harrington,E.A., Bruce,J.L., Harlow,E., and Dyson,N. (1998). pRB plays an essential role in cell cycle arrest induced by DNA damage. *Proc. Natl. Acad. Sci. U. S. A* 95, 11945-11950.
- Harrington,M.A., Jones,P.A., Imagawa,M., and Karin,M. (1988). Cytosine methylation does not affect binding of transcription factor Sp1. *Proc. Natl. Acad. Sci. U. S. A* 85, 2066-2070.
- Heard,E. (2004). Recent advances in X-chromosome inactivation. *Curr. Opin. Cell Biol.* 16, 247-255.
- Hegde,S., Ni,S., He,S., Yoon,D., Feng,G.S., Watowich,S.S., Paulson,R.F., and Hankey,P.A. (2009). Stat3 promotes the development of erythroleukemia by inducing Pu.1 expression and inhibiting erythroid differentiation. *Oncogene* 28, 3349-3359.
- Heinz,S., Benner,C., Spann,N., Bertolino,E., Lin,Y.C., Laslo,P., Cheng,J.X., Murre,C., Singh,H., and Glass,C.K. (2010). Simple combinations of lineage-determining transcription factors prime cis-regulatory elements required for macrophage and B cell identities. *Mol. Cell* 38, 576-589.
- Hendrich,B., Hardeland,U., Ng,H.H., Jiricny,J., and Bird,A. (1999). The thymine glycosylase MBD4 can bind to the product of deamination at methylated CpG sites. *Nature* 401, 301-304.
- Hesson,L.B., Cooper,W.N., and Latif,F. (2007). Evaluation of the 3p21.3 tumour-suppressor gene cluster. *Oncogene* 26, 7283-7301.
- Hewitson,K.S., McNeill,L.A., Riordan,M.V., Tian,Y.M., Bullock,A.N., Welford,R.W., Elkins,J.M., Oldham,N.J., Bhattacharya,S., Gleadle,J.M., Ratcliffe,P.J., Pugh,C.W., and Schofield,C.J. (2002). Hypoxia-inducible factor (HIF) asparagine hydroxylase is identical to factor inhibiting HIF (FIH) and is related to the cupin structural family. *J. Biol. Chem.* 277, 26351-26355.
- Hoffman,L.M., Jensen,C.C., Kloeker,S., Wang,C.L., Yoshigi,M., and Beckerle,M.C. (2006). Genetic ablation of zyxin causes Mena/VASP mislocalization, increased motility, and deficits in actin remodeling. *J. Cell Biol.* 172, 771-782.
- Hogg,R.P., Honorio,S., Martinez,A., Agathangelou,A., Dallol,A., Fullwood,P., Weichselbaum,R., Kuo,M.J., Maher,E.R., and Latif,F. (2002). Frequent 3p allele loss and epigenetic inactivation of the RASSF1A tumour suppressor gene from region 3p21.3 in head and neck squamous cell carcinoma. *Eur. J. Cancer* 38, 1585-1592.
- Hollenhorst,P.C., Jones,D.A., and Graves,B.J. (2004). Expression profiles frame the promoter specificity dilemma of the ETS family of transcription factors. *Nucleic Acids Res.* 32, 5693-5702.

- Hollenhorst,P.C., Shah,A.A., Hopkins,C., and Graves,B.J. (2007). Genome-wide analyses reveal properties of redundant and specific promoter occupancy within the ETS gene family. *Genes Dev.* *21*, 1882-1894.
- Hsieh,C.L. (1997). Stability of patch methylation and its impact in regions of transcriptional initiation and elongation. *Mol. Cell Biol.* *17*, 5897-5904.
- Hsu,T., Trojanowska,M., and Watson,D.K. (2004). Ets proteins in biological control and cancer. *J. Cell Biochem.* *91*, 896-903.
- Huang,L.E., Arany,Z., Livingston,D.M., and Bunn,H.F. (1996). Activation of hypoxia-inducible transcription factor depends primarily upon redox-sensitive stabilization of its alpha subunit. *J. Biol. Chem.* *271*, 32253-32259.
- Huang,L.E., Gu,J., Schau,M., and Bunn,H.F. (1998). Regulation of hypoxia-inducible factor 1alpha is mediated by an O₂-dependent degradation domain via the ubiquitin-proteasome pathway. *Proc. Natl. Acad. Sci. U. S. A* *95*, 7987-7992.
- Hubbi,M.E., Luo,W., Baek,J.H., and Semenza,G.L. (2011). MCM proteins are negative regulators of hypoxia-inducible factor 1. *Mol. Cell* *42*, 700-712.
- Huggins,C.J. and Andrusis,I.L. (2008). Cell cycle regulated phosphorylation of LIMD1 in cell lines and expression in human breast cancers. *Cancer Lett.* *267*, 55-66.
- Illingworth,R.S. and Bird,A.P. (2009). CpG islands--'a rough guide'. *FEBS Lett.* *583*, 1713-1720.
- Imataka,H., Sogawa,K., Yasumoto,K., Kikuchi,Y., Sasano,K., Kobayashi,A., Hayami,M., and Fujii-Kuriyama,Y. (1992). Two regulatory proteins that bind to the basic transcription element (BTE), a GC box sequence in the promoter region of the rat P-4501A1 gene. *EMBO J.* *11*, 3663-3671.
- Imreh,S., Kost-Alimova,M., Kholodnyuk,I., Yang,Y., Szeles,A., Kiss,H., Liu,Y., Foster,K., Zabarovsky,E., Stanbridge,E., and Klein,G. (1997). Differential elimination of 3p and retention of 3q segments in human/mouse microcell hybrids during tumor growth. *Genes Chromosomes. Cancer* *20*, 224-233.
- Ivan,M., Kondo,K., Yang,H., Kim,W., Valiando,J., Ohh,M., Salic,A., Asara,J.M., Lane,W.S., and Kaelin,W.G., Jr. (2001). HIFalpha targeted for VHL-mediated destruction by proline hydroxylation: implications for O₂ sensing. *Science* *292*, 464-468.
- Iyer,N.G., Ozdag,H., and Caldas,C. (2004). p300/CBP and cancer. *Oncogene* *23*, 4225-4231.
- Iyer,N.V., Kotch,L.E., Agani,F., Leung,S.W., Laughner,E., Wenger,R.H., Gassmann,M., Gearhart,J.D., Lawler,A.M., Yu,A.Y., and Semenza,G.L. (1998). Cellular and developmental control of O₂ homeostasis by hypoxia-inducible factor 1 alpha. *Genes Dev.* *12*, 149-162.
- Jaakkola,P., Mole,D.R., Tian,Y.M., Wilson,M.I., Gielbert,J., Gaskell,S.J., Kriegsheim,A., Hebestreit,H.F., Mukherji,M., Schofield,C.J., Maxwell,P.H., Pugh,C.W., and Ratcliffe,P.J. (2001). Targeting of HIF-alpha to the von Hippel-Lindau ubiquitylation complex by O₂-regulated prolyl hydroxylation. *Science* *292*, 468-472.

- James,V., Zhang,Y., Foxler,D.E., de Moor,C.H., Kong,Y.W., Webb,T.M., Self,T.J., Feng,Y., Lagos,D., Chu,C.Y., Rana,T.M., Morley,S.J., Longmore,G.D., Bushell,M., and Sharp,T.V. (2010). LIM-domain proteins, LIMD1, Ajuba, and WTIP are required for microRNA-mediated gene silencing. *Proc. Natl. Acad. Sci. U. S. A* *107*, 12499-12504.
- Jemal,A., Siegel,R., Xu,J., and Ward,E. (2010). Cancer statistics, 2010. *CA Cancer J. Clin.* *60*, 277-300.
- Jiang,B.H., Rue,E., Wang,G.L., Roe,R., and Semenza,G.L. (1996). Dimerization, DNA binding, and transactivation properties of hypoxia-inducible factor 1. *J. Biol. Chem.* *271*, 17771-17778.
- Jones,P.L., Veenstra,G.J., Wade,P.A., Vermaak,D., Kass,S.U., Landsberger,N., Strouboulis,J., and Wolffe,A.P. (1998). Methylated DNA and MeCP2 recruit histone deacetylase to repress transcription. *Nat. Genet.* *19*, 187-191.
- Juven-Gershon,T., Hsu,J.Y., Theisen,J.W., and Kadonaga,J.T. (2008). The RNA polymerase II core promoter - the gateway to transcription. *Curr. Opin. Cell Biol.* *20*, 253-259.
- Kadonaga,J.T. (2002). The DPE, a core promoter element for transcription by RNA polymerase II. *Exp. Mol. Med.* *34*, 259-264.
- Kadmas,J.L. and Beckerle,M.C. (2004). The LIM domain: from the cytoskeleton to the nucleus. *Nat. Rev. Mol. Cell Biol.* *5*, 920-931.
- Kafri,T., Ariel,M., Brandeis,M., Shemer,R., Urven,L., McCarrey,J., Cedar,H., and Razin,A. (1992). Developmental pattern of gene-specific DNA methylation in the mouse embryo and germ line. *Genes Dev.* *6*, 705-714.
- Kafri,T., Gao,X., and Razin,A. (1993). Mechanistic aspects of genome-wide demethylation in the preimplantation mouse embryo. *Proc. Natl. Acad. Sci. U. S. A* *90*, 10558-10562.
- Kalantry,S. (2011). Recent advances in X-chromosome inactivation. *J. Cell Physiol* *226*, 1714-1718.
- Kallio,P.J., Okamoto,K., O'Brien,S., Carrero,P., Makino,Y., Tanaka,H., and Poellinger,L. (1998). Signal transduction in hypoxic cells: inducible nuclear translocation and recruitment of the CBP/p300 coactivator by the hypoxia-inducible factor-1alpha. *EMBO J.* *17*, 6573-6586.
- Kantarjian,H., Issa,J.P., Rosenfeld,C.S., Bennett,J.M., Albitar,M., DiPersio,J., Klimek,V., Slack,J., de,C.C., Ravandi,F., Helmer,R., III, Shen,L., Nimer,S.D., Leavitt,R., Raza,A., and Saba,H. (2006). Decitabine improves patient outcomes in myelodysplastic syndromes: results of a phase III randomized study. *Cancer* *106*, 1794-1803.
- Kantarjian,H.M., O'Brien,S., Cortes,J., Giles,F.J., Faderl,S., Issa,J.P., Garcia-Manero,G., Rios,M.B., Shan,J., Andreeff,M., Keating,M., and Talpaz,M. (2003). Results of decitabine (5-aza-2'-deoxycytidine) therapy in 130 patients with chronic myelogenous leukemia. *Cancer* *98*, 522-528.
- Kanungo,J., Pratt,S.J., Marie,H., and Longmore,G.D. (2000). Ajuba, a cytosolic LIM protein, shuttles into the nucleus and affects embryonal cell proliferation and fate decisions. *Mol. Biol. Cell* *11*, 3299-3313.

- Karlsson,O., Thor,S., Norberg,T., Ohlsson,H., and Edlund,T. (1990). Insulin gene enhancer binding protein Isl-1 is a member of a novel class of proteins containing both a homeo- and a Cys-His domain. *Nature* 344, 879-882.
- Karsenty,G. and Wagner,E.F. (2002). Reaching a genetic and molecular understanding of skeletal development. *Dev. Cell* 2, 389-406.
- Karube,Y., Tanaka,H., Osada,H., Tomida,S., Tatematsu,Y., Yanagisawa,K., Yatabe,Y., Takamizawa,J., Miyoshi,S., Mitsudomi,T., and Takahashi,T. (2005). Reduced expression of Dicer associated with poor prognosis in lung cancer patients. *Cancer Sci.* 96, 111-115.
- Kastner,P. and Chan,S. (2008). PU.1: a crucial and versatile player in hematopoiesis and leukemia. *Int. J. Biochem. Cell Biol.* 40, 22-27.
- Kholodnyuk,I., Kost-Alimova,M., Kashuba,V., Gizatuln,R., Szeles,A., Stanbridge,E.J., Zabarovsky,E.R., Klein,G., and Imreh,S. (1997). A 3p21.3 region is preferentially eliminated from human chromosome 3/mouse microcell hybrids during tumor growth in SCID mice. *Genes Chromosomes. Cancer* 18, 200-211.
- Kholodnyuk,I.D., Kost-Alimova,M., Yang,Y., Kiss,H., Fedorova,L., Klein,G., and Imreh,S. (2002). The microcell hybrid-based "elimination test" identifies a 1-Mb putative tumor-suppressor region at 3p22.2-p22.1 centromeric to the homozygous deletion region detected in lung cancer. *Genes Chromosomes. Cancer* 34, 341-344.
- Kihara-Negishi,F., Yamamoto,H., Suzuki,M., Yamada,T., Sakurai,T., Tamura,T., and Oikawa,T. (2001). In vivo complex formation of PU.1 with HDAC1 associated with PU.1-mediated transcriptional repression. *Oncogene* 20, 6039-6047.
- Kim,J.H., Dhanasekaran,S.M., Prensner,J.R., Cao,X., Robinson,D., Kalyana-Sundaram,S., Huang,C., Shankar,S., Jing,X., Iyer,M., Hu,M., Sam,L., Grasso,C., Maher,C.A., Palanisamy,N., Mehra,R., Kominsky,H.D., Siddiqui,J., Yu,J., Qin,Z.S., and Chinnaiyan,A.M. (2011). Deep sequencing reveals distinct patterns of DNA methylation in prostate cancer. *Genome Res.* 21, 1028-1041.
- Kim,J.H., Konieczkowski,M., Mukherjee,A., Schechtman,S., Khan,S., Schelling,J.R., Ross,M.D., Bruggeman,L.A., and Sedor,J.R. (2010a). Podocyte injury induces nuclear translocation of WTIP via microtubule-dependent transport. *J. Biol. Chem.* 285, 9995-10004.
- Kim,J.K., Samaranyake,M., and Pradhan,S. (2009). Epigenetic mechanisms in mammals. *Cell Mol. Life Sci.* 66, 596-612.
- Kim,J.W., Tchernyshyov,I., Semenza,G.L., and Dang,C.V. (2006). HIF-1-mediated expression of pyruvate dehydrogenase kinase: a metabolic switch required for cellular adaptation to hypoxia. *Cell Metab* 3, 177-185.
- Kim,M.S., Oh,J.E., Kim,Y.R., Park,S.W., Kang,M.R., Kim,S.S., Ahn,C.H., Yoo,N.J., and Lee,S.H. (2010b). Somatic mutations and losses of expression of microRNA regulation-related genes AGO2 and TNRC6A in gastric and colorectal cancers. *J. Pathol.* 221, 139-146.
- Kiss,H., Kedra,D., Yang,Y., Kost-Alimova,M., Kiss,C., O'Brien,K.P., Fransson,I., Klein,G., Imreh,S., and Dumanski,J.P. (1999). A novel gene containing LIM domains (LIMD1) is located within the common eliminated region 1 (C3CER1) in 3p21.3. *Hum. Genet.* 105, 552-559.

- Kiss,H., Yang,Y., Kiss,C., Andersson,K., Klein,G., Imreh,S., and Dumanski,J.P. (2002). The transcriptional map of the common eliminated region 1 (C3CER1) in 3p21.3. *Eur. J. Hum. Genet.* *10*, 52-61.
- Klemsz,M.J. and Maki,R.A. (1996). Activation of transcription by PU.1 requires both acidic and glutamine domains. *Mol. Cell Biol.* *16*, 390-397.
- Klemsz,M.J., McKercher,S.R., Celada,A., Van,B.C., and Maki,R.A. (1990). The macrophage and B cell-specific transcription factor PU.1 is related to the ets oncogene. *Cell* *61*, 113-124.
- Knudson,A.G., Jr. (1971). Mutation and cancer: statistical study of retinoblastoma. *Proc. Natl. Acad. Sci. U. S. A* *68*, 820-823.
- Kok,K., van den Berg,A., Veldhuis,P.M., van der Veen,A.Y., Franke,M., Schoenmakers,E.F., Hulsbeek,M.M., van der Hout,A.H., de,L.L., van,d., V, and . (1994). A homozygous deletion in a small cell lung cancer cell line involving a 3p21 region with a marked instability in yeast artificial chromosomes. *Cancer Res.* *54*, 4183-4187.
- Kokura,K., Kaul,S.C., Wadhwa,R., Nomura,T., Khan,M.M., Shinagawa,T., Yasukawa,T., Colmenares,C., and Ishii,S. (2001). The Ski protein family is required for MeCP2-mediated transcriptional repression. *J. Biol. Chem.* *276*, 34115-34121.
- Kondo,E., Gu,Z., Horii,A., and Fukushige,S. (2005). The thymine DNA glycosylase MBD4 represses transcription and is associated with methylated p16(INK4a) and hMLH1 genes. *Mol. Cell Biol.* *25*, 4388-4396.
- Kong,K.Y., Owens,K.S., Rogers,J.H., Mullenix,J., Velu,C.S., Grimes,H.L., and Dahl,R. (2010). MIR-23A microRNA cluster inhibits B-cell development. *Exp. Hematol.* *38*, 629-640.
- Koslowski,M., Luxemburger,U., Tureci,O., and Sahin,U. (2011). Tumor-associated CpG demethylation augments hypoxia-induced effects by positive autoregulation of HIF-1alpha. *Oncogene* *30*, 876-882.
- Kost-Alimova,M. and Imreh,S. (2007). Modeling non-random deletions in cancer. *Semin. Cancer Biol.* *17*, 19-30.
- Kovesdi,I., Reichel,R., and Nevins,J.R. (1987). Role of an adenovirus E2 promoter binding factor in E1A-mediated coordinate gene control. *Proc. Natl. Acad. Sci. U. S. A* *84*, 2180-2184.
- Kundu,T.K. and Rao,M.R. (1999). CpG islands in chromatin organization and gene expression. *J. Biochem.* *125*, 217-222.
- Kutach,A.K. and Kadonaga,J.T. (2000). The downstream promoter element DPE appears to be as widely used as the TATA box in *Drosophila* core promoters. *Mol. Cell Biol.* *20*, 4754-4764.
- Lagrange,T., Kapanidis,A.N., Tang,H., Reinberg,D., and Ebright,R.H. (1998). New core promoter element in RNA polymerase II-dependent transcription: sequence-specific DNA binding by transcription factor IIB. *Genes Dev.* *12*, 34-44.
- Lander,E.S., Linton,L.M., Birren,B., Nusbaum,C., Zody,M.C., Baldwin,J., Devon,K., Dewar,K., Doyle,M., FitzHugh,W., Funke,R., Gage,D., Harris,K., Heaford,A., Howland,J., Kann,L.,

- Lehoczky,J., LeVine,R., McEwan,P., McKernan,K., Meldrim,J., Mesirov,J.P., Miranda,C., Morris,W., Naylor,J., Raymond,C., Rosetti,M., Santos,R., Sheridan,A., Sougnez,C., Stange-Thomann,N., Stojanovic,N., Subramanian,A., Wyman,D., Rogers,J., Sulston,J., Ainscough,R., Beck,S., Bentley,D., Burton,J., Clee,C., Carter,N., Coulson,A., Deadman,R., Deloukas,P., Dunham,A., Dunham,I., Durbin,R., French,L., Grafham,D., Gregory,S., Hubbard,T., Humphray,S., Hunt,A., Jones,M., Lloyd,C., McMurray,A., Matthews,L., Mercer,S., Milne,S., Mullikin,J.C., Mungall,A., Plumb,R., Ross,M., Shownkeen,R., Sims,S., Waterston,R.H., Wilson,R.K., Hillier,L.W., McPherson,J.D., Marra,M.A., Mardis,E.R., Fulton,L.A., Chinwalla,A.T., Pepin,K.H., Gish,W.R., Chissoe,S.L., Wendl,M.C., Delehaunty,K.D., Miner,T.L., Delehaunty,A., Kramer,J.B., Cook,L.L., Fulton,R.S., Johnson,D.L., Minx,P.J., Clifton,S.W., Hawkins,T., Branscomb,E., Predki,P., Richardson,P., Wenning,S., Slezak,T., Doggett,N., Cheng,J.F., Olsen,A., Lucas,S., Elkin,C., Uberbacher,E., Frazier,M., Gibbs,R.A., Muzny,D.M., Scherer,S.E., Bouck,J.B., Sodergren,E.J., Worley,K.C., Rives,C.M., Gorrell,J.H., Metzker,M.L., Naylor,S.L., Kucherlapati,R.S., Nelson,D.L., Weinstock,G.M., Sakaki,Y., Fujiyama,A., Hattori,M., Yada,T., Toyoda,A., Itoh,T., Kawagoe,C., Watanabe,H., Totoki,Y., Taylor,T., Weissenbach,J., Heilig,R., Saurin,W., Artiguenave,F., Brottier,P., Bruls,T., Pelletier,E., Robert,C., Wincker,P., Smith,D.R., Doucette-Stamm,L., Rubenfield,M., Weinstock,K., Lee,H.M., Dubois,J., Rosenthal,A., Platzer,M., Nyakatura,G., Taudien,S., Rump,A., Yang,H., Yu,J., Wang,J., Huang,G., Gu,J., Hood,L., Rowen,L., Madan,A., Qin,S., Davis,R.W., Federspiel,N.A., Abola,A.P., Proctor,M.J., Myers,R.M., Schmutz,J., Dickson,M., Grimwood,J., Cox,D.R., Olson,M.V., Kaul,R., Raymond,C., Shimizu,N., Kawasaki,K., Minoshima,S., Evans,G.A., Athanasiou,M., Schultz,R., Roe,B.A., Chen,F., Pan,H., Ramser,J., Lehrach,H., Reinhardt,R., McCombie,W.R., de la Bastide,M., Dedhia,N., Blocker,H., Hornischer,K., Nordsiek,G., Agarwala,R., Aravind,L., Bailey,J.A., Bateman,A., Batzoglou,S., Birney,E., Bork,P., Brown,D.G., Burge,C.B., Cerutti,L., Chen,H.C., Church,D., Clamp,M., Copley,R.R., Doerks,T., Eddy,S.R., Eichler,E.E., Furey,T.S., Galagan,J., Gilbert,J.G., Harmon,C., Hayashizaki,Y., Haussler,D., Hermjakob,H., Hokamp,K., Jang,W., Johnson,L.S., Jones,T.A., Kasif,S., Kasprzyk,A., Kennedy,S., Kent,W.J., Kitts,P., Koonin,E.V., Korf,I., Kulp,D., Lancet,D., Lowe,T.M., McLysaght,A., Mikkelsen,T., Moran,J.V., Mulder,N., Pollara,V.J., Ponting,C.P., Schuler,G., Schultz,J., Slater,G., Smit,A.F., Stupka,E., Szustakowski,J., Thierry-Mieg,D., Thierry-Mieg,J., Wagner,L., Wallis,J., Wheeler,R., Williams,A., Wolf,Y.I., Wolfe,K.H., Yang,S.P., Yeh,R.F., Collins,F., Guyer,M.S., Peterson,J., Felsenfeld,A., Wetterstrand,K.A., Patrinos,A., Morgan,M.J., de,J.P., Catanese,J.J., Osoegawa,K., Shizuya,H., Choi,S., and Chen,Y.J. (2001). Initial sequencing and analysis of the human genome. *Nature* 409, 860-921.
- Lando,D., Peet,D.J., Gorman,J.J., Whelan,D.A., Whitelaw,M.L., and Bruick,R.K. (2002a). FIH-1 is an asparaginyl hydroxylase enzyme that regulates the transcriptional activity of hypoxia-inducible factor. *Genes Dev.* 16, 1466-1471.
- Lando,D., Peet,D.J., Whelan,D.A., Gorman,J.J., and Whitelaw,M.L. (2002b). Asparagine hydroxylation of the HIF transactivation domain a hypoxic switch. *Science* 295, 858-861.
- Landolin,J.M., Johnson,D.S., Trinklein,N.D., Aldred,S.F., Medina,C., Shulha,H., Weng,Z., and Myers,R.M. (2010). Sequence features that drive human promoter function and tissue specificity. *Genome Res.* 20, 890-898.
- Langer,E.M., Feng,Y., Zhaoyuan,H., Rauscher,F.J., III, Kroll,K.L., and Longmore,G.D. (2008). Ajuba LIM proteins are snail/slug corepressors required for neural crest development in *Xenopus*. *Dev. Cell* 14, 424-436.

- Lapidot,T., Sirard,C., Vormoor,J., Murdoch,B., Hoang,T., Caceres-Cortes,J., Minden,M., Paterson,B., Caligiuri,M.A., and Dick,J.E. (1994). A cell initiating human acute myeloid leukaemia after transplantation into SCID mice. *Nature* 367, 645-648.
- Lawrie,C.H., Cooper,C.D., Ballabio,E., Chi,J., Tramonti,D., and Hatton,C.S. (2009). Aberrant expression of microRNA biosynthetic pathway components is a common feature of haematological malignancy. *Br. J. Haematol.* 145, 545-548.
- Lee,E.S., Issa,J.P., Roberts,D.B., Williams,M.D., Weber,R.S., Kies,M.S., and El-Naggar,A.K. (2008). Quantitative promoter hypermethylation analysis of cancer-related genes in salivary gland carcinomas: comparison with methylation-specific PCR technique and clinical significance. *Clin. Cancer Res.* 14, 2664-2672.
- Lee,R.C., Feinbaum,R.L., and Ambros,V. (1993). The *C. elegans* heterochronic gene *lin-4* encodes small RNAs with antisense complementarity to *lin-14*. *Cell* 75, 843-854.
- Lee,W.H., Bookstein,R., Hong,F., Young,L.J., Shew,J.Y., and Lee,E.Y. (1987). Human retinoblastoma susceptibility gene: cloning, identification, and sequence. *Science* 235, 1394-1399.
- Lee,Y., Ahn,C., Han,J., Choi,H., Kim,J., Yim,J., Lee,J., Provost,P., Radmark,O., Kim,S., and Kim,V.N. (2003). The nuclear RNase III Drosha initiates microRNA processing. *Nature* 425, 415-419.
- Lee,Y., Kim,M., Han,J., Yeom,K.H., Lee,S., Baek,S.H., and Kim,V.N. (2004). MicroRNA genes are transcribed by RNA polymerase II. *EMBO J.* 23, 4051-4060.
- Leeb,M., Steffen,P.A., and Wutz,A. (2009). X chromosome inactivation sparked by non-coding RNAs. *RNA. Biol.* 6, 94-99.
- Lei,H., Oh,S.P., Okano,M., Juttermann,R., Goss,K.A., Jaenisch,R., and Li,E. (1996). De novo DNA cytosine methyltransferase activities in mouse embryonic stem cells. *Development* 122, 3195-3205.
- Leprince,D., Gegonne,A., Coll,J., de,T.C., Schneeberger,A., Lagrou,C., and Stehelin,D. (1983). A putative second cell-derived oncogene of the avian leukaemia retrovirus E26. *Nature* 306, 395-397.
- Li,L., Bin,L.H., Li,F., Liu,Y., Chen,D., Zhai,Z., and Shu,H.B. (2005). TRIP6 is a RIP2-associated common signaling component of multiple NF-kappaB activation pathways. *J. Cell Sci.* 118, 555-563.
- Li,L. and Davie,J.R. (2010). The role of Sp1 and Sp3 in normal and cancer cell biology. *Ann. Anat.* 192, 275-283.
- Li,P.M., Reichert,J., Freyd,G., Horvitz,H.R., and Walsh,C.T. (1991). The LIM region of a presumptive *Caenorhabditis elegans* transcription factor is an iron-sulfur- and zinc-containing metallodomain. *Proc. Natl. Acad. Sci. U. S. A* 88, 9210-9213.
- Li,S.H., Chun,Y.S., Lim,J.H., Huang,L.E., and Park,J.W. (2011). von Hippel-Lindau protein adjusts oxygen sensing of the FIH asparaginyl hydroxylase. *Int. J. Biochem. Cell Biol.* 43, 795-804.

- Liu,W., Xin,H., Eckert,D.T., Brown,J.A., and Gnarra,J.R. (2011). Hypoxia and cell cycle regulation of the von Hippel-Lindau tumor suppressor. *Oncogene* 30, 21-31.
- Lloberas,J., Soler,C., and Celada,A. (1999). The key role of PU.1/SPI-1 in B cells, myeloid cells and macrophages. *Immunol. Today* 20, 184-189.
- Lorincz,M.C., Dickerson,D.R., Schmitt,M., and Groudine,M. (2004). Intragenic DNA methylation alters chromatin structure and elongation efficiency in mammalian cells. *Nat. Struct. Mol. Biol.* 11, 1068-1075.
- Magdinier,F., Billard,L.M., Wittmann,G., Frappart,L., Benchaib,M., Lenoir,G.M., Guerin,J.F., and Dante,R. (2000). Regional methylation of the 5' end CpG island of BRCA1 is associated with reduced gene expression in human somatic cells. *FASEB J.* 14, 1585-1594.
- Mahon,P.C., Hirota,K., and Semenza,G.L. (2001). FIH-1: a novel protein that interacts with HIF-1alpha and VHL to mediate repression of HIF-1 transcriptional activity. *Genes Dev.* 15, 2675-2686.
- Makino,Y., Cao,R., Svensson,K., Bertilsson,G., Asman,M., Tanaka,H., Cao,Y., Berkenstam,A., and Poellinger,L. (2001). Inhibitory PAS domain protein is a negative regulator of hypoxia-inducible gene expression. *Nature* 414, 550-554.
- Makino,Y., Uenishi,R., Okamoto,K., Isoe,T., Hosono,O., Tanaka,H., Kanopka,A., Poellinger,L., Haneda,M., and Morimoto,C. (2007). Transcriptional up-regulation of inhibitory PAS domain protein gene expression by hypoxia-inducible factor 1 (HIF-1): a negative feedback regulatory circuit in HIF-1-mediated signaling in hypoxic cells. *J. Biol. Chem.* 282, 14073-14082.
- Marie,H., Pratt,S.J., Betson,M., Epple,H., Kittler,J.T., Meek,L., Moss,S.J., Troyanovsky,S., Attwell,D., Longmore,G.D., and Braga,V.M. (2003). The LIM protein Ajuba is recruited to cadherin-dependent cell junctions through an association with alpha-catenin. *J. Biol. Chem.* 278, 1220-1228.
- Martinet,W., Schrijvers,D.M., and Kockx,M.M. (2003). Nucleofection as an efficient nonviral transfection method for human monocytic cells. *Biotechnol. Lett.* 25, 1025-1029.
- Marxsen,J.H., Stengel,P., Doege,K., Heikkinen,P., Jokilehto,T., Wagner,T., Jelkmann,W., Jaakkola,P., and Metzen,E. (2004). Hypoxia-inducible factor-1 (HIF-1) promotes its degradation by induction of HIF-alpha-prolyl-4-hydroxylases. *Biochem. J.* 381, 761-767.
- Masayesva,B.G., Ha,P., Garrett-Mayer,E., Pilkington,T., Mao,R., Pevsner,J., Speed,T., Benoit,N., Moon,C.S., Sidransky,D., Westra,W.H., and Califano,J. (2004). Gene expression alterations over large chromosomal regions in cancers include multiple genes unrelated to malignant progression. *Proc. Natl. Acad. Sci. U. S. A* 101, 8715-8720.
- Masson,N., Willam,C., Maxwell,P.H., Pugh,C.W., and Ratcliffe,P.J. (2001). Independent function of two destruction domains in hypoxia-inducible factor-alpha chains activated by prolyl hydroxylation. *EMBO J.* 20, 5197-5206.
- Mavrothalassitis,G. and Ghysdael,J. (2000). Proteins of the ETS family with transcriptional repressor activity. *Oncogene* 19, 6524-6532.

- Maxwell,P.H., Wiesener,M.S., Chang,G.W., Clifford,S.C., Vaux,E.C., Cockman,M.E., Wykoff,C.C., Pugh,C.W., Maher,E.R., and Ratcliffe,P.J. (1999). The tumour suppressor protein VHL targets hypoxia-inducible factors for oxygen-dependent proteolysis. *Nature* 399, 271-275.
- Mayer,W., Niveleau,A., Walter,J., Fundele,R., and Haaf,T. (2000). Demethylation of the zygotic paternal genome. *Nature* 403, 501-502.
- McKeon,C., Ohkubo,H., Pastan,I., and de,C.B. (1982). Unusual methylation pattern of the alpha 2 (I) collagen gene. *Cell* 29, 203-210.
- Meehan,R.R., Lewis,J.D., McKay,S., Kleiner,E.L., and Bird,A.P. (1989). Identification of a mammalian protein that binds specifically to DNA containing methylated CpGs. *Cell* 58, 499-507.
- Meissner,A., Mikkelsen,T.S., Gu,H., Wernig,M., Hanna,J., Sivachenko,A., Zhang,X., Bernstein,B.E., Nusbaum,C., Jaffe,D.B., Gnirke,A., Jaenisch,R., and Lander,E.S. (2008). Genome-scale DNA methylation maps of pluripotent and differentiated cells. *Nature* 454, 766-770.
- Melo,S.A., Ropero,S., Moutinho,C., Aaltonen,L.A., Yamamoto,H., Calin,G.A., Rossi,S., Fernandez,A.F., Carneiro,F., Oliveira,C., Ferreira,B., Liu,C.G., Villanueva,A., Capella,G., Schwartz S Jr, Shiekhhattar,R., and Esteller,M. (2009). A TARBP2 mutation in human cancer impairs microRNA processing and DICER1 function. *Nat. Genet.* 41, 365-370.
- Merritt,W.M., Lin,Y.G., Han,L.Y., Kamat,A.A., Spannuth,W.A., Schmandt,R., Urbauer,D., Pennacchio,L.A., Cheng,J.F., Nick,A.M., Deavers,M.T., Mourad-Zeidan,A., Wang,H., Mueller,P., Lenburg,M.E., Gray,J.W., Mok,S., Birrer,M.J., Lopez-Berestein,G., Coleman,R.L., Bar-Eli,M., and Sood,A.K. (2008). Dicer, Drosha, and outcomes in patients with ovarian cancer. *N. Engl. J. Med.* 359, 2641-2650.
- Metcalf,D., Dakic,A., Mifsud,S., Di,R.L., Wu,L., and Nutt,S. (2006). Inactivation of PU.1 in adult mice leads to the development of myeloid leukemia. *Proc. Natl. Acad. Sci. U. S. A* 103, 1486-1491.
- Michelsen,J.W., Schmeichel,K.L., Beckerle,M.C., and Winge,D.R. (1993). The LIM motif defines a specific zinc-binding protein domain. *Proc. Natl. Acad. Sci. U. S. A* 90, 4404-4408.
- Michiels,C., Minet,E., Michel,G., Mottet,D., Piret,J.P., and Raes,M. (2001). HIF-1 and AP-1 cooperate to increase gene expression in hypoxia: role of MAP kinases. *IUBMB. Life* 52, 49-53.
- Mighell,A.J., Markham,A.F., and Robinson,P.A. (1997). Alu sequences. *FEBS Lett.* 417, 1-5.
- Millar,C.B., Guy,J., Sansom,O.J., Selfridge,J., MacDougall,E., Hendrich,B., Keightley,P.D., Bishop,S.M., Clarke,A.R., and Bird,A. (2002). Enhanced CpG mutability and tumorigenesis in MBD4-deficient mice. *Science* 297, 403-405.
- Minet,E., Michel,G., Mottet,D., Raes,M., and Michiels,C. (2001). Transduction pathways involved in Hypoxia-Inducible Factor-1 phosphorylation and activation. *Free Radic. Biol. Med.* 31, 847-855.

- Mishra,D.K., Chen,Z., Wu,Y., Sarkissyan,M., Koeffler,H.P., and Vadgama,J.V. (2010). Global methylation pattern of genes in androgen-sensitive and androgen-independent prostate cancer cells. *Mol. Cancer Ther.* *9*, 33-45.
- Mitelman,F., Mertens,F., and Johansson,B. (1997). A breakpoint map of recurrent chromosomal rearrangements in human neoplasia. *Nat. Genet.* *15 Spec No*, 417-474.
- Moik,D.V., Janbandhu,V.C., and Fassler,R. (2011). Loss of migfilin expression has no overt consequences on murine development and homeostasis. *J. Cell Sci.* *124*, 414-421.
- Monk,M., Boubelik,M., and Lehnert,S. (1987). Temporal and regional changes in DNA methylation in the embryonic, extraembryonic and germ cell lineages during mouse embryo development. *Development* *99*, 371-382.
- Monticone,M., Biollo,E., Maffei,M., Donadini,A., Romeo,F., Storlazzi,C.T., Giaretti,W., and Castagnola,P. (2008). Gene expression deregulation by KRAS G12D and G12V in a BRAF V600E context. *Mol. Cancer* *7*, 92.
- Moreau-Gachelin,F., Tavitian,A., and Tambourin,P. (1988). Spi-1 is a putative oncogene in virally induced murine erythroleukaemias. *Nature* *331*, 277-280.
- Moreau-Gachelin,F., Wendling,F., Molina,T., Denis,N., Titeux,M., Grimber,G., Briand,P., Vainchenker,W., and Tavitian,A. (1996). Spi-1/PU.1 transgenic mice develop multistep erythroleukemias. *Mol. Cell Biol.* *16*, 2453-2463.
- Morison,I.M., Ramsay,J.P., and Spencer,H.G. (2005). A census of mammalian imprinting. *Trends Genet.* *21*, 457-465.
- Mueller,B.U., Pabst,T., Osato,M., Asou,N., Johansen,L.M., Minden,M.D., Behre,G., Hiddemann,W., Ito,Y., and Tenen,D.G. (2002). Heterozygous PU.1 mutations are associated with acute myeloid leukemia. *Blood* *100*, 998-1007.
- Murata,Y., Tamari,M., Takahashi,T., Horio,Y., Hibi,K., Yokoyama,S., Inazawa,J., Yamakawa,K., Ogawa,A., Takahashi,T., and . (1994). Characterization of an 800 kb region at 3p22-p21.3 that was homozygously deleted in a lung cancer cell line. *Hum. Mol. Genet.* *3*, 1341-1344.
- Nakajima,N., Horikoshi,M., and Roeder,R.G. (1988). Factors involved in specific transcription by mammalian RNA polymerase II: purification, genetic specificity, and TATA box-promoter interactions of TFIID. *Mol. Cell Biol.* *8*, 4028-4040.
- Nan,X., Ng,H.H., Johnson,C.A., Laherty,C.D., Turner,B.M., Eisenman,R.N., and Bird,A. (1998). Transcriptional repression by the methyl-CpG-binding protein MeCP2 involves a histone deacetylase complex. *Nature* *393*, 386-389.
- Naoghare,P.K., Tak,Y.K., Kim,M.J., Han,E., and Song,J.M. (2011). Knockdown of Argonaute 2 (AGO2) Induces Apoptosis in Myeloid Leukaemia Cells and Inhibits siRNA-Mediated Silencing of Transfected Oncogenes in HEK-293 Cells. *Basic Clin. Pharmacol. Toxicol.*
- Ng,H.H., Zhang,Y., Hendrich,B., Johnson,C.A., Turner,B.M., Erdjument-Bromage,H., Tempst,P., Reinberg,D., and Bird,A. (1999). MBD2 is a transcriptional repressor belonging to the MeCP1 histone deacetylase complex. *Nat. Genet.* *23*, 58-61.

- Nishioka,K., Rice,J.C., Sarma,K., Erdjument-Bromage,H., Werner,J., Wang,Y., Chuikov,S., Valenzuela,P., Tempst,P., Steward,R., Lis,J.T., Allis,C.D., and Reinberg,D. (2002). PR-Set7 is a nucleosome-specific methyltransferase that modifies lysine 20 of histone H4 and is associated with silent chromatin. *Mol. Cell* 9, 1201-1213.
- Nishiyama,C., Nishiyama,M., Ito,T., Masaki,S., Masuoka,N., Yamane,H., Kitamura,T., Ogawa,H., and Okumura,K. (2004). Functional analysis of PU.1 domains in monocyte-specific gene regulation. *FEBS Lett.* 561, 63-68.
- Nix,D.A., Fradelizi,J., Bockholt,S., Menichi,B., Louvard,D., Friederich,E., and Beckerle,M.C. (2001). Targeting of zyxin to sites of actin membrane interaction and to the nucleus. *J. Biol. Chem.* 276, 34759-34767.
- O'Rourke,J.F., Tian,Y.M., Ratcliffe,P.J., and Pugh,C.W. (1999). Oxygen-regulated and transactivating domains in endothelial PAS protein 1: comparison with hypoxia-inducible factor-1alpha. *J. Biol. Chem.* 274, 2060-2071.
- O'Shea-Greenfield,A. and Smale,S.T. (1992). Roles of TATA and initiator elements in determining the start site location and direction of RNA polymerase II transcription. *J. Biol. Chem.* 267, 1391-1402.
- Ohh,M., Park,C.W., Ivan,M., Hoffman,M.A., Kim,T.Y., Huang,L.E., Pavletich,N., Chau,V., and Kaelin,W.G. (2000). Ubiquitination of hypoxia-inducible factor requires direct binding to the beta-domain of the von Hippel-Lindau protein. *Nat. Cell Biol.* 2, 423-427.
- Oikawa,T. and Yamada,T. (2003). Molecular biology of the Ets family of transcription factors. *Gene* 303, 11-34.
- Okada,Y., Nobori,H., Shimizu,M., Watanabe,M., Yonekura,M., Nakai,T., Kamikawa,Y., Wakimura,A., Funahashi,N., Naruse,H., Watanabe,A., Yamasaki,D., Fukada,S., Yasui,K., Matsumoto,K., Sato,T., Kitajima,K., Nakano,T., Aird,W.C., and Doi,T. (2011). Multiple ETS Family Proteins Regulate PF4 Gene Expression by Binding to the Same ETS Binding Site. *PLoS. One.* 6, e24837.
- Okano,M., Bell,D.W., Haber,D.A., and Li,E. (1999). DNA methyltransferases Dnmt3a and Dnmt3b are essential for de novo methylation and mammalian development. *Cell* 99, 247-257.
- Okano,M., Xie,S., and Li,E. (1998a). Cloning and characterization of a family of novel mammalian DNA (cytosine-5) methyltransferases. *Nat. Genet.* 19, 219-220.
- Okano,M., Xie,S., and Li,E. (1998b). Dnmt2 is not required for de novo and maintenance methylation of viral DNA in embryonic stem cells. *Nucleic Acids Res.* 26, 2536-2540.
- Ott,M.O., Sperling,L., Cassio,D., Levilliers,J., Sala-Trepat,J., and Weiss,M.C. (1982). Undermethylation at the 5' end of the albumin gene is necessary but not sufficient for albumin production by rat hepatoma cells in culture. *Cell* 30, 825-833.
- Papachristou,D.J., Gkretsi,V., Tu,Y., Shi,X., Chen,K., Larjava,H., Rao,U.N., and Wu,C. (2007). Increased cytoplasmic level of migfilin is associated with higher grades of human leiomyosarcoma. *Histopathology* 51, 499-508.

- Papandreou,I., Cairns,R.A., Fontana,L., Lim,A.L., and Denko,N.C. (2006). HIF-1 mediates adaptation to hypoxia by actively downregulating mitochondrial oxygen consumption. *Cell Metab* 3, 187-197.
- Papetti,M. and Skoultchi,A.I. (2007). Reprogramming leukemia cells to terminal differentiation and growth arrest by RNA interference of PU.1. *Mol. Cancer Res.* 5, 1053-1062.
- Pasanen,A., Heikkila,M., Rautavuoma,K., Hirsila,M., Kivirikko,K.I., and Myllyharju,J. (2010). Hypoxia-inducible factor (HIF)-3alpha is subject to extensive alternative splicing in human tissues and cancer cells and is regulated by HIF-1 but not HIF-2. *Int. J. Biochem. Cell Biol.* 42, 1189-1200.
- Pazin,M.J. and Kadonaga,J.T. (1997). What's up and down with histone deacetylation and transcription? *Cell* 89, 325-328.
- Pennacchio,L.A. and Rubin,E.M. (2001). Genomic strategies to identify mammalian regulatory sequences. *Nat. Rev. Genet.* 2, 100-109.
- Perez-Alvarado,G.C., Miles,C., Michelsen,J.W., Louis,H.A., Winge,D.R., Beckerle,M.C., and Summers,M.F. (1994). Structure of the carboxy-terminal LIM domain from the cysteine rich protein CRP. *Nat. Struct. Biol.* 1, 388-398.
- Perez-Ordóñez,B., Beauchemin,M., and Jordan,R.C. (2006). Molecular biology of squamous cell carcinoma of the head and neck. *J. Clin. Pathol.* 59, 445-453.
- Petit,M.M., Fradelizi,J., Golsteyn,R.M., Ayoubi,T.A., Menichi,B., Louvard,D., Van de Ven,W.J., and Friederich,E. (2000). LPP, an actin cytoskeleton protein related to zyxin, harbors a nuclear export signal and transcriptional activation capacity. *Mol. Biol. Cell* 11, 117-129.
- Petit,M.M., Meulemans,S.M., Alen,P., Ayoubi,T.A., Jansen,E., and Van de Ven,W.J. (2005). The tumor suppressor Scrib interacts with the zyxin-related protein LPP, which shuttles between cell adhesion sites and the nucleus. *BMC. Cell Biol.* 6, 1.
- Petit,M.M., Mols,R., Schoenmakers,E.F., Mandahl,N., and Van de Ven,W.J. (1996). LPP, the preferred fusion partner gene of HMGIC in lipomas, is a novel member of the LIM protein gene family. *Genomics* 36, 118-129.
- Petursdottir,T.E., Thorsteinsdottir,U., Jonasson,J.G., Moller,P.H., Huiping,C., Bjornsson,J., Egilsson,V., Imreh,S., and Ingvarsson,S. (2004). Interstitial deletions including chromosome 3 common eliminated region 1 (C3CER1) prevail in human solid tumors from 10 different tissues. *Genes Chromosomes. Cancer* 41, 232-242.
- Pfeifer,G.P. and Damman,R. (2005). Methylation of the tumor suppressor gene RASSF1A in human tumors. *Biochemistry (Mosc.)* 70, 576-583.
- Place,T.L., Fitzgerald,M.P., Venkataraman,S., Vorrink,S.U., Case,A.J., Teoh,M.L., and Domann,F.E. (2011). Aberrant promoter CpG methylation is a mechanism for impaired PHD3 expression in a diverse set of malignant cells. *PLoS. One.* 6, e14617.

- Pongubala, J.M., Van, B.C., Nagulapalli, S., Klemsz, M.J., McKercher, S.R., Maki, R.A., and Atchison, M.L. (1993). Effect of PU.1 phosphorylation on interaction with NF-EM5 and transcriptional activation. *Science* 259, 1622-1625.
- Posfai, J., Bhagwat, A.S., Posfai, G., and Roberts, R.J. (1989). Predictive motifs derived from cytosine methyltransferases. *Nucleic Acids Res.* 17, 2421-2435.
- Primeau, M., Gagnon, J., and Momparler, R.L. (2003). Synergistic antineoplastic action of DNA methylation inhibitor 5-AZA-2'-deoxycytidine and histone deacetylase inhibitor depsipeptide on human breast carcinoma cells. *Int. J. Cancer* 103, 177-184.
- Pugh, C.W., O'Rourke, J.F., Nagao, M., Gleadle, J.M., and Ratcliffe, P.J. (1997). Activation of hypoxia-inducible factor-1; definition of regulatory domains within the alpha subunit. *J. Biol. Chem.* 272, 11205-11214.
- Raisz, L.G. (2005). Pathogenesis of osteoporosis: concepts, conflicts, and prospects. *J. Clin. Invest* 115, 3318-3325.
- Rehli, M., Poltorak, A., Schwarzfischer, L., Krause, S.W., Andreesen, R., and Beutler, B. (2000). PU.1 and interferon consensus sequence-binding protein regulate the myeloid expression of the human Toll-like receptor 4 gene. *J. Biol. Chem.* 275, 9773-9781.
- Richard, D.E., Berra, E., Gothie, E., Roux, D., and Pouyssegur, J. (1999). p42/p44 mitogen-activated protein kinases phosphorylate hypoxia-inducible factor 1alpha (HIF-1alpha) and enhance the transcriptional activity of HIF-1. *J. Biol. Chem.* 274, 32631-32637.
- Rico, M., Mukherjee, A., Konieczkowski, M., Bruggeman, L.A., Miller, R.T., Khan, S., Schelling, J.R., and Sedor, J.R. (2005). WT1-interacting protein and ZO-1 translocate into podocyte nuclei after puromycin aminonucleoside treatment. *Am. J. Physiol Renal Physiol* 289, F431-F441.
- Rosenbauer, F., Wagner, K., Kutok, J.L., Iwasaki, H., Le Beau, M.M., Okuno, Y., Akashi, K., Fiering, S., and Tenen, D.G. (2004). Acute myeloid leukemia induced by graded reduction of a lineage-specific transcription factor, PU.1. *Nat. Genet.* 36, 624-630.
- Rougier, N., Bourc'his, D., Gomes, D.M., Niveleau, A., Plachot, M., Paldi, A., and Viegas-Pequignot, E. (1998). Chromosome methylation patterns during mammalian preimplantation development. *Genes Dev.* 12, 2108-2113.
- Rozenberg, J.M., Shlyakhtenko, A., Glass, K., Rishi, V., Myakishev, M.V., FitzGerald, P.C., and Vinson, C. (2008). All and only CpG containing sequences are enriched in promoters abundantly bound by RNA polymerase II in multiple tissues. *BMC. Genomics* 9, 67.
- Ruthenburg, A.J., Li, H., Patel, D.J., and Allis, C.D. (2007). Multivalent engagement of chromatin modifications by linked binding modules. *Nat. Rev. Mol. Cell Biol.* 8, 983-994.
- Saito, M. and Ishikawa, F. (2002). The mCpG-binding domain of human MBD3 does not bind to mCpG but interacts with NuRD/Mi2 components HDAC1 and MTA2. *J. Biol. Chem.* 277, 35434-35439.
- Salceda, S. and Caro, J. (1997). Hypoxia-inducible factor 1alpha (HIF-1alpha) protein is rapidly degraded by the ubiquitin-proteasome system under normoxic conditions. Its stabilization by hypoxia depends on redox-induced changes. *J. Biol. Chem.* 272, 22642-22647.

- Saletta,F., Suryo,R.Y., Noulsri,E., and Richardson,D.R. (2010). Iron chelator-mediated alterations in gene expression: identification of novel iron-regulated molecules that are molecular targets of hypoxia-inducible factor-1 alpha and p53. *Mol. Pharmacol.* **77**, 443-458.
- Sanchez-Elsner,T., Botella,L.M., Velasco,B., Langa,C., and Bernabeu,C. (2002). Endoglin expression is regulated by transcriptional cooperation between the hypoxia and transforming growth factor-beta pathways. *J. Biol. Chem.* **277**, 43799-43808.
- Sarraf,S.A. and Stancheva,I. (2004). Methyl-CpG binding protein MBD1 couples histone H3 methylation at lysine 9 by SETDB1 to DNA replication and chromatin assembly. *Mol. Cell* **15**, 595-605.
- Saxonov,S., Berg,P., and Brutlag,D.L. (2006). A genome-wide analysis of CpG dinucleotides in the human genome distinguishes two distinct classes of promoters. *Proc. Natl. Acad. Sci. U. S. A* **103**, 1412-1417.
- Schaefer,M. and Lyko,F. (2010). Solving the Dnmt2 enigma. *Chromosoma* **119**, 35-40.
- Schaefer,M., Pollex,T., Hanna,K., Tuorto,F., Meusburger,M., Helm,M., and Lyko,F. (2010). RNA methylation by Dnmt2 protects transfer RNAs against stress-induced cleavage. *Genes Dev.* **24**, 1590-1595.
- Schnitzler,G.R. (2008). Control of nucleosome positions by DNA sequence and remodeling machines. *Cell Biochem. Biophys.* **51**, 67-80.
- Schodel,J., Oikonomopoulos,S., Ragoussis,J., Pugh,C.W., Ratcliffe,P.J., and Mole,D.R. (2011). High-resolution genome-wide mapping of HIF-binding sites by ChIP-seq. *Blood* **117**, e207-e217.
- Schramm,L. and Hernandez,N. (2002). Recruitment of RNA polymerase III to its target promoters. *Genes Dev.* **16**, 2593-2620.
- Schuster,S.J., Badiavas,E.V., Costa-Giomi,P., Weinmann,R., Erslev,A.J., and Caro,J. (1989). Stimulation of erythropoietin gene transcription during hypoxia and cobalt exposure. *Blood* **73**, 13-16.
- Sciandra,J.J., Subjeck,J.R., and Hughes,C.S. (1984). Induction of glucose-regulated proteins during anaerobic exposure and of heat-shock proteins after reoxygenation. *Proc. Natl. Acad. Sci. U. S. A* **81**, 4843-4847.
- Scott,E.W., Fisher,R.C., Olson,M.C., Kehrl,E.W., Simon,M.C., and Singh,H. (1997). PU.1 functions in a cell-autonomous manner to control the differentiation of multipotential lymphoid-myeloid progenitors. *Immunity* **6**, 437-447.
- Scott,M.P., Tamkun,J.W., and Hartzell,G.W., III (1989). The structure and function of the homeodomain. *Biochim. Biophys. Acta* **989**, 25-48.
- Sementchenko,V.I. and Watson,D.K. (2000). Ets target genes: past, present and future. *Oncogene* **19**, 6533-6548.
- Semenza,G.L. (1999). Regulation of mammalian O₂ homeostasis by hypoxia-inducible factor 1. *Annu. Rev. Cell Dev. Biol.* **15**, 551-578.

- Semenza,G.L. (2003). Targeting HIF-1 for cancer therapy. *Nat. Rev. Cancer* 3, 721-732.
- Semenza,G.L. (2011). Hypoxia. Cross talk between oxygen sensing and the cell cycle machinery. *Am. J. Physiol Cell Physiol* 301, C550-C552.
- Semenza,G.L., Neufelt,M.K., Chi,S.M., and Antonarakis,S.E. (1991). Hypoxia-inducible nuclear factors bind to an enhancer element located 3' to the human erythropoietin gene. *Proc. Natl. Acad. Sci. U. S. A* 88, 5680-5684.
- Semenza,G.L. and Wang,G.L. (1992). A nuclear factor induced by hypoxia via de novo protein synthesis binds to the human erythropoietin gene enhancer at a site required for transcriptional activation. *Mol. Cell Biol.* 12, 5447-5454.
- Seo,S., Zhang,Q., Bugge,K., Breslow,D.K., Searby,C.C., Nachury,M.V., and Sheffield,V.C. (2011). A novel protein LZTFL1 regulates ciliary trafficking of the BBSome and Smoothed. *PLoS. Genet.* 7, e1002358.
- Sharp,T.V., Al-Attar,A., Foxler,D.E., Ding,L., de,A., V, Zhang,Y., Nijmeh,H.S., Webb,T.M., Nicholson,A.G., Zhang,Q., Kraja,A., Spendlove,I., Osborne,J., Mardis,E., and Longmore,G.D. (2008). The chromosome 3p21.3-encoded gene, LIMD1, is a critical tumor suppressor involved in human lung cancer development. *Proc. Natl. Acad. Sci. U. S. A* 105, 19932-19937.
- Sharp,T.V., Munoz,F., Bourbouli,D., Presneau,N., Darai,E., Wang,H.W., Cannon,M., Butcher,D.N., Nicholson,A.G., Klein,G., Imreh,S., and Boshoff,C. (2004). LIM domains-containing protein 1 (LIMD1), a tumor suppressor encoded at chromosome 3p21.3, binds pRB and represses E2F-driven transcription. *Proc. Natl. Acad. Sci. U. S. A* 101, 16531-16536.
- Sharrocks,A.D. (2001). The ETS-domain transcription factor family. *Nat. Rev. Mol. Cell Biol.* 2, 827-837.
- Shen,L., Kondo,Y., Guo,Y., Zhang,J., Zhang,L., Ahmed,S., Shu,J., Chen,X., Waterland,R.A., and Issa,J.P. (2007). Genome-wide profiling of DNA methylation reveals a class of normally methylated CpG island promoters. *PLoS. Genet.* 3, 2023-2036.
- Shen,W.J., Dai,D.Q., Teng,Y., and Liu,H.B. (2008). Regulation of demethylation and re-expression of RASSF1A gene in gastric cancer cell lines by combined treatment of 5-Aza-CdR and NaB. *World J. Gastroenterol.* 14, 595-600.
- Shogren-Knaak,M., Ishii,H., Sun,J.M., Pazin,M.J., Davie,J.R., and Peterson,C.L. (2006). Histone H4-K16 acetylation controls chromatin structure and protein interactions. *Science* 311, 844-847.
- Shyu,K.G., Hsu,F.L., Wang,M.J., Wang,B.W., and Lin,S. (2007). Hypoxia-inducible factor 1alpha regulates lung adenocarcinoma cell invasion. *Exp. Cell Res.* 313, 1181-1191.
- Simmen,M.W. (2008). Genome-scale relationships between cytosine methylation and dinucleotide abundances in animals. *Genomics* 92, 33-40.
- Smale,S.T. and Kadonaga,J.T. (2003). The RNA polymerase II core promoter. *Annu. Rev. Biochem.* 72, 449-479.

- Smiraglia,D.J., Rush,L.J., Fruhwald,M.C., Dai,Z., Held,W.A., Costello,J.F., Lang,J.C., Eng,C., Li,B., Wright,F.A., Caligiuri,M.A., and Plass,C. (2001). Excessive CpG island hypermethylation in cancer cell lines versus primary human malignancies. *Hum. Mol. Genet.* *10*, 1413-1419.
- Smith,M.F., Jr., Carl,V.S., Lodie,T., and Fenton,M.J. (1998). Secretory interleukin-1 receptor antagonist gene expression requires both a PU.1 and a novel composite NF-kappaB/PU.1/GA-binding protein binding site. *J. Biol. Chem.* *273*, 24272-24279.
- Song,L.P., Zhang,J., Wu,S.F., Huang,Y., Zhao,Q., Cao,J.P., Wu,Y.L., Wang,L.S., and Chen,G.Q. (2008). Hypoxia-inducible factor-1alpha-induced differentiation of myeloid leukemic cells is its transcriptional activity independent. *Oncogene* *27*, 519-527.
- Sparkes,R.S., Murphree,A.L., Lingua,R.W., Sparkes,M.C., Field,L.L., Funderburk,S.J., and Benedict,W.F. (1983). Gene for hereditary retinoblastoma assigned to human chromosome 13 by linkage to esterase D. *Science* *219*, 971-973.
- Sparkes,R.S. and Sparkes,M.C. (1983). Esterase D studies in human retinoblastoma. *Isozymes. Curr. Top. Biol. Med. Res.* *11*, 173-182.
- Spendlove,I., Al-Attar,A., Watherstone,O., Webb,T.M., Ellis,I.O., Longmore,G.D., and Sharp,T.V. (2008). Differential subcellular localisation of the tumour suppressor protein LIMD1 in breast cancer correlates with patient survival. *Int. J Cancer* *123*, 2247-2253.
- Srichai,M.B., Konieczkowski,M., Padiyar,A., Konieczkowski,D.J., Mukherjee,A., Hayden,P.S., Kamat,S., El-Meanawy,M.A., Khan,S., Mundel,P., Lee,S.B., Bruggeman,L.A., Schelling,J.R., and Sedor,J.R. (2004). A WT1 co-regulator controls podocyte phenotype by shuttling between adhesion structures and nucleus. *J. Biol. Chem.* *279*, 14398-14408.
- Srinivas,V., Zhang,L.P., Zhu,X.H., and Caro,J. (1999). Characterization of an oxygen/redox-dependent degradation domain of hypoxia-inducible factor alpha (HIF-alpha) proteins. *Biochem. Biophys. Res. Commun.* *260*, 557-561.
- Stamatoyannopoulos,J.A. (2010). Illuminating eukaryotic transcription start sites. *Nat. Methods* *7*, 501-503.
- Stebbins,C.E., Kaelin,W.G., Jr., and Pavletich,N.P. (1999). Structure of the VHL-ElonginC-ElonginB complex: implications for VHL tumor suppressor function. *Science* *284*, 455-461.
- Stein,R., Razin,A., and Cedar,H. (1982). In vitro methylation of the hamster adenine phosphoribosyltransferase gene inhibits its expression in mouse L cells. *Proc. Natl. Acad. Sci. U. S. A* *79*, 3418-3422.
- Stein,R., Sciaky-Gallili,N., Razin,A., and Cedar,H. (1983). Pattern of methylation of two genes coding for housekeeping functions. *Proc. Natl. Acad. Sci. U. S. A* *80*, 2422-2426.
- Stewart,C.L., Stuhlmann,H., Jahner,D., and Jaenisch,R. (1982). De novo methylation, expression, and infectivity of retroviral genomes introduced into embryonal carcinoma cells. *Proc. Natl. Acad. Sci. U. S. A* *79*, 4098-4102.
- Stiehl,D.P., Wirthner,R., Koditz,J., Spielmann,P., Camenisch,G., and Wenger,R.H. (2006). Increased prolyl 4-hydroxylase domain proteins compensate for decreased oxygen levels. Evidence for an autoregulatory oxygen-sensing system. *J. Biol. Chem.* *281*, 23482-23491.

- Stirewalt,D.L. (2004). Fine-tuning PU.1. *Nat. Genet.* 36, 550-551.
- Stolze,I.P., Tian,Y.M., Appelhoff,R.J., Turley,H., Wykoff,C.C., Gleadle,J.M., and Ratcliffe,P.J. (2004). Genetic analysis of the role of the asparaginyl hydroxylase factor inhibiting hypoxia-inducible factor (FIH) in regulating hypoxia-inducible factor (HIF) transcriptional target genes [corrected]. *J. Biol. Chem.* 279, 42719-42725.
- Strathdee,G., Sim,A., and Brown,R. (2004). Control of gene expression by CpG island methylation in normal cells. *Biochem. Soc. Trans.* 32, 913-915.
- Strathdee,G., Sim,A., Soutar,R., Holyoake,T.L., and Brown,R. (2007). HOXA5 is targeted by cell-type-specific CpG island methylation in normal cells and during the development of acute myeloid leukaemia. *Carcinogenesis* 28, 299-309.
- Stroh,T., Erben,U., Kuhl,A.A., Zeitz,M., and Siegmund,B. (2010). Combined pulse electroporation--a novel strategy for highly efficient transfection of human and mouse cells. *PLoS. One.* 5, e9488.
- Sugatani,T. and Hruska,K.A. (2007). MicroRNA-223 is a key factor in osteoclast differentiation. *J. Cell Biochem.* 101, 996-999.
- Sugatani,T. and Hruska,K.A. (2009). Impaired micro-RNA pathways diminish osteoclast differentiation and function. *J. Biol. Chem.* 284, 4667-4678.
- Sun,Z., Asmann,Y.W., Kalari,K.R., Bot,B., Eckel-Passow,J.E., Baker,T.R., Carr,J.M., Khrebtukova,I., Luo,S., Zhang,L., Schroth,G.P., Perez,E.A., and Thompson,E.A. (2011). Integrated analysis of gene expression, CpG island methylation, and gene copy number in breast cancer cells by deep sequencing. *PLoS. One.* 6, e17490.
- Suzuki,M., Yamada,T., Kihara-Negishi,F., Sakurai,T., Hara,E., Tenen,D.G., Hozumi,N., and Oikawa,T. (2006). Site-specific DNA methylation by a complex of PU.1 and Dnmt3a/b. *Oncogene* 25, 2477-2488.
- Suzuki,M., Yamada,T., Kihara-Negishi,F., Sakurai,T., and Oikawa,T. (2003). Direct association between PU.1 and MeCP2 that recruits mSin3A-HDAC complex for PU.1-mediated transcriptional repression. *Oncogene* 22, 8688-8698.
- Suzuki,M.M. and Bird,A. (2008). DNA methylation landscapes: provocative insights from epigenomics. *Nat. Rev. Genet.* 9, 465-476.
- Suzuki,Y., Tsunoda,T., Sese,J., Taira,H., Mizushima-Sugano,J., Hata,H., Ota,T., Isogai,T., Tanaka,T., Nakamura,Y., Suyama,A., Sakaki,Y., Morishita,S., Okubo,K., and Sugano,S. (2001). Identification and characterization of the potential promoter regions of 1031 kinds of human genes. *Genome Res.* 11, 677-684.
- Takai,D. and Jones,P.A. (2002). Comprehensive analysis of CpG islands in human chromosomes 21 and 22. *Proc. Natl. Acad. Sci. U. S. A* 99, 3740-3745.
- Tan,M., Gu,Q., He,H., Pamarthy,D., Semenza,G.L., and Sun,Y. (2008). SAG/ROC2/RBX2 is a HIF-1 target gene that promotes HIF-1 alpha ubiquitination and degradation. *Oncogene* 27, 1404-1411.

- Tenen,D.G. (2003). Disruption of differentiation in human cancer: AML shows the way. *Nat. Rev. Cancer* 3, 89-101.
- Thomlinson,R.H. and Gray,L.H. (1955). The histological structure of some human lung cancers and the possible implications for radiotherapy. *Br. J. Cancer* 9, 539-549.
- Tian,H., McKnight,S.L., and Russell,D.W. (1997). Endothelial PAS domain protein 1 (EPAS1), a transcription factor selectively expressed in endothelial cells. *Genes Dev.* 11, 72-82.
- Tondravi,M.M., Mckercher,S.R., Anderson,K., Erdmann,J.M., Quiroz,M., Maki,R., and Teitelbaum,S.L. (1997). Osteopetrosis in mice lacking haematopoietic transcription factor PU.1. *Nature* 386, 81-84.
- Tu,Y., Wu,S., Shi,X., Chen,K., and Wu,C. (2003). Migfilin and Mig-2 link focal adhesions to filamin and the actin cytoskeleton and function in cell shape modulation. *Cell* 113, 37-47.
- Tuveson,D.A., Shaw,A.T., Willis,N.A., Silver,D.P., Jackson,E.L., Chang,S., Mercer,K.L., Grochow,R., Hock,H., Crowley,D., Hingorani,S.R., Zaks,T., King,C., Jacobetz,M.A., Wang,L., Bronson,R.T., Orkin,S.H., DePinho,R.A., and Jacks,T. (2004). Endogenous oncogenic K-ras(G12D) stimulates proliferation and widespread neoplastic and developmental defects. *Cancer Cell* 5, 375-387.
- Valencak,J., Schmid,K., Trautinger,F., Wallnofer,W., Muellauer,L., Soleiman,A., Knobler,R., Haitel,A., Pehamberger,H., and Raderer,M. (2011). High expression of Dicer reveals a negative prognostic influence in certain subtypes of primary cutaneous T cell lymphomas. *J. Dermatol. Sci.*
- van Wijk,N.V., Witte,F., Feike,A.C., Schambony,A., Birchmeier,W., Mundlos,S., and Stricker,S. (2009). The LIM domain protein Wtip interacts with the receptor tyrosine kinase Ror2 and inhibits canonical Wnt signalling. *Biochem. Biophys. Res. Commun.* 390, 211-216.
- Venter,J.C., Adams,M.D., Myers,E.W., Li,P.W., Mural,R.J., Sutton,G.G., Smith,H.O., Yandell,M., Evans,C.A., Holt,R.A., Gocayne,J.D., Amanatides,P., Ballew,R.M., Huson,D.H., Wortman,J.R., Zhang,Q., Kodira,C.D., Zheng,X.H., Chen,L., Skupski,M., Subramanian,G., Thomas,P.D., Zhang,J., Gabor Miklos,G.L., Nelson,C., Broder,S., Clark,A.G., Nadeau,J., McKusick,V.A., Zinder,N., Levine,A.J., Roberts,R.J., Simon,M., Slayman,C., Hunkapiller,M., Bolanos,R., Delcher,A., Dew,I., Fasulo,D., Flanigan,M., Florea,L., Halpern,A., Hannenhalli,S., Kravitz,S., Levy,S., Mobarry,C., Reinert,K., Remington,K., Abu-Threideh,J., Beasley,E., Biddick,K., Bonazzi,V., Brandon,R., Cargill,M., Chandramouliswaran,I., Charlab,R., Chaturvedi,K., Deng,Z., Di,F., V, Dunn,P., Eilbeck,K., Evangelista,C., Gabrielian,A.E., Gan,W., Ge,W., Gong,F., Gu,Z., Guan,P., Heiman,T.J., Higgins,M.E., Ji,R.R., Ke,Z., Ketchum,K.A., Lai,Z., Lei,Y., Li,Z., Li,J., Liang,Y., Lin,X., Lu,F., Merkulov,G.V., Milshina,N., Moore,H.M., Naik,A.K., Narayan,V.A., Neelam,B., Nuskern,D., Rusch,D.B., Salzberg,S., Shao,W., Shue,B., Sun,J., Wang,Z., Wang,A., Wang,X., Wang,J., Wei,M., Wides,R., Xiao,C., Yan,C., Yao,A., Ye,J., Zhan,M., Zhang,W., Zhang,H., Zhao,Q., Zheng,L., Zhong,F., Zhong,W., Zhu,S., Zhao,S., Gilbert,D., Baumhueter,S., Spier,G., Carter,C., Cravchik,A., Woodage,T., Ali,F., An,H., Awe,A., Baldwin,D., Baden,H., Barnstead,M., Barrow,I., Beeson,K., Busam,D., Carver,A., Center,A., Cheng,M.L., Curry,L., Danaher,S., Davenport,L., Desilets,R., Dietz,S., Dodson,K., Doup,L., Ferreira,S., Garg,N., Gluecksmann,A., Hart,B., Haynes,J., Haynes,C., Heiner,C., Hladun,S., Hostin,D., Houck,J., Howland,T., Ibegwam,C., Johnson,J., Kalush,F., Kline,L., Koduru,S., Love,A., Mann,F., May,D., McCawley,S., McIntosh,T., McMullen,I., Moy,M., Moy,L., Murphy,B., Nelson,K., Pfannkoch,C., Pratts,E., Puri,V., Qureshi,H., Reardon,M., Rodriguez,R.,

Rogers,Y.H., Romblad,D., Ruhfel,B., Scott,R., Sitter,C., Smallwood,M., Stewart,E., Strong,R., Suh,E., Thomas,R., Tint,N.N., Tse,S., Vech,C., Wang,G., Wetter,J., Williams,S., Williams,M., Windsor,S., Winn-Deen,E., Wolfe,K., Zaveri,J., Zaveri,K., Abril,J.F., Guigo,R., Campbell,M.J., Sjolander,K.V., Karlak,B., Kejariwal,A., Mi,H., Lazareva,B., Hatton,T., Narechania,A., Diemer,K., Muruganujan,A., Guo,N., Sato,S., Bafna,V., Istrail,S., Lippert,R., Schwartz,R., Walenz,B., Yooseph,S., Allen,D., Basu,A., Baxendale,J., Blick,L., Caminha,M., Carnes-Stine,J., Caulk,P., Chiang,Y.H., Coyne,M., Dahlke,C., Mays,A., Dombroski,M., Donnelly,M., Ely,D., Esparham,S., Fosler,C., Gire,H., Glanowski,S., Glasser,K., Glodek,A., Gorokhov,M., Graham,K., Gropman,B., Harris,M., Heil,J., Henderson,S., Hoover,J., Jennings,D., Jordan,C., Jordan,J., Kasha,J., Kagan,L., Kraft,C., Levitsky,A., Lewis,M., Liu,X., Lopez,J., Ma,D., Majoros,W., McDaniel,J., Murphy,S., Newman,M., Nguyen,T., Nguyen,N., and Nodell,M. (2001). The sequence of the human genome. *Science* 291, 1304-1351.

Verger,A. and Duterrque-Coquillaud,M. (2002). When Ets transcription factors meet their partners. *Bioessays* 24, 362-370.

Wagner,K.D., Wagner,N., Wellmann,S., Schley,G., Bondke,A., Theres,H., and Scholz,H. (2003). Oxygen-regulated expression of the Wilms' tumor suppressor Wt1 involves hypoxia-inducible factor-1 (HIF-1). *FASEB J.* 17, 1364-1366.

Wakefield,R.I., Smith,B.O., Nan,X., Free,A., Soteriou,A., Uhrin,D., Bird,A.P., and Barlow,P.N. (1999). The solution structure of the domain from MeCP2 that binds to methylated DNA. *J. Mol. Biol.* 291, 1055-1065.

Wang,G.L., Jiang,B.H., Rue,E.A., and Semenza,G.L. (1995a). Hypoxia-inducible factor 1 is a basic-helix-loop-helix-PAS heterodimer regulated by cellular O₂ tension. *Proc. Natl. Acad. Sci. U. S. A* 92, 5510-5514.

Wang,G.L., Jiang,B.H., and Semenza,G.L. (1995b). Effect of altered redox states on expression and DNA-binding activity of hypoxia-inducible factor 1. *Biochem. Biophys. Res. Commun.* 212, 550-556.

Wang,G.L. and Semenza,G.L. (1993a). Characterization of hypoxia-inducible factor 1 and regulation of DNA binding activity by hypoxia. *J. Biol. Chem.* 268, 21513-21518.

Wang,G.L. and Semenza,G.L. (1993b). Desferrioxamine induces erythropoietin gene expression and hypoxia-inducible factor 1 DNA-binding activity: implications for models of hypoxia signal transduction. *Blood* 82, 3610-3615.

Wang,G.L. and Semenza,G.L. (1993c). General involvement of hypoxia-inducible factor 1 in transcriptional response to hypoxia. *Proc. Natl. Acad. Sci. U. S. A* 90, 4304-4308.

Wang,G.L. and Semenza,G.L. (1995). Purification and characterization of hypoxia-inducible factor 1. *J. Biol. Chem.* 270, 1230-1237.

Wang,J., Liu,X., Ni,P., Gu,Z., and Fan,Q. (2010). SP1 is required for basal activation and chromatin accessibility of CD151 promoter in liver cancer cells. *Biochem. Biophys. Res. Commun.* 393, 291-296.

Wang,Y. and Gilmore,T.D. (2001). LIM domain protein Trip6 has a conserved nuclear export signal, nuclear targeting sequences, and multiple transactivation domains. *Biochim. Biophys. Acta* 1538, 260-272.

- Wang,Y., Liu,Y., Malek,S.N., Zheng,P., and Liu,Y. (2011). Targeting HIF1alpha eliminates cancer stem cells in hematological malignancies. *Cell Stem Cell* 8, 399-411.
- Warburg,O. (1956). On the origin of cancer cells. *Science* 123, 309-314.
- Way,J.C. and Chalfie,M. (1988). *mec-3*, a homeobox-containing gene that specifies differentiation of the touch receptor neurons in *C. elegans*. *Cell* 54, 5-16.
- Webster,K.A. (1987). Regulation of glycolytic enzyme RNA transcriptional rates by oxygen availability in skeletal muscle cells. *Mol. Cell Biochem.* 77, 19-28.
- Wei,Q., Zhou,W., Wang,W., Gao,B., Wang,L., Cao,J., and Liu,Z.P. (2010). Tumor-suppressive functions of leucine zipper transcription factor-like 1. *Cancer Res.* 70, 2942-2950.
- Wenger,R.H., Kvietikova,I., Rolfs,A., Camenisch,G., and Gassmann,M. (1998). Oxygen-regulated erythropoietin gene expression is dependent on a CpG methylation-free hypoxia-inducible factor-1 DNA-binding site. *Eur. J. Biochem.* 253, 771-777.
- Wigler,M., Levy,D., and Perucho,M. (1981). The somatic replication of DNA methylation. *Cell* 24, 33-40.
- Wigler,M.H. (1981). The inheritance of methylation patterns in vertebrates. *Cell* 24, 285-286.
- Wijnhoven,B.P., Dinjens,W.N., and Pignatelli,M. (2000). E-cadherin-catenin cell-cell adhesion complex and human cancer. *Br. J. Surg.* 87, 992-1005.
- Wijnhoven,S.W., Kool,H.J., van Teijlingen,C.M., van Zeeland,A.A., and Vrieling,H. (2001). Loss of heterozygosity in somatic cells of the mouse. An important step in cancer initiation? *Mutat. Res.* 473, 23-36.
- Wood,A.J. and Oakey,R.J. (2006). Genomic imprinting in mammals: emerging themes and established theories. *PLoS. Genet.* 2, e147.
- Wu,C. (2005). Migfilin and its binding partners: from cell biology to human diseases. *J. Cell Sci.* 118, 659-664.
- Wu,J.F., Shen,W., Liu,N.Z., Zeng,G.L., Yang,M., Zuo,G.Q., Gan,X.N., Ren,H., and Tang,K.F. (2010). Down-regulation of Dicer in hepatocellular carcinoma. *Med. Oncol.*
- Xia,X. and Kung,A.L. (2009). Preferential binding of HIF-1 to transcriptionally active loci determines cell-type specific response to hypoxia. *Genome Biol.* 10, R113.
- Xia,X., Lemieux,M.E., Li,W., Carroll,J.S., Brown,M., Liu,X.S., and Kung,A.L. (2009). Integrative analysis of HIF binding and transactivation reveals its role in maintaining histone methylation homeostasis. *Proc. Natl. Acad. Sci. U. S. A* 106, 4260-4265.
- Xie,S., Wang,Z., Okano,M., Nogami,M., Li,Y., He,W.W., Okumura,K., and Li,E. (1999). Cloning, expression and chromosome locations of the human DNMT3 gene family. *Gene* 236, 87-95.

- Yang,S.H., Vickers,E., Brehm,A., Kouzarides,T., and Sharrocks,A.D. (2001). Temporal recruitment of the mSin3A-histone deacetylase corepressor complex to the ETS domain transcription factor Elk-1. *Mol. Cell Biol.* *21*, 2802-2814.
- Yang,Y., Kiss,H., Kost-Alimova,M., Kedra,D., Fransson,I., Seroussi,E., Li,J., Szeles,A., Kholodnyuk,I., Imreh,M.P., Fodor,K., Hadlaczky,G., Klein,G., Dumanski,J.P., and Imreh,S. (1999). A 1-Mb PAC contig spanning the common eliminated region 1 (CER1) in microcell hybrid-derived SCID tumors. *Genomics* *62*, 147-155.
- Yee,K.M., Spivak-Kroizman,T.R., and Powis,G. (2008). HIF-1 regulation: not so easy come, easy go. *Trends Biochem. Sci.* *33*, 526-534.
- Yi,J. and Beckerle,M.C. (1998). The human TRIP6 gene encodes a LIM domain protein and maps to chromosome 7q22, a region associated with tumorigenesis. *Genomics* *49*, 314-316.
- Yi,R., Qin,Y., Macara,I.G., and Cullen,B.R. (2003). Exportin-5 mediates the nuclear export of pre-microRNAs and short hairpin RNAs. *Genes Dev.* *17*, 3011-3016.
- Yoder,J.A. and Bestor,T.H. (1998). A candidate mammalian DNA methyltransferase related to pmt1p of fission yeast. *Hum. Mol. Genet.* *7*, 279-284.
- Yu,F., White,S.B., Zhao,Q., and Lee,F.S. (2001). HIF-1 α binding to VHL is regulated by stimulus-sensitive proline hydroxylation. *Proc. Natl. Acad. Sci. U. S. A* *98*, 9630-9635.
- Zabarovsky,E.R., Lerman,M.I., and Minna,J.D. (2002). Tumor suppressor genes on chromosome 3p involved in the pathogenesis of lung and other cancers. *Oncogene* *21*, 6915-6935.
- Zagorska,A. and Dulak,J. (2004). HIF-1: the knowns and unknowns of hypoxia sensing. *Acta Biochim. Pol.* *51*, 563-585.
- Zelko,I.N., Mueller,M.R., and Folz,R.J. (2008). Transcription factors sp1 and sp3 regulate expression of human extracellular superoxide dismutase in lung fibroblasts. *Am. J. Respir. Cell Mol. Biol.* *39*, 243-251.
- Zendman,A.J., Ruiter,D.J., and van Muijen,G.N. (2003). Cancer/testis-associated genes: identification, expression profile, and putative function. *J. Cell Physiol* *194*, 272-288.
- Zhang,H., Feng,X., Liu,W., Jiang,X., Shan,W., Huang,C., Yi,H., Zhu,B., Zhou,W., Wang,L., Liu,C., Zhang,L., Jia,W., Huang,W., Li,G., Shi,J., Wanggou,S., Yao,K., and Ren,C. (2011a). Underlying mechanisms for LTF inactivation and its functional analysis in nasopharyngeal carcinoma cell lines. *J. Cell Biochem.* *112*, 1832-1843.
- Zhang,H., Kolb,F.A., Jaskiewicz,L., Westhof,E., and Filipowicz,W. (2004a). Single processing center models for human Dicer and bacterial RNase III. *Cell* *118*, 57-68.
- Zhang,Q., Zhang,Z.F., Rao,J.Y., Sato,J.D., Brown,J., Messadi,D.V., and Le,A.D. (2004b). Treatment with siRNA and antisense oligonucleotides targeted to HIF-1 α induced apoptosis in human tongue squamous cell carcinomas. *Int. J. Cancer* *111*, 849-857.
- Zhang,Y., Ng,H.H., Erdjument-Bromage,H., Tempst,P., Bird,A., and Reinberg,D. (1999). Analysis of the NuRD subunits reveals a histone deacetylase core complex and a connection with DNA methylation. *Genes Dev.* *13*, 1924-1935.

- Zhang,Y., Wang,R., Song,H., Huang,G., Yi,J., Zheng,Y., Wang,J., and Chen,L. (2011b). Methylation of multiple genes as a candidate biomarker in non-small cell lung cancer. *Cancer Lett.* 303, 21-28.
- Zheng,Y., Zhang,W., Ye,Q., Zhou,Y., Xiong,W., He,W., Deng,M., Zhou,M., Guo,X., Chen,P., Fan,S., Liu,X., Wang,Z., Li,X., Ma,J., and Li,G. (2012). Inhibition of Epstein-Barr Virus Infection by Lactoferrin. *J. Innate. Immun.*
- Zhong,H., Agani,F., Baccala,A.A., Laughner,E., Rioseco-Camacho,N., Isaacs,W.B., Simons,J.W., and Semenza,G.L. (1998). Increased expression of hypoxia inducible factor-1alpha in rat and human prostate cancer. *Cancer Res.* 58, 5280-5284.
- Zhong,H., De Marzo,A.M., Laughner,E., Lim,M., Hilton,D.A., Zagzag,D., Buechler,P., Isaacs,W.B., Semenza,G.L., and Simons,J.W. (1999). Overexpression of hypoxia-inducible factor 1alpha in common human cancers and their metastases. *Cancer Res.* 59, 5830-5835.
- Zhou,X., Popescu,N.C., Klein,G., and Imreh,S. (2007). The interferon-alpha responsive gene TMEM7 suppresses cell proliferation and is downregulated in human hepatocellular carcinoma. *Cancer Genet. Cytogenet.* 177, 6-15.
- Zhou,Y., Chen,L., Barlogie,B., Stephens,O., Wu,X., Williams,D.R., Cartron,M.A., van,R.F., Nair,B., Waheed,S., Pineda-Roman,M., Alsayed,Y., Anaissie,E., and Shaughnessy,J.D., Jr. (2010). High-risk myeloma is associated with global elevation of miRNAs and overexpression of EIF2C2/AGO2. *Proc. Natl. Acad. Sci. U. S. A* 107, 7904-7909.
- Zhu,J., He,F., Hu,S., and Yu,J. (2008). On the nature of human housekeeping genes. *Trends Genet.* 24, 481-484.
- Zhu,W.G., Srinivasan,K., Dai,Z., Duan,W., Druhan,L.J., Ding,H., Yee,L., Villalona-Calero,M.A., Plass,C., and Otterson,G.A. (2003). Methylation of adjacent CpG sites affects Sp1/Sp3 binding and activity in the p21(Cip1) promoter. *Mol. Cell Biol.* 23, 4056-4065.